Climate, Fine-Sediment Transport Linkages, Coast Mountains, British Columbia

by

Brian Peter Menounos

B.A., The University of Colorado, Boulder, 1994
M.A., The University of Colorado, Boulder, 1996

A THESIS SUBMITTED IN PARTIAL FULFILMENT OF
THE REQUIREMENTS FOR THE DEGREE OF

DOCTOR OF PHILOSOPHY

in

THE FACULTY OF GRADUATE STUDIES

(Department of Geography)

We accept this thesis as conforming
to the required standard

THE UNIVERSITY OF BRITISH COLUMBIA

April 22, 2002

Department of Geography

The University Of British Columbia
Vancouver, Canada

Date 25 April 2002

Abstract

The relation between climate and sediment yield remains poorly defined in regions of high relief and where sediment sources are numerous. This study examines the climatic controls associated with fine sediment production and yield for six glacierized watersheds in the Coast Mountains, British Columbia, Canada. Contemporary monitoring of suspended sediment transport was undertaken to detail the hydrologic conditions responsible for the entrainment and production of fine-grained sediment production and transport. The analysis of lake sediments recovered from outlet lake basins provided a means of documenting changes in sediment delivery over century to millennia time scales. Four of the lake basins contain finely laminated sediments which are interpreted to be clastic varves and so detail lake sedimentation at annual to event time scales.

The results indicate that much of the variance in sediment transport records can be attributed to hydro-climatic variability at all time scales under consideration and much like other geophysical time series, a 1/frequency-variance scaling is apparent within the yield proxies of this study. Climatological conditions important for sediment production and entrainment at event to annual scales include those processes responsible for high flow events in the study area. Decadal-scale variations in sediment delivery coincide with sustained periods of ice melt. Sediment delivery from the watersheds at century to millennial time scales reflects major changes in ice cover. The correspondence between long records of lake sedimentation and air-temperature proxies developed from tree rings and ice cores suggests that changes in sediment yield from the watersheds reflects changes in air temperatures in the study area. Variations in air temperature appear to influence sediment transfers by controlling the intensity of glacial runoff during the ablation season. Highest sensitivity (i.e. those records where geomorphic filtering of the climate signal has not occurred) is noted for those basins which have active glaciers and the opportunity for sediment storage of fine-grained sediment in the fluvial system is low.

Contents

Abstract ii

Contents iii

List of Tables viii

List of Figures ix

Dedication xii

Acknowledgements xiii

1 Introduction 1
- 1.1 Statement of the Problem 1
- 1.2 Framework for Analysis 2
- 1.3 Previous Work on the Climate-Sediment Discharge Relation in the Coast Mountains 3
- 1.4 Objectives 4
  - 1.4.1 Thesis Outline 6

2 Climatic Controls on Sediment Production and Yield 7
- 2.1 Introduction 7
- 2.2 North Pacific Climate Variability and Hydrologic Response 7
  - 2.2.1 North Pacific Atmospheric Dynamics 8
    - 2.2.1.1 Ocean-Atmospheric Linkages for North Pacific Climate Variability (ENSO and the PDO) 10
  - 2.2.2 Climate Variability Influencing Glacial Mass Balance 14
- 2.3 Floods and Flood Generating Mechanisms 15
- 2.4 Summary 16
- 2.5 Sediment Production, Storage and Transfers: The fine Sediment Cascade 17
  - 2.5.1 Glaciers 17
  - 2.5.2 Sub-glacial Erosion 17
  - 2.5.3 Glacial Response Times 18
  - 2.5.4 Rapid Mass Movement 19
    - 2.5.4.1 Debris Flows, Torrents and Landsliding 19
    - 2.5.4.2 Snow Avalanches 19
  - 2.5.5 Intermediate Sediment Storage: the Fluvial System 20
- 2.6 Climate and Fine Sediment Cascade Linkages: The Conceptual Model 20
- 2.7 Conclusions 23

3 Study Area, Data Collection, Acquisition and Analysis 24
3.1 Introduction 24
3.2 Study Area Watershed Selection 24
3.3 Sediment Source Identification and Morphometric Controls of Sediment Production . 27
3.3.0.1 Duffey 27
3.3.0.2 Birkenhead Lake Basin 29
3.3.0.3 Joffre Lake Basin 30
3.3.0.4 Green Lake 31
3.3.0.5 Cheakamus 32
3.3.0.6 Glacier Lake Basin 32
3.3.1 Geology 33
3.3.2 Basin Morphometry 35
3.3.2.1 Coupling Number 38
3.3.3 Watershed Similarity 39
3.4 Data Acquisition and Analysis (Climate and Sediment Discharge) 40
3.4.1 Hydro-climatic Data (this study) 40
3.4.1.1 Stream Gauging and SSC Collection 41
3.4.1.2 Lake Sedimentation 41
3.4.2 Hydro-Climatic Data 42
3.5 Paleo-environmental Data (this study) 42
3.5.1 Sediment Archives 42
3.5.2 Development of Varve Chronologies 43
3.5.3 Age Control of Sediment Archives 43
3.5.4 Paleo-environmental Data (other sources) 44
3.5.4.1 Tree Ring Data 44
3.5.4.2 Ice Core Record 44

4 Event to Inter-annual Time Scales: Sediment Transport 45
4.1 Introduction 45
4.2 Large-Scale Climate Conditions During the Period of Study 45
4.3 Observed Streamflow Variability 46
4.4 Fine Sediment Sources and Seasonality of Transport 48
4.4.1 Sediment Source Areas 48
4.4.2 Seasonality of Transport 51
4.4.3 Seasonal Dependent Sediment Storage 52
4.4.4 SSC Modeling and Estimates of Sediment Yields 53
4.4.4.1 Van Horlick, Cayoosh and Fitzsimmons Creeks 59
4.4.4.2 Assessment of Bias During Glacial Runoff 62
4.4.4.3 Phelix Creek 63
4.4.5 The Significance of the Infrequent Event 63
4.5 Lake Monitoring 64
4.6 Conclusion 68

5 Inter-annual to Decadal Scales: Fine-Sediment Production and Transport . . . 70
5.1 Introduction 70
5.2 Analysis of Hydro-climatic Variability During the Contemporary Period 70
5.2.1 Temperature and Precipitation Variability 70
5.2.2 Inter-annual Variations in Discharge and Flood Frequency 75

5.2.2.1 Lillooet and Cheakamus Discharge Records . . . 75
5.2.3 Conclusion . . . 80
5.3 Analysis of Sedimentary Archives Within the Lake Basins . . . 80
5.3.1 Massive Sediments . . . 86
5.3.2 Indistinctly-laminated sediments . . . 86
5.3.3 Distinctly-laminated Sediments . . . 88
5.3.4 Bedded Sediments . . . 91
5.4 Interpretation: Inter and Intra-lake Sedimentation Processes . . . 92
5.4.0.1 Factors Governing Bioturbation . . . 93
5.4.1 Decadal Scale Variations in Sediment Delivery to the Lake Basins . . . 94
5.4.2 Varve Interpretation of Finely-Laminated Sediment Archive . . . 97
5.4.2.1 Seasonal Recovery . . . 97
5.4.2.2 Radiometric Dating (^{137}Cs) . . . 97
5.4.2.3 Hydrologic Correlations . . . 98
5.4.3 Spatial and Temporal Variations in Varve Thickness . . . 98
5.4.3.1 Spatial Patterns of Sedimentation . . . 100
5.4.3.2 Temporal Variability . . . 100
5.4.3.3 Climatic Controls on Varve Departures . . . 101
5.4.3.4 Duffey . . . 101
5.4.3.5 Green, Cheakamus and Glacier Lakes . . . 102
5.4.4 Extreme Sedimentation Events and Seasonality . . . 107
5.4.4.1 Discussion . . . 110
5.4.5 Sediment Source Changes Indirectly Related to Climate: Changes in Glacial Extent During the 20th Century . . . 111
5.4.5.1 Discussion . . . 115
5.4.5.2 Glacial Activity and Lake Sedimentation . . . 115
5.4.5.3 Climatic Controls on Sediment Source Variability: Limitations for Environmental Reconstruction . . . 116
5.4.6 Internal Controls on Sediment Delivery: Land Use and Natural Diversions . . 117
5.5 Lake-Based Sediment Yield Estimates . . . 120
5.5.0.1 Discussion . . . 121
5.6 Conclusions . . . 122

6 Century to Millennial Time Scales: Variations in Sediment Production and Delivery . . . 124
6.1 Changes in Sediment Production-Glacial Fluctuations during the last 600 Years . . . 124
6.2 Decadal-to-Century Scale Climate Variability and Sediment Transfers . . . 128
6.2.1 Data Retrieval, Analysis, and Calibration . . . 131
6.2.2 Calibration Datasets: Temperature and Precipitation . . . 133
6.2.3 Results-Temperature and Precipitation . . . 134
6.2.4 Results-Tree Ring Patterns and Correspondence to Temperature, Precipitation Fields, and Large-Scale Climate Indices . . . 139
6.2.4.1 Orthogonal Linear Regression (OLR) . . . 143
6.2.4.2 Results . . . 143
6.2.4.3 Temperature and Precipitation Reconstruction (1400-1979AD) . . . 146
6.2.4.4 Large-scale, climate indices . . . 147
6.3 Climate-Sediment Transport Linkages over the past 600 years: Varve Chronologies From Green and Duffey Lake Basins . . . 151

6.3.0.5 Results-Green Lake . . . 151
6.3.0.6 Results-Duffey Lake . . . 153
6.3.1 Removal of Temperature Signal from the Green Lake Varve Chronology . . . 158
6.3.1.1 Temperature Model Residual Analysis . . . 159
6.3.1.2 Reconstruction of Varve Thickness . . . 161
6.3.2 Discussion . . . 161
6.3.2.1 Sediment Residuals and their Relation to Glacial Extent . . . 165
6.4 Millennial-Scale Changes in Sediment Delivery . . . 166
6.4.1 Bulk Physical Properties and Dating Control . . . 166
6.4.2 Duffey Lake . . . 168
6.4.2.1 Interpretation . . . 173
6.4.3 Green Lake . . . 174
6.4.3.1 Interpretation . . . 178
6.4.4 Joffre Lake . . . 178
6.4.4.1 Interpretation . . . 180
6.4.5 Depth-Age Sedimentation Models . . . 181
6.4.5.1 Results . . . 182
6.4.5.2 Sedimentation Indices . . . 185
6.4.5.3 Green Lake Varve Index . . . 185
6.4.6 Discussion -Glacial fluctuations and Changes in Sediment Supply . . . 188
6.4.6.1 Early Holocene Glacial Advances (?) . . . 190
6.4.6.2 Middle Holocene Glacial Advances . . . 191
6.4.6.3 Late Neoglacial Advances and the Inception of the 'Little Ice Age' . 192
6.4.6.4 Deposit Preservation and Apparent Magnitude of Glacial Events . . 193
6.4.7 Comparison of the Sediment Indices to Climate Based Proxies from the Greenland Ice Cores . . . 194
6.4.8 Results . . . 195
6.4.8.1 Varve Records . . . 195
6.4.8.2 Clastic Indices and Joffre Lake DN Record . . . 197
6.4.8.3 Discussion . . . 199
6.5 Conclusions . . . 201

7 Conclusions . . . 203
7.1 Introduction . . . 203
7.2 Sediment Production, Transport and its Linkage to Climate: Time and Space Scaling 203
7.3 Other Important Findings . . . 205
7.3.0.4 Importance of Glacial Cover . . . 206
7.3.0.5 Sediment Relaxation . . . 206
7.4 Limitations of the Study and Directions for Further Research . . . 207
7.4.0.6 Glacial Sediment Budgets and Provenance . . . 208
7.4.0.7 Multi-basin Varve Network . . . 209

Bibliography . . . 210

A Detailed Methodology . . . 230
A.1 Discharge Records . . . 230
A.1.1 Cayoosh Creek Discharge . . . 232
A.2 Lake Sediment Core Recovery . . . 233

A.3 Laboratory Techniques 234
A.3.1 Organic Carbon 234
A.3.2 Volumetric Sampling and Particle Size Analysis 235
A.3.3 Sediment Slabbing and Embedding Techniques 235

B TRIM, Geologic and Glacial Mapping 237
B.1 LIA Mapping 237
B.2 Rectification from air photos 238

C EOF, Spectral Analysis, and Effective Degrees of Freedom 239
C.1 EOF and PCA 239
C.1.1 Simplification of spatio-temporal patterns: Rotated Solution 241
C.2 Autocorrelation and the Color of Noise 241
C.2.1 Autocorrelation and Effective Degrees of Freedom 242

D Varve Measurements and Uncertainties 243

List of Tables

3.1 monitoring table 25
3.2 Basin Morphometric Characteristics 37

4.1 Hydro-climatic Variability During Period of Monitoring 46
4.2 Flow Statistics of Monitored Streams During Period of Study 48
4.3 Ln(SSC)-Linear(Q) Rating Curve Models 61
4.4 Load Estimates (Metric Tonnes) Obtained From the Rating Curves 63

5.1 Available Long Term (n≈100yr) Records of Monthly Precipitation and Temperature Anomalies 1889-1997 72
5.2 Pearson Correlation Coefficients for Varve Records 106
5.3 Changes in Areal and Downvalley Extent of Glaciers Within or Near Study Basins During Contemporary Period 114

6.1 Summary Statistics of RPCA Analysis of Gridded Monthly Temperature and Precipitation Analysis 138
6.2 Statistics of Tree-Ring Networks 139
6.3 EOF Statistics From the Tree-Ring Network 142
6.4 Summary Statistics from multiple regression models 145
6.5 PDO Model, Verification, and Calibration Statistics 149
6.6 20th Century Varve Prediction Model 161
6.7 Radiocarbon Ages Used in This Study 167
6.8 Bedded Sediment Characteristics, Duffey Lake 172
6.9 Spectral Power in the GISP2 and Green Lake Varve Series 197

D.1 Uncertainty (percent) in Varve Chronologies, Duffey and Green Lake Basins 244

List of Figures

2.1 PNA 9
2.2 ENSO 11
2.3 PDO Anomalies 13
2.4 Proposed Climate-Fine Sediment Cascade Linkages 22

3.1 Study area location 26
3.2 Variability in Flood Generating Mechanisms Across the Study Area 28
3.3 DEMs of Duffey and Joffre Basins 30
3.4 DEM of Birkenhead Lake Basin 31
3.5 DEMs of Cheakamus and Green Lake Basins 33
3.6 DEM of Glacier Basin 34
3.7 Generalized Geology of the Study Area. 35
3.8 Bivariate Distributions of Slope-Elevational Data 39
3.9 Dendrogram of Watershed Similarity 40

4.1 Van Horlick, Cayoosh and Phelix Creek Hydrographs 47
4.2 Median SSC (log) Estimates for Sub-basins and Main-stem Channels 49
4.3 Median Concentration of Mainstem and Tributary Channels and Contemporary Ice Cover 50
4.4 Hydrologic Season and Sediment Transport 55
4.5 Discharge-SSC Relations 56
4.6 Power Spectrum of 500hPa Anomalies 58
4.7 Fractional Load Estimates 66
4.8 Stream Discharge, Lake Sediment Flux, Birkenhead and Duffey Lakes 67
4.9 Sediment Flux, Organic Matter Relations, Birkenhead and Duffey Lakes 68

5.1 Regional Departures in Monthly Precipitation and Temperatures 74
5.2 Cumulative Standardized Departures of PDO, Temperature and Precipitation for the Period 1900-1990 76
5.3 Q_{max}, Spring (3/1-8/1), and Autumn (8/15-12/15) Flood Distributions, Lillooet River 77
5.4 Spatial Distribution of Specific Flow ($m^3km^{-2}s^{-1}$) When Lillooet River Discharge Exceeds 700 m^3s^{-1} 78
5.5 Daily and Annual Discharge of the Lillooet and Cheakamus Rivers 81
5.6 Cumulative Departures and Cross Correlation Between SOI and Lillooet River Autumn Flood Events 82
5.7 Bathymetry and Core Locations, Duffey and Birkenhead Lakes 83
5.8 Bathymetry and Core Locations, Green and Joffre Lakes 84
5.9 Bathymetry and Core locations, Cheakamus and Glacier lakes 85
5.10 Representative Sediment Cores from Duffey and Green Lake Basins 87
5.11 Photo-micrograph of Sedimentary Couplets from Duffey Lake 89

5.12 Photo-micrographs of Thin Section Samples from Cheakamus, Glacier, Green and Duffey Lakes . . . 90
5.13 Particle Size Distribution of the Laminated Sediments . . . 91
5.14 Organic Matter Content of Surface Sediments From the Lake Basins . . . 96
5.15 Cesium Profiles for Green and Duffey Lake Basins . . . 99
5.16 Varve Thickness Departures . . . 104
5.17 Varve Thickness-Q_{max} Relations . . . 105
5.18 Channel Changes of Cayoosh and Van Horlick Creeks, Duffey Lake Basin . . . 108
5.19 Channel-change Following 1991 Flood (Lower Cheakamus River) . . . 109
5.20 Channel-change of Fitzsimmons Following 1991 Flood . . . 110
5.21 Contemporary record of terminus fluctuations, Fitzsimmons Glacier . . . 112
5.22 Residuals of Varve Thickness From Green Lake After Controlling for Flood Intensity 119

6.1 DEM and Moraine Record near the Joffre Lakes Basin . . . 127
6.2 Observed Trends in Glaciation Levels and Relation to April 1 SWE . . . 129
6.3 a) North American (1800-1979AD) Tree-ring Network Recovered From the ITRDB 132
6.4 First 5 EOFs of Monthly Temperature Anomalies (1900-1998AD) . . . 135
6.5 First 5 EOFs of Monthly Precipitation Anomalies (1900-1998AD) . . . 136
6.6 Amplitudes and Spatial Loadings of the First 4 EOFs From the 1800-1980AD (n=678) Tree-Ring Network . . . 141
6.7 Reconstructed Annual Temperature and Precipitation Variability for the Study Area 148
6.8 PDO Model . . . 150
6.9 Raw and Standardized Varve Thickness, Green Lake (1387-1999AD) . . . 152
6.10 Reconstructed Annual Temperature and Green Lake Varve Departures . . . 154
6.11 Northern Hemispheric Air Temperature and Green Lake Varve Departures . . . 155
6.12 Raw and Standardized Varve Thickness, Duffey Lake (1465-1999AD) . . . 156
6.13 Smoothed (lowess-53yr) Varve Departures, Duffey (top) and Green (bottom) Lakes . 157
6.14 Reconstructed Temperature and Varve Thickness Variations . . . 160
6.15 Modeled Versus Observed Varve Thickness . . . 163
6.16 Lithostratigraphy and Bulk Physical Properties of Core 98-Duf(E) . . . 169
6.17 Lithostratigraphy and Bulk Physical Properties of Core 97-Duf(09) . . . 170
6.18 Lithostratigraphy and Bulk Physical Properties of Cores 00-Grn(AB) . . . 176
6.19 Couplet Thickness, Green Lake Core (00-Grn(A)) . . . 177
6.20 Lithostratigraphy and Bulk Physical Properties of Core 99-Jof(01) . . . 179
6.21 Depth-Age Models and Uncertainties . . . 184
6.22 Clastic Sedimentation Indices and Terrestrial Evidence for Glacial Advances in the North Pacific . . . 187
6.23 Comparison of Green (upper), Moose (middle), and Hector (lower) Lake Varve Chronologies . . . 189
6.24 Spectra of $EOF_{geochem}$and Varve Series . . . 196
6.25 Terrestrial Glacial Record (top) , Greyscale Value (DN) of Lower Joffre Lake Sediments (middle) and Oxygen Isotope Variations (bottom) of GRIP core . . . 198
6.26 $EOF_{geochem}$ and Clastic Indices . . . 200

7.1 Spectrum of observed climate variability in instrumental and proxy climate-proxy records . . . 204
7.2 Time-Space Scaling of observed and inferred climate-sediment transport linkages, Coast Mountains BC . . . 205

A.1 Stage-Discharge Relations 231
A.2 Electrical Noise in Cayoosh Stage Measurement 233
A.3 LOI TOC Relation 234

Dedication

This thesis is dedicated to my family and friends as they were by far the most important but often neglected components of this study.

Acknowledgements

This project was made possible by many individuals and organizations. First and foremost I would like to thank my thesis advisor, Dr. Olav Slaymaker for providing academic and financial support throughout the duration of the study. This work would have been severely at a loss without his critical eye and more importantly, his insight into process geomorphology and Quaternary studies. Members of my committee, Drs. John Clague and Kurt Grimm provided very thorough reviews of drafts and have been entirely supportive of this study from day one. This work has also benefitted from numerous discussions with Drs. Dan Moore and Marwan Hassan (UBC Geography) and Dr. Robert Gilbert (Queen's University). Thin section and varve counting techniques benefitted greatly from discussions with Drs. Scott Lamoureux and Robert Gilbert (Queen's University).

Financial support for this study was provided by grants from Forest Renewal British Columbia, the Natural Sciences and Engineering Research Council of Canada and the Geological Society of America.

Per-gratis laboratory analysis was provided by Dr. T. Jull (University of Arizona's NSF, AMS Laboratory) for AMS ^{14}C dating and by Dr. S. Sonoc (University of Toronto, Department of Chemical Engineering) for ^{137}Cs measurements. Other individuals who provided crucial advice and or help with laboratory analysis included M. Soon (UBC Earth and Ocean Sciences), R. Beukens (ISOTRACE),and R. Enkin (Geomatics Laboratory, Geological Survey of Canada).

Organizations and individuals paramount for providing important datasets included M. Demuth of the GSC (Glacial mass balance data), L. Campo of atmospheric environment service of Canada (streamflow records). Availability and free access to on-line climate and climate proxy data provided by the National Oceanic and Atmospheric Administration (NOAA) is gratefully acknowledged. This study especially acknowledges efforts by the International Tree Ring Data Bank (ITRDB) in their effort to make public a tremendously useful and important climate-proxy datasets. Northern hemispheric temperature data were provided by Dr. M. Mann (University of Virginia). Varve chronologies for Lillooet and Hector Lakes were made available by Drs. J. Desloges (University of Toronto) and E. Leonard (Colorado College) respectively. Dr. M. Journeay (GSC) made his electronic bedrock and surficial geology data available for this study.

I wish to especially thank those individuals which loaned research equipment for this study and include Dr. S. Calvert (UBC Earth and Ocean Sciences), Dr. M. Church (UBC Geography), Dr. R. Gilbert, and Dr. N. Smith (University of Calgary).

B. Schultz, (BC Parks) assisted in securing permission to conduct fieldwork within the Duffey, Birkenhead and Joffre Lake parks.

Technical thanks to Vincent Kujala (UBC Geography) for teaching me how to avoid the evil empire (Microsoft) with Linux and LaTeX, to Darren Ham and Erik Schiefer for helping with ARCINFO crises, to Phil Austin (UBC Geography) for introducing me to the power of Python, and to Chris Jeffrey (UBC Geography) for introducing a better and free statistical alternative, (R). Ivan Liu (UBC) provided technical help with the construction of laboratory and field equipment used in this study.

This study would not have been possible without amazing abilities of my friends and paid field assistants in the field. Food, beer and or trips to Skookumchuck hot springs provided payment in kind to those individuals who helped on a volunteer basis. They include E. Arnaud, S. Aycock, B.

Beierle, M. Evans, C. Gold, W. Hales, J. Hales, D. Hamm, A. Joseph, D. Mazzuchi, R.D. Moore, T. Newton, D. Pellerin, D. Ray, K. Ray, E. Schiefer, J. Stockwell, M. Szczodrak, S.Talwar, J. Tutchener, J. Venditti, P. Villard, R. Wilson, and R. White.

Finally, I would like to thank the love of my life Ms. Kimberley Ray. She was there when everyone else wasn't, period.

Chapter 1

Introduction

1.1 Statement of the Problem

Geomorphologists have long recognized the complex relation between climate and sediment transport. Langbein and Schumm (1958), for example, compared regional patterns of sediment yield data within the United States and found that the relation between sediment yield and effective precipitation was non-linear. Vegetative cover, they hypothesized, was the primary factor that introduced complexities into the underlying relation. Since Langbein and Schumm's study, the sample size, duration and spatial coverage of sediment yield studies have markedly increased (e.g. Walling and Webb, 1996), but the relation between climate and sediment yield remains especially obscure in mountain environments where spatial variability of sediment sources and sediment transport mechanisms is extreme.

This thesis investigates climatic controls of suspended sediment transport and yield for six, glacierized watersheds ($\approx$10-250 km^2) over time scales ranging from days to millennia in southwestern British Columbia. Contemporary monitoring of suspended sediment transport was undertaken to detail the major climatological controls of suspended sediment production and transport at event to seasonal time scales. This information is then used in conjunction with lake sediment deposits from outlet lake basins to develop proxy records of sediment yield over time scales which far exceed the length of sediment monitoring programs.

Watersheds in southwestern British Columbia were chosen for this study for a number of reasons: 1) their proximity to UBC (2-3 hours) provides an opportunity to investigate the processes of sediment transport over event to seasonal time scale; 2) an evaluation of the regional representativeness associated with specific hydrologic events which can be shown to be important for sediment production and transfers is possible given the relatively dense network of hydro-meteorological stations in the study area; 3) lake sedimentation rates within this region are commonly high (> 1mm yr^{-1}) so that event to annual-scale resolution of lake sedimentation is possible; and 4) previous work on lake sedimentation, sediment transport and sediment budgets in the southern Coast Mountains is available for purposes of comparison.

Glacierized watersheds were chosen for two complementary reasons. First, glaciers represent hydrologic elements that are particularly sensitive to changes in precipitation and temperature. Studies have shown that inter-annual changes in mass balance of glaciers within the North Pacific region can be explained by large-scale variations in winter precipitation patterns (e.g. Walters and Meier, 1989; Hodge et al., 1998; Bitz and Battisti, 1999). At inter-decadal to century time scales persistence in these anomalies likely influences rates of sub-glacial erosion leading to an indirect proxy of glacial fluctuations and millennium-scale changes in climate (e.g. Souch, 1994; Leonard, 1997).

Secondly, glacierized watersheds provide an opportunity to investigate the scaling (time and space) behavior associated with fine sediment transport because of the transitory storage of fine sediments within glacierized terrain. Sediment transport from proglacial settings is primarily governed by rates of sediment production and entrainment, and through secondary effects such as changes in sediment storage in the fluvial environment. By combining the temporal record of past glacial activity from the Canadian Cordillera (e.g. Ryder and Thomson, 1986; Desloges and Ryder,

1990; Luckman, 1993) with inter-annual to inter-decadal records of fine-sediment export, major changes in sedimentation rates attributed to variation in ice cover may be evaluated (e.g. Leonard, 1997). These data can then be used in conjunction with reconstructed time series of temperature and precipitation variability within the study area to control for climatic factors which may be responsible for sediment production and transport. It is the isolation of climatic and geomorphic information from sediment yield records that is the central objective of this study.

1.2 Framework for Analysis

Neglecting tectonic inputs, fine sediment discharge[1] records over some time scale (t) can be envisioned as the linear combination of climatic factors, namely those that control the entrainment and production of sediment:

$$Qs_{(t)} = C_{(t)} + G_{(t)} + \sigma_{(t)} \tag{1.1}$$

where $Qs_{(t)}$ is fine-grained sediment discharge ($kg\ s^{-1}$) at some time (t) and C is an index of climate which depends on the time scale in question. For example, at very short time scales (scale of monitoring), C may be a single variable (i.e. water discharge) which influences the proportion of driving stress (shear stress and turbulence) available for sediment entrainment and suspension. At longer (e.g. annual to century) time scales, C itself becomes a variate and depends to a large degree on those climatic parameters (e.g. temperature and or precipitation) which can influence changes in sediment production. G represents a geomorphic filter and σ represents a noise component which represents random and unpredictable fluctuations in sediment discharge (not climatic noise) which are stochastic and unpredictable. The underlying distribution from which σ is drawn is unknown but it will be assumed to be normally distributed (σ ; 0,1) with no autocorrelation (red noise). Although noise in most geophysical time series is characteristically autocorrelated, any memory in the system is assumed to arise from the imposed geomorphic filter.

A geomorphic filter is herein defined as an operator which, much like filters employed in signal processing, serves to alter the input signal in some specified manner. Such an effect is analogous to convolution in time series analysis (Press et al., 1986). Deconvolution (the aim of this research) is a trivial task in the frequency domain if the response function (G) is known but for most cases this in not obtainable and isolation of the filter from noise and signal in the time domain is required. Geomorphic filtering represents an abstraction of how earth-surface processes serve to dissipate climatic energy on fine sediment cascades within mountain environments. Geomorphic thresholds (e.g. Schumm, 1979), landscape sensitivity (e.g. Brunsden, 1990, 1996; Evans, 1997) and sediment relaxation effects (e.g. Allen, 1974) are the primary controls that dictate the overall response function associated with a given filter. An example of a threshold that is perceived to be important for this study is the relative size of a glacier or snow field; insufficient ice depth may fail to produce sediment because basal sliding does not occur. Sensitivity is used in this thesis to imply that that there has been minimal geomorphic filtering of the original climate forcing record (temperature or precipitation time series). High sensitivity implies a rapid, detectable response of the system to external forcing is similar to Brunsden and Thornes' (1979) original definition of landscape sensitivity.

[1] In the rest of the thesis the term 'fine sediment' is analogous with that inorganic component which is transported in stream systems as suspended sediment. It represents a combination of wash ($< 63\mu m$) and bed load, the boundary varying depending on the river and flow regime. An upper size boundary of 125 μm is implied for this work as most of the recovered sediments (both in the lakes and those collected during the suspended sediment monitoring of the streams) are below this size fraction.

Geomorphic filtering may occur at a number of sites within fine sediment cascades of glacierized watersheds and the amplitude may vary considerably. For example, effective (minimal) hillslope-channel coupling (e.g. Caine, 1989) may serve to amplify (mute) Qs. Filters which introduce a phase change between signal and response can be associated with sediment production systems prone to lag effects such as glaciers (e.g. Bahr et al., 1998) or they may represent time transgressive changes introduced during transport over time scales of hours (e.g. Williams, 1989) to millennia (e.g. Church et al., 1989). Finally, filter response (linear, exponential or power function) is controlled by characteristics of the transported sediment such as its caliber, transport distance, sediment reservoir type (e.g. moraine or floodplain) and re-vegetation rates.

1.3 Previous Work on the Climate-Sediment Discharge Relation in the Coast Mountains

The current research stems in part from observations of the climate-fine sediment response detailed in four studies completed within the Coast Mountains. Desloges (1987) investigated the response of several bio-geophysical systems (glaciers, proglacial lake deposits, tree-rings, floodplain sediments) to late-Holocene climate change. Those results indicate that although there was sufficient evidence for past climate variability the ability for any archive to record such change faithfully depended on sensitivity, record length, and accuracy. In general Desloges (1987) observed that climate was a poor predictor of biogeophysical response. It is unknown whether this was due to complacency effects (e.g. tree rings) or low sensitivity as defined in this thesis.

Souch (1990) documented the timing and magnitude of glacial advances for a medium-scale watershed within the Coast Mountains. Her study reconstructed past glacial activity by decomposing lacustrine sediments into glacial and non-glacial components utilizing a variety of laboratory techniques. From those data, she inferred that glaciers underwent expansion during three separate episodes within the region during the Holocene Epoch. Low sedimentation rates and limited dating control prevented an analysis of whether these phases of glacial activity were coeval across the Canadian Cordillera and the degree to which these phases can be further sub-divided.

Gilbert (1975) and Desloges and Gilbert (1994b) investigated the processes of underflow and general hydro-climatic controls associated with sediment delivery for Lillooet Lake. They suggested that despite the limited areal extent of contemporary glaciers (14 %), they represent the primary sediment source for fine sediments deposited in the lake basin. A large proportion of sediment is mobilized and delivered to the lake basin during high magnitude discharge events. This observation was based on correlation of 3-day maximum discharge (Lillooet River) for a given year to a composite series of varve thickness over the period common to both (1923-1988). Unfortunately, logistical difficulties (e.g. lake depth and no winter ice cover) prevented recovery of sediment records older than approximately 150 years.

Evans (1997) examined the geomorphic sensitivity of 4 small-scale alpine systems to Holocene climatic change. An assessment of this sensitivity was obtained by examining the between-lake variability associated with changes in lake-based sediment yields during the Holocene. The major conclusion which can be drawn from that study is that sensitivity of watershed response to imposed climatic variability depended to a large degree on effective coupling between hillslopes and stream networks. These observations agree with findings made in similar alpine environments (e.g. Caine, 1989).

These studies suggest that the ability to demonstrate a process-response relation between climate and sediment yield depends to a large degree upon the sensitivity of sediment production systems to imposed forcing and secondly, upon efficient routing of this fine sediment with minimal

possibility of transient storage. High resolution (annual) sediment yield proxies from glacierized watersheds are likely to clarify the climate-sediment yield relation.

1.4 Objectives

The research topic is evaluated by testing two premises:

Premise 1: Records of sediment yield from climatically-sensitive watersheds can be decomposed into endogenic and exogenic components.

In the glacially-conditioned landscape of British Columbia, paraglacial sedimentation represents one of the major endogenic controls of Holocene sediment yields. In contemporary time, land-use within many mountain watersheds has likewise altered the internal production and transfers of fine-sediment (for this thesis, land use will be defined as a form of endogenic forcing because those processes that redistribute and alter the fine-sediment cascade are operating within the watershed). In both examples, changes in fine sediment discharge arise through the alteration or emplacement of new sediment sources. Over time, sediment yields decline as these new sediment sources stabilize.

In addition to endo-deterministic components, annual sediment yield data may also be controlled by random fluctuations in fine-sediment discharge resulting from processes which are entirely stochastic. A small debris flow which terminates into a stream reach is an example of such a stochastic event and may influence sediment yields over time scales of weeks to years. Although the location of failure may be determined by localized conditions allowing failure, the timing of the mass movement event can not be predicted. Exogenic controls of sediment yield can be viewed as processes originating external to the watershed but they operate on internal processes responsible for both sediment production and entrainment (e.g. weathering rates and streamflow). In the Coast Mountains of British Columbia, three principal exogenic forcing mechanisms control sediment yield rates; climate, tectonic activity, and volcanism, though this thesis assumes that the latter two mechanisms have been more or less constant over the Holocene. Climate may enhance both sediment supply and rates of its entrainment while the last two mechanisms influence sediment supply. Exogenic forces can likewise be classified into deterministic and stochastic components. Winter precipitation may be related to patterns of sea surface temperature in the North Pacific, while extreme precipitation events that initiate debris flow activity may be entirely stochastic in nature.

Premise 2: A statistically significant proportion of the variance in sediment yields from climatically-sensitive mountain watersheds is attributed to measurable change in the mean climate state which influences sediment production, entrainment or its export. It is assumed that similarities between records of climate and sediment yield (i.e. similar trend, and periodic components) reflect forcing by the former on the latter. This thesis will not be concerned with the partitioning of climatic components into predictable and/or random events.

Although many studies have attempted to address premise 1, less work has been directed toward rigorously testing premise 2. In order to investigate premise 2, the explicit assumption that premise 1 is true must be made. This assumption is based on numerous regional and global studies which link the variance associated with high resolution sediment archives to the timing and magnitude of exogenic controls of sediment yield. The methods that will be utilized to test premise 2 rely on four main stages.

Stage 1: Construct sediment yield records and proxies from glacierized mountain watersheds

This stage entails selection of watersheds where sediment production and transport is largely controlled by variations in climate. The environment in which such a direct process-response linkage is perceived to exist are glacierized watersheds where relative relief is high and where the glacial,

fluvial and hillslope systems are directly coupled to downvalley lake systems. This study focuses explicitly on that portion of the total yield which is suspended in river flow and represents both washload and a smaller but undifferentiated fraction which is derived from river banks. The focus on suspended sediments provides a means of linking fluvial sediment transport with lacustrine deposition and is perceived to be that fraction which is most sensitive to inter-annual to inter-decadal climate variability.

It is hypothesized that catchment scale operates as a signal filter and therefore, is important in controlling the climatic sensitivity of sediment-yield data. Based on prior work (e.g. Evans, 1997) and similarity to other environments, it is believed that small scale watersheds (order $0.1 - 10km^2$) are not suitable for this project. Although a suite of geomorphic processes operating within small watersheds may be sensitive to changes in climate, decoupling within the sediment cascade (e.g. Caine, 1989) based on morphometric relations may fail to produce a yield signal which reflects variations in climate. In this situation, signal dampening has occurred and only the most notable departures in climate will produce a recognizable response. This situation would produce an output analogous to one where geomorphic thresholds are in operation (e.g. Schumm, 1979; Brunsden, 1996)but the lack of correspondence between forcing and response is due to faulty linkages in the fine-sediment cascade of such systems.

At the larger scale (order 1000-10,000 km^2) the original signal associated with climate change may undergo a different type of modification known as a phase change. This phase change is commonly a delay of the original signal which should scale to the volume of sediment produced (reworked) during the climatic event and its caliber. In addition, drainage basin scale can also dissipate the original signal of climate through storage effects as the perturbation wave (here it is envisioned as a pulse of sediment) moves downstream to the catchment outlet. Such effects have been demonstrated in fluvial environments impacted by upland mining (e.g. Gilbert, 1917) and those associated with volcanic eruptions (e.g. Simon, 1999). Medium-scale watersheds (order 10-1000 km^2) represent a compromise between signal loss associated with smaller watersheds and phase changes and or dissipation that can occur in larger systems. Because the objective of this project is to assess the proportion of variance in sediment yield data explained by changes in climate, medium-scale watersheds appear to represent the scale at which signal filtering is minimized.

Stage 2: Construct and assess variance in the sediment-yield records from sensitive watersheds.

This component of the research will partition the variance associated with the sediment yield data into trend, periodic, and noise components.

Stage 3: Construct and assess variance in hydro-climatic time series that influence the production and entrainment of fine sediment

In order to partition sediment yield data into exo- and endogenic components, it is necessary to document the trend and potential periodic components associated with hydro-climatic variability within the study area over the contemporary period (1880-present). Inter-annual variation in the behavior of these systems, in addition to larger-scale atmospheric and ocean variability which affects the study area will be compared to records of sediment transport to assess the dominant controls associated with sediment production and transport. The hydro-climatic series will be used to calibrate longer proxy records of climate such as tree ring chronologies from the North Pacific and North America.

Stage 4: Compare and remove the periodic components common to both the sediment yield and hydro-climatic time series from the sediment yield records

At this stage it will be possible to evaluate statistically the proportion of variance explained by climate variability within the sediment discharge records by removing climate 'signals' from the records. The residuals from the analysis will be evaluated and tested against white noise models in an attempt to understand any geomorphic filtering which may have occurred. In short, the proposed methodology should provide a means of evaluating the proportion of climatic and geomorphic variance within the fine sediment records. After controlling for this climatic variance, an appraisal of the degree of geomorphic filtering within the records can then be made.

1.4.1 Thesis Outline

Variations in sediment yield reflect earth-surface processes governing sediment production and availability, its entrainment and time-transgressive patterns of storage. All of these processes are highly dependent upon the time scale under consideration and so time is a logical way of organizing the results of the study. Chapter 2 provides an overview of North Pacific climate variability and how such variability may be expected to control the production and rates of sediment export from the watersheds. Sediment sources within the watersheds and basin morphometry are evaluated and the methodology and datasets used in this study are summarized in Chapter 3 and in Appendix A. Chapter 4 details observations made concerning sediment sources, seasonality of transport and spatial controls on sediment discharge within the study area over event to inter-annual time scales. Chapter 5 examines the fine sediment response of the watersheds to climate variability over longer time scales (inter-annual to decadal) while Chapter 6 investigates climate-sediment yield relations over century to millennial time scales. Conclusions from the study are provided in Chapter 7.

Chapter 2

Climatic Controls on Sediment Production and Yield

2.1 Introduction

This chapter reviews the current understanding of North Pacific hydro-climate variability with an aim of detailing the principal external control of sediment production and transport for the Coast Mountains of British Columbia. Geomorphic elements which could change the timing, amplitude or introduce noise into the relation between hydro-climatic forcing and sediment response are summarized. Finally, a conceptual model illustrates how variations in North Pacific climate might be expected to influence various components of a fine-sediment cascade.

2.2 North Pacific Climate Variability and Hydrologic Response

Understanding the evolution of large-scale patterns of atmospheric circulation over seasonal to inter-decadal time scales is important to this study because such factors are believed to control the frequency and magnitude of sediment-transporting events. As discussed shortly, such circulation anomalies can be shown to influence the spatial and temporal characteristics of temperature and precipitation variability within the North Pacific region and more locally, within southern British Columbia. At event to inter-annual time scale, changes in precipitation and temperature largely govern sediment production and entrainment by controlling the magnitude of nival melt, glacial runoff and the intensity of flooding. Thus, the literature review is limited to those hydro-climatic studies which have examined variations in glacial mass balance, snowmelt runoff, or extreme precipitation events and potential links to circulation anomalies. The large-scale structure associated with atmospheric anomalies common to the North Pacific allows conclusions made by others for regions outside of the Coast Mountains such as the Pacific Northwest and maritime Alaska to be pertinent to this study. There have been relatively few studies examining inter-annual variations in streamflow and potential linkages to North Pacific climate variability (though see Cayan et al., 1989; Cayan and Peterson, 1989; Cayan et al., 1998). Such variability may cause changes in the mean flow and or frequency of extreme runoff events.

Climate within the southern Coast Mountains can be broadly characterized as temperate-maritime with most of the annual precipitation occurring during the autumn and winter seasons (October-March). The westerlies and jet stream direct eastward mid-latitude cyclones and frontal systems originating in the Gulf of Alaska and areas to the south. Such systems deliver much of observed wintertime precipitation totals with snow falling at higher elevations. An easterly origin for this cyclonic activity and the north-south trending nature of the Pacific Ranges cause precipitation totals to decline from west to east (Cayan and Peterson, 1989). Springtime weather is characteristically unpredictable but improves during the summer months (June-September) as latitudinal differences in heating decrease and high pressure builds over the southern portion of British Columbia and the Pacific Ocean.

2.2.1 North Pacific Atmospheric Dynamics

A disproportionate number of studies has examined hydrologic response during the winter (October-March) hydrologic season. Annual runoff in the North Pacific is largely from snowmelt and streamflow variability has important implications ranging from fisheries management to hydro-electric power generation. Connections between the different elements within the climate system (e.g. ocean-atmosphere, circulation-precipitation anomalies) are strongest during the winter when latitudinal temperature gradients are highest allowing the development of large-scale, seasonally-persistent centers of low and high pressure.

Early studies (c.f. Redmond and Koch, 1991) investigating hydrologic variability (streamflow and precipitation totals) within the western United States and Pacific Northwest observed two dominant wintertime patterns: 1) a coherent variation (i.e. spatial homogeneity of similar inter-annual magnitude) and 2) an opposing pattern of winter precipitation in which the Pacific Northwest experiences positive (negative) anomalies in precipitation in years that the southwest was dry (wet). Later work showed that such a pattern extends as far north as western Canada and maritime portions of Alaska (Cayan and Peterson, 1989; Walters and Meier, 1989) but that wintertime streamflow variability of Alaska was similar in phase to variability in the southwest. This apparent spatial pattern of streamflow is partially controlled by the magnitude and location of dominant high and low pressure centers (500 hPa) during winter (DJF) in North America. This feature is known as the Pacific North American Pattern (PNA) and its strong (weak) phase is characterized by an intensified (reduced) Aleutian low and a heightened (weaker) ridge of high pressure over western North America (Wallace and Gutzler, 1981). The PNA controls the variability of winter precipitation over the Pacific North American Region largely by controlling the position and behavior of the jet stream and westerly flow aloft; during a strong (weak) phase of the PNA, zonal winds decrease (increase) and the jet stream is directed (diverted) across the Pacific Northwest. The lower-tropospheric manifestation of this pattern leads to lower (higher) sea surface pressures in the North Pacific when the PNA is in a weak (strong) phase (figure 2.1).

Global climate model data compiled by the National Center for Environmental Prediction (NCEP) were examined to understand how large scale ocean-atmospheric anomalies may affect temperature and precipitation patterns in the study area for the 1948-2000 period. The NCEP reanalysis project and data quality are discussed elsewhere (Kalnay and Coauthors, 1996). Composite anomalies for strong and weak phases of the PNA reveal the following: wintertime air temperatures are warmer than average with close to normal precipitation rates when the PNA is in a strong phase while much cooler air temperatures and slightly enhanced precipitation occur during the weak phase of the PNA (figure 2.1).

Such changes appear to influence the depth of snowcover and the intensity of snowmelt runoff in the North Pacific. In an analysis of snowcourse sites from western United States, Cayan (1996) found that anomalies in snow water equivalence (SWE) for April 1 (1930-1989) resembled the PNA pattern with positive (negative) snow loading anomalies in the Pacific Northwest when the PNA was in a weak (strong) phase. A similar observation was made for snowpack anomalies (1966-1992) in British Columbia (Moore and McKendry, 1996) but in this study, an areally-weighted index of surface pressure variations (Trenberth and Hurrell, 1994) over the North Pacific [30-65 °N and 140-160° W] was used[1].

[1]The correlation between the NP and the PNA is strong as they are based on pressure fields from similar regions

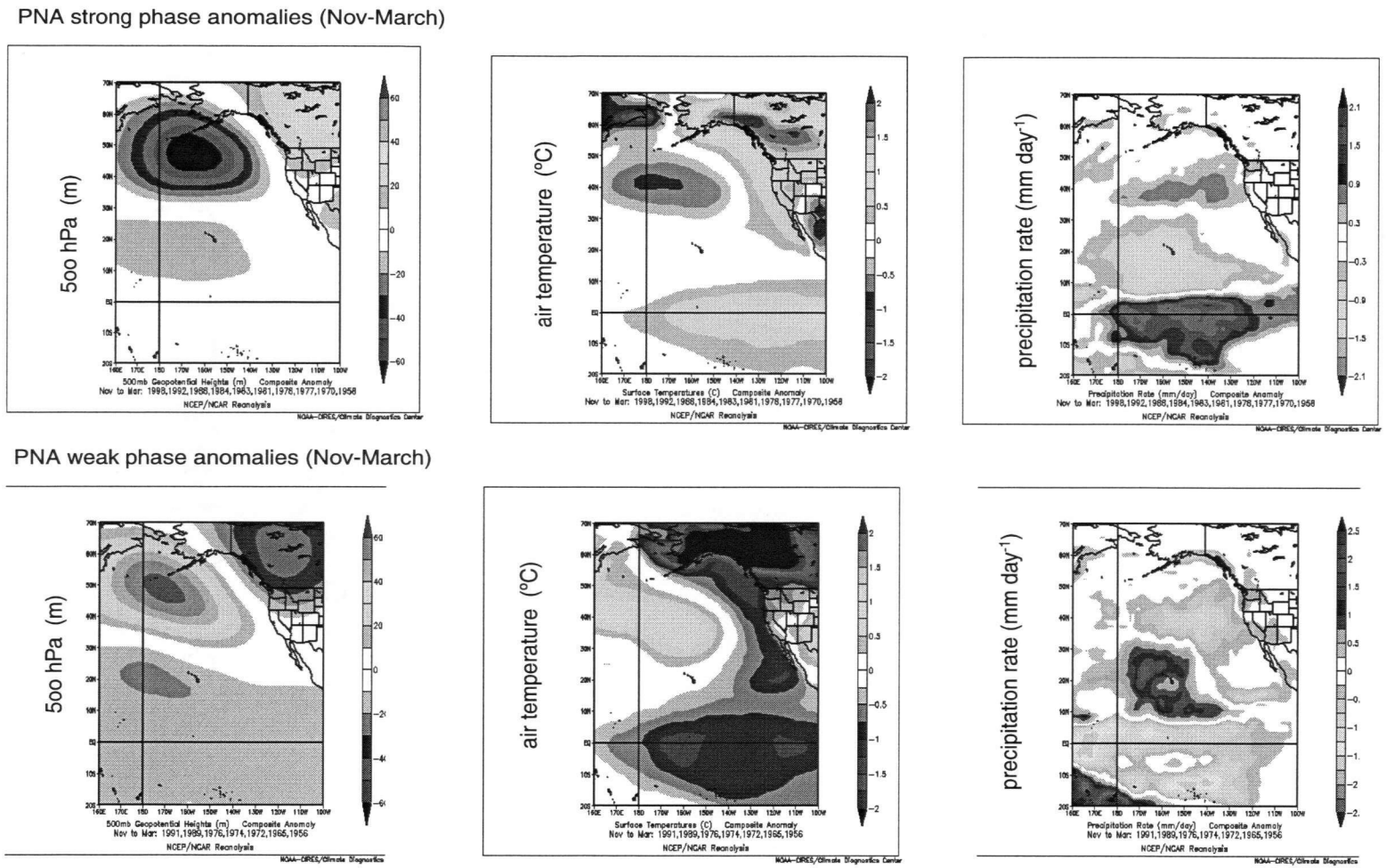

Figure 2.1: PNA
Composites showing strong (top panel) and weak (bottom panel) phases of the PNA during wintertime (Nov.-March). Climate anomalies generated from NCEP/NCAR reanalysis data (www.cdc.noaa.gov). Years of composite anomalies represent strong ($> 1.0\ \sigma$) and weak ($< 1.0\ \sigma$) phase of the PNA during period 1948-2000.

Moore and Mckendry (1996) noted a general north-south polarity between snowcourse sites in BC that was largely caused by precipitation variations and to a lesser degree by mean winter temperatures. In addition, they found that snowpacks in the southern portion of the province underwent a step change following 1976 to smaller than average SWE. Such a change has been observed in numerous hydro-climatic studies both within the North Pacific and within the Northern Hemisphere (e.g. Ebbesmeyer et al., 1991).

2.2.1.1 Ocean-Atmospheric Linkages for North Pacific Climate Variability (ENSO and the PDO)

An ocean-atmospheric coupled phenomenon (ENSO) is believed to be responsible for creating the PNA and/or a PNA-like pattern within North America but mechanisms for explaining such teleconnections between the tropics and extra-tropics are poorly understood. Nevertheless, statistically significant correlation between indices of ENSO (e.g. the SOI) and hydrologic time series (e.g. winter precipitation , glacial mass balance, streamflow, April 1 SWE anomalies) from the North Pacific (e.g. Cayan and Peterson, 1989; Walters and Meier, 1989; Moore and McKendry, 1996) suggests that such linkages exist. Shabbar et al. (1996; 1997) examined the way in which ENSO influences precipitation and temperature fields (1910-1990AD) over Canada and found a negative (positive) relation between the SOI and wintertime temperature (precipitation) anomalies for western Canada. They showed that atmospheric circulation during warm (cold) phases of ENSO resembled the strong (weak) PNA pattern. Similar to inferences made by Walters and Meier (1989), Shabbar et al. (1996) observed that much of the reason for the low wintertime precipitation totals in western Canada is caused by the bifurcation of the jet stream and diversion of storm tracks around a ridge of high pressure over western Canada and the Pacific Northwest. The strength of such relations increased when only strong phases of ENSO (e.g. $1.0 < SOI > 1.0$) were considered and suggests that teleconnections between the North Pacific and the tropics depend to a large degree on the strength of ENSO (figure 2.2).

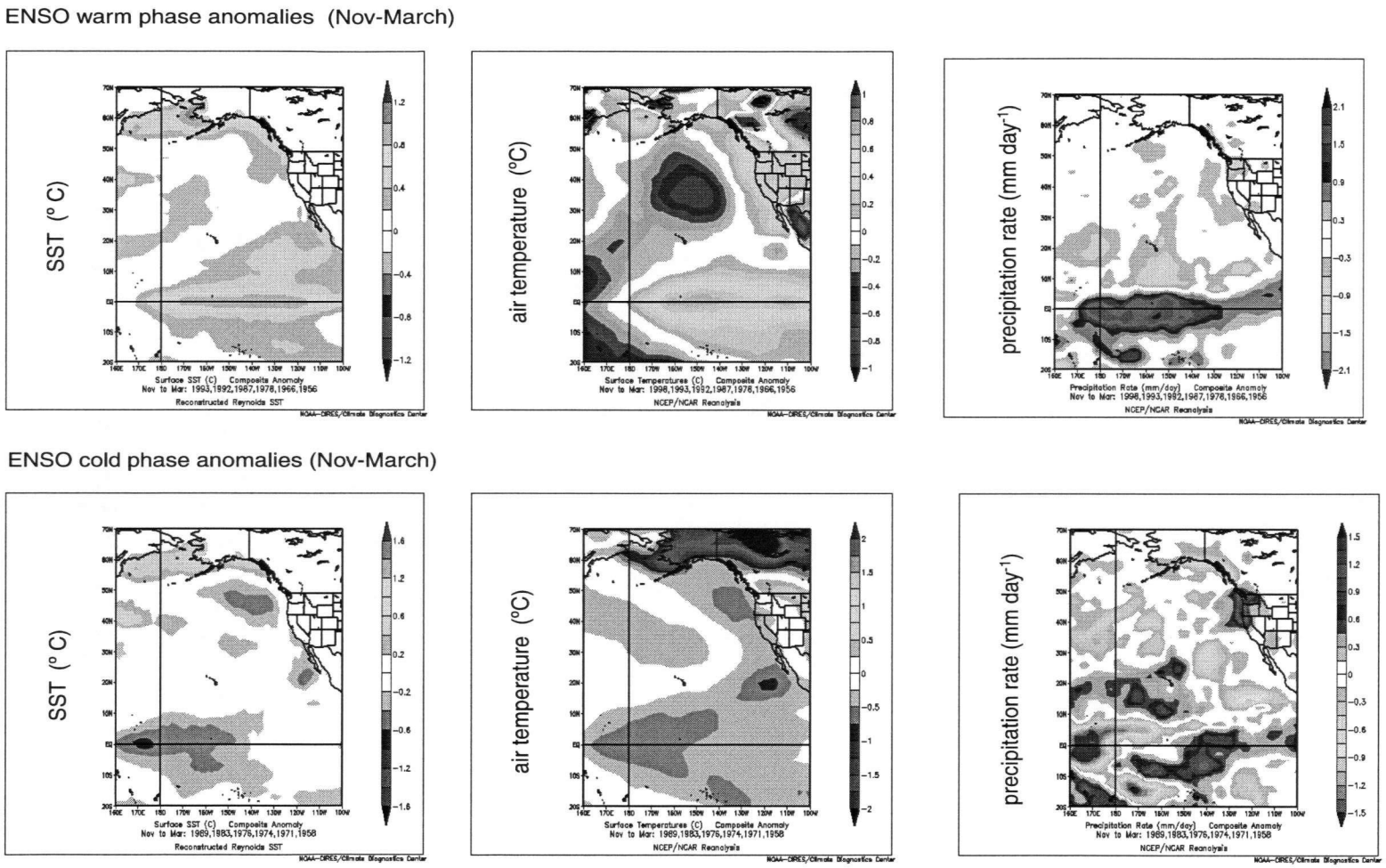

Figure 2.2: ENSO
As in figure 2.1 but for warm (top panel) and cold (bottom) phases of ENSO. Years represent winter season (Nov.-March) composites when -1.0 < SOI > 1.0.

Recent research investigating climate variability in the North Pacific and elsewhere (e.g. Zhang et al., 1997; Mantua et al., 1997) has suggested that it is sea surface temperature (SST) patterns in the extra-tropics (northern Pacific) rather than the tropics which appear to be the principal controls of large scale atmospheric features in the North Pacific region. Zhang et al. (1997) found that the PNA was positively correlated to an index of global SST (with anomalies from ENSO removed) called the globalized residual index (GR). The results are similar to those found by Mantua et al., (1997) but that study concentrated on North Pacific SST variability (1900-1992) in the north Pacific (north of 20° latitude). The expansion coefficient of the leading principal component from this analysis is known as the Pacific Decadal Oscillation (PDO). A similar aggregation of positive ($> 1.0\sigma$) and negative ($< 1.0\sigma$) wintertime anomalies of NCEP data (figure 2.3) indicates that temperature and precipitation fields in western North American and southern British Columbia are influenced by such SST variability. This SST variability shows much visual (and statistical) correspondence to atmospheric circulation (c.f. figure 2.1). In particular there is a southward (northward) displacement of the Aleutian low during years when the PDO is in a negative (positive) phase.

In addition to highlighting the apparent polarity in the climate states of the Pacific Northwest and the Gulf of Alaska, Mantua et al. (1997) demonstrated that this polarity and abrupt shifts (regime shifts) in the mean climate state for the North Pacific and western United States corresponded to the time varying spatial structure of North Pacific SST patterns. These regime shifts and linkages to the PDO could be detected in diverse indicators of climate from the North Pacific ranging from observations of fish catches to variations in stream flow. Significance of the most recent regime shift (1976-1977) had been previously recognized by others (e.g. Ebbesmeyer et al., 1991) but does not appear to be the consequence of human-induced climate change; similar step-like changes are recognized in high resolution, climate-proxy records from the North Pacific prior to 1850AD (e.g. Minobe, 1997; Gedalof and Smith, 2001).

There is ongoing debate surrounding the mechanisms and possible interactions of tropical and extra-tropical SST variability (e.g. Gershunoz and Barnett, 1998; Barnett et al., 1999; Hunt and Tsonis, 2000). Though it is not the purpose of this review to discuss the origins of tropical and extra-tropical SST variability, possible interaction between the PDO and ENSO may amplify circulation anomalies during particular years. For example, years of similar SOI values may experience considerably different precipitation or temperature anomalies. Indeed, Gershunov and Barnett (1998) show that such anomalies are amplified when ENSO and the PDO are in similar phase (i.e. negative SOI and warm North Pacific).

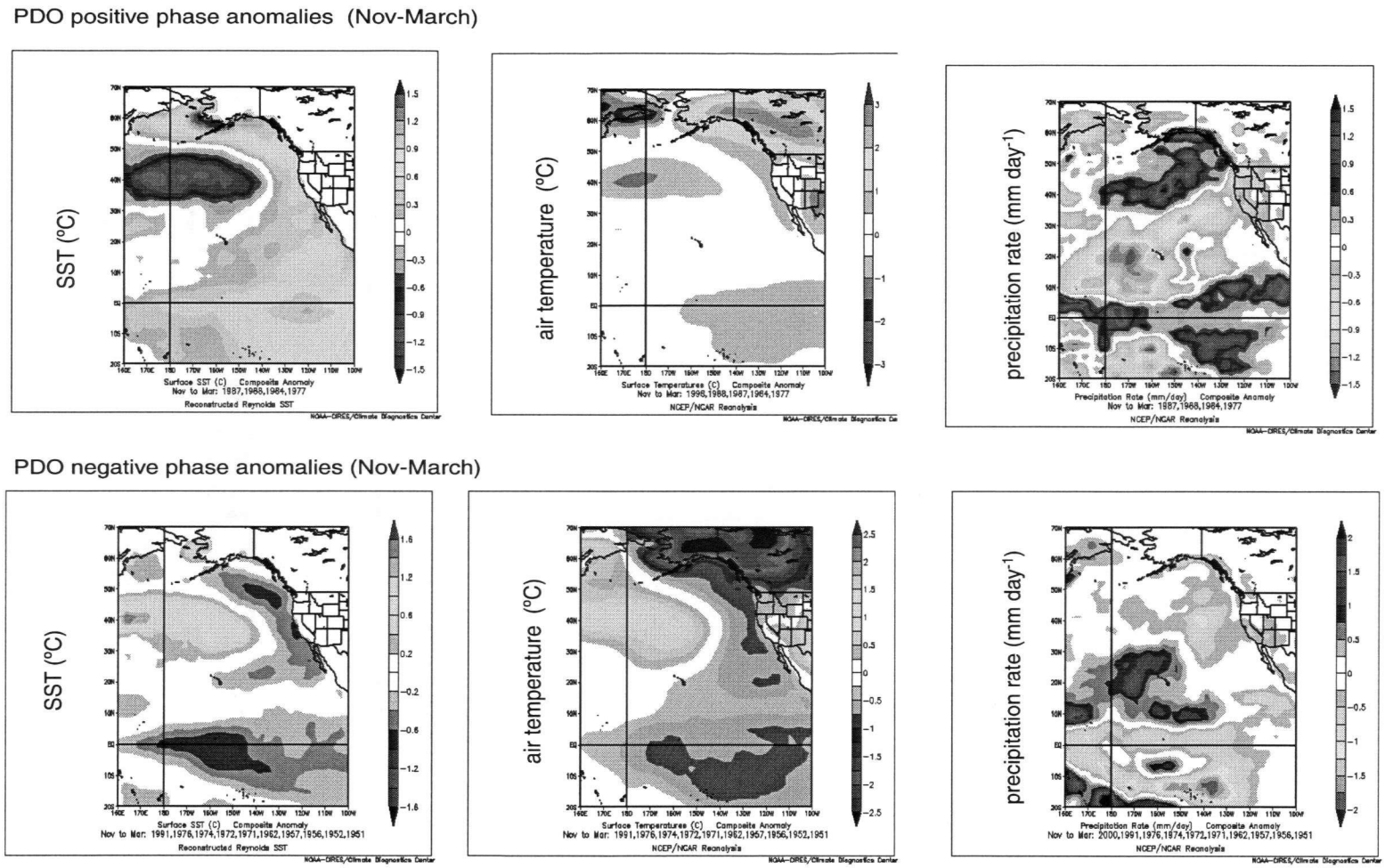

Figure 2.3: PDO Anomalies
Corresponding climate states during positive (top panel) and negative (bottom panel) years of the PDO. Composite represent years when -1.0 < PDO > 1.0.

To summarize, North Pacific wintertime climate variability is conditioned to a large degree by both tropical and extra-tropical SST anomalies. Atmospheric variability (e.g. circulation patterns) may occur over time scales considerably longer (inter-annual to decadal) than that which commonly occurs in the atmosphere because they are partly forced by SST variations which change much more slowly. Despite the apparent ocean-climate linkage demonstrated in these studies, a large component of stochasticity remains in the climate system. Neglecting such effects, the ocean-atmospheric indices (e.g. ENSO, PDO and PNA) will be used in this study to characterize inter-annual to decadal climate variability in the study area. How such large-scale, ocean-atmospheric variability is likely to control the production and transport of fine sediments within the watersheds is considered below.

2.2.2 Climate Variability Influencing Glacial Mass Balance

Variations in glacial mass balance are reviewed under wintertime variability because for (maritime) glaciers in the study area, net mass balance is most strongly controlled by variations in winter precipitation (e.g. Hodge et al., 1998; Bitz and Battisti, 1999). For glaciers in more continental settings within the Coast Mountains, variations in summer temperature and circulation patterns can be as important as inter-annual variations in wintertime conditions (Bitz and Battisti, 1999) but few studies have linked summer mass balance variability to atmospheric circulation patterns. Because large-scale atmospheric circulation anomalies appear to influence inter-annual variations in glacial mass balance, there is reason to expect a coincident response of glaciers within large spatial domains.

Despite the large number of glaciers within the Coast Mountains there have been surprisingly few studies linking climate variability with changes in mass balance (net, winter or summer) and that work has focused primarily on Place and Sentinel glaciers (e.g. Yarnal, 1984; Moore and Demuth, 2001). Other mass balance studies from the North Pacific region will be discussed because they are controlled by atmospheric anomalies which affect large spatial scales. Such studies are useful for illuminating the most likely response of glaciers to climate forcing within the study area.

Glaciological studies began early in the Coast Mountains (e.g. Taylor, 1936) and by the 1950's, linkages between climate and glacial response were being tested (Mathews, 1951). Mathews' work in Garibaldi Provincial Park (1951) compared contemporary and former evidence of glacial fluctuations to climatic parameters such as summer air temperature and winter precipitation totals and the results indicated that glaciers within Garibaldi Provincial Park reached their maximum downvalley positions during the Holocene between the 18th and 19th centuries. Rapid recession occurred during 1920-1940 and based on climatological data, it was believed to be the result of an anomalous warm and dry period. Similar rates of glacial recession during the early part of the century have been reported for eastern ranges in the Canadian Cordillera (e.g. Luckman and Osborn, 1979).

Detailed mass balance studies in the Canadian Cordillera began in 1965 with the start of the International Hydrologic Decade. A west-east transect through the southern Canadian Cordillera was chosen to show how the climate-glacial linkage changes from maritime (Sentinel, Helm), to transitional (Place) and to continental (Peyto) environments. Yarnal (1984) found that mass balance changes at Sentinel and Peyto glaciers (1965-1974) were explained by recurring synoptic features during the accumulation and ablation periods gleaned from classification of charts of geopotential surface (500 hPa). Both glaciers experience net increases (decreases) in mass under conditions of cyclonic (anti-cyclonic) activity during winter and synoptic conditions which favored cloudy, cool (sunny, warm) conditions. Similar synoptic-mass balance linkages were obtained by Walters and Meier (1989) who analyzed a longer and more complete data set for other North Pacific glaciers

(South Cascade, Sentinel, Place, Peyto, Wolverine, Gulkana). This study suggested that wintertime balance variability could be largely explained by changes in atmospheric circulation similar to the PNA. Such upper level anomalies were also believed to explain the out of phase relation between southern and northern glaciers. Similar to western US and Pacific Northwest studies examining wintertime streamflow response, Walters and Meier (1989) hinted at an apparent ENSO-PNA linkage but they concluded it was not strong.

Two recent studies (Hodge et al., 1998; Bitz and Battisti, 1999) have likewise demonstrated that mass balance of maritime glaciers in the North Pacific is largely controlled by large-scale atmospheric circulation anomalies during the winter (Nov-March) season. These studies show that net mass balance of the maritime glaciers is most strongly controlled by wintertime variability in precipitation. Consequently, enhanced (reduced) wintertime precipitation occurs the PNA is in a negative (positive) phase and appears to be controlled by both ENSO and the PDO (c.f. figures 2.1, 2.2, 2.3). Similar to Yarnal (1984), Bitz et al. (1999) found that mass balance (winter and net) of North Pacific glaciers is controlled by storminess and that the largest fraction of variance in North Pacific glacial mass balance time series (winter and net) can be explained by changes in North Pacific SST (i.e. the PDO).

2.3 Floods and Flood Generating Mechanisms

Floods are usually the result of climatological processes that deliver exceptional quantities of precipitation to a watershed or conditions which favor rapid melting of snowpacks. Unlike atmospheric anomalies that influence wintertime precipitation, synoptic features associated with flood events are usually more spatially restricted and generalizations for the North Pacific region become more tenuous. Nevertheless, their ability to mobilize significant quantities of sediment within the Coast Mountains is well known (e.g. Hickin, 1989; Church et al., 1989; Desloges and Gilbert, 1994b). What is much less known, however, are the large scale atmospheric conditions responsible for such floods. Only recently have there been systematic attempts to understand broad-scale atmospheric controls of such extreme events within the North Pacific (Higgins et al., 2000; Cayan et al., 1999). Floods have been shown to be particularly important for controlling sediment transport in Coast Mountain watersheds (Church et al., 1989).

Most floods within the Coast Mountains occur during fall, winter, and spring months and result from cyclogenesis. Floods in the study area can be classified as rain fall (R), rain-on-snow (ROS), or snowmelt (S) in origin. Though ROS floods are particularly important in the Pacific Northwest and in low (< 500m) watersheds, such events are probably less significant hydrologically in the higher elevation watersheds. Melone (1985) found that R events accounted for approximately 66% of flood events at 76 streamflow stations in coastal BC while S or ROS events constituted about 8% of the stations. The remaining stations (25%) had mixed flood populations. Floods from coastal stations have significantly higher unit discharges ($m^3 s^{-1} km^{-2}$) than interior watersheds and is similar to a more recent study of flood magnitude for British Columbia (Church, 1997). For the storms which caused autumn and winter flooding, Melone (1985) found that they shared common meteorological conditions including: 1) deep low pressure centers from which frontal activity developed and; 2) strong southwesterly winds aloft. These upper level winds provide moist, sub-tropical air which causes freezing levels to rise and are known informally as "Pineapple Express" storms because moisture sources for such systems originate near the Hawaiian Islands.

Not all cyclones (even intense ones) cause flooding within the Coast Mountains and flood occurrence commonly depends on unique atmospheric and watershed conditions. For example, a ROS event will do little to elevate streamflow if the snowpack is not isothermal or if such a snowcover is thin and discontinuous. Thus, unlike wintertime precipitation and temperature anomalies, a

"climatology" associated with flooding events in the Coast Mountains is unlikely and characterization of flood frequencies may be largely limited to descriptions of their underlying probability distributions (i.e. a stochastic process).

Cayan et al. (1999) find that ENSO increases (decreases) the probability of observing extreme events (> 90 percentile between October-April) in precipitation and streamflow (> 90 percentile between January-July) during its cold (warm) phase in the Pacific Northwest. Streamflow from these basins is primarily snowmelt driven, but because precipitation totals were not calculated during the snowmelt period, flood-generating mechanisms (e.g. ROS or S) remain unknown. Such events most likely result from larger than average snowpack depth given the observed ENSO-snowpack relation for the region (e.g. Cayan, 1996; Moore and McKendry, 1996).

Higgins et al., (2000) describe a lead-lag relation between extreme precipitation events in the western United States (coastal California and the Pacific Northwest) and ENSO which suggests that extreme precipitation events may be a precursor to the warm phase of ENSO. Through correlation and analysis of gridded daily precipitation and atmospheric datasets, they demonstrate that the largest proportion (after accounting for individual probabilities) of extreme 3-day precipitation events occur during neutral (with respect to ENSO) winters (Nov-March) preceding the development of ENSO's warm phase. Moisture sources for the events originate from deep convection in the tropics which become advected northward and across the west coast. However, unlike those studies which find a di-pole pattern of precipitation anomalies between the south and north, their results indicate that all portions of the coast may experience extreme precipitation events which depend to a large degree on specific configuration of the jet stream. Testing such a mechanism for extreme precipitation and or discharge events during the fall season (SON) for British Columbia is required because Higgins et al., 2000 only examined precipitation events during the winter months (Nov-March), and fall-season storms are well known for their ability to entrain sediment within the Coast Mountains (Gilbert, 1975; Desloges and Gilbert, 1994b).

2.4 Summary

North Pacific climate and hydrologic response is controlled to a large degree by large-scale wintertime circulation anomalies (e.g. PNA) whereby deficits (surplus) of wintertime precipitation in the North Pacific contrast rather remarkably with net surplus (deficits) observed in areas to the north and south. Such atmospheric patterns are influenced by both tropical and extra-tropical SST-atmosphere interactions with forcing which can occur in both directions (i.e. atmosphere forcing ocean and vice versa). ENSO and the PDO have differing frequencies at which they operate and interactions between these states are likely to amplify circulation anomalies for a given year.

The hypothesized fine-sediment response according to this atmospheric variability would be as follows: Nival transfers (sediment entrainment) would be expected to increase during cold (positive) phases of ENSO (PDO) due largely to heavier snowpacks and/or the potential for an increased probability of ROS or S flooding. Increased sediment transfers during glacial melt could conceivably occur during hydrologic years of shallow snowpacks because less snowcover on a glacier will allow more available energy (short wave and sensible) to be used for melting glacial ice and establishing meltwater conduits between the glaciers' surface and sole (developed in more detail in section 2.5). Sediment transfers during autumn will be most likely limited to those precipitation events which generate high discharge events and those in which warm air temperatures prevent the accumulation of snow at higher elevations.

2.5 Sediment Production, Storage and Transfers: The fine Sediment Cascade

It is not the purpose of this section to review exhaustively what is known about the dynamics and controls of sediment production and transfers within mountainous regions but rather to highlight those processes which are perceived to play an important role in sediment production and or its transfers. Major fine sediment production sites include glaciers and steep hillslopes coupled to the fluvial system while storage reservoirs include glacial forefields and moraines and floodplain environments.

2.5.1 Glaciers

Glaciers represent an important mechanism of sediment production within many mountain systems and although there remains considerable controversy concerning the overall ranking of glacial erosion as a denudation process (Harbor and Warburton, 1993; Hicks et al., 1990; Hallet et al., 1996), the effectiveness of Quaternary glaciation on Coast Mountain landform evolution is rarely questioned. Over time scales of centuries, several studies have indicated that variations in the intensity of sediment transfers within watersheds is in part modulated by percent glacial cover (Souch, 1994; Leonard, 1997; Leonard and Reasoner, 1999). Though a relation between sediment yield and percent glacier cover appears to exist for the global dataset, much of the scatter could potentially be reduced by relating yield to variables which more faithfully represent erosion intensity such as ice flux (Hallet et al., 1996). Glaciers are likewise important for sediment transfers as they elevate discharge within watersheds during seasons usually characterized by low precipitation.

2.5.2 Sub-glacial Erosion

Glacial erosion in temperate environments (i.e. when ice is at the pressure melting point) is controlled primarily by abrasion and quarrying effects but effectiveness also requires evacuation of sediment away from the bed of a glacier. Abrasion and quarrying rates are controlled mainly by variability in down-valley (u_x) ice velocity (Boulton, 1979; Hallet, 1979) and concentration of debris in subglacial ice. U_x scales to ice flux (m^3s^{-1}) and commonly to annual precipitation in maritime settings. Glacial motion (warm-based ice) occurs by both creep and basal sliding, but it is the sliding component which is most effective for the production of fine-grained sediment. Erosion by ice sliding over lithified substrate has been confirmed both by theoretical and empirical data (Drewry, 1986). Though few data exist, it appears that there is a direct relation between down-valley ice velocity and sub-glacial erosion rates (e.g. Humphrey and Raymond, 1994). The fine-grained ($> 63\mu m$) fraction of subglacial till is believed to result from abrasion processes during basal sliding (e.g. Haldorsen, 1981) rather than those associated with rock fracture.

Glaciological studies indicate a wide range of basal sliding rates (both between and within individual glaciers) but averaged together for non-surging glaciers, this motion accounts for approximately one-half of total ice movement (Patterson, 1994). Initial studies suggested that regelation was the primary mechanism of basal movement but it is now realized that sub-glacial water pressure plays an important role in controlling glacial sliding (Patterson, 1994). Water pressure is highest during the ablation season due to effective routing of firn and snow meltwater to the base of temperate glacier (e.g. Iken et al., 1983) and can greatly affect u_x (Iken and Bindshadler, 1986; Rothlisberger and Lang, 1987).

Like u_x, meltwater produced during the ablation season plays an important role in sediment cascades within glacierized terrain by providing a means to evacuate and expose lithified substrate which can subsequently be eroded. High sediment concentrations of meltwater can arise from melt-

ing of sediment-laden ice in the ablation zone or routing of surface melt across and through subglacial sediments. Those studies which have monitored suspended sediment transport in proglacial settings (e.g. Richards, 1984; Gurnell, 1987, 1995; Bogen, 1996; Richards, 2001) have found significant hysteresis effects in discharge-suspended sediment relations for individual ablation seasons and between specific years and this time dependence is likely influenced by changes in water flow patterns beneath a glacier. A large fraction of sediment entrained subglacially probably remains in suspension as washload.

2.5.3 Glacial Response Times

The response time of a glacier is the duration for a glacier to adjust to some specified change in mass balance and is equal to the filling time (analogous to residence time of water in a lake). This parameter has important implications in the current study because it is one type of geomorphic filter that may cause notable phase lags between changes in climate and fine-sediment discharge (see Chapter 1). Although the original derivation (Nye, 1963) suggested that response scaled to glacial length divided by down-glacial ice velocity, response time t can also be approximated by (Jhannesson et al., 1989a,b):

$$t \propto \frac{h}{-\dot{b}} \tag{2.1}$$

h represents the average thickness (m) and $-\dot{b}$ is the net mass balance rate (myr^{-1}) evaluated at the terminus. Although it is often assumed that larger glaciers respond more slowly to mass balance perturbations (i.e. they are thicker and or longer), scaling analysis (Bahr et al., 1998) suggests that this notion may be incorrect . They suggest that for larger valley glaciers, $-\dot{b}$ increases at a faster rate than h because enhanced ice velocity allows the terminus to extend to lower elevations. Despite this argument, glaciers with dimensions that are relevant to this study (order 1-10 km^2) should exhibit dimensional adjustments to mass-balance perturbations within 20-50 years.

Empirical data on terminus variations from the European Alps (see summary in Patterson, 1994), the Cascades (e.g. Spicer, 1989; Harper, 1993) and the Canadian Cordillera (e.g. Luckman and Osborn, 1979) seem to contradict equation 2.1 and may suggest deficits in our understanding on how temperate glaciers respond to mass balance perturbations. For this study, however, changes in glacial length are arguably the most important for the production of fine-grained sediment since changes in length likely alter u_x and rates of meltwater production. Such length scale changes often produce terrestrial deposits which can also be used to document prior glacial extent and may represent important sediment sources (e.g. Richards, 1984; Holmlund et al., 1996).

To summarize, the primary factors which control fine-grained sediment production from glaciers are the total area of sub-glacial ice which is in contact with lithified substrates, u_x, and available meltwater which can influence u_x but is also important for sediment entrainment. Thus, as a first order approximation, sediment production is facilitated by high proportions of the catchment which are glacierized and the intensity of glacial runoff for a year. Over inter-annual to decadal time scales, low rates of primary (subglacial erosion) and secondary (subglacial reworking) production of fine grained sediment would be expected during years of positive mass balance as the magnitude of glacial runoff would be lower. Persistence (decadal to century) in these departures would be expected to increase the proportion of the catchment which is ice covered and elevate the total basal area over which the glacial may flow. Such conditions would be expected to increase sediment yields. Both effects when combined with intermittent transport of sediments in proglacial sites of transitory sediment storage would be expected to introduce considerable scatter into the relation between climate change and sediment export from such environments.

2.5.4 Rapid Mass Movement

Controlling factors of hillslope instability in the Coast Mountains include high local relief (often exceeding 1000 m) and the occurrence of meteorological events required for failure. Lithology, morphometry, seismicity and glacial recession play secondary, but important roles in rapid mass movement rates. Processes believed to be important for influencing fine sediment discharge in this environment include snow avalanching, debris flow activity and landsliding. These types of hillslope processes vary in their degree of influence; their deposits or failure sites can be active sediment sources or they can play secondary roles by blocking stream channels.

2.5.4.1 Debris Flows, Torrents and Landsliding

Pleistocene and contemporary glacial deposits such as moraines are an important sediment source of fine grained sediments which are commonly modified by debris flows, landsliding and slope-wash processes. Though landslides can be an important source of fine-grained sediment especially if failed material reaches stream systems (e.g. Bovis and Jakob, 2000), these deposits quickly stabilize and do not appear to be as tightly coupled to stream systems as debris torrents or debris flows. Exceptions occur and especially when such deposits are large ($> 500{,}000\ m^3$), comprised of volcanic lithologies, and deposited in steep stream reaches where significant incision can occur (Slaymaker, 1993). Debris-flows are hypothesized to play a more important role in the fine-sediment cascades of this study because such events are directly coupled to stream systems. Jordan and Slaymaker (1991) found that debris flows (small and large scale) represented an important sediment source for a detailed sediment budget of the Lillooet River basin. A later study, however, suggested that the proportion of fine-grained ($< 63\ \mu m$) sediments originating from such events contributed only marginally to the yield from the basin (Desloges and Gilbert, 1994b) .

Meteorological events required for hillslope instability within the Coast Mountains are precipitation events of high magnitude and or intensity (e.g. Church and Miles, 1987; Jakob, 1996) but failure can also occur during synoptic conditions favorable for high rates of snowmelt (Bovis and Jakob, 2000). Important controls on debris flow activity also relate to antecedent conditions ranging from climatic effects (e.g. pore water pressure build up due to series of precipitation events) to limitations imposed by rates of physical weathering (e.g. Jakob, 1996). The climatic conditions responsible for debris-flow activity, much like exceptional flooding, are likely to be spatially discontinuous and highly unpredictable so that a down-valley, climate-debris flow signal within sediment yield records is unlikely. Despite the unpredictable nature of such events, detachment from colluvial and glacial deposits is likely to contribute a sizable fraction of sediments to stream systems of the study. Detachment from glacial deposits is likely to be considerable though the intensity of detachment would be expected to be a function of particle size characteristics of the deposits. Neglecting lithologic differences, subglacially-deposited (lodgement) till is comprised of a sizable fraction of silts and clays (Haldorsen, 1981) whereas particle size distributions for sediments in moraines reveal a much smaller fine-sediment component (Small, 1987).

2.5.4.2 Snow Avalanches

Little published work has been conducted on the effects of snow avalanches on controlling sediment production and transfers within the Coast Mountains. Research within the Canadian Rockies (e.g. Gardner, 1970; Luckman, 1975, 1977) has demonstrated that erosion and subsequent transport of debris by snow avalanches is most effective when the water content of the snow is high and when failure occurs down to the snow-ground interface. Particle size data from avalanched snow (e.g. Ackroyd, 1986) indicates a lack of fines (<2 mm) limiting their importance as a fine sediment source.

Though recent work (Smith et al., 1994) has examined the erosional potential associated with the impact pressures of snow avalanches, such effects are so localized that they too are assumed to have a negligible influence on basin-scale fine sediment production and transfers. Such activity can be expected to complicate the sedimentation records in lakes when it is proximal to the lake system.

2.5.5 Intermediate Sediment Storage: the Fluvial System

Floodplain, Pleistocene valley fills, and glacial forefields represent significant sources of sediment which contribute substantially to sediment transfers during times of lateral or vertical channel change. The flux of fine sediment from these reservoirs depends on particle size characteristics and their degree of coupling to the active stream system (Jordan and Slaymaker, 1991). Depletion of such deposits relates to volume of material stored divided by the net gain of transport (i.e. $Q_{s(in)} - Q_{s(out)}¿0.0$) and time scale over which such deposits affect downvalley sediment discharge can range from years to millennia. In river reaches where streams have incised into these sedimentary stores, contribution from undercutting and or lateral instability along scarp edges is locally important. It is important to note that in contrast to the apparent model of sediment yield for British Columbia (e.g. Church and Ryder, 1972; Church and Slaymaker, 1989; Church et al., 1989) data for the Squamish river basin (Hickin, 1989) and its tributaries (Brooks, 1994) indicates that the paraglacial[2] phase within these watersheds was short-lived and contemporary sediment transfers are dominated by contemporary glacial sources. Erosion from such fluvial sites in the Coast Mountains appears to be primarily during floods (e.g. Desloges, 1987; Ham and Church, 2000) and it may be expected that time-transgressive changes in flood frequency will control the release of fine sediments from such reservoirs. Desloges (1987) noted that although channel changes (e.g. width variability) on the Bella Coola River corresponded to periods of increased and variable discharge (1957-1976), most of channel change occurred during exceptional flow events.

2.6 Climate and Fine Sediment Cascade Linkages: The Conceptual Model

The previous discussion concluded that temperature and precipitation fields over the study area are directly modulated by large-scale variations in ocean-atmospheric variability over inter-annual to decadal time scales. Given the sensitivity of the fine sediment cascade to changes in the intensity of sediment production and entrainment caused by such climatological process, it is hypothesized that a significant fraction of this climatic variance is recoverable from proxies (monitoring data and sedimentary deposits) of sediment yield. The sensitivity is believed to arise from direct coupling between major sites of sediment production (contemporary glaciers and forefield areas) and the caliber of transported sediments. Geomorphic filtering is likely to arise from intermediate storage of this sediment in the fluvial system, a time-transgressive change in Q_s due to lags introduced by glacial response times or changes in sediment availability due to variation in ice cover. The linkages between climate and fine sediment yield within glacierized watersheds of the Coast Mountains (figure 2.4) can be viewed as a process-response system (e.g. Slaymaker, 1991) and the dominant controls on sediment discharge are summarized below.

Wintertime variations in temperature and precipitation can be expected to influence directly the intensity of fine sediment discharge to outlet lake basins but the overall significance with respect to sediment transport depends to a large degree on synoptic-scale variations during runoff. For

[2]Paraglacial effects are a function of scale. In the context of Pleistocene Glaciation, adjustments to the sediment cascade reflect reworking of till on upland surfaces and sediments stored in the fluvial network. With respect to contemporary glaciation, sediment sources may reflect those which are sub-glacial (i.e. primary or secondary sediment production) and/or sediment mobilized from recently deglaciated (forefield) areas.

example, high Q_s rates during the nival period may be expected following winters of large snowpacks but only if snowpacks are depleted quickly (e.g. during prolonged warm weather conditions or during rain on snow events). Such transfers would be expected to reflect sediments originating from fluvial sources.

Shallow snowcover (warmer temperatures or reduced snowfall) would be expected to decrease Q_s during the snowmelt-runoff season but increase the intensity of Q_s during the glacial season. The caliber of that fraction of sediment produced by glacial sliding during the ablation season would limit storage in the fluvial system and direct export as washload is expected. Warm air temperatures during summer would allow the lakes to become thermally stratified, facilitating the transport of glacially-derived sediments throughout the lake basin.

Infrequent, intense rainstorms could entrain significant quantities of sediment though their effectiveness will depend on the proportion of the watershed which is snow covered during the runoff event (Caine, 1995) and thermal characteristics during the inflow event (e.g. Gilbert, 1973, 1975). Though such precipitation events may cause rapid mass movements, fine-grained sediments originating from hillslope instability are likely to be related to large-scale climate variability in a complex fashion because initiation of failure is governed by other factors which may or may not be linked to climate. The proportion of sediments reaching the lake basins which originate from glacial forefield and moraine sources will depend on how quickly these exposed surfaces stabilize. This period can be expected to depend on the rates of vegetative re-growth, the intensity of precipitation events responsible for detachment and or mass movement and grain size characteristics of the sediment entering the fluvial network.

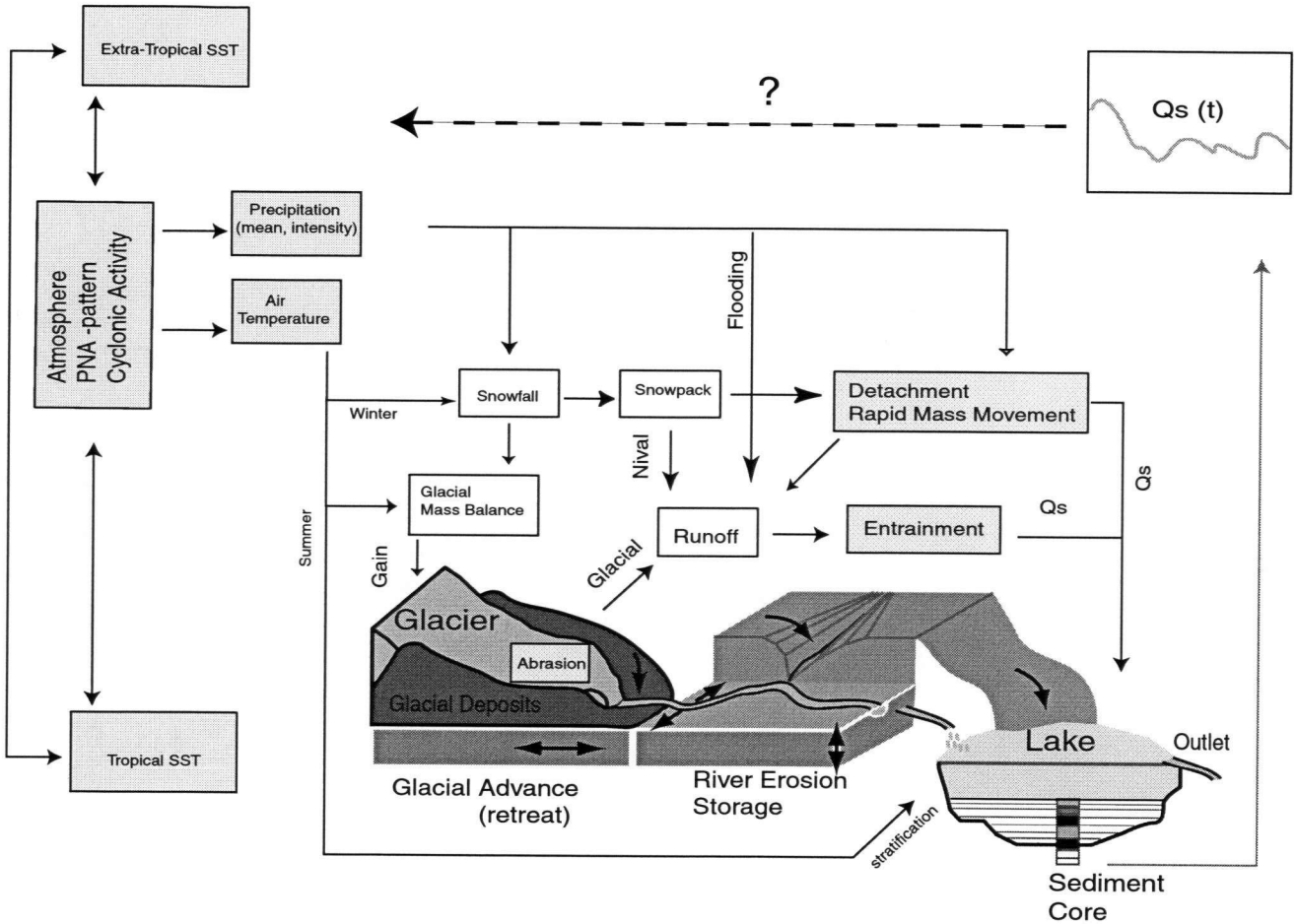

Figure 2.4: Proposed Climate-Fine Sediment Cascade Linkages
Detailed process-response relations (e.g. mechanisms of glacial runoff) have been omitted for clarity. Examining the linkage between fine sediment records (lake deposits) and climatic variance and the degree of filtering (upper dashed arrow) is the purpose of the present study.

2.7 Conclusions

This chapter has summarized the way in which climate variability is hypothesized to influence the production and transport of fine-grained sediments for Coast Mountains watersheds. Wintertime atmospheric circulation patterns and the way in which they control precipitation totals (e.g. Yarnal, 1984) and hydrologic response (Desloges, 1987) in the North Pacific region have been examined in previous studies. Recent work indicates that the origins of such circulation anomalies during wintertime are controlled by large-scale SST variability in the tropics and extra-tropics. The potential for the transmission of such climatic information through the fine sediment cascade is likely to be large given the overall sensitivity of the fine-sediment cascade to variations in glacial sediment production and runoff during the nival and glacial meltwater seasons. Geomorphic filtering of this climatic information may be caused by such factors as glacial response times, fluvial sediment storage or complexities introduced by sediment transfers during extreme runoff events. Despite such filtering, the linkages between large-scale atmospheric variability and sediment production and transfers within the study area suggest that inter-annual to inter-decadal climate variability within the southern Coast Mountains is likely preserved within short to long-term records of sediment yield.

Chapter 3

Study Area, Data Collection, Acquisition and Analysis

3.1 Introduction

The construction and analysis of several types of contemporary and climate-proxy data are required in order to examine the climatic controls of fine sediment discharge over inter-annual to millennial time scales. Morphometric characteristics of the watersheds, sediment source identification and its routing through the watersheds are discussed as they relate primarily to the intensity and magnitude of potential filtering imposed by the watersheds. Description of data type, including a wider discussion of methodological procedures, can be found in the appendix. Datasets collected and analyzed in this thesis correspond to three general time scales: 1) Seasonal to inter-annual (i.e. observational); 2) inter-annual to decadal (i.e. hydro-climatic time series encompassing the contemporary period (1900AD to present) and; 3) century to millennial (climate proxy records preserved within tree rings and ice core records).

3.2 Study Area Watershed Selection

The southern Coast Mountains are comprised of NNW-SSE trending mountain ranges where morphology has been controlled by high uplift rates during the last 10 myr, multiple glaciation during the Quaternary (Ryder, 1981; Muhs et al., 1986), and generally resistant bedrock assemblages (Monger and Journeay, 1994). Similar to other mountain ranges which lie leeward of dominant weather systems, large precipitation and temperature gradients exist across the southern Coast Mountains and are largely expressed in a west-east rise in contemporary glaciation levels from 1200 m along the coast to 2450 m inland (Evans, 1990).

Six lake basins were selected to provide a regional perspective of contemporary and paleo response of fine-sediment cascades to climate forcing. Criteria for selection of these six in order of importance were: a) the presence of contemporary ice cover; b) the size of the watersheds; c) access to lake basins for core recovery; and d) the availability of hydro-meteorological data from within or in proximity to the watersheds. Collected data types, duration and hydrologic datasets collected by other agencies (Environment Canada) are summarized in table 3.1.

Two of the watersheds were chosen late in the project (Glacier and Cheakamus Lake Basins) in order to understand the regional pattern of 20th century sediment transport. Contemporary (1880-2000AD) sediment records were recovered from these lake basins to assess the regional representativeness of sedimentation trends from Duffey and Green Lake basins. A more complete understanding of recent changes in sediment transport is important because it is during this time that most climatological data exist and provide a more rigorous approach of assessing the fraction of variance attributable to hydro-climate variability. Together, the six watersheds encompass an area of roughly 900 km^2 and are centered around the Lillooet River Basin (figure 3.1).

Basin	*Data Collected*[a]	*Duration*	*Other Monitoring Data*[b]
Duffey	q, c, lm, sv	May 1997-Oct. 2001	–
Birkenhead	q, c, lm, sm	May 1997-Oct. 2001	–
Cheakamus	sv	–	q (1924-1948; 1982-1999)[c]
Glacier	sv	–	–
Green	sv	May 1999-Oct. 2001	q (1922-1948; 1993-1999)[d]
Joffre	sm	–	–

Table 3.1: monitoring table

a. (q) Discharge records;(c) climate data [air temperature, precipitation]; (lm) lake monitoring; (sm) sediment record [massive]; (sv) sediment record [varved].

b. Collected by Water Survey of Canada

c. Station re-located 5 km downstream from outlet of lake

d. Lake Outlet (1922-1948); Fitzsimmons Creek (1993-1999)

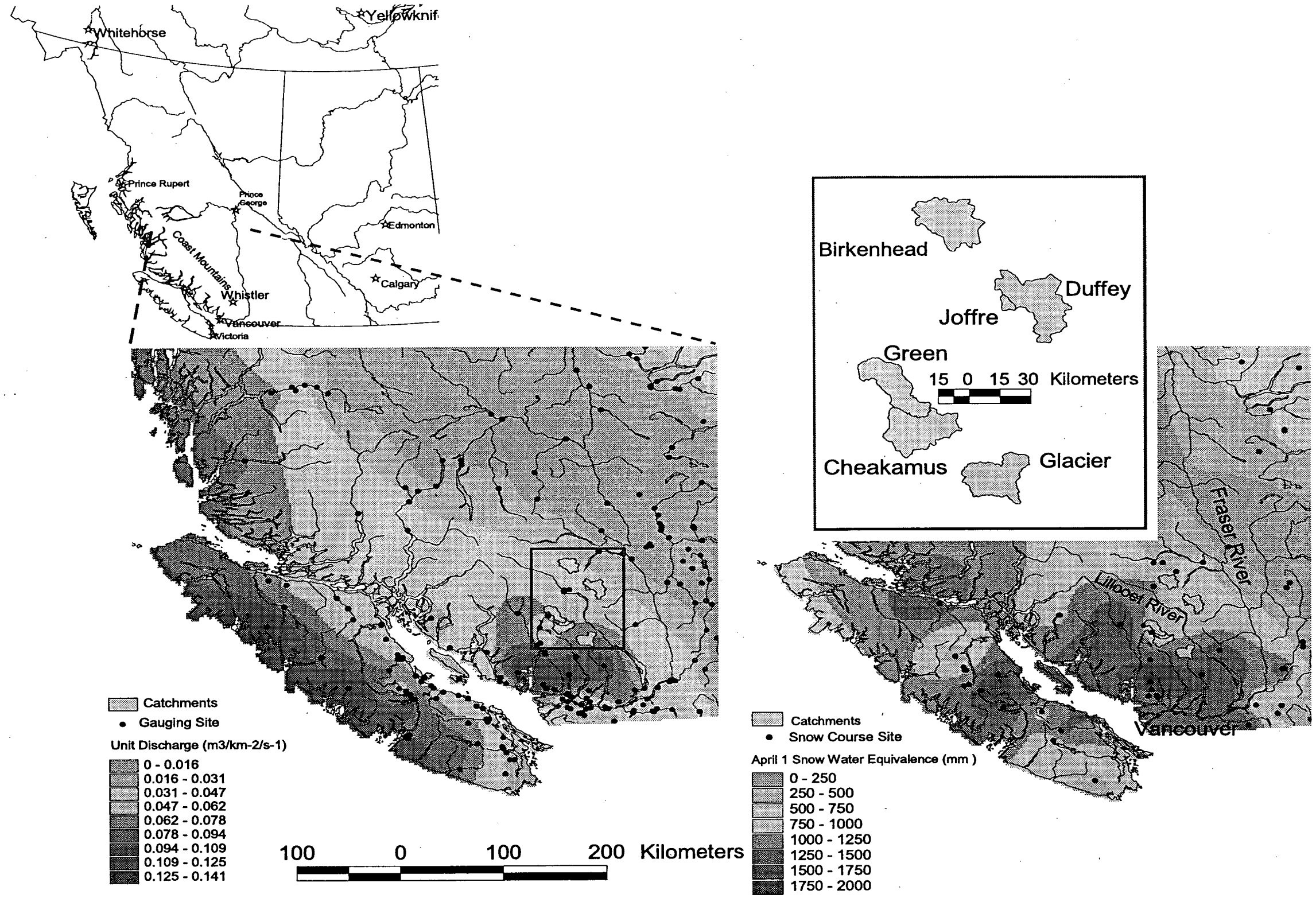

Figure 3.1: Study area location

Location of study area basins (upper right panel) in southwest British Columbia and average, yearly specific flow (1950-1996) and April 1 snow water equivalence from snowcourse sites. Streamflow (unit discharge) and April 1 snow water equivalence were calculated using total number of available years rather than common period of record providing a more detailed spatial assessment of mean annual runoff.

Those watersheds southwest of Lillooet River (Green, Cheakamus, Glacier) lie windward to moist maritime air masses while the basins of Duffey, Birkenhead and Lower Joffre are situated in environments which can be expected to reflect more continental conditions. Annual runoff is reduced by half across the study area caused by heavier snowpacks for those basins to the southwest of Lillooet River (figure 3.1). Annual precipitation ranges from 1700 $mmyr^{-1}$ near the southwest corner of the study area and declines to approximately 700 $mmyr^{-1}$ near Birkenhead Lake.

Similar to mean annual runoff and winter precipitation, flood generating mechanisms differ significantly across the study area. Those basins closer to the coast are more susceptible to rainfall generated floods while runoff from basins situated to the lee of the Coast Divide are predominantly snowmelt driven (figure 3.2). The importance and stability of this hydro-climatic divide is also reflected in ecosystem zonation: Coastal western hemlock comprises the dominant tree species southwest of Lillooet River while more continental species such as Englemann Spruce are located on the northeast side of the Lillooet River Basin.

3.3 Sediment Source Identification and Morphometric Controls of Sediment Production

To understand differences in the relative intensities of sediment production within the watersheds, identification of major sediment sources was made through air photo analysis and site visitation. Morphometric controls influencing both production or the relative rates of transfers were examined and analyzed primarily through the use of planimetric data and digital elevation models constructed for the watersheds. Such results and a description of the basins are summarized below.

3.3.0.1 Duffey

The Duffey Lake basin (250 km^2) is a catchment whose morphometry has been heavily influenced by Quaternary glaciation. Lying immediately east of the Coast Mountains divide, the catchment is lightly glacierized (1.7 percent) with 40 percent of the catchment above treeline (Figure 3.3). The majority of the watershed (85 percent) is drained by two main stream systems, Cayoosh and Van Horlick Creeks where discharge has been continuously recorded since 1997. The lake (3.8 km^2) is a deep (90m depth) elongated basin which is oriented parallel to the main valley axis of Cayoosh Creek. Cayoosh and Van Horlick Creeks flow parallel to the main valley axis for approximately 1km before entering the lake basin. Small tributaries enter the lake from the north and south side and steep slopes on the north side of lake basin are additional sediment source areas for the lake basin. Several colluvial cones and avalanche plunge pools (c.f. Corner, 1980) terminate directly into the lake.

The behavior of Cayoosh and Van Horlick creeks during the Holocene may be more a function of contrasting morphometric controls rather than variations in climate (Brooks, 1994). Van Horlick is a tortuous sandbed river draining 118 km^2 of sub-alpine to alpine terrain while Cayoosh Creek is largely a gravel bed river draining a slightly smaller, less elongated 98 km^2 watershed. Based on isolated terraces and late glacial (?) outwash fans from some of the larger tributaries, Cayoosh Creek has incised 10-30 m into valley floor deposits for its final 1-3 km before flowing parallel to Van Horlick Creek and creating the contemporary deltaic environment of Duffey Lake. The age and general deglacial history of this area is poorly documented but a minimum-limiting estimate is provided by a single radiocarbon date (9520±70 ^{14}C yr BP; TO-7580; see table 6.7) approximately 30m above the contemporary floodplain of Cayoosh Creek. The surface of the exposure appears to be the remnant of a former river terrace. The wood was located in a 30cm unit of organic sediment underlain by 50cm of gravel which overlies at least 3m of grey, poorly sorted diamict interpreted

to be lodgement till. The organic unit is overlain by 2m of alternating peat and minerogenic beds. The clastic sediments are interpreted to be distal fines derived from debris-flow activity from a large gully complex above the exposure. This interpretation is based on recent deposition of minerogenic matter on top of the sequence following a debris flow which occurred in late summer 1998. These Pleistocene deposits are believed to be important fine-grained sediment sources for Cayoosh Creek.

In contrast, episodes of large-scale channel aggradation, channel abandonment and or modification by snow avalanches, appear to have characterized the history of Van Horlick Creek during recent (Neoglacial to present) time. Active glaciers within the eastern and western branches of

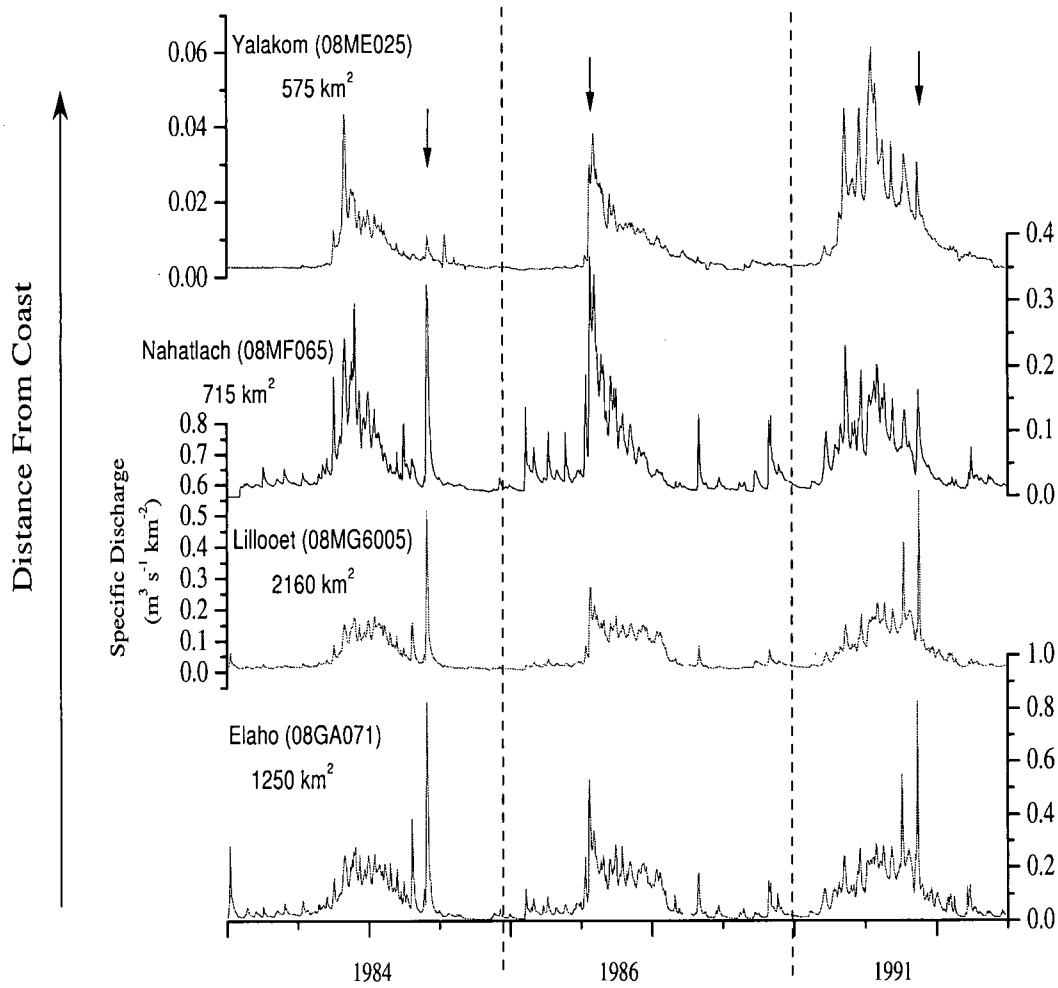

Figure 3.2: Variability in Flood Generating Mechanisms Across the Study Area
Differences in flood type (arrows) and intensity are evident across the Coast Mountains for three recent floods (2 autumn and 1 snowmelt).

Van Horlick appear to be the dominant sediment sources for the fine-grained sand currently being transported by the river. Some of this sediment has formed a large sandur-like slug of sediment 2-3km downvalley from an active glacier in the east fork of Van Horlick Creek. In general, there is a surprising lack of landforms within the valley floor which could be attributed to deglaciation within the catchment or changes in base level of the creek. Bedrock near the contemporary channel can be found in several reaches and appears to be a natural control of baselevel. Upstream of such outcroppings, channel gradients are low, sinuosity increases and there appears to be a general pattern of channel aggradation. In two reaches, radiocarbon dates (2230±60 ^{14}C yr BP and 180±45 ^{14}C yr BP, table 6.7) obtained from vegetation overlain by weakly stratified sediments in close proximity (20 m) to the contemporary channel provide limited but important chronologic control for gross-scale changes in channel aggradation during the Neoglacial period. The radiocarbon ages and their association with lake sedimentation are discussed in greater detail in Chapter 6.

Forestry activity and general land use within the Duffey Lake watershed began in 1970 when a logging road connecting the towns of Pemberton and Lillooet was constructed. This road was initially constructed for timber extraction but jurisdiction and maintenance was transferred to the Ministry of Highways in the late 1970s. In 1990 the Duffey Lake road was re-surfaced and paved thereby minimizing one potential source of fine sediments to the lake basin. Forest harvesting was moderate in the early 1970s within the catchment and was concentrated along the valley floors of the Cayoosh and Van Horlick Stream systems. Approximately 8.6 percent of the catchment has been logged. During the late 1970's and 1980's timber harvesting moved further up the mainstem reaches of the Van Horlick and Cayoosh Creeks. As of 1994, total road length in the Duffey catchment totaled 121.7 km or a density of 0.48 $km\ km^{-2}$. The Duffey Lake Road makes up 17 percent of this total while logging companies have built and continue to maintain the other 83 percent. Although timber harvesting has taken place since 1994 those areas were not on the available forestry-cover map sheets.

3.3.0.2 Birkenhead Lake Basin

Birkenhead Lake drains 222km^2 of sub-alpine to alpine terrain northeast of Lillooet River. Water and sediment enter the lake primarily from two tributaries, Sockeye and Phelix Creek. Phelix Creek drains rugged terrain which is largely ice-free except for 1.5km^2 Birken Glacier (figure 3.4). Phelix Creek was chosen for establishment of water and sediment monitoring because access is easier and a suitable gauging site for Sockeye Creek could not be found. Birken Glacier represents an important sediment source for Birkenhead Lake as few intervening lakes exist between the glacier and the lake basin.

Sockeye Creek is steep and drains lightly glacierized terrain. The creek has built a large alluvial fan where it enters Birkenhead Lake though it likely was constructed soon after retreat of Pleistocene ice (Church and Ryder, 1972). Unlike Phelix Creek, numerous natural sediment traps (lake basins and wetlands) exist between contemporary ice and Birkenhead Lake. Bathymetric data indicate that the lake consists of two deeper basins apparently created by the progradation of the Sockeye Creek alluvial fan. Smaller alluvial/colluvial cones have developed under large gully/ couloir complexes on the east side of the lake and may introduce localized inputs of clastic material to the lake basin. Land use effects (recreation, logging, home construction and agriculture) imposed by development and or forestry are likely to be minimal given the low (1-2 percent) proportion of the watershed where such activity has taken place.

3.3.0.3 Joffre Lake Basin

Lower Joffre lake drains 14.5 km^2 of sub-alpine to alpine terrain and lies immediately west of the Duffey Lake basin (figure 3.3). The catchment is the most heavily glacierized (25 percent) of the study but two intervening lakes between contemporary ice and the lower-most lake likely trap the majority of sediment produced by contemporary ice cover. The catchment was chosen to provide a lower resolution albeit longer record with which to examine the fine sediment response of the basin to low frequency climate variability. Few point sources of clastic sediments are recognizable outside of those glacial deposits immediately downvalley of contemporary ice masses. Unweathered, lateral moraines terminate into the uppermost lake basin. The lake is small (1.04 ha), shallow (d_{max} =12m) and characterized by simple bathymetry with a single inflow and outlet channel. No land use has

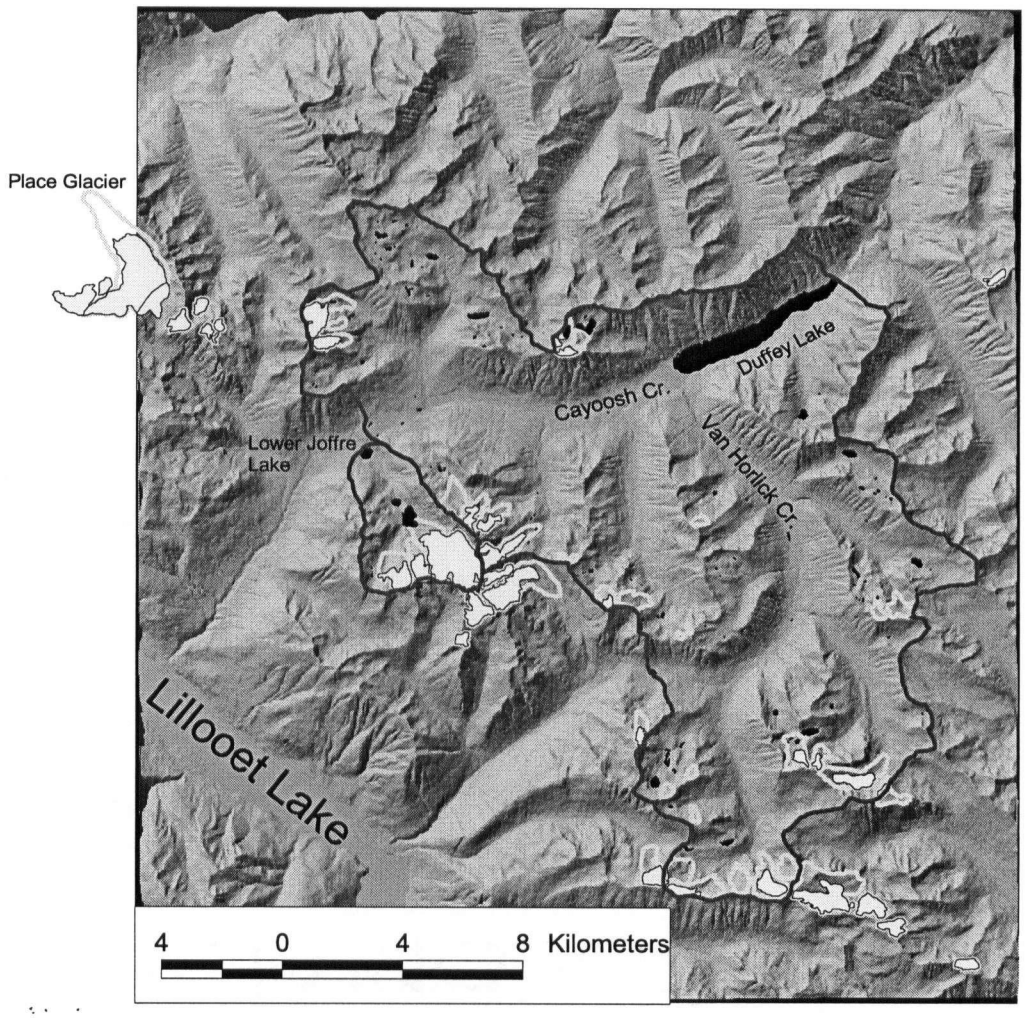

Figure 3.3: DEMs of Duffey and Joffre Basins
Solid (light blue) and outlined (light green) polygons show ice extent today and during the Little Ice Age. Larger outlined polygons (red) denote watershed boundaries.

occurred in the catchment during the contemporary period.

3.3.0.4 Green Lake

Green Lake receives sediment and water from approximately 180 km^2 but the watershed boundary is poorly defined in the main valley (figure 3.5). Three creeks enter the lake basin but only one (Fitzsimmons Creek) appears to deliver the majority of sediment to the lake basin. This statement is based on sequential air photos which reveal the lack of turbid river plumes entering the lake from these tributaries and a notable lack of delta development associated with these other tributaries. At no time during the study were the waters entering the lake basin from these streams turbid or discolored. Fitzsimmons Creek is a 19.5 km long mountain creek draining rugged, glacierized (9 %) terrain. The creek is steep (average channel gradient $=0.072m\ m^{-1}$) and has incised into

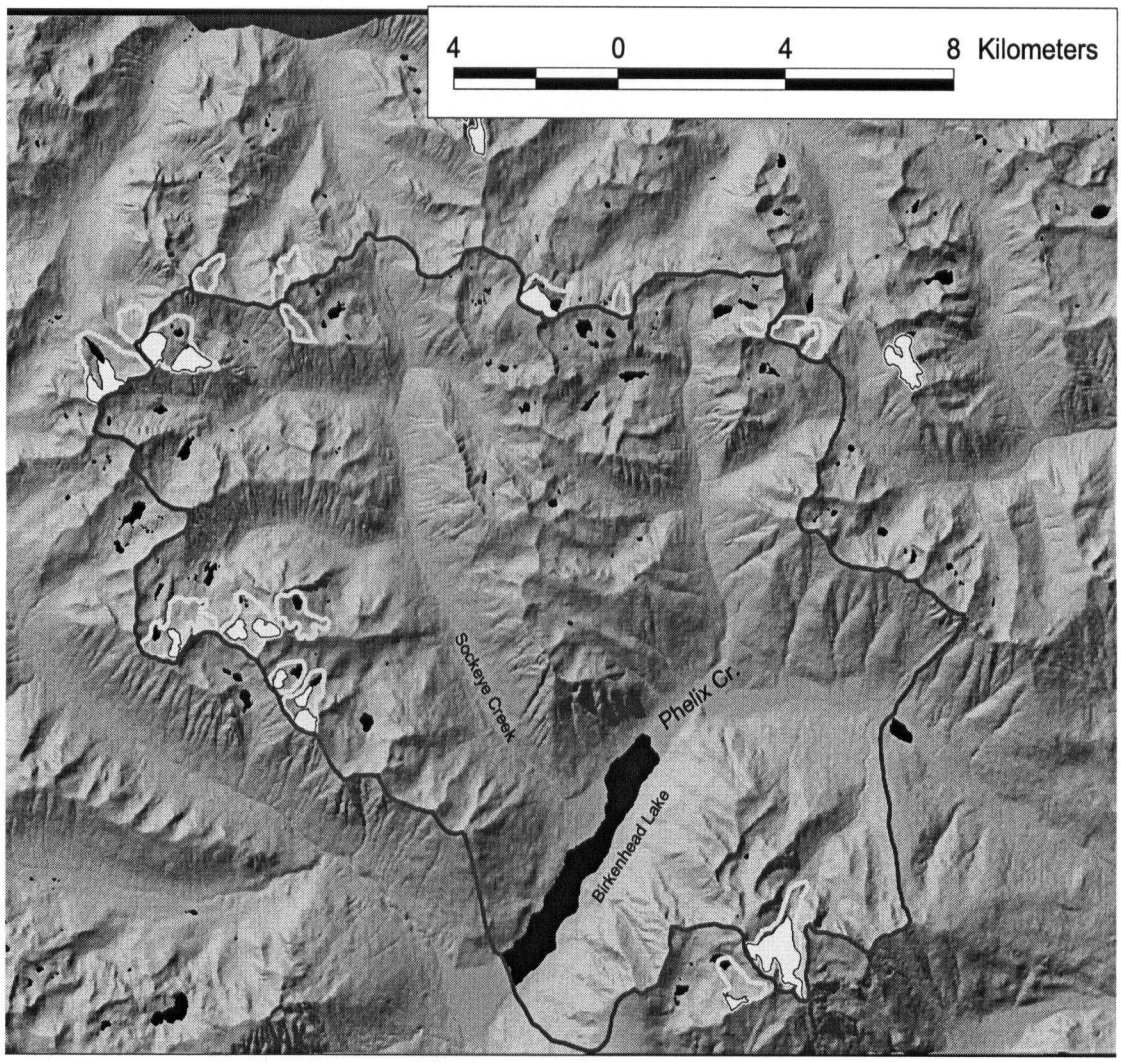

Figure 3.4: DEM of Birkenhead Lake Basin

thick (50m+) sequences of valley fill predominantly comprised of lodgement and or ablation tills which are overlain by glacio-fluvial sediments (Golder Associates, 1992). This fill likely represents an important sediment source to the channel as the active channel of Fitzsimmons is deeply incised in many locations and numerous failure scarps can be identified on air photos and through field visitation. Two active glaciers within the Fitzsimmons Creek sub-basin (Fitzsimmons and Overlord) likely represent other important fine-grained sediment sources and much like the Duffey Lake basin, there is little opportunity for deposition of fine grained sediment outside of intermediate storage in the channel. Green Lake (2.0 km^2) is characterized by an irregular bottom with two main basins; the proximal being largest and moderately deep (40m) and a shallower ($d_{max} = 30m$) distal basin.

Land use within the catchment has changed dramatically since the formation of Whistler and Blackcomb ski resorts though most of this development (outside of ski run and building construction on the slopes of Blackcomb and Whistler Mountains) has been on the lower elevation, de-coupled areas between Alpha Lake and the delta of Green Lake. Land use began as early as the beginning of the 20th century with the construction of the Pacific Great Eastern Railway though the general phase of development begin during the 1950's when logging began in the Fitzsimmons Creek valley.

3.3.0.5 Cheakamus

Cheakamus Lake catchment (216 km^2) is moderately glacierized (23 percent) and there are few intervening lakes between major sites of sediment production and the lake basin (figure 3.5). Upstream of the lake basin, Cheakamus River flows as a multi-thread to braided system over a low elevation valley floor. Tributaries which appear to deliver significant quantities of sediment to the main channel originate from active glaciers and unstable glacial forefield areas. Several active colluvial cones constraining the upper reaches of Cheakamus River likely deliver colluvial sediments to the channel. Lateral instability of the main channel and distributaries on the delta are clearly evident and a Gilbert-style delta has prograded beyond the more uniform (wave modified ?) deltaic region of the lake basin. Snow avalanche tracks terminate directly into many reaches of Cheakamus River, though channel abandonment and re-routing appear to be largely absent based on analysis of sequential air photos. Overall, there is limited evidence for large scale introduction of sediment to the main channel by landsliding and or debris flows. Glaciers and glacial forefields appear to be the dominant sediment source for Cheakamus River and by inference, the lake basin. Both Cheakamus and Glacier Lake basins are pristine watersheds. They became protected land with the designation of Garibaldi Provincial Park in the beginning of the 20th century.

3.3.0.6 Glacier Lake Basin

Glacier Lake basin (192 km^2) is covered with approximately 12.6 percent contemporary ice cover (figure 3.6). The terrain is steep and several proglacial lakes have formed between unweathered moraines and contemporary ice fronts. The basin is unique to this study in that outside of proglacial lake formation, it is the only example of a basin where fine sediment cascades can be shown to have been dramatically altered by internal geomorphic processes operating within the catchment. Following glacial recession from maximum downvalley extent during the 'Little Ice Age' (LIA), a major tributary to the lake incised into a moraine that was damming a large lake basin, and diverted runoff from 10 percent (5 percent contemporary ice cover) of the watersheds to the Pitt River system. This date of the diversion is unknown but apparently occurred before 1931 (Ricker, 1978). Two colluvial cones fringe the western side of the lake basin but they are heavily vegetated and have likely delivered negligible quantities of sediments to the lake during contemporary time (1948 to present). Several sites of colluvial sediment production are evident within the air photos of

the basin and include debris flow and or debris torrents originating in gully and couloir complexes to the south of the lake basin. Continued failures in these areas are evidenced by un-vegetated failure scarps and the large spatial extent of colluvium at their bases.

3.3.1 Geology

Overall, lithologic differences between the basins which could dramatically alter the production of fine sediment through enhanced glacial erosion or physical weathering appear to be slight but may be responsible for high, localized rates of rapid mass movement. Bedrock is primarily resistant, intrusive lithologies which characterize the Coast Plutonic Complex of the Southern Coast Mountains (Monger and Journeay, 1994). Mid-Cretaceous to mid-Jurassic age granodiorites, diorites and quartzdiorites are the dominant rock types within Joffre, Duffey and Birkenhead basins (figure 3.7)

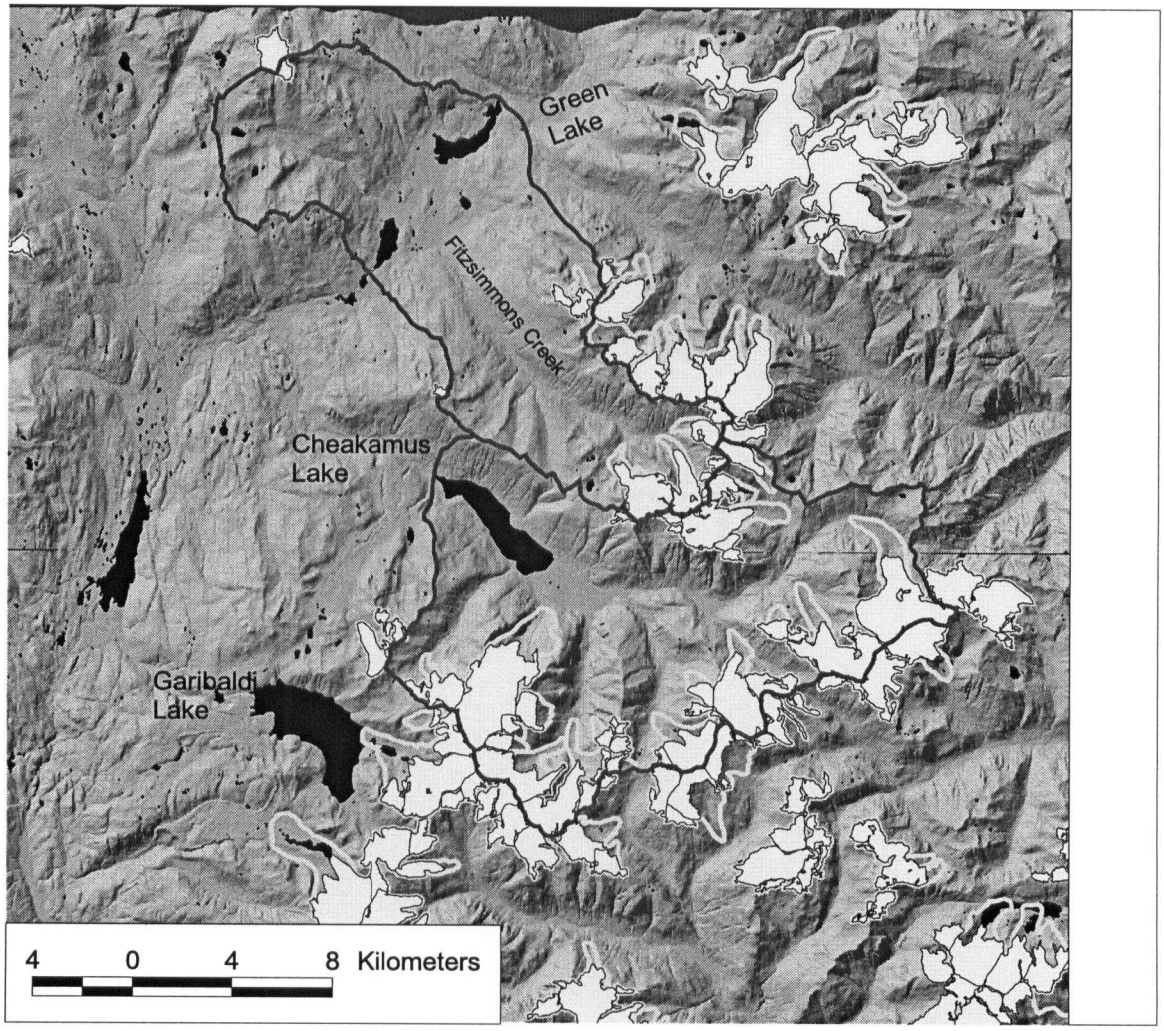

Figure 3.5: DEMs of Cheakamus and Green Lake Basins

while equal proportions of metamorphosed volcani-clastics and conglomerates (Gambier Group) can be found within the watersheds of Cheakamus, Green and Glacier Lakes. One may expect rates to be higher for the Gambier Group and undifferentiated conglomerates and volcaniclastic rock types but such suspicion is largely speculative given the lack of lithologic-specific weathering data for the Coast Mountains. Equally speculative, it is believed that variations in rock type play a subordinate role to the availability and caliber of surficial materials deposited during the last glaciation in controlling patterns of sediment supply within the watersheds. An exception to this is the notable hillslope instability observed in volcanic lithologies in the southeastern portion of the Glacier Lake basin. Continual debris flow and torrenting in Holocene time has produced a large colluvial cone which abuts the main inflow to the lake basin (Snowcap Creek). This cone has

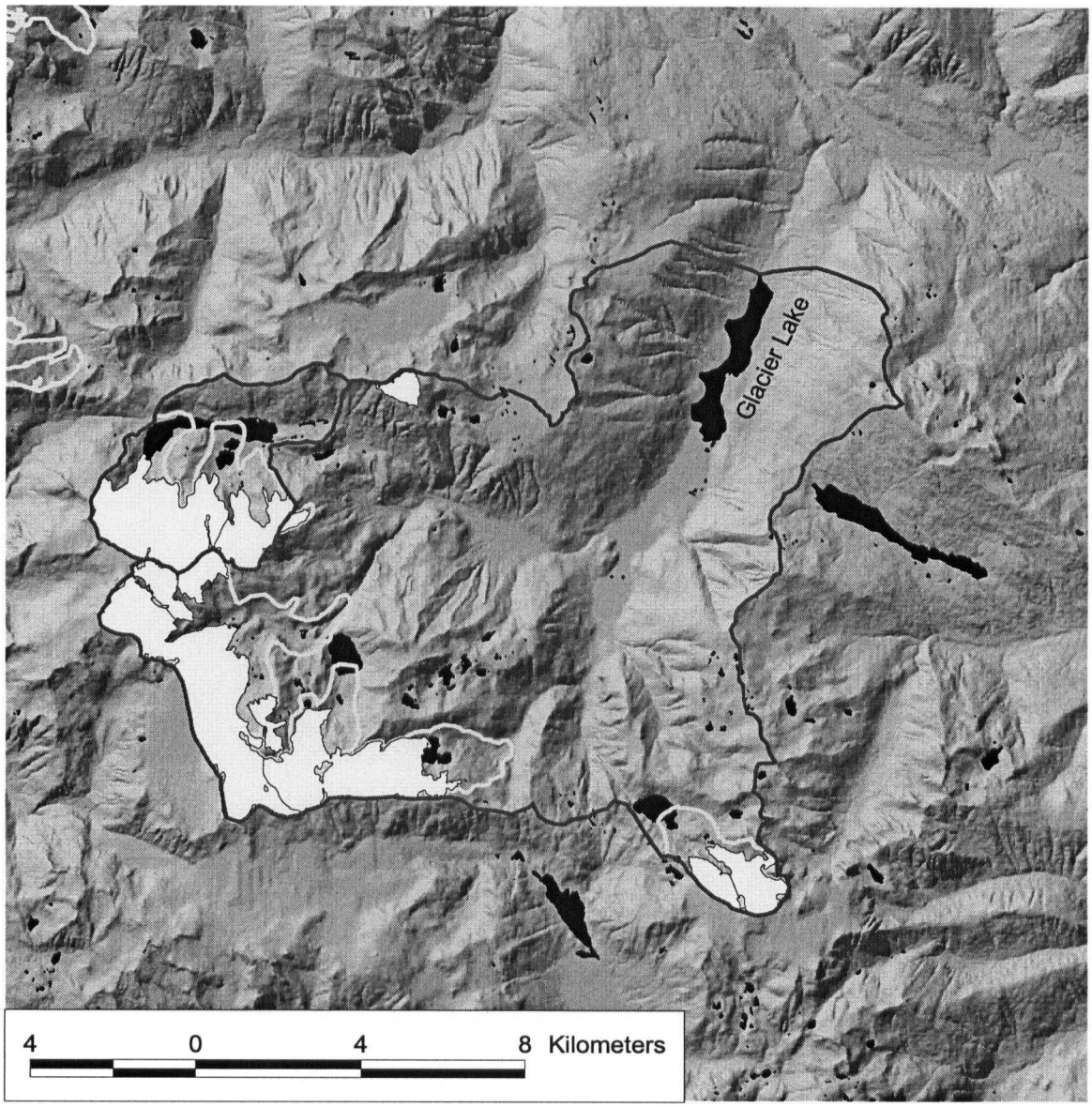

Figure 3.6: DEM of Glacier Basin
Water from snowcap watershed (smaller outlined watershed) now flows into the Pitt River system. See text for discussion.

remained active since at least 1931.

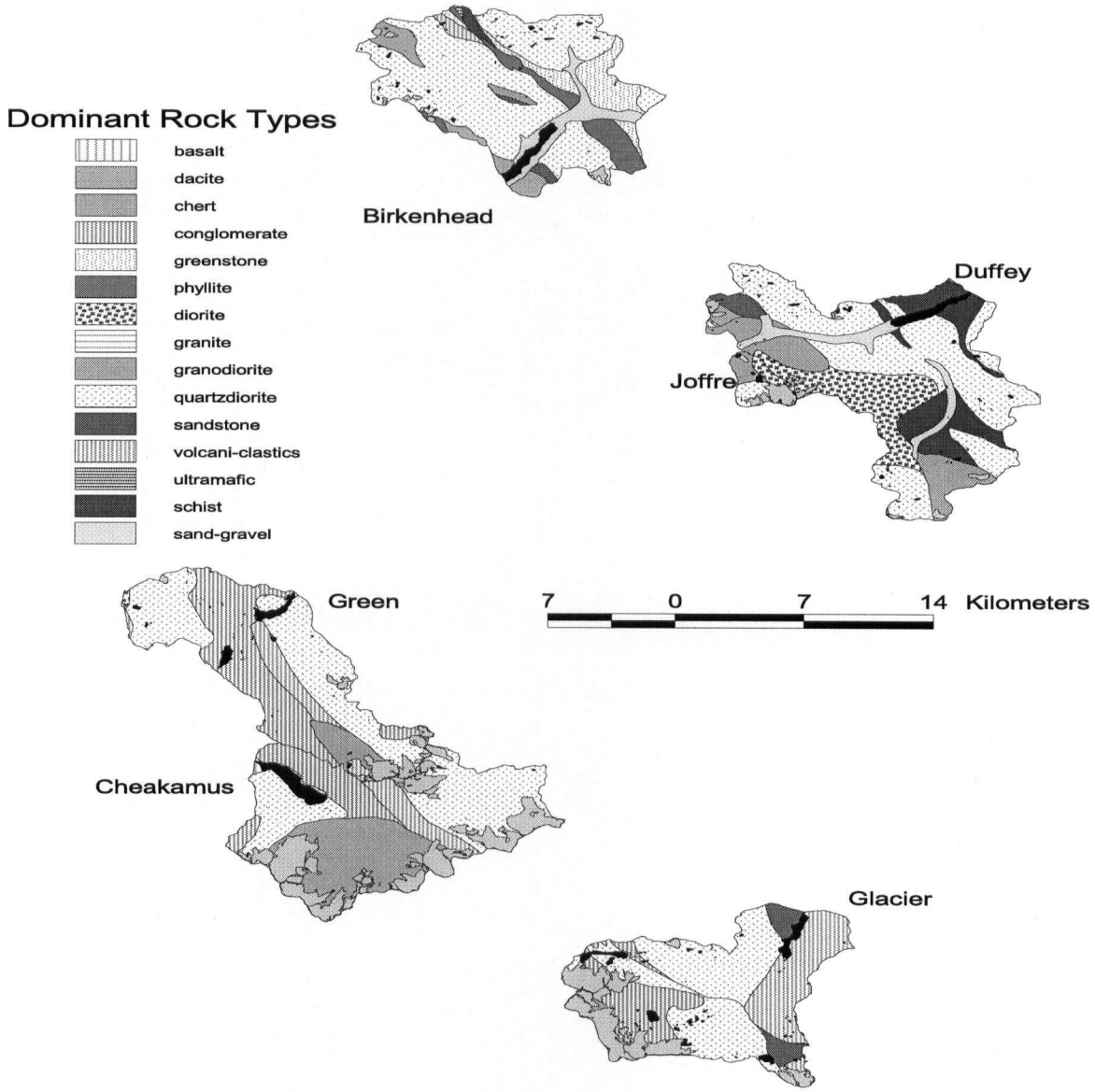

Figure 3.7: Generalized Geology of the Study Area.
Geologic data kindly provided by Dr. Murray Journeay, Geological Survey of Canada. Appendix A details the merging of the TRIM and geologic data.

3.3.2 Basin Morphometry

In addition to variations in climate and lithology, morphometric characteristics such as slope and relief can often be important controls of sediment production and storage patterns within earth surface systems (e.g. Schumm, 1956; Hooke, 2000). General morphometric characteristics of the watersheds were calculated from the DEM data and digital map sheets (see Appendix A for details) in order to understand and control for endogenic factors in fine sediment production, intermittent storage and final sedimentation within the studied lake basins (table 3.2). The characteristics include those which are believed to influence the production or transfers of fine sediments within

the watersheds and include among others contemporary ice cover, stream density, percentage of total intervening lakes and average hillslope gradient. The planimetric and digital elevation model were obtained from the Terrain Resources Inventory Mapping (TRIM) project, Ministry of Environment, British Columbia. Zonal vegetation data for the province (biogeoclimatic zones) was also obtained and the percentage of alpine tundra (AT) was used as an index of geomorphic intensity given its low vegetation density; geomorphic processes responsible for physical weathering become increasingly important in this environment.

Parameter	*Duffey*	*Birkenhead*	*Joffre*	*Green*	*Glacier*	*Cheakamus*
Area (km^2)	252	222	14.5	174	205	216
Drainage Density ($km\ km^{-2}$)	2.98	2.88	1.48	1.18	1.07	1.37
Relief (m)	1600	1870	1560	2060	2100	1580
Relief Ratio [a]	0.059	0.085	0.260	0.090	0.096	0.061
Ruggedness Number[b]	0.010	0.013	0.041	0.017	0.015	0.011
Elevation (μ, σ), (m)	1755±317	1604±450	1925±353	1422±488	1342±530	1680±431
Slope (μ, σ), (percent)	26±12	27±12	28±13	21±11	25±11	27±12
Coupling Number[c]	0.428	0.419	0.570	0.334	0.639	0.455
Intervening Lakes (percent)[d]	0.52	0.59	2.17	1.01	1.29	0.071
Ice Cover (percent)	1.71	1.21	25.2	6.0	12.0	23.2
LIA Ice Cover (percent)[e]	5	3	30	12.1	15	30
AT Biozone (percent) [f]	49	42	66	30	45	60

Table 3.2: Basin Morphometric Characteristics

a. $\frac{Basin\ Relief}{Basin\ Length}$

b. $\frac{Basin\ Relief}{\sqrt{Basin\ Area}}$

c. See text

d. Percentage of upstream lakes from examined lake basins

e. Assessed through mapping of visible trimlines and unweathered terminal and lateral moraines from air photos

f. Alpine Tundra Biogeoclimatic zones mapped (1:100,000) by the Ministry of Environment and co-registered to TRIM data

Slope and elevation are important controls on fine sediment production within mountain environments (e.g. Schumm, 1956; Hooke, 2000) largely because such variables control the spatial distribution of potential energy and rates of sediment detachment (fluvial, hillslope or glacial). For example, assessing the relative proportion of surface area within a given watershed which is both steep and above treeline may provide an index of sediment production. Slope (s) and elevation (z) data for the DEM data can be combined to produce bivariate distributions for the catchments because each cell ($25m$) within a given DEM has an elevation (z) and slope (s)component:

$$\sum_{i=1}^{i=n} p(z,s) = 1.0 = \frac{\sum_{i=1}^{i=n} \phi((z-z_i)/h_z)\phi((s-s_i)/h_s))}{nh_s h_x} \tag{3.1}$$

where $p(z,s)$ represents the joint probability function of z and s, h represents the bin width (frequency distribution), and ϕ is a Gaussian-shaped kernel (Venables and Ripley, 1999). Comparison of 2-dimensional histograms for a given basin highlights the relative proportion of the the land surface (e.g. steep and high elevation) which may be expected to contribute sediment through physical or mechanical weathering (figure 3.8). Conversely, such graphs allow a quick assessment concerning the elevational distribution of major sites of sediment traps and areas characterized by overall sediment deposition. Though it is often assumed that slope is normally distributed in most environments (Schumm, 1956; Hooke, 2000), the DEM data indicates that both elevation and slope are non-normally distributed.

Significant proportions within Glacier and Joffre basins appear to be major sediment traps at intermediate elevations and are likely to attenuate the flux of fine-sediments produced in higher, steeper environments. Large percentages within the watersheds are characterized as low elevation-low gradient representing sites characterized by net sediment storage (figure 3.8). Though low elevation fluvial sediment storage is not apparent in the bivariate data from Joffre (figure 3.8), intervening lakes within the basin can be expected to significantly decrease the amplitude of sediment export from the watershed.

3.3.2.1 Coupling Number

In addition to slope and elevation, sediment transfers in mountain watersheds depend on the ability of sediment generated on hillslopes to reach the stream system (e.g. Caine, 1989; Whiting and Bradley, 1993). A simple coupling index was developed to summarize this likelihood of clastic sediment (hillslope derived colluvium or alluvium) entering the stream system within a given watershed. The index is derived from stream and DEM data obtained from the Ministry of Environment, British Columbia (TRIM data). Slope data (mm^{-1}) for a given pixel within the DEM was divided by the distance (m) to the stream network. The operation produces a resulting grid in which higher values correspond to steeper terrain in close proximity to stream reaches. In order to make meaningful comparisons between basins, the value for each pixel (dimensions of m^{-1}) is multiplied by the area it represents (625 m^2), summed for the entire watershed and then divided by total stream length (m) within the watershed. Division by total stream length is necessary in order to normalize for drainage density.

Highest coupling is observed in the Glacier Lake basin while lowest values are found for Green Lake (table 3.2). This index of coupling is particularly high near couloir and gully networks and lowest in wide floodplain areas. Unfortunately the index can only provide the potential for sediment flux rather than an estimated value. Estimates of flux rates would require detailed information concerning regolith thickness and identification of event versus weathering-limited terrain (e.g. Jakob, 1996). Nevertheless the parameter provides an integrated measure of overall hillslope-

fluvial coupling within the watersheds and will prove useful for assessing the internal controls of fine sediment transport within the watersheds.

3.3.3 Watershed Similarity

The degree of morphometric similarity between watersheds was assessed by combining data from table 3.2 and calculating a dissimilarity matrix for the entire data set (Davis, 1986). Morphometric similarity provides important *a priori* information regarding fine sediment discharge and should be useful for understanding the geomorphic controls of sediment variability as assessed in Chapters 5 and 6. The degree of similarity can be estimated by first standardizing the variables and then calculating the Euclidean distances between the 6 basins in 12 parameter space and assessing

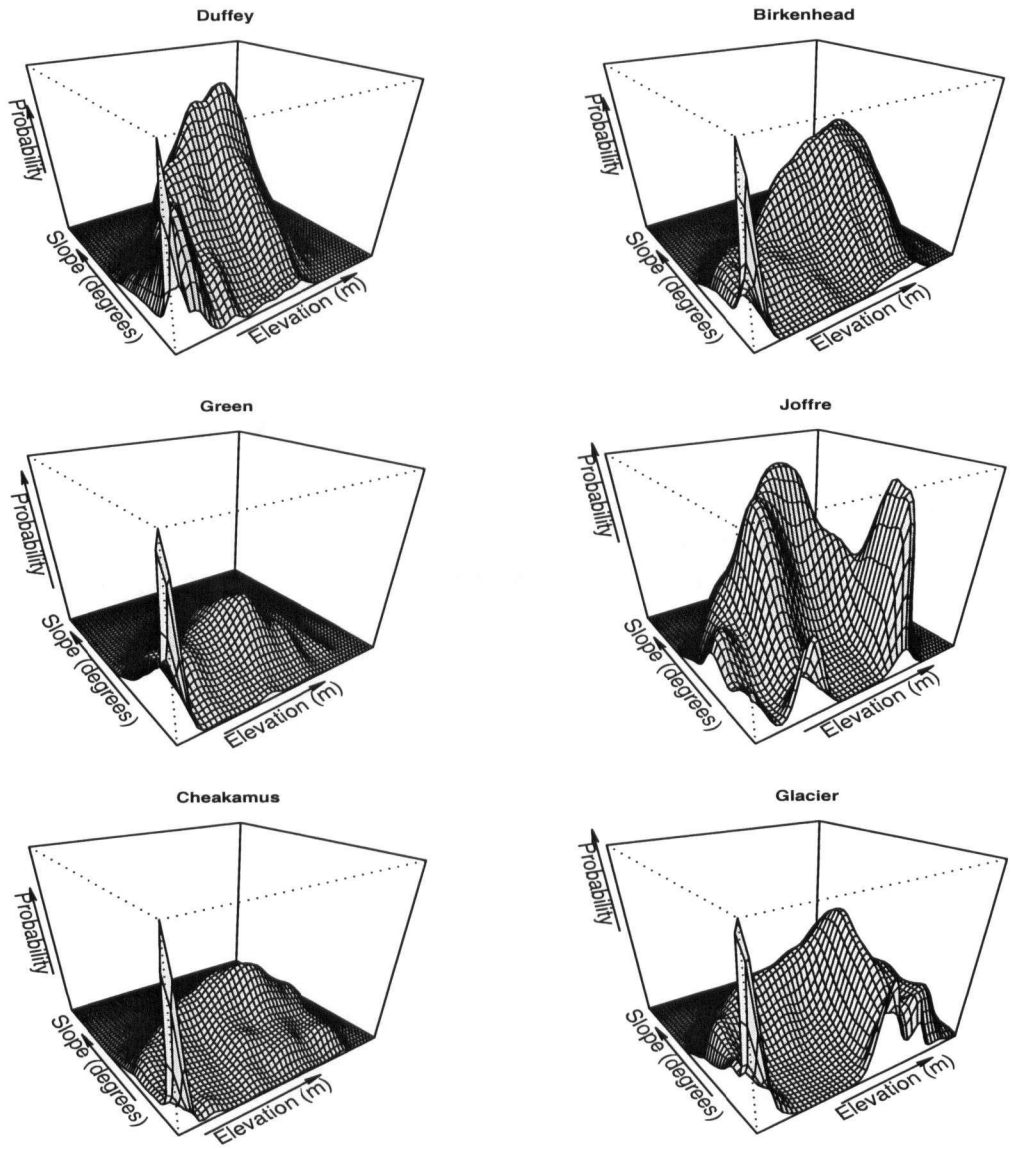

Figure 3.8: Bivariate Distributions of Slope-Elevational Data
Total probability under the surfaces normalized to unity.

the linkages between basins graphically (figure 3.9). The similarity between basins is inversely proportional to the length of lines joining adjacent basins. Changing the algorithm for centroid determination (mean, median or non-parametric) did not alter the results shown here.

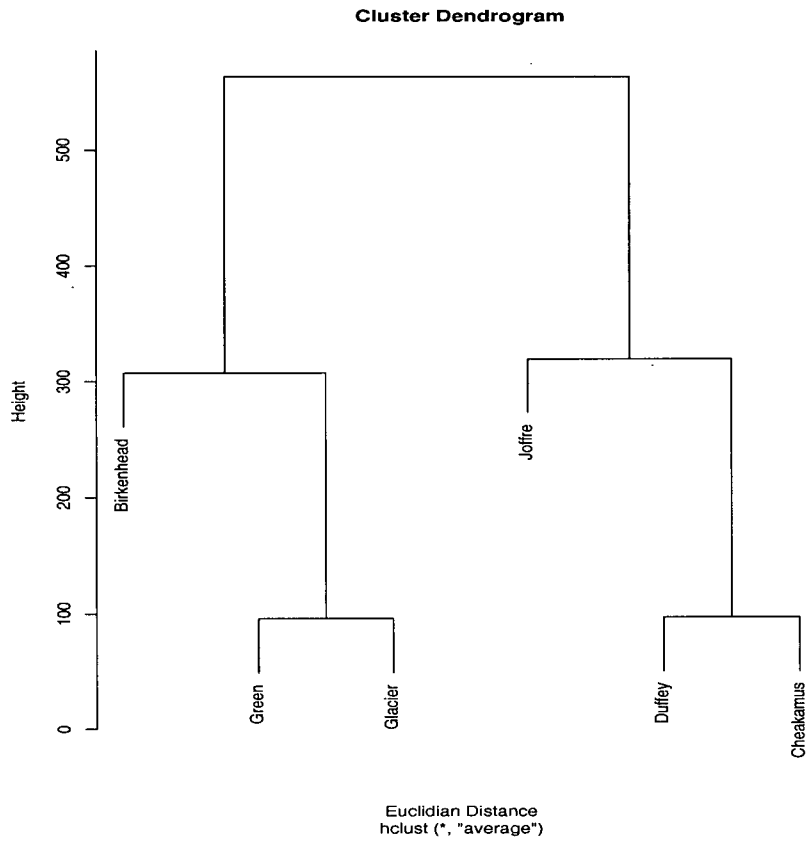

Figure 3.9: Dendrogram of Watershed Similarity

Similarities between watersheds based on morphometric characteristics indicate that the basins cluster into two groups; one consisting of Birkenhead, Green and Glacier while the other group is comprised of Joffre, Duffey and Cheakamus lake basins. Based on correlation between the variables of table 3.2, this split is believed to be largely the result of relief, ruggedness number and elevational differences. These data and their overall significance in terms of sediment yields will be re-examined in subsequent chapters.

3.4 Data Acquisition and Analysis (Climate and Sediment Discharge)

3.4.1 Hydro-climatic Data (this study)

Stream discharge (water and sediment) and concurrent lake sedimentation (pelagic) events were monitored in the Duffey and Birkenhead Lake basins between May, 1997-October, 2000 to document the timing, magnitude and climatic significance of sediment inflow events. Sediment sampling for Fitzsimmons Creek (Green Lake) began in Spring 1999 and was used in conjunction with streamflow data from the basin to estimate the seasonality and magnitude of sediment transport.

3.4.1.1 Stream Gauging and SSC Collection

Suitable sites were chosen within the the Duffey and Birkenhead catchments to record important meteorological events responsible for fine-grained sediment transport. Those events included sustained periods of warm weather important for snowmelt and or glacial melt runoff and high-intensity rainstorms. Water level (stage) and temperature (water and air) were collected (10-minute sampling interval) on three major streams (one in Birkenhead, two in Duffey) and converted to discharge following standard procedures (World Meteorological Organization, 1980). Detailed methods pertinent to the development of the discharge records including reliability of the stage-discharge relations can by found in Appendix A. Tipping bucket rain gauges (non-shielded) were located leeward of natural windbreaks but distant enough to prevent interception losses or additions from foliage. Precipitation totals and estimates derived from the rain gauges provide, at best, a first order approximation of precipitation fields over the study area given the size of the watersheds. Shielded thermistors (± 0.5 °C) were mounted 1.5m above the ground and recorded variations in air temperature throughout the period of study.

Major sediment discharge events for three of the watersheds (Duffey, Birkenhead, Green) were documented by collection of depth-integrated (using a DH-48 sampler) suspended sediment samples (SSC). Sampling locations were chosen where the creeks exhibited fully turbulent (lateral and vertical) flow and sampling locations were not altered throughout the duration of the study. Replication of instantaneous SSC was determined by collecting duplicate (concurrent sampling in time) and paired (i.e. left and right-bank samples) suspended sediment samples and provided a means of evaluating sampling error as a function of discharge or texture (related to hydrologic season). The results indicated no difference between replicate samples (time and space). Pump sampling (ISCO sampler) was attempted but abandoned after it became apparent that insufficient pump suction did not allow the collection of representative SSC samples for the streams.

The timing and intensity of SSC sampling were controlled primarily by high flow events (precipitation or snowmelt induced) or prolonged warm spells during late summer during the period of glacial melt. Sampling strategy reflected a bias toward capturing high flow events because most sediment transport within mountain watersheds of British Columbia occurs during these times (Church et al., 1989). Sampling during high discharge events was often hourly and was decreased to bi-daily sampling when sediment concentrations within the creeks declined. Significantly fewer samples were collected for Phelix Creek (Birkenhead Lake catchment) due to the manual nature of the sampling program and the decision to make more detailed hydrologic studies within the Duffey Lake catchment the main objectives of the contemporary monitoring portion of the study. The combination of watershed size (order 100 km^2) and runoff generation mechanism (mainly snowmelt) caused the creeks to experience high discharge events close to midnight creating a situation where sampling intensity following peak flows was much less than those preceding daily peak flows. The SSC samples were vacuum filtered ($0.45\mu m$) and oven dried (105 °C) to determine sediment concentration (mgl^{-1}). Particle size characteristics of the samples were qualitatively assessed through examination of the the filter papers under a binocular microscope.

3.4.1.2 Lake Sedimentation

Processes governing the physics of sediment delivery and re-distribution within temperate lakes are complex (c.f. Gilbert, 1975; Smith, 1978) and relate primarily to the magnitude of inflow event, particle size characteristics, lake stratification and wind stress. In glacierized catchments, this complexity increases due in part to changing intensities and type of inflow events (i.e. nival and or glacial runoff). To understand some of these processes and to link in a more direct manner fluvial

sediment transport and concurrent lake sedimentation events, sediment traps were installed in 1997 in Birkenhead and Duffey Lakes in distal and proximal locations with respect to major inflows to the lake basin. Each trap was constructed of two, 4 inch diameter settling chambers approximately 50cm long mounted vertically to a support line. The traps were fitted with interior baffles to inhibit current and faunal (e.g. fish) disturbance. They were positioned 2m above the lake floor and remained suspended in the water column by floats at the water surface; large cinderblocks provided suitable anchors. No preservative was used to inhibit bioturbation or diagenesis of the sediment collected within the traps. Traps were emptied four times yearly at the start of each hydrologic season (i.e. nival, glacial, autumn rainstorm, winter) and allowed estimates to be made concerning: a) the hydrologic season most responsible for the highest sediment fluxes to the lake floors; b) the year-to-year variations in sediment delivery to the lake; and c) between-lake comparisons of contemporary sediment fluxes.

The sediment traps remained in the lake during the winter hydrologic season by reducing the length of trap line until the surface float was under 1-2m of water. No attempt was made to document or estimate the significance of turbidity currents in re-distributing sediments within the lake basins though such processes have been shown to be important mechanisms of sediment transport within temperate lake systems (e.g. Gilbert, 1975; Lambert et al., 1976). Given the morphometry of the lakes examined in this project, it is suspected that underflow events represent a significant albeit spatially discontinuous mechanism of sediment transport and redistribution.

3.4.2 Hydro-Climatic Data

Ancillary data which was not collected in this study include streamflow and climate time series (temperature and precipitation) collected by Environment Canada (streamflow data formerly collected by Water Survey of Canada). Discharge data were used to develop sediment rating relations for Fitzsimmons Creek and for assessing the hydro-climatic variability of the watersheds both during the period of monitoring and throughout the instrumental period of record. Data were accessible from electronic media. Snow course data provide aggregated information concerning winter precipitation and temperature anomalies (Moore and McKendry, 1996) and electronic data were readily available from the Ministry of Environment, British Columbia.

3.5 Paleo-environmental Data (this study)

Paleo-environmental archives utilized in this study encompass primarily fine-sediments preserved in lake basins within the study area. Those data provide indices of lake-based sedimentation patterns over event to millennial time scales. Given the length of recovered records, paleo-environmental data (tree rings and ice cores) recording regional-to-hemispheric climate variability were also analyzed to detect and remove (if possible) climatic signals from the sediment records. This is necessary if partitioning of the sediment records into climatic and geomorphic components is to be accomplished.

3.5.1 Sediment Archives

The spatial and temporal patterns of lake sedimentation within the lake basins were determined by recovery and subsequent analysis of lake sediment cores. Coring density and location were chosen to meet two criteria; a) numerous short cores were collected to characterize the spatial pattern of sedimentation in those lakes investigated in detail (Green, Birkenhead, Duffey Lake) and b) recovery of high resolution sediment records which suitable resolution (order 1-10 yr) appropriate for this project. Recovery of multiple short cores allowed an assessment to be made concerning

the representativeness of these longer archives with respect to lake-wide sedimentation patterns. It also provides a means of estimating sediment yields estimates earlier than the short cores allow but requires that lake sedimentation patterns do not change through time (e.g. Lamoureux, 1999b). Recovery of long cores (>1m) was accomplished during winter using a percussion coring system (Reasoner, 1993) and by vibracoring (Smith, 1998). Shorter, gravity cores (10-80 cm) and Ekman dredges (Desloges and Gilbert, 1995) were recovered from an inflatable boat. After splitting, cores were photographed, logged and sampled for bulk physical properties (i.e. water content, bulk density, organic matter content, carbonate content, texture, particle size, magnetic susceptibility) using standard procedures (e.g. Gale and Hoare, 1991). Detailed descriptions of laboratory techniques can be found in appendix A.

3.5.2 Development of Varve Chronologies

Varve identification and measurements were made on photographs of partially-dried cores (e.g. Gilbert, 1975; Desloges and Gilbert, 1995), embedded sediment slabs, and thin sections (Lamoureux, 1994). Varve thickness (± 0.05mm) was measured with illuminated (polished slab and photographs) and transmitted (thin sections) light with a binocular microscope under low magnification (10x). Repeat thickness measurements generally differed by less than 5 percent. Counting errors were assessed by repeat counts along the same section of core after a period of time (interpretive error) and by cross-dating different cores based on the presence of marker horizons such as turbidites or uniquely colored varves (e.g. Lamoureux and Bradley, 1996). Assessment of absolute error is in part provided by independent depth-age estimates provided by AMS ^{14}C dating while relative or counting error is evaluated by recounting varve series and by developing multiple core chronologies (Appendix D).

3.5.3 Age Control of Sediment Archives

Depth-age models of sedimentation for the lakes are provided by cesium (^{137}Cs) activity determination, lead (^{210}Pb) series, and AMS ^{14}C dating, tephrochronology, and by varve counting. ^{137}Cs activity levels (gamma ray counting) of 1.0cm thick sediment slices were measured at the University of Toronto's Department of Chemical Engineering. The activity profiles were used to independently date and confirm the varved interpretation of the sediment archives of Green and Duffey lake sediments. Ten samples from Birkenhead Lake were analyzed for unsupported ^{210}Pb activity at the Department of Earth and Ocean Sciences, University of British Columbia. Accelerator mass spectrometry (AMS) was applied to determine the ^{14}C activity of terrestrial macrofossils found at various depths within the cores. Suitable macrofossils (usually conifer needles) could usually be found within 1cm thick slices of sediment though larger intervals had to be utilized in cores where macrofossils were rare or absent. Sediment was passed through a 63 μm sieve and macrofossils were collected with tweezers, oven dried (70 °C) and placed in sealed glass vials prior to submission for ^{14}C activity determination (1-6 months after collection). Radiocarbon ages were converted to calendric age by the calibration program Calib 4.2 (Stuiver et al., 1998a,b). Tephrochronology provides a check against the validity of depth-age models constructed with the AMS ^{14}C ages. Two types of tephra have been previously identified in the study area; a) Bridge River tephra (BRT) which was deposited ca. 2400 cal. yr BP and b) air-fall from Mt. Mazama (MAZ) which erupted ca. 7700 cal. yr BP (Hallett et al., 1997; Zdanowicz et al., 1999).

3.5.4 Paleo-environmental Data (other sources)

3.5.4.1 Tree Ring Data

Growth patterns of trees provide one method of extending short and spatially discontinuous precipitation and climate records (e.g. Bradley, 1999; Mann et al., 1999). Tree ring records from British Columbia and western North America were obtained from the International Tree Ring Data Bank (ITRDB) (Contributors of the International Tree-Ring Data Bank, 2001). These chronologies are commonly deep in sample depth (>20 trees), have undergone rigorous cross-dating and non-climatic trends (i.e. removal of trends due to tree growth) are often removed (standardization) from the records. One of the major limitations from these records, however, is that the standardization process often removes lower frequency climate variability from the records. Chronologies from the Pacific Northwest and western North America were combined and analyzed using principal component analysis (PCA) to extract the dominant temporal-spatial patterns which were then compared to temperature and precipitation variability within southern British Columbia. The large spatial domain was necessary in order to examine variability in tree growth response during the first half of the millennium given low number of chronologies within British Columbia which exceed 500 years. Though several studies have previously examined regional tree-growth response over western North America and the Pacific Northwest, many new sites have been added to the ITRDB including those in sparsely sampled locations as well as several chronologies developed from Mountain Hemlock (*Tsuga mertensiana*), a tree species which is sensitive to variations in winter accumulation (Gedalof and Smith, 2001). Multi-proxy derived and calibrated records (Mann et al., 1998, 1999) provide estimates of Northern Hemispheric temperature variability for the past 6 centuries.

3.5.4.2 Ice Core Record

Climate proxy indices recorded in ice cores obtained from the Greenland Ice Sheet[1] were used to supplement and extend climatological indices developed from tree ring records over time scales of centuries to millennia. Though the Greenland Ice Sheet is distant from the study area, the high elevation at which the ice cores recovered allows the site to record major changes in global atmospheric circulation (Hammer et al., 1997).

[1]Data from both the Greenland Ice Core Project (GRIP) and the Greenland Ice Sheet Project 2 (GISP2) were accessible online (www.ngdc.noaa.gov) from the National Geophysical Data Center and major findings from the ice cores are summarized in a special issue of the Journal of Geophysical Research (vol. 102, 1997).

Chapter 4

Event to Inter-annual Time Scales: Sediment Transport

4.1 Introduction

This chapter summarizes the results obtained from the contemporary monitoring program which began in 1997 and continued until late 2000. The monitoring program was structured into two principal stages and provided information concerning major sediment sources and more importantly, the relative magnitude of event to inter-annual sediment transfers. The first phase was directed toward an attempt to quantify those sub-basins which contributed the largest proportion of washload to the monitored streams of the study. Such data, when combined with sediment source identification through field visits and air photo analysis, revealed that glacierized areas are the main sediment source within the watersheds. The second phase of the monitoring entailed more regular collection of suspended sediment samples from those watersheds chosen to be representative and where permanent monitoring sites were established. Such data also allow a first-order comparison to be made between fluvial and lacustrine based sediment yields.

4.2 Large-Scale Climate Conditions During the Period of Study

The monitoring program was conducted over a period that coincided with some of the most notable climatic departures observed in the historical record of hydro-climatic variability within southwest British Columbia. This was an excellent opportunity to test the inferred climatic controls of fine-sediment production and discharge as outlined in Chapter 2. Such variability included significant inter-annual variations in winter snowfall accumulation, glacial runoff and rainfall-generated floods during the autumn and allowed estimates to be placed on the relative importance of sediment transport during these contrasting hydrologic seasons.

During the period of study, one of the largest ENSO events (20th century) began with anomalously warm SST forming in the eastern Pacific Basin in early summer, 1997. The conditions continued into early spring 1998 when tropical SST anomalies dissipated, reversed in sign and initiated a strong La Niña event lasting until early spring of 2000. Similar scale variations in SST formed in the North Pacific Basin and together, they are believed to have influenced atmospheric circulation patterns over the study area during winter 1997-1998 (table 4.1). During the winter of 1997-1998, snowpacks were thinner on average and southern British Columbia experienced early-season peak flows on major snowmelt-dominated river systems due in part to shallow snowpacks but generally warmer than average spring time temperatures. This thin snowpack in addition to a particularly warm summer caused monitored glaciers in the study area to experience a large loss in net mass (table 4.1). Winter accumulation the following year was in sharp contrast to 1997-1998. Record-breaking snowfall occurred over much of the Pacific Northwest and southern British Columbia. Unsettled and cool conditions during spring and summer prolonged the timing of snowmelt runoff and for the first time since 1976, accumulation exceeded ablation for Place Glacier (table 4.1).

4.3 Observed Streamflow Variability

The hydrologic monitoring indicated that, as expected, yearly discharge is controlled primarily by winter precipitation totals and synoptic conditions during the runoff season. What was not anticipated was the large inter-annual variability of runoff generated by glacial melt and late summer-autumn precipitation events. Runoff processes important for fine-grained sediment production and transfers can be summarized as follows:

a) Runoff response from the three sub-basins (Phelix, Cayoosh and Van Horlick Creeks) are nearly identical throughout a given hydrologic season but also over inter-annual time scales (table 4.2; figure 4.1). The similarity of streamflow response is not surprising as the basins are in close proximity to one another and the majority of precipitation experienced by these watersheds falls as snow.

Integration of total runoff observed during the snow free period (April -December) indicates that the watersheds receive between 1500-2300 $mm\,yr^{-1}$of precipitation neglecting the effects of evapo-transpiration.

b) During and up to peakflow during nival runoff, discharge variations on 3-10 day time scales are well correlated with air temperature fluctuations and lag air temperature by about 2-3 days (figure 4.4). Short-term variability in air temperature appears to be caused by large scale patterns in atmospheric circulation (NCEP data) and is supported by the positive correlation between observed daily air temperature and average height (m) of the 500 hPa surface over the study area (45-55N; 120-140 W).

Following peak flows during spring, air temperature and discharge continue to be related but in a non-linear fashion as snowpacks become depleted. Such nival runoff dependence upon air temperature variations is normal for snowmelt dominated watersheds in southern British Columbia and has been shown to extend over sub-continental scales in western United States (Peterson et al., 2000). Following peak flows during spring, the amplitude of the diurnal hydrograph decreases

	1996-1997	1997-1998	1998-1999	1999-2000
ENSO[a]	0.23	-2.35	1.20	1.18
PDO	0.15	1.30	-0.61	-1.45
PNA	-0.32	1.18	-0.20	0.08
Winter Anomalies[b]	29 [33]	45 [4]	1 [9]	50 [16]
Summer Anomalies	4 [6]	47 [3]	19 [41]	15 [21]
April 1 SWE[c]	0.73	-0.17	2.56	0.25
Glacial Mass Balance[d]	-1073(-888)	-2850 (-2450)	1500 (620)	110 (130)

Table 4.1: Hydro-climatic Variability During Period of Monitoring

[a] Values for ENSO, PDO and PNA represent wintertime (October-March) averages.

[b] Rank (highest to lowest) of precipitation [temperature] anomalies from coastal climate network for period 1948-2000 (Climate Trends and Variations Bulletin, Meteorological Service of Canada)

[c] Standardized departures (average) of April 1 snow water equivalence (SWE) from 5 (Grouse, Tenquille Lake, Nahatlach, McGilvery, Duffey) snow course sites.

[d] Net Mass Balance [$mm\,H_2O$] for Helm and (Place) Glaciers

and is interpreted to reflect continual depletion and ripening of the snowpack (e.g. Caine, 1992). Continued depletion of snowcover through summer allows additional receipts of net radiation to be used for melting firn and glacial ice. The onset of glacial melt is characterized by a return to diurnal cycles but of much lesser magnitude caused by low proportions of the watersheds which are currently glacierized. Precipitation events during spring (rain on snow), summer and autumn

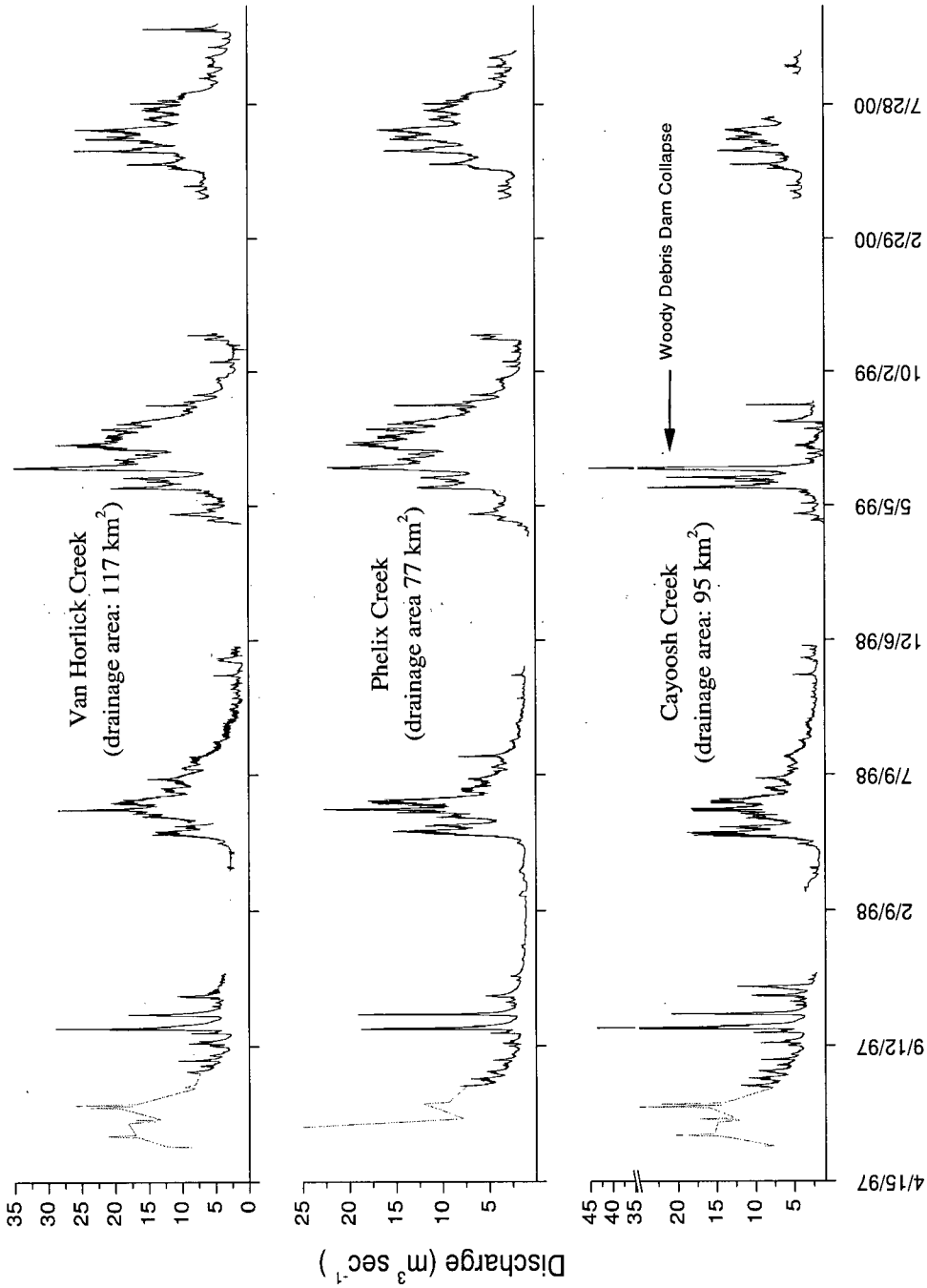

Figure 4.1: Van Horlick, Cayoosh and Phelix Creek Hydrographs
Logger malfunction and organic-debris dam collapse are responsible for the observed gaps in the discharge records from Cayoosh Creek during the snowmelt and snow free period.

increase discharge but do so only temporarily. The magnitude of such runoff events varies depending on overall precipitation intensities but freezing levels during the event are also important.

c) Response times (hourly data) of the basins vary according to runoff generating mechanisms and basin morphometry. Daily peakflows during snowmelt occur close to midnight in all of the basins. Based on air temperature data, this is approximately 7-8 hours following maximum daytime heating. It would be expected that as snowpacks within the study become depleted, the duration between maximum daytime heating and peakflow would increase as the snowline increases in elevation but such phase changes are largely absent from these data. This differs from results reported for other well-instrumented alpine catchments (e.g. Caine, 1992). Reasons for this stationarity may include such factors as seasonal changes in snow metamorphism and/or snow permeability (R.D. Moore, pers. comm.) or perhaps that reduced meltwater production late in the snowmelt season is compensated by increasing distance between sites of meltwater production and monitoring sites as the snowline increases in elevation. Hydrologic response of Van Horlick Creek lags that of Cayoosh and Phelix Creeks by approximately 4 hours presumably because of channel length and basin shape.

4.4 Fine Sediment Sources and Seasonality of Transport

To reiterate, suspended sediment sampling was carried out to meet three objectives: 1) to identify those sub-basins which appeared to contribute the majority of fine grained sediments to the main stem channels; 2) to collect an adequate number of samples over a range of discharges so that the major sediment-transporting events could be detected and compared to weather events and; 3) to provide short-term, fluvially-based yield estimates for the sub basins. Sediment sources were inferred by partitioning the watersheds of the study into sub-basins and collecting SSC samples from those tributaries believed to contribute the greatest proportion of sediments to Duffey, Birkenhead and Green lake basins. The majority of SSC collection occurred before the Green Lake basin was chosen for detailed investigation so a partitioning of its watershed was not completed. Based on air photo analysis and site visitation, SSC samples were collected from the creek which appeared to be the dominant contributor of fine sediments to the lake basin (Fitzsimmons Creek). The collection and analysis of SSC data for Fitzsimmons Creek is considered important to this study because its closer proximity to the coast may cause sediment transfers within the watershed to differ in timing and intensity from those basins which are more continental in nature (e.g. Duffey, Joffre, Birkenhead).

4.4.1 Sediment Source Areas

Suspended sediment samples collected from the sub-basins and mainstem channels within the catchment are markedly skewed and were log transformed in order to make between-basin comparisons

Year	*Van Horlick (117km^2)*	*Cayoosh Creek (95km^2)*	*Phelix (77 km^2)*
	mean (max) skew		
1997	9.4 (35.0) 1.40	8.8 (43.7) 1.85	7.1 (30.9) 1.47
1998	5.9 (28.5) 1.08	4.9 (18.8) 1.47	4.17 (22.7) 1.70
1999	9.39 (36.9) 0.90	6.7 (46.1) 1.68	7.20 (22.2) 0.73
2000	8.96 (25.9) 0.96	6.0 (14.8) 0.86	6.6 (16.8) 0.55
mean	8.41 (31.6) 1.09	6.4 (30.9) 1.47	5.7 (20.2) 1.03

Table 4.2: Flow Statistics of Monitored Streams During Period of Study
Estimates based on hourly discharge (m^3s^{-1}) during the snow free period (mid April-mid December)

(figure 4.2). Low sample size associated with several sub-basins (e.g. Birken, Caspar, Cerise) and non-uniform temporal sampling severely limits the degree of confidence associated with estimating average or median SSC for most of the sub-basins. In addition, these data only provide an

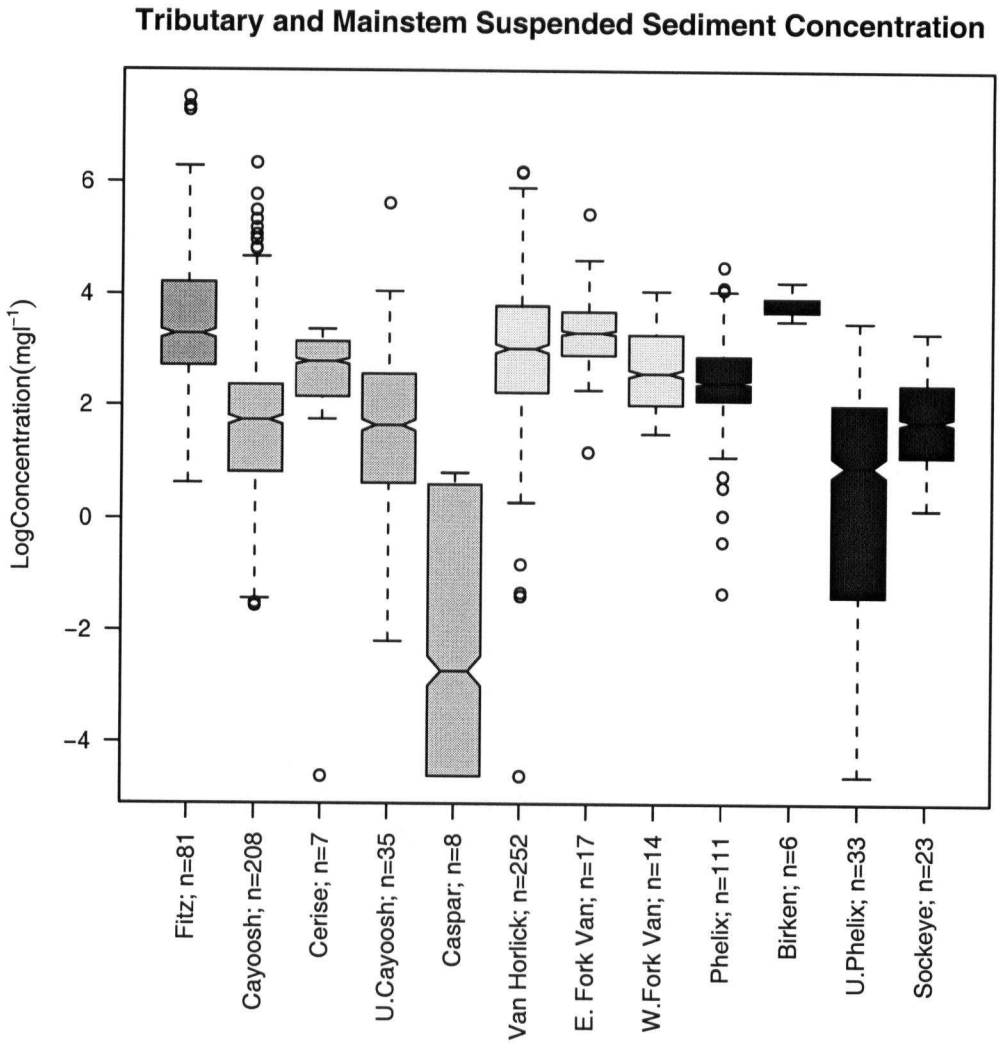

Figure 4.2: Median SSC (log) Estimates for Sub-basins and Main-stem Channels
Boxes and whiskers indicates 25-75 and 5-95 percent quantile estimates of the distributions respectively. Observations which lie outside of the 5-95 percent quantile ranges of the data are shown as points. Notch width indicates 2σ range in median estimates for the distribution and non-overlapping notches can be taken to represent statistically different populations ($p = 0.05$).

estimate of sediment source location because no attempt was made to collect hydrologic data for these systems which are required to estimate sediment yield. Nevertheless, the data hint at those sub-basins which appear to be the largest contributors to total load for the monitored streams of this study. Highest median SSC are observed in Fitzsimmons and Van Horlick creeks. Air photo analysis of the sub-basins, in addition to field visitation, indicates that most unvegetated areas

within the sub-basins correspond to glacial forefields and unstable glacial deposits adjacent to the contemporary channels (especially for Fitzsimmons).

Though many have suggested that glaciers represent an important explanatory variable in controlling sediment delivery from mountain environments (e.g. Hicks et al., 1990; Harbor and Warburton, 1993; Hallet et al., 1996) the relation is not simple and by no means universally accepted . Part of the difficulty relates to the use of glacial cover as a surrogate for more physically-based but much less understood sub-glacial processes that control sediment production and delivery (e.g. Hallet et al., 1996). For lack of a more meaningful index for contemporary glacial erosion and or sediment production, percent glacial cover is used to examine the relation between median SSC and contemporary ice (figure 4.3). Based on this limited data set the relation between glacial cover and mean SSC (and by inference yield) over the period of monitoring becomes evident.

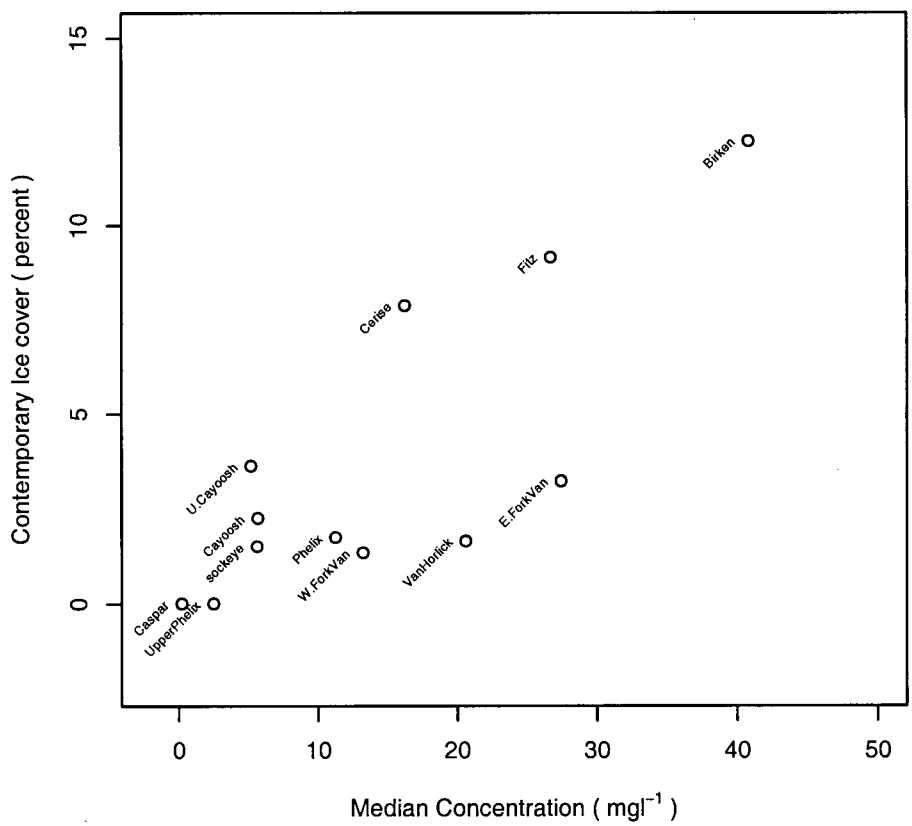

Figure 4.3: Median Concentration of Mainstem and Tributary Channels and Contemporary Ice Cover

It is believed that SSC is influenced by glacial cover both during periods of sustained glacial runoff when those streams draining glaciated terrain are carrying fine-grained sediments (rockflour) as wash load and by intermediate storage of sediment within the channel which can be mobilized during infrequent high flows. The degree to which these effects influence SSC is not simple but does appear to be partly controlled by the presence of intervening lake basins between active ice masses and downvalley monitoring sites. The reduction in sediment availability caused by intervening

lake basins has been inferred to decrease sediment yield from other glacierized Coast Mountain watersheds (e.g. Desloges and Gilbert, 1998).

The degree to which sediment delivery is attenuated by intervening lakes is well illustrated for the Duffey Lake catchment where the monitoring program has been most ambitious. Sediment yields (discussed shortly) are significantly higher for Van Horlick than for Cayoosh Creek despite the slightly more extensive glacial cover in the latter. The sand bed morphology of Van Horlick is likely the result of low valley gradients, active valley glaciers, and lack of intermediate sediment storage sites. Sediment comprising the channel and immediate floodplain (sand to silt) can be intermittently entrained and transported during high flow events. In contrast, sediment transfers between glaciers and downvalley monitoring sites are reduced by intervening lake basins except perhaps for the finest size fraction during time of sustained glacial melt and subsequent lake stratification. In short, sediment supply within Cayoosh is hypothesized to be largely a function of the rate of sediment detachment from exposed land surfaces and bankfull discharge events which create lateral or vertical instability.

4.4.2 Seasonality of Transport

Based on the monitoring program, most of the observed sediment transport occurs during three main hydrologic seasons: 1) runoff during the snowmelt period; 2) runoff coinciding with glacial ablation, and 3) during infrequent precipitation events of late summer and autumn. To summarize:

1) Snowmelt and rain-on-snow (ROS) floods appear to be particularly important processes for sediment transport for all of the monitored streams in the study though the period of principal transport occurs during a relatively short period. High sediment concentrations ($100 - 500 mg\, l^{-1}$)are observed for the creeks during the main period of snowmelt (mid May -mid July) following 3-5 days of warm sunny weather. During this hydrologic season, the majority of sediments appears to originate from channel and floodplain sources (figure 4.4).

Snowmelt runoff during spring 1999 was particularly intense for both Cayoosh and Van Horlick Creeks. The record-breaking snowpack and sustained warm conditions in June 1999 yielded snowmelt runoff that produced bankfull conditions in both channels. Following peakflows, there was much evidence of morphologic change within the creeks such as recently deposited and re-organized sand and gravel bars. In Cayoosh Creek, the failure of a major organic debris dam lowered bed elevation of the channel by 1m near the stage recorder. Consequently, the stage recorder required relocation following the flood (see Appendix A).

2) Sediment transport during late summer appears to be caused by increases in the relative contribution of proglacial sediments though its overall magnitude at least during the period of study was minor (figure 4.4). The transition between nival and glacial runoff was qualitatively assessed by observing changes of streamflow turbidity: following peak Q during spring those streams draining glacierized terrain in the study area commonly become clear for about 2-3 weeks with further reduction in flow. In hydrologic years 1997, 1998 and 2000, streamflow turbidity began to increase under clear sky conditions and stream color changed from clear to light green and in many cases light grey. Coincident with such color changes is the return of the diurnal cycle (figure 4.4), though its amplitude is greatly reduced ($\approx 1\ m^3 s^{-1}$). The timing associated with this nival-glacial transition varies from year to year and depends on the magnitude and timing of snowmelt runoff which is heavily influenced by total snowpack thickness and total energy available for meltwater generation. For example, glacial runoff varied greatly during the study ranging from over 2 months during 1998 to a little over 2 weeks during 1999. Such variability confounds yearly sediment transport interpretation because those years characterized by sustained glacial runoff may be expected to deliver less sediment during the nival period and vice versa.

3) Rainfall generated floods occur during autumn and this is the third hydrologic season important for sediment detachment and transport. Their significance within the study, however, appear to be spatially variable. The importance of such events is well exemplified by observed sediment discharge during an intense storm on 1 October, 1997 (figure 4.4) which delivered 33-43 mm of precipitation within a 24 hour period. Maximum discharge was reached 3 hours (Cayoosh) and 6 hours (Van Horlick) after maximum precipitation intensity (4.25 $mm\,hr^{-1}$). Although precipitation totals for this storm were moderate, pre-event flows in both creeks were elevated by precipitation on 30 September. Total precipitation between 29 September and 4 October, 1997 was approximately 100mm (figure 4.4). Temperatures for the event were relatively warm and no protective snowcover existed preceding the event. The event produced bankfull discharges in both Cayoosh and Van Horlick Creeks (bedload movement could be heard). Based on sediment yield estimates obtained from rating curves (discussed shortly), the quantity of sediment transported between 29 September and 4 October was comparable in magnitude to the suspended sediment discharge for the previous months of August and September (1997). This suggests that, if antecedent conditions are right, (e.g. no snowcover and mild storm), autumn precipitation events are significant in mobilizing both fluvial and non-fluvial sediments within the catchments.

4) Though precipitation-induced floods are significant within the study area, their relative importance appears to be related to distance from the coast. Such spatial influence was apparent during the passage of a late-summer frontal system during 1999. The event produced bankfull discharge in Fitzsimmons Creek with instantaneous SSC exceeding 1000 $mg\,l^{-1}$ and although discharge records for the event are not available (gauge malfunction, Lynne Campo (Environment Canada) pers. comm) peakflow is estimated to have been between 20-30 m^3s^{-1}. The estimate is based on regression analysis of the pre-event Fitzsimmons data with regional station data. In contrast, the storm elevated Q and SSC only slightly in the Duffey Lake basin. Such precipitation events, in addition to entraining fluvial sediments, can introduce considerable quantities of hillslope sediments through detachment effects (e.g. Gilbert, 1917). Based on field observations, hillslope detachment sites include unvegetated terrace scarps, and road surfaces. Recently de-glaciated terrain (moraines and forefields) is an other important sediment source where detachment effects can be locally significant (e.g. Richards, 1984). Holman et al. (1996), for example, found that close to 50 percent of calculated load from a proglacial stream originated from glacial forefield areas. Additional sediment may be entrained sub-glacially if the precipitation events occur during times of strong glacial ablation. It is during this time that additions of water to the glacial surface (either by ice melt or additions by precipitation) are easily routed to subglacial areas where they can elevate sub-basal water pressure and entrain fine-grained sediment. Elevated discharge caused by ice melt during the event is likely to be minimal given the high energy requirements for solid-to-liquid conversion of water (Rothlisberger and Lang, 1987).

4.4.3 Seasonal Dependent Sediment Storage

Similar to seasonally-dependent sediment sources, variations in sediment storage patterns can influence the apparent significance of sediment entrainment and discharge for a given hydrologic season. Such transitory sediment storage patterns may inflate the relative importance of sediment production and transport during a particular hydrologic season. In-channel storage of fine grained sediments was noted for most of the stream systems and was most apparent during the recessional limb of the seasonal hydrograph. Following peakflows, protruding boulders (0.2-0.5m) were often covered with 0.2-1mm accumulations of sediment. The sediments collected in 2000 from Van Horlick were very fine sand (D_{50} =79 μm) but with a larger than expected proportion (12 percent) of clay-sized (¡3.8μm) material. It is hypothesized that the sand-sized proportion of sediment is

transported primarily during high flow events during nival melt and that the finest grained fraction of the sediment is glacial rock flour deposited on the boulders during declining flows during summer. These channel storage patterns likely introduce seasonally-dependent hysteresis effects into sediment discharge from this channel as such material may be mobilized from these storage sites much later than when it was deposited (e.g. during autumn runoff events). Similar deposits of fine-grained sediment have been found in other proglacial streams in the study area (Richards, 2001) and the significance of such in-channel storage patterns requires further study.

4.4.4 SSC Modeling and Estimates of Sediment Yields

Sediment yield was estimated for three of the basins of this study through development of multiple regression models and provide a means of gauging the regional representativeness of observed sediment transport to those estimates for British Columbia (Church and Slaymaker, 1989; Church et al., 1989). More importantly, the estimates allow calibration of longer but more indirect estimates of sediment yield archived within the lake sediments of this study. Suspended sediment yield for most Canadian rivers is commonly estimated from daily SSC and discharge data but such an approach is likely to bias load estimates from small mountain watersheds where the majority of sediment is transported over a very short period of time (Thompson et al., 1987). Changes in observed SSC and Q within the study area can vary greatly within a given day and to reduce potential errors introduced by estimating load on a daily basis, hydrologic data (Q, SSC, precipitation, and air temperature) were averaged into hourly data. This sampling interval was chosen because of equipment malfunction for Cayoosh Creek which did not allow stage to be estimated at a finer resolution (see Appendix A) and the hourly format of streamflow data for Fitzsimmons Creek and Lillooet River.

An increase in sediment concentration with higher discharge is expected because the mechanism keeping sediment in suspension (turbulence) covaries with Q in open channel flow. Though a simple, linear relation between SSC and Q may exist for some river systems, variable sediment sources and availability often complicate the relation by introduction of a third variable into the relation, namely time (Williams, 1989). Linearization of the Q-SSC relation is often possible by log transforming of both variates. Most studies investigating suspended sediment transport find most success by transforming both Q and SSC. Such transformation helps to linearize the relation but also has an additional advantage of reducing heteroscadasticity within the data. An unfortunate result of the transformation is the biased estimate of the first moment of the distribution, more closely approximating the geometric rather than the arithmetic mean (Finney, 1941). The end effect causes negative bias in sediment transport rates but the effects can be reduced through parametric or non-parametric methods (Thompson et al., 1987; Ferguson, 1986).

A transformation of SSC data is also required when predicting loads through least squares regression because such methods require variables to be normally distributed. Both Q and SSC data for all the basins failed a Shapiro-Wilks test for normality. A Box-Cox procedure was used in an attempt to transform the data into more normally-distributed datasets. The family of Box-Cox transformations is continuous and can be approximated by (Box and Cox, 1964) :

$$y^{(\lambda)} = \begin{cases} \frac{(y^{\lambda}-1)}{\lambda} & \lambda \neq 0 \\ log(y) & \lambda = 0 \end{cases} \tag{4.1}$$

where λ is real number. Maximum likelihood methods (Box and Cox, 1964) can be used to find λ which transforms the data into the most normally distributed form. An alternative procedure was adopted via a computer algorithm in which λ was optimized by maximizing the probability

value (H_o : *data are normally distributed*) obtained from a Shapiro Wilks normality test for a given λ. For Van Horlick, a transformation function of the form $y^{-0.1}$ produced the most normally distributed data ($p = 0.26$, Shapiro-Wilks) but a log transform was only marginally rejected. The power transform only marginally (5 percent) improved the explained covariance between Q and SSC. In the end a log transformation was favored because bias correction procedures for log-transformed data are well known and the Q-logSSC relation could be more easily interpreted on physical grounds. Similar results were obtained for the other data sets of this study.

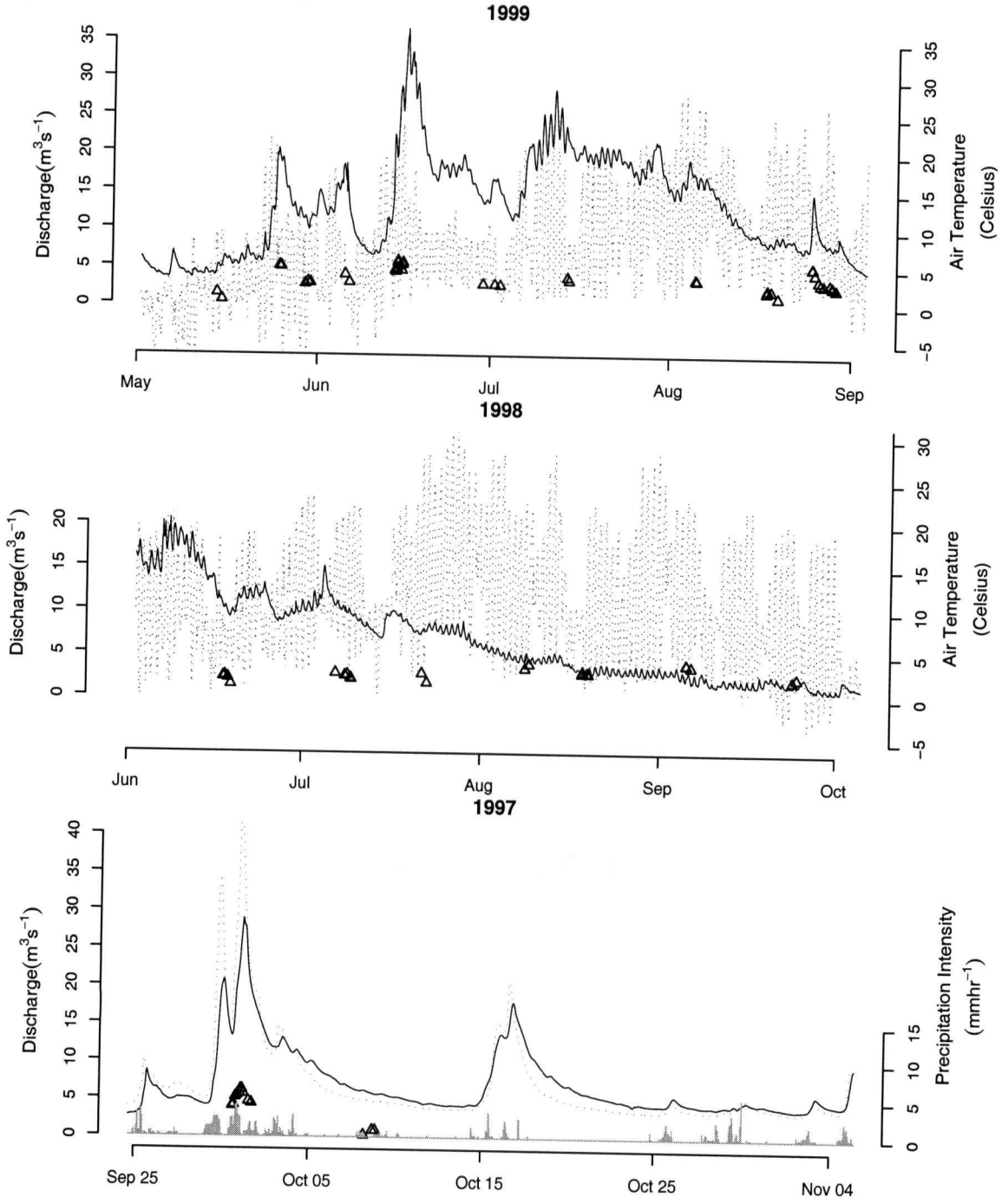

Figure 4.4: Hydrologic Season and Sediment Transport
Examples of SSC response (black triangles-ln transformed data) to runoff during nival (top), glacial (middle) and autumn (bottom panel) seasons for Van Horlick Creek. Air temperature (dotted line) shown for two upper plots. Hydrograph from nearby Cayoosh Creek (lower panel, dotted line) indicates a more flashy response than Van Horlick to precipitation (grey bars).

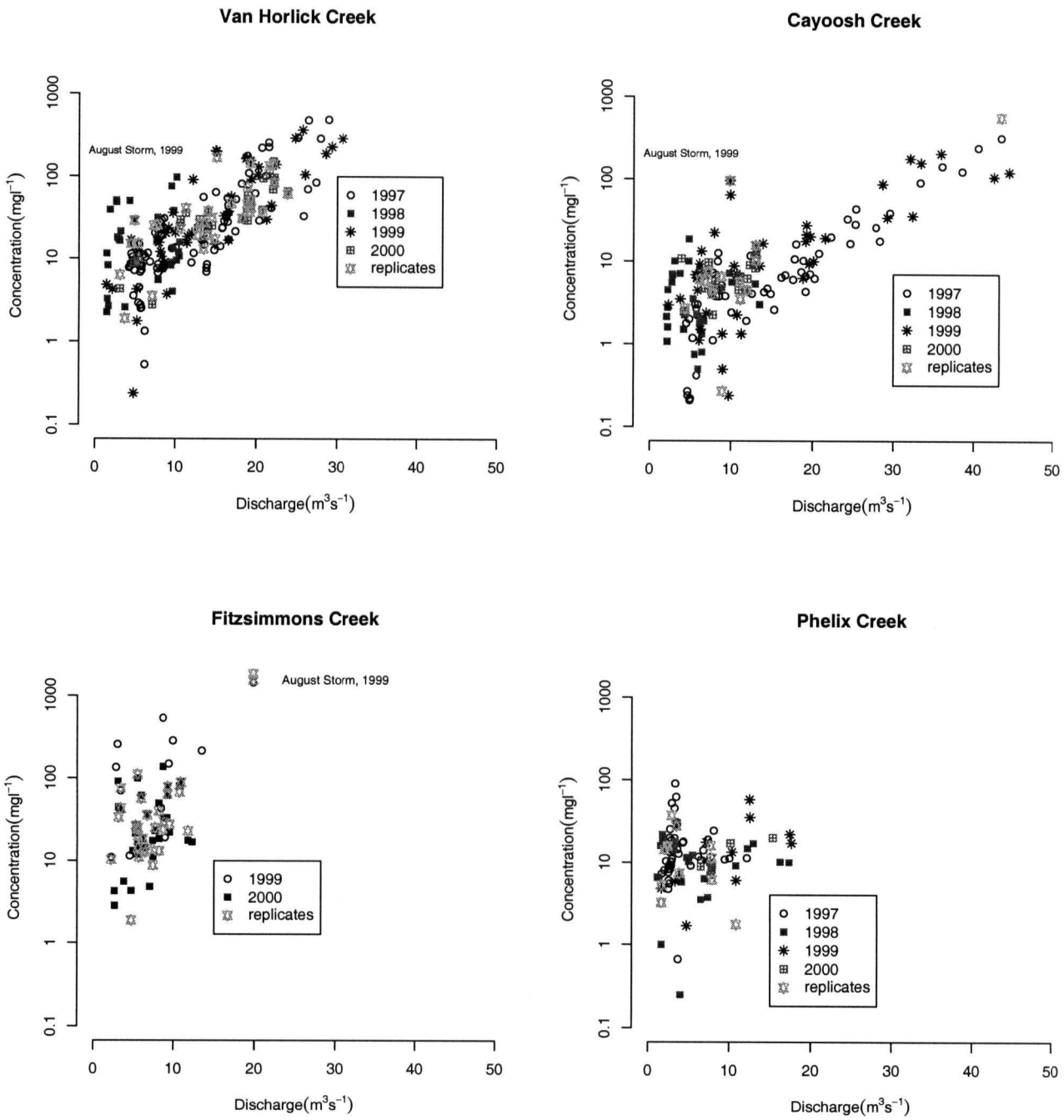

Figure 4.5: Discharge-SSC Relations

Significant scatter remained in the Q-SSC relation after a log transform which likely arises from hysteresis effects (figure 4.5). Observed hysteresis within this study is clockwise during sediment transport events at diurnal time scales but counterclockwise over a given hydrologic season. Sediment availability-exhaustion effects are believed to control this short term hysteresis (Williams, 1989) while changes in sediment texture (and inferred sediment sources) cause the reverse time dependence at seaonal cycles; during nival runoff (snowmelt) sediments available for entrainment are relatively coarse grained and transport can be characterized as supply-limited whereas during glacial runoff sediment availability is unlimited. In addition, entrained glacial sediment can be transported during low water discharge because it is commonly finer-grained than sediments transported during nival runoff. Similar observations have been made for the time-varying nature of sediment transport in glacierized watersheds (e.g. Richards, 1984; Bogen, 1995).

An attempt was made to control some of this hysteresis by examining the relation between other, less direct controls of SSC namely those variables which might control sediment availability or its rate of detachment. These included precipitation intensity $mm\,hr^{-1}$, air temperature and change in discharge (ΔQ). Air temperature was initially included in the regression models as it was hypothesized to influence sediment production and/or variability during periods of sustained glacial runoff. However, it did not appear to increase the predictive capability of the models. ΔQ is calculated by differencing the current flow (lag $_{t=0}$) with discharge at various times in the past. This index has been shown to be an effective explanatory variable in statistical modeling of SSC over a range of spatial scales (e.g. Richards, 1984; Thompson et al., 1987) with the effective lag increasing with increasing drainage area. ΔQ is believed to reduce hysteresis effects (sediment source availability and exhaustion) in the relation between Q and SSC. ΔQ was optimized by determining the highest correlation between SSC and ΔQ for lags between 1 and 500 hours for each of the streams.

For those streams with most complete discharge and SSC records (Cayoosh and Van Horlick), ΔQ was most correlated with SSC at the time scale of approximately one week. Perhaps coincidentally, this is a similar ΔQ time scale observed to influence sediment transport on the Fraser River (Thompson et al., 1987; Thompson, 1987). The similarity in the time scale of such hysteresis effects between these studies would suggest that time-varying patterns of sediment availability are set by climatological events common to the watersheds. To test such a claim, time series of daily 500hPa anomalies between April-November during the period of study (1997-2000) were constructed from NCEP re-analysis data for the study region (45-55N, 120-140W). The annual cycle was removed from the series by subtracting the low frequency trend (lowess fitted curve with 50 percent window) from the data. Spectral analysis of such series (see appendix C) indicates significant power (P¡0.01) at periods between 5-10 days when tested against a red noise background (figure 4.6). Such analysis confirms the suspicion that observed patterns of hysteresis with the SSC data (and Q variations at these time scales) from this study are likely caused by synoptic-scale variations in discharge which are primarily controlled by variations in atmospheric circulation during nival runoff. Such variability is hypothesized to largely control within channel pattern of fine-grained sediment storage and availability. Such synoptic variability relates primarily to snowmelt rather and rainfall-generated runoff.

Hysteresis at seasonal time scales likely creates the observed scatter in lnSSC-Q relations (figure 4.5). More scatter is observed at low flow conditions and contrasts with commonly observed patterns of increasing heteroscadasticity within Q-SSC datasets. Such low flow scatter is believed to be cause by the inter-annual variability of glacial runoff. As the basins are only lightly glacierized, average SSC increases during the glacial melt season but stream discharge is comparable in magnitude to flow during autumn or early spring. Such scatter might be expected to bias load estimates during

years of sustained glacial runoff and the severity of such bias is addressed shortly.

Weighted least squares analysis was used in regression model formulation as a means of stabilizing the variance observed at moderate to low flow conditions. Discharge was used as the weighting function which is a sensible choice in this study as the objectives are to estimate total yield for the basins. The importance of floods in influencing total yield from mountain watersheds is well known (e.g. Church et al., 1989; Pitlick, 1993; Costa and O'Connor, 1995). As in general least squares analysis, outliers have a profound influence on parameter estimation and general goodness of fit tests. Several robust alternatives to least squares exist but because inferential theory and parameter error estimation is largely lacking for such models (e.g. Hocking, 1996) they were not used. Instead, Q-SSC data for each creek were examined graphically noting observations which departed significantly from the main trend in the data and through analysis of the residuals obtained from

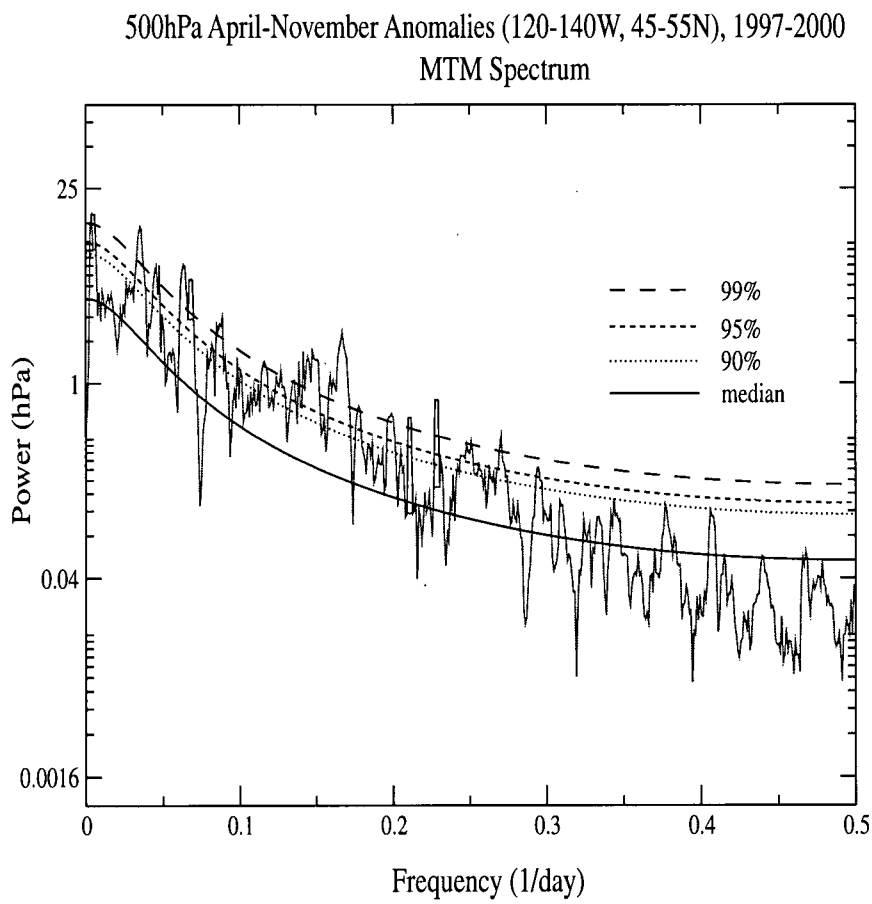

Figure 4.6: Power Spectrum of 500hPa Anomalies
Continuous time series (April-November) of seasonally differenced 500hPa anomalies for area encompassing 120-140W, 45-55N for period (1997-2000). Anomalies obtained by differencing daily average from seasonal trend (derived from fitting lowess regression (window =50 percent of time series) to dataset). Uppermost lines denote 99, 95, 90 percent confidence limits (in order from top) while lowermost line denotes median-reshaped spectrum. Note significance of power at 5-10 day period. Spectra of individual years give similar results. Power calculation and red noise background estimation are discussed in Appendix C.

the least squares models. Adequacy of the models was assessed by plotting the residuals obtained from the linear models and those expected from a normal distribution (quantile-quantile plots). Leverages of outliers from the models were examined using Cook's distance plots and model performance was re-evaluated following their removal. Most outliers occurred at low flow conditions with SSC data usually less than 1.0 $mg\,l^{-1}$ (c.f. figure 4.5) . This mass is close to the analytical precision of the laboratory methods. Because these samples were taken at low flow conditions (late Autumn to early Spring) their removal should not affect sediment transport estimates for the range of flows which are important for the majority of sediment transporting events. Few outliers exist at the opposite end (high flow/SSC) but they were purposely retained in the models given their significance in estimating sediment transport. SSC samples collected during the 1999 August rainstorm are examples of high-end outliers within the Q-SSC data for Cayoosh and Van Horlick Creeks but not for Fitzsimmons most likely due to higher precipitation intensities experienced in the Green Lake basin for this storm. It is likely that additional scatter would occur in the Q-SSC relations if additional SSC data were available which reflected sediments produced during detachment.

Development of individual regression models for each hydrologic season was attempted given the changes in sediment source/texture characteristics through a given hydrologic season. Such partitioning, however, did not improve the predictive ability to model SSC and it remains unknown whether this failure relates to low sample size or whether it reflects a lack of true differences (and or predictability) in sediment transport between season. Many studies have observed significant inter-annual variations in simple rating curves (i.e. Q-SSC relation) in glacierized catchments (e.g Fenn, 1989; Bogen, 1996). Such scatter is believed to relate to complexities in sub-glacial sediment supply and storage processes which are likely to change over inter annual time scales. Indeed, such inter-annual complexities during glacial runoff have recently been observed for a nearby proglacial stream (Place Creek; G. Richards, pers. comm.).

4.4.4.1 Van Horlick, Cayoosh and Fitzsimmons Creeks

Using a minimum number of predictors, sediment transport can be modeled for three of the streams over the period of study. Residuals from the models are autocorrelated, in violation of linear regression theory. The structure likely arises from the sampling design where SSC was collected intensively over time periods of several days and major sampling separated by intervals of a week or more. Standard techniques which could utilize such autocorrelation to improve the predictive capabilities of the model (c.f. Gurnell and Fenn, 1984), however, could not be employed since the time intervals between collection were non-uniform. The addition of air temperature and precipitation decreased the predictive ability of the models. The most likely reasons that sediment transport is poorly predicted by precipitation is the inverse relation between air temperature and precipitation (a surrogate for reduced insolation). Most precipitation events observed in this study were low intensity events and any improvement to the models would occur above some threshold. Similarly, it is also likely that early and late season precipitation events occur as snowfall at higher elevation. Precipitation events during spring may not cause significant detachment if large portions are protected by from rainsplash or rilling by snowcover (Caine, 1976, 1995).

The quality of the regressions and confidence of yield estimates (based on sample size, discharge data availability, and length of record) is highest for Van Horlick and lowest for Fitzsimmons Creek (table 4.3). Malfunction of the Fitzsimmons gauge in 1999 and 2000 precluded the use of hourly discharge data for Fitzsimmons Creek and discharge was estimated by regressing daily flow data for those years of nearly complete record (1993, 1995) for the nival period against flow data from Lillooet River (08MG005) and using this model ($r^2 = 0.87$) to estimate hourly discharge for 1999 and 2000. Inspection of Fitzsimmons SSC time series (not shown) revealed the presence of a

declining trend in sediment transport through the period of monitoring. This trend (t) was used as a third variable in model development and increased the explained variance by approximately 10 percent. The trend is likely real and reflects continual stabilization of fluvial and hillslope sediment sources following a catastrophic flood in 1991. The significance of the event within the context of long-term records of sediment transport will be discussed in Chapters 5 and 6.

Stream	*Model*	*Goodness of fit (model)*	*Goodness of fit (parameters)*
Van Horlick	$ln(\widehat{ssc}) = Q(0.08) + \Delta Q^{a}_{174}(0.07) + 2.05$	$r^2_{adj} = 0.79$; $SE = 1.98$; $d.f. = 185$	$p¡2e^{-16}$for all parameters
Cayoosh	$ln(\widehat{ssc}) = Q(0.06) + \Delta Q_{168}(0.05) + 1.11$	$r^2_{adj} = 0.80$; $SE = 2.35$; $d.f. = 147$	$p¡\begin{cases} 1.95e-08 & int. \\ 6.23e-04 & Q \\ 3,97e-04 & \Delta Q_{174} \end{cases}$
Fitzsimmons	$ln(\widehat{ssc}) =$ $Q_{lill}(1.4e-03) + \Delta Q_{263}(5.72e-03) - (1.48e-04)t^b + 4.58$	$r^2_{adj} = 0.72$; $SE = 11.47$; $d.f. = 47$	$p¡\begin{cases} 1.47e-11 & int. \\ 0.277 & Q_{lill} \\ 7.11e-04 & \Delta Q_{263} \\ 1.34e-04 & t \end{cases}$

Table 4.3: Ln(SSC)-Linear(Q) Rating Curve Models

a. Change in discharge in hours

b. Linear trend through the data

note. Replicate samples were not used in the development of the regression models as they do not represent independent data. Model parameter estimation and general goodness of fits are identical if they are included but their significance changes due to the increased degrees of freedom.

The regression models were used to estimate suspended sediment transport for Fitzsimmons, Van Horlick and Cayoosh Creeks for those periods corresponding to collection of SSC data (1997-2000 for Van Horlick and Cayoosh; 1999-2000 for Fitzsimmons). In addition to gauge malfunction of Fitzsimmons, regression methods were required to estimate discharge for Van Horlick and Cayoosh before installation of stage recorders (May-July 1997) and data gaps introduced by channel change and logger malfunction for the Cayoosh record (appendix A). Based on hydrograph similarity noted between hourly flow data from snowmelt-dominated Nahatlach River (08MF065; 575 km^2), regression models were developed for estimating hourly discharge for both records. Both models explain over 95 percent of the variance in the datasets during snowmelt-runoff.

Load estimates were corrected for negative bias introduced by the log transformations and vary greatly both between station and between year (table 4.4). Estimated load for Fitzsimmons during 1999 is the highest recorded yearly load estimate and was over 6 times greater than the load estimate for the following year. Van Horlick apparently transports over seven times more suspended sediment on average than Cayoosh Creek; reasons for this difference are likely caused by greater sediment availability in the Van Horlick basin. The glaciers in the Van Horlick watershed have well-developed snouts (greater ice flux and perhaps higher basal sliding velocity) and few intervening lakes exist between the glaciers and the monitoring site.When load estimates are normalized by basin area (yield) sediment discharge for Cayoosh Creek ($0.03 \pm 0.02 Mgkm^{-2}day^{-1}$) plot exactly on the regional trend of sediment delivery observed for British Columbia (Church and Slaymaker, 1989; Church et al., 1989). The average yield from Fitzsimmons basin is considerably higher ($0.46 \pm 0.47 Mgkm^{-2}day^{-1}$) and falls within that quadrant characterized as disturbed (by land use and or glaciers). The estimate is also the most uncertain given the use of synthetic hourly discharge data and low number of years (2) contributing to the estimate. Nevertheless, the yield estimate compares favorably to a long term estimate ($0.6 \pm 0.3 Mgkm^{-2}day^{-1}$) derived from additional SSC sampling and the use of daily Lillooet Q data over the period 1947-1999 (Pepola, 2001). Entrenchment into and subsequent failure of Pleistocene valley fill, combined with active contemporary glaciers is believed to be the primary reason for high yields for Fitzsimmons Creek.

According to the regional trend, yield estimates for Van Horlick ($0.17 \pm 0.11\ Mg\ km^{-2}day^{-1}$) could be classified as borderline disturbed while those obtained for Cayoosh Creek are close to the lower bounds of the envelope for British Columbia. The monitoring data confirm the observations made concerning the general lack of fine grained sediment within this sub-basins. When the data from both tributary basins to Duffey Lake are combined, the aggregated yield estimate is very close to the regional trend. The differences between the basins highlights the importance of intervening lakes in influencing sediment yields and the heterogeneity associated with yield estimates from smaller watersheds.

4.4.4.2 Assessment of Bias During Glacial Runoff

Average SSC in all of the streams increased notably during the glacial runoff season (mid July-early September) but bears little direct relation to Q and only weakly to air temperature. Greater availability of sub-glacial sediment (either through enhanced production or entrainment) is the likely reason for this increase as it commonly occurred under clear sky conditions and during late summer. Whatever its source, such an increase would be expected to negatively bias load estimates derived from the regression models. To assess the magnitude of such a bias, sediment loads during a particularly strong glacial melt year (1998) and one with minimal precipitation events were estimated for Van Horlick Creek. A continuous estimate of hourly SSC was constructed through linear interpolation. The interpolation procedure increases estimated loads by 8 percent and indicates that the bias imposed by the regression is relatively minor. True bias, however, is

unknown given the lack of continuous SSC data for the study. Over the period of monitoring, sediment transport during the glacial melt season appears to be less significant than during the nival season. During periods when ice cover was more extensive the contribution of glacial runoff would increase may increase this bias. Thus, the relative importance of nival transfers compared to glacial runoff will be addressed in chapters 5 and 6 through the use of laminated sediment records from Duffey Lake.

Stream	correction factor[a]	1997	1998	1999	2000	mean	sd	c.v.
Van Horlick	1.19	8,722	2,890	13,156	4,385	7288	4628	0.64
Cayoosh	1.33	2,004	698	1,827	618	965	547	0.55
Fitzsimmons	1.33	na	na	22,434	3,506	12,970	13,383	1.03

Table 4.4: Load Estimates (Metric Tonnes) Obtained From the Rating Curves

a. Correction factor applied to load estimates to account for bias introduced in estimating central moment from log normally distributed data. Correction factor non-parametrically estimated from $\Sigma_{i=1}^{n} exp(e_i)/n$ where e_i represents the ith standardized residual from the multiple regression model (Thompson, 1987).

4.4.4.3 Phelix Creek

Sediment discharge from Phelix Creek can not be predicted with any degree of confidence. This complexity between runoff and SSC exists within a given year but also throughout the period of monitoring (figure 4.5). Instantaneous discharge and SSC are not significantly correlated ($r = 0.034; n = 89; p = 0.75$) but there is a weak correlation ($r = 0.44; n = 79; p¡4.0e^{-05}$) between ΔQ_{159} and SSC. The poor relation between Q and SSC may result from a combination of factors including inadequate sampling (frequency and design), physical characteristics of the channel, or non-linear availability of sediment available for transport. Phelix Creek was less intensively sampled during this study due in part to logistical reasons but also because the non-predictable nature of suspended sediment transport was observed early in the project. Channel morphology and sediment storage patterns are also hypothesized to contribute to the inability to predict sediment transport. Upstream and downstream (about 1 km each direction) of the monitoring site, Phelix Creek flows across a broad delta surface as a single to multi-thread channel with significant stores of in and across-channel woody debris behind which sediment wedges have accumulated. Above the monitoring site the channel is constrained from lateral shifting along its left bank by a terrace of unknown age and there is much evidence for intermittent failure of the material. It is speculated that sediment is supplied to the channel from such sites in an unpredictable fashion. Other confounding effects that may influence sediment transport at this site include variable delivery of sediments introduced by recent land use (forest clearance and or limited agriculture) in low lying areas above the monitoring site. Whatever its cause, sediment transport over at least the period of monitoring can not be predicted in any meaningful way.

4.4.5 The Significance of the Infrequent Event

In many environments bankfull discharge occurs infrequently but transports the majority of total load especially in small, mountain catchments (e.g Baker and Costa, 1987; Church et al., 1989; Costa and O'Connor, 1995). Such effects are evident for the basins of this study when the data

are normalized by total load and the duration of its transport (figure 4.7). For example, over 60 percent of annual load in 1997 was routed past the gauging site on Cayoosh Creek in a period of 2 days (one day during snowmelt, the other during autumn). Such effects are also noted for Van Horlick but based on the load estimates of this study, autumn precipitation events appear to be less important for overall sediment transport during the year. Such differences are believed to reflect not only differences in hydrologic response times, but also suggest important controls of sediment availability within the sub-catchments. Fine-grained sediment storage in the channel of Van Horlick and directly (i.e. no intervening lakes) coupled contemporary glaciers likely explain the 4-8 fold difference in sediment yields from the corresponding sub-basins of Duffey Lake. Though the data are less secure, extreme events within the Fitzsimmons load time series are also evident where approximately 60 percent of the calculated load was mobilized and routed over 2 events in 1999 (nival and late summer event discussed earlier). In short, the monitoring data indicate that a large proportion of the year's total sediment load is mobilized and routed to the lake systems of this study infrequently and over a relatively short duration and agree with lake-based estimates of sediment yield for larger watersheds within the southern Coast Mountains (e.g. Desloges and Gilbert, 1994a,b).

4.5 Lake Monitoring

Limited CTD profiles from Duffey and Green Lakes indicate that the lakes become weakly to moderately stratified during summer primarily caused by net additions of energy to the water surface as the waters are low in dissolved and suspended sediments (2-30 mgl^{-1}). Lack of detailed temperature profiling through the summer does not allow an assessment of whether inflow events or climatological events favoring large wind stresses disrupts summer stratification as observed by Gilbert (Gilbert, 1975) for Lillooet Lake. Such temporary disruptions probably do not completely destroy the overall seasonal thermal structure. Five of the lakes developed a shallow (20-30cm) ice cover which usually forms in late December and lasts through April. Logistical difficulties prevented an assessment of whether the sixth (Glacier Lake) was ice covered during winter. Based on the limited data collected, the lakes can be classified as dimictic, with overturning occurring during early spring and late autumn, a common feature of temperate lakes (Hkanson and Jansson, 1983).

Stratification is likely to be an important factor in effective sediment transport within the epilimnion during the snow free period. Before stratification develops, sediments entering to the lake basins are most likely those channel sediments entrained during early season snowmelt runoff. The coarser texture and lack of thermal structure (isothermal lake water and low temperature of inflowing streams) likely delivers the sediment to deepest, unobstructed areas of the lake basins as low concentration turbidity flows. As stratification develops, a coincident increase in glacially derived sediment allows more effective sediment transport throughout the lake basin. The significance of stratification was apparent during late summer, 1998, when an apparent overflow event was observed. Surface waters of both lakes during this time were between 12-15 °C. Over an approximate 2 week period during late August, high loading of glacial silts from major inflows to Duffey and Birkenhead Lake significantly increased lake turbidity and lake outlet streams which are almost always visibly clear were grey-green in color. Such overflow events appear to be particularly effective in distributing fine grained sediments throughout the lake basins of this study and elsewhere (Gilbert, 1975).

The sediment traps located in proximal and distal settings of the lake basins (Duffey and Birkenhead) provided a means of quantifying which hydrologic season was most important for pelagic sedimentation in proximal and distal setting of the lakes. Daily sediment flux ($g\ m^{-2}\ day^{-1}$) to the lake floors as recorded by the four lake sediment traps over a given year and over

inter-annual time scales reveal:

1) Sedimentation patterns within the lake basins, as expected, mirror the seasonal hydrographs of the basins with maximum flux rates observed during nival runoff (figure 4.8). Though lake sedimentation follows the annual hydrologic cycle, high fluxes can occur in years with sustained glacial runoff (e.g. 1998) or during those years with early-season (i.e. snow free) autumn precipitation events (1997). Maximum hourly discharge over the observed hydrologic season is most highly correlated with lake sedimentation but the strength of the relation varies within and between lake (figure 4.8). Relation between sedimentation and other indices of discharge (mean or total flow) give much poorer results. For Duffey Lake, there appears to be a simple, linear-log relation between maximum discharge events and concurrent lake sedimentation but the clarity of the relation decreases downlake. This likely indicates that although sediment transport to the lake basin can be predicted easily, its transport to deeper water environments is complicated by within-lake processes of sediment re-distribution.

2) Minimal lag exists between fluvial sediment transport and lake sedimentation events, as observed in other mountain lake systems (e.g. Gilbert, 1975; Smith, 1978) within the Canadian Cordillera (figure 4.8). In contrast to commonly observed sedimentation events induced by lake overturning (e.g. Hkanson and Jansson, 1983) sedimentation events during autumn appear to be directly controlled by the frequency and intensity of rain-fall generated floods. Generally low sediment fluxes during autumn were observed in those years of negligible autumn runoff events (e.g. 1998, 1999, figure 4.1).

3) Highest sediment fluxes are recorded closest to areas of major lake inflow (figure 4.8) and interpreted to reflect sediment transported by both interflow and overflow processes. Low concentration turbidity flows often exceed 2m in thickness (e.g. Gilbert, 1973; Lambert and Hs, 1976; Lambert et al., 1976), the height at which the sediment traps were suspended above the lake floor. The significance of turbidity currents in controlling unconformable sedimentation within the lake basins is likely to be great.

4) Clastic and organic sedimentation appear to be non-linearly related (figure 4.9). The inverse relation has been qualitatively (Desloges and Gilbert, 1998; Leonard, 1986b) and quantitatively (e.g. Souch, 1990, 1994) inferred for oligotrophic lakes though the form of the relation has varied between studies. In this study, the relation appears to be non-linear for both lakes in contrast to the data presented by Souch (1994) for a proglacial lake in the Coast Mountains. Reasons for the difference are unknown. The relatively simple relations provide a means of inferring gross-scale changes in sedimentation rates within the non-laminated portions of the sediment archives as a function of bulk physical property changes.

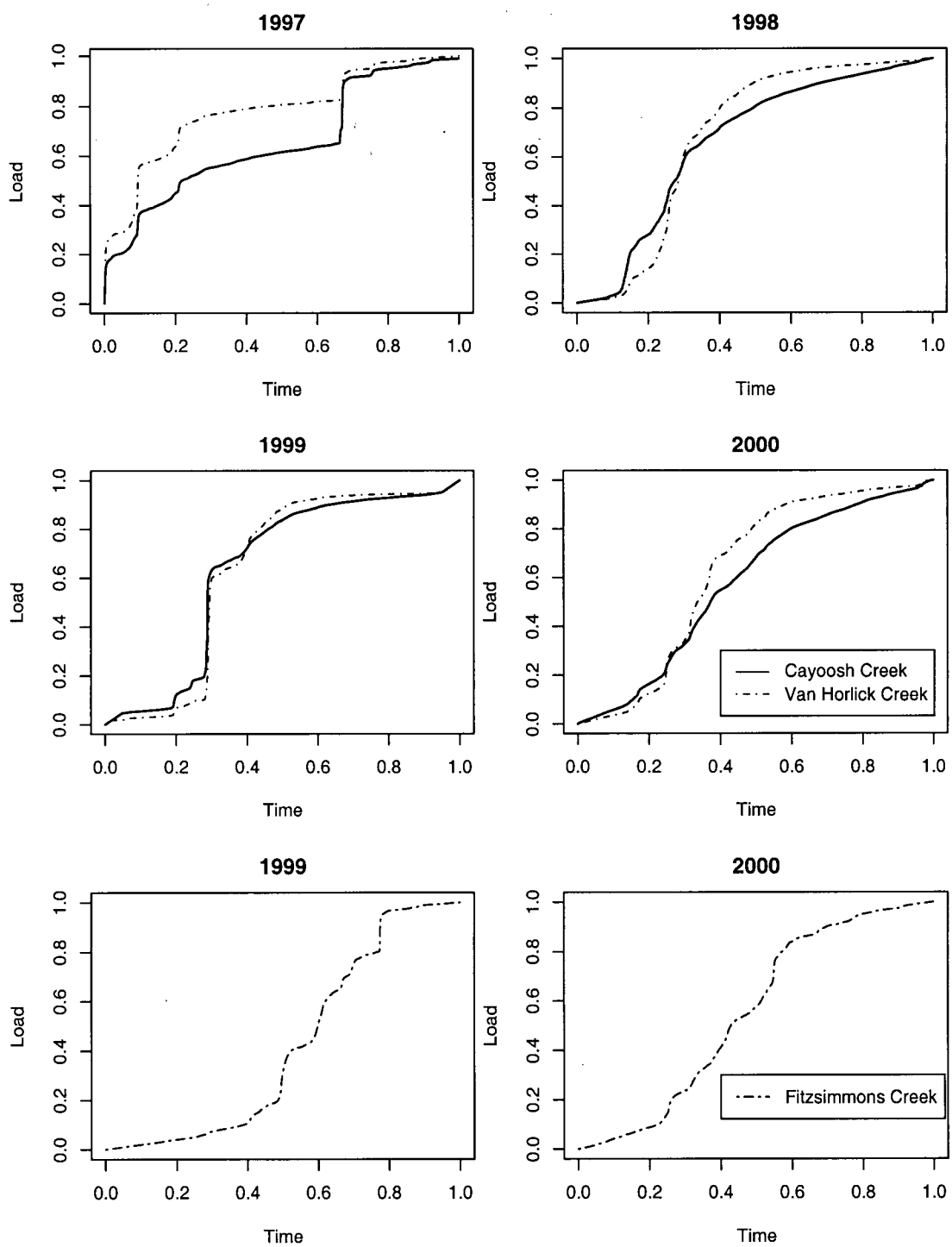

Figure 4.7: Fractional Load Estimates
Load estimates for Cayoosh, Van Horlick (first 4 panels) and Fitzsimmons (last 2 panels) Creeks during the study. Loads appear artificially high for 1997 during early season because SSC collection commenced in mid-May when flows were of moderate discharge.

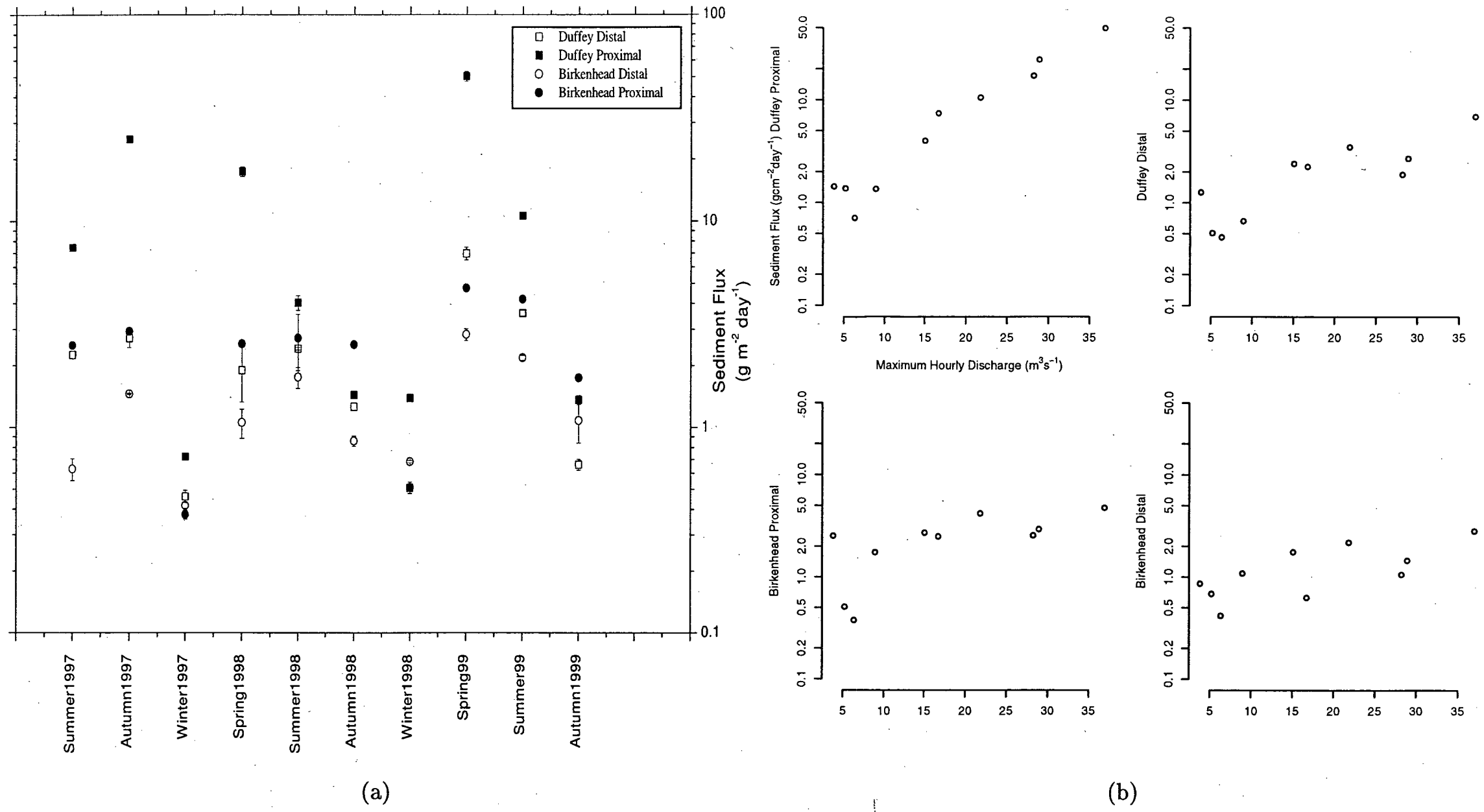

Figure 4.8: Stream Discharge, Lake Sediment Flux, Birkenhead and Duffey Lakes

a. Seasonal sediment flux to lake floor ($gm^{-2}day^{-1}$) for Birkenhead and Duffey Lake Basins. Error bars denote ($\pm 1\sigma$) uncertainty in estimate.

b. Relation to maximum hourly discharge (Van Horlick Creek) as a function of location and lake. Maximum discharge was better predictor of lake sedimentation than average discharge or total inflow. Discharge estimates for winter required interpolating between early winter-early spring hydrographs due to ice within channel. Use of Phelix Creek data for Birkenhead does not decrease scatter for Birkenhead Lake.

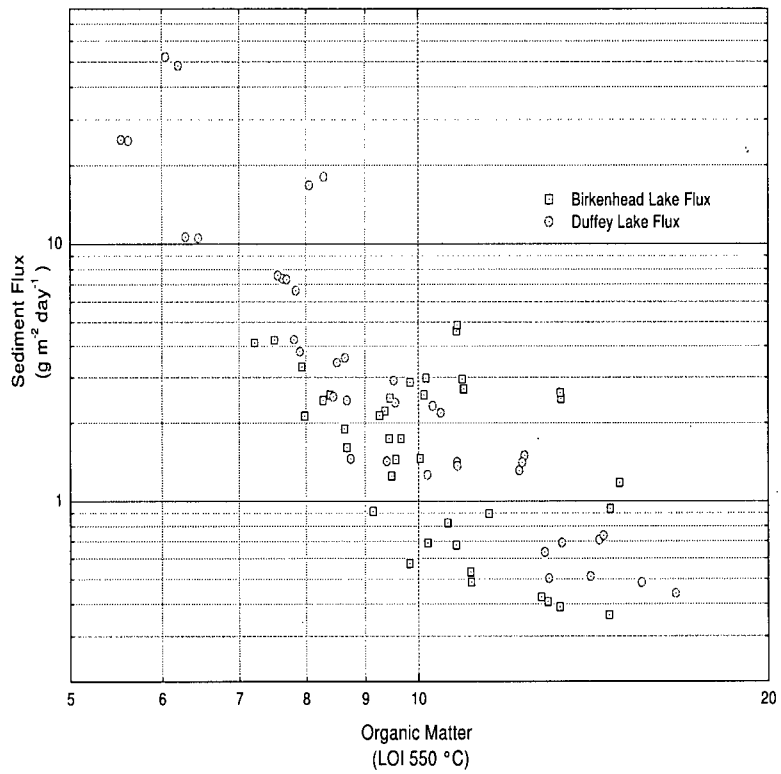

Figure 4.9: Sediment Flux, Organic Matter Relations, Birkenhead and Duffey Lakes

4.6 Conclusion

The monitoring program indicates that streamflow variability from the basins examined in this study originates from snowmelt. There is much similarity in flow events at event to seasonal time scales. Sediment transport occurs most regularly during nival runoff with major sediment sources located in those sub-basins with contemporary ice cover and little opportunity sediment storage such as in proglacial lake basins. A large majority of sediment transport in Fitzsimmons Creek occurs infrequently and during hydrologic events which favor detachment of sediment from exposed surfaces such as fluvial scarps and failing terraces in the main valley and glacial forefield areas. For the Duffey Lake basin which is located further from the Coast and is higher in elevation, most sediment transport during high flow events occurs during snowmelt runoff and can be predicted using only discharge and change in discharge with an acceptable degree of confidence. Sediment transport for the fourth stream (Phelix Creek) is unpredictable and reasons for the unpredictable nature of sediment transport remain uncertain. Speculatively, the factors may include irregular release and entrainment of sediment due to large woody debris. Sediment transport during sustained glacial melt increases SSC but because low fractions of the watersheds are glacierized, there is no coincident increase in runoff. Glacial runoff during periods when contemporary ice cover is more extensive may be expected to alter the overall significance of SSC production and transport during the glacial runoff season.

Linkages between sediment transport and climate appear to be complex at the monitoring scale and controlled primarily by flood magnitude. For those streams entering Duffey Lake, the linkages between major modes of wintertime climate and high runoff events are likely to be greatest because the basin experiences most sediment transport during snowmelt dominant floods. Although

such floods can occur in low snowpack years, intense floods generated during snowmelt require deep snowpacks which are common during years when wintertime temperatures are cool and precipitation anomalies are large. The stability of the observed climate-sediment transport relations over longer time periods is considered in Chapter 5.

Chapter 5

Inter-annual to Decadal Scales: Fine-Sediment Production and Transport

5.1 Introduction

The results from the previous chapter indicate that fine sediment production, entrainment and ultimate deposition within the lake basins of the study area are primarily controlled by the frequency and intensity of high magnitude runoff events resulting from snowmelt and or precipitation events. Smaller quantities of sediment are delivered to the lake basins during the glacial runoff season. This chapter examines the stability of such relations during the contemporary period (1880-2000AD). Sediment yields for three of the lake basins (Duffey, Birkenhead, and Green) are compared to those estimates derived from the monitoring program as a means of comparing the methodologies but more importantly, to assess the reliability of using sediment indices developed from spatially restricted coring sites to represent lake-wide patterns in sedimentation. Laminated sediments with resolution sufficient to assess spatial and temporal patterns of inter-annual sedimentation were present in four of the lake basins of this study and are interpreted to be clastic varves. A varve interpretation can be verified in two of those basins through radiometric dating (^{137}Cs) and by repeat coring during the period of study. Correlation of varve thickness to hydroclimatic data for the other two basins strongly suggests that these lake basins also contain annually resolvable sediment archives though an unequivocal varve interpretation awaits independent dating. The chapter begins by first detailing the contemporary record of hydro-climate variability within the study area. Description and interpretation of the sediment archives are then discussed and the fraction of variance within the varve chronologies which can be attributed to hydro-climate are detailed. Those effects caused by changes in sediment availability are discussed and followed by a comparison between the fluvial and lake-sediment yield estimates for the watersheds.

5.2 Analysis of Hydro-climatic Variability During the Contemporary Period

There is sufficient reason to expect linkages between fine sediment transport and climate variability, because as discussed in Chapter 2, sediment production and entrainment is partially controlled by variations in precipitation and temperature anomalies. One of the principal reasons for selecting southwest British Columbia for this project was that a relatively dense network of long term, hydro-meteorological stations has likely captured variations in climate which are believed to influence sediment transfers within the study area. Such data provide a means to assess and calibrate spatial and temporal variations in sediment delivery for the last 100 years. Important trends and departures from those records are isolated as they provide a means of controlling for climate variations within the study area.

5.2.1 Temperature and Precipitation Variability

A closer inspection of the meteorological and streamflow data from the region indicates that few high quality records exist where large data gaps are absent or where station relocation has severely compromised the usefulness of the records for calibration and or removal of climatic signals from the sediment records. There is an effort to rehabilitate some of the meteorological records within

Canada (e.g. Mekis and Hogg, 1999) but at the time of this writing, the number of available stations within the southern Coast Mountains is severely limited. Fortunately, one of the longest (> 100 years), and most complete records of monthly precipitation and temperature anomalies is close to the study site (Aggasiz) and effects imposed by human development (e.g. heat island) are minimized because the site and surrounding area remains undeveloped. The data are part of the WMO's national historical climatological network and passes most tests for inhomogeneity and stationarity with respect to location and scale statistics (Zhang et al., 2000; Peterson and Vose, 1997). Nine additional stations (7 from WA, 1 from BC) were analyzed in conjunction with the data from Aggasiz because of their proximity to the study area, their high quality, and the length of usable record (table 5.1).

The use of multiple stations from within a homogeneous climate region minimizes possibility of false or erroneous trends arising from equipment malfunction and or effects of urbanization. The data set contains relatively few missing values (table 5.1) and where possible, missing data were replaced by estimating (least squares regression) the values from other stations within the network which were most highly correlated to the station of interest. Mean temperatures represent the average of monthly averaged daily maximum and minimum temperatures. Two distant stations (Olympia, WA and Big Creek BC) are combined with the more local meteorological network because the analysis seeks to extract that proportion of the variance common to all stations. Thus, a common signature between the stations is taken to indicate changes in precipitation or temperature trends likely arising from large-scale changes in atmospheric circulation patterns.

Station	Location	Useable Record (yr)	Temp (°C)	Precip ($mm\ month^{-1}$)
Aggasiz (BC)	49.25N 121.77W	97.58 (99.5)[a]	10.4±5.7	136± 91
Bellingham (WA)	48.72N 122.52W	NA (92.08)	NA	72± 48
Big Creek (BC)	51.70N 123W	83.58 (NA)	2.9±8.6	NA
Blaine (WA)	49N 122.75W	NA (93.75)	NA	86± 51
Clearbrook (WA)	48.97N 122.33W	92 (NA)	9.3±5.4	NA
Olga (WA)	48.62N 122.80W	104 (100)	9.6±4.3	61±45
Port Angeles (WA)	48.12N 123.43W	103.25 (93.75)	9.1± 4.2	NA
Port Townsend (WA)	48.12N 122.75W	98.75 (97.5)	9.8± 4.3	40±27
Sedro Wolley (WA)	48.50N 122.90W	98.92 (93.33)	10.2± 4.8	97 ±63
Olympia (WA)	46.97N 122.90W	NA (92.42)	NA	109± 95

Table 5.1: Available Long Term (n≈100yr) Records of Monthly Precipitation and Temperature Anomalies 1889-1997

a. Years of usable record. Temperature (precipitation)

Stations were chosen to according to quality of the data, length of usable record, and proximity to the study area. Long records exist which are closer to the study area (e.g. Gozales Heights, Victoria B.C.) but have not been corrected for significant inhomogeneities detected in the datasets. Monthly precipitation (1889-1989) and temperature (1890-1997) reflect largest common period of overlap with the least amount of missing data. Station statistics (mean and variance) determined before replacement of missing values

Location and scale statistics from the stations in the network are largely similar for the analyzed stations with the exception of the more northerly and interior location of Big Creek, BC where average monthly temperature is significantly lower (one sided t-test) than the average of the combined station network (table 5.1). Very good ($r^2 > 0.9$), linear relations exist between stations (not shown) but the relation between Big Creek (temperature) and the other stations is slightly non-linear suggesting inhomogeneity in the dataset presumably from instrument relocation, malfunction or both. In order to guard against such effects, principal component analysis (PCA; Appendix C) was used to extract the "signal" common to all stations (e.g Mann et al., 1998). The first principal component (PC) from the temperature and precipitation data explains over 91 and 84% of the variance within each dataset respectively and are believed to represent the dominant precipitation and temperature variations over the contemporary monitoring period for study area. The PC's were not rotated as second and successive eigenvalues are poorly differentiable and because they explain such small proportions of variance within a climatically homogeneous region, they likely carry minimal climatic information (Preisendorfer, 1988; Cheng et al., 1995).

Secular trends and low frequency components of the first principal components revealed by Lowess regression (e.g. Cleveland, 1979)and cumulative departure plots (e.g. Buishand, 1982) indicate cool and wet conditions in the 1920's and late 1970's and warmer and drier conditions during the late 1890's, 1935-1945 and following 1980 (figure 5.1).

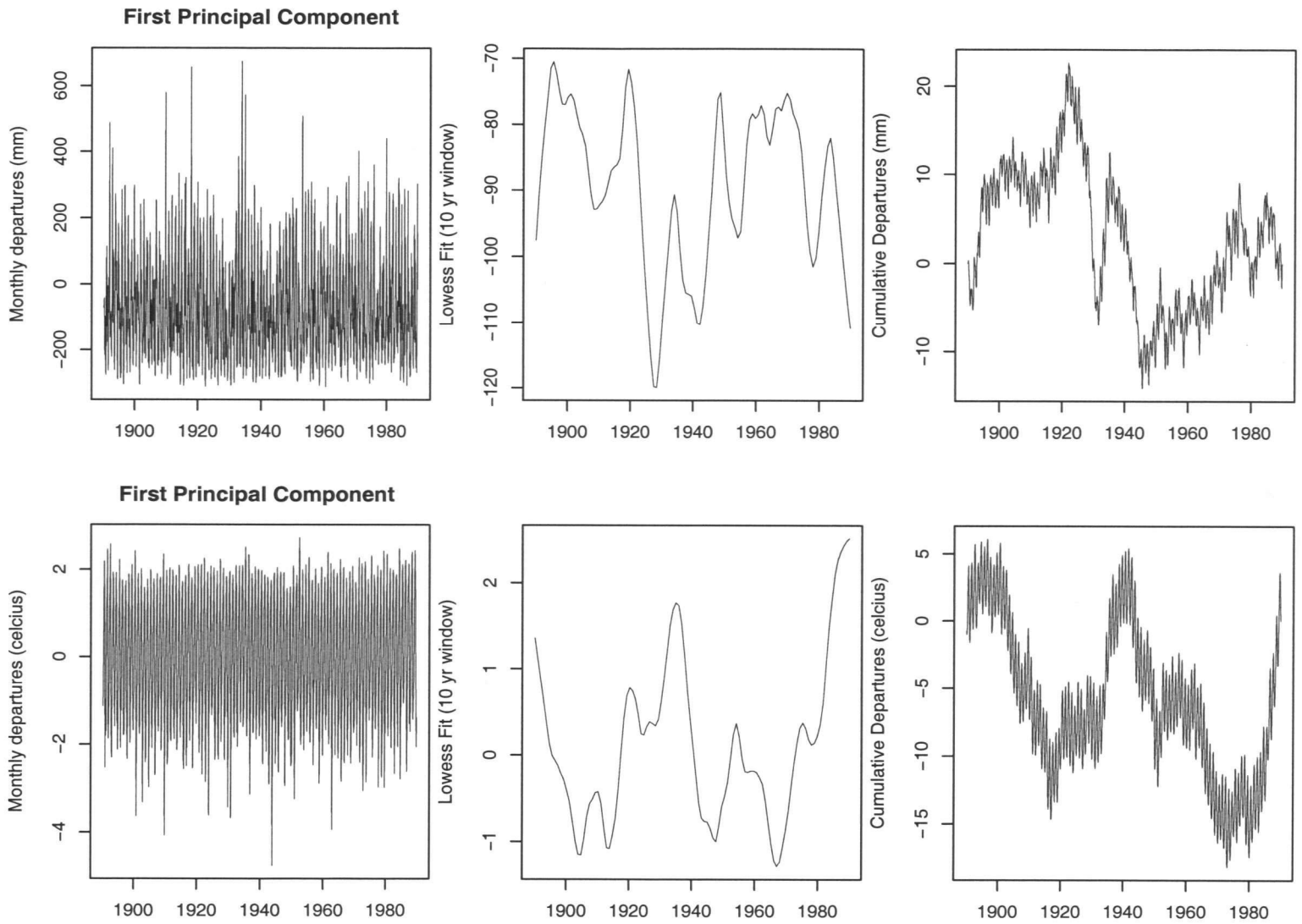

Figure 5.1: Regional Departures in Monthly Precipitation and Temperatures
Regional anomalies based on 1889-1989 (precipitation) and 1890-1997 (temperature) period. Normals shown in table 5.1.

Seasonal decomposition of the records indicates that both precipitation and temperature during the winter season (November-March) explain most of the variance within the annually aggregated data. Monthly precipitation and temperature are inversely correlated ($r = -0.49$; $n = 1200$; $p < 2.2e^{-16}$) and remain highly significant ($n = 200$; $p < 9.6e^{-14}$) when corrected for effective sample size (Appendix C). The PC's were compared to large-scale atmospheric indices (e.g. PDO, ENSO and PNA) discussed in Chapter 2 but only variations in the PDO were similar in phase and amplitude to those changes found in monthly temperature and precipitation anomalies. Zero-lag correlation between the PDO and the temperature and precipitation time series are only weakly correlated. Autocorrelation functions of the PDO time series (entire monthly record) indicate statistically significant persistence in the time series up to 7 years when tested against a white noise model. Such memory and its apparent influence on inter-decadal climate variations in the study area can be readily seen by comparing cumulative departure plots of the first principal components (temperature or precipitation) and the PDO (figure 5.2). Cumulative departure time series of the PDO and air temperature track one another for most of the period of common overlap (1920-1996) but diverge in the early portion of the records (1900-1920). The reason for the divergence is unknown but may include errors in early air temperature measurements or problems in the sea surface temperature dataset from this time caused by either low number of observations and or changes in measurement procedures. Similar, early 20th century discrepancies are noted between comparisons of the PDO and proxy (Linsey et al., 2000) and historic constructions of sea surface temperature variations in the Pacific and North Pacific region.

Frequency decomposition of the temperature and precipitation time series indicate a significant proportion of the variance is at the decadal scale, an observation made for gridded precipitation data from the Pacific Northwest over approximately the same period (Cayan et al., 1998). Most notable in all of the time series (ppt., temperature, and the PDO) is the very large anomalous behavior during the late 1920's to the mid 1940's coincident with large-scale drought conditions in North America. This period is known informally as the 'Dust Bowl' and the 'Dirty 30's' (figure 5.1).

5.2.2 Inter-annual Variations in Discharge and Flood Frequency

Changes in mean flow or flood frequency can be expected to influence fine-sediment entrainment and transport. Therefore, an evaluation of inter-annual to inter-decadal changes in extreme runoff events may highlight trends that explain changes in sediment delivery to the lake basins. The monitoring results indicated the importance of flood on total sediment transport and so it is important to determine the stationarity of flooding in the study area and whether such events represent climatic noise or are related to a particular climate state. If they are unpredictable and completely random through time then they likely represent climatic noise and will not provide any insight into past climate variability despite their significance for sediment transport.

5.2.2.1 Lillooet and Cheakamus Discharge Records

Similar to the meteorological data, a closer inspection of streamflow records in proximity to the study area (c.f. figure 3.1) reveals few long-term, hydrologic records without large data gaps. A stream gauging site existed near the outlet of Green Lake from 1922-1948 but almost half of the reported daily data are estimates rather than true measurements. One of the longest and most complete records from southern British Columbia is from Lillooet River (08MG026) and its central location in the study area makes it a particularly useful dataset. The streamflow record is considered to be high quality and there does not appear to be any rating shift or gauge malfunction over the

period of record (Mr. Duncan, Environment Canada, pers. comm).

Runoff from the Lillooet River is a combination of snowmelt and glacial runoff (14% glacierized) and there is high inter-annual variability in mean annual flow and skewness of the annual hydrograph. Long-term variations in discharge reflect primarily variations in winter snowfall and trends are similar to those snowmelt dominated catchments in southern British Columbia. The transitional environment of the Lillooet River basin causes the annual flood (Q_{max}) distribution to be mixed between snowmelt (S), rain-on-snow (ROS) and rainstorm (R) generated floods (figure 5.3).

R floods are most common during autumn when frontal precipitation originating from cyclonic activity crosses the study area. In general the most intense floods occur during autumn but are limited in their spatial extent. Snowmelt floods are more common, less intense and appear to be more regionally distributed across the Coast Mountains but occur infrequently whereas snowmelt generated annual floods are less intense but occur with much greater frequency (figure 5.4).

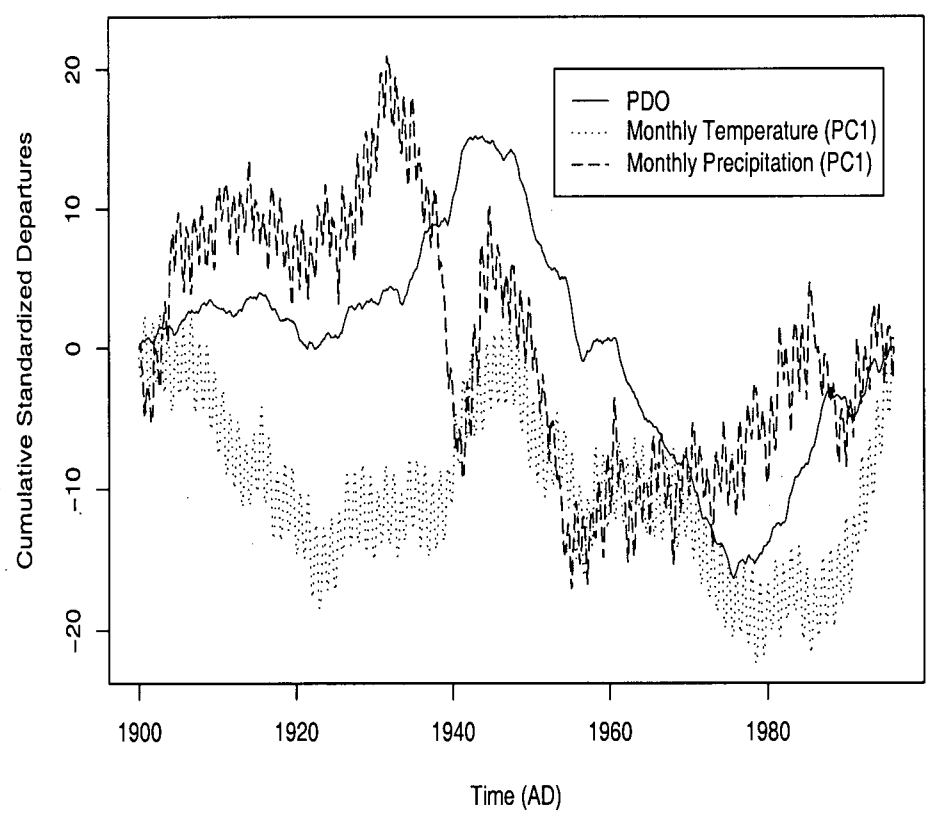

Figure 5.2: Cumulative Standardized Departures of PDO, Temperature and Precipitation for the Period 1900-1990

PDO values (monthly) scaled (divided by 10) to allow comparison to monthly average temperature and precipitation PC's. Precipitation PC based on monthly precipitation total (mm) and temperature PC represents average of monthly min-max values.

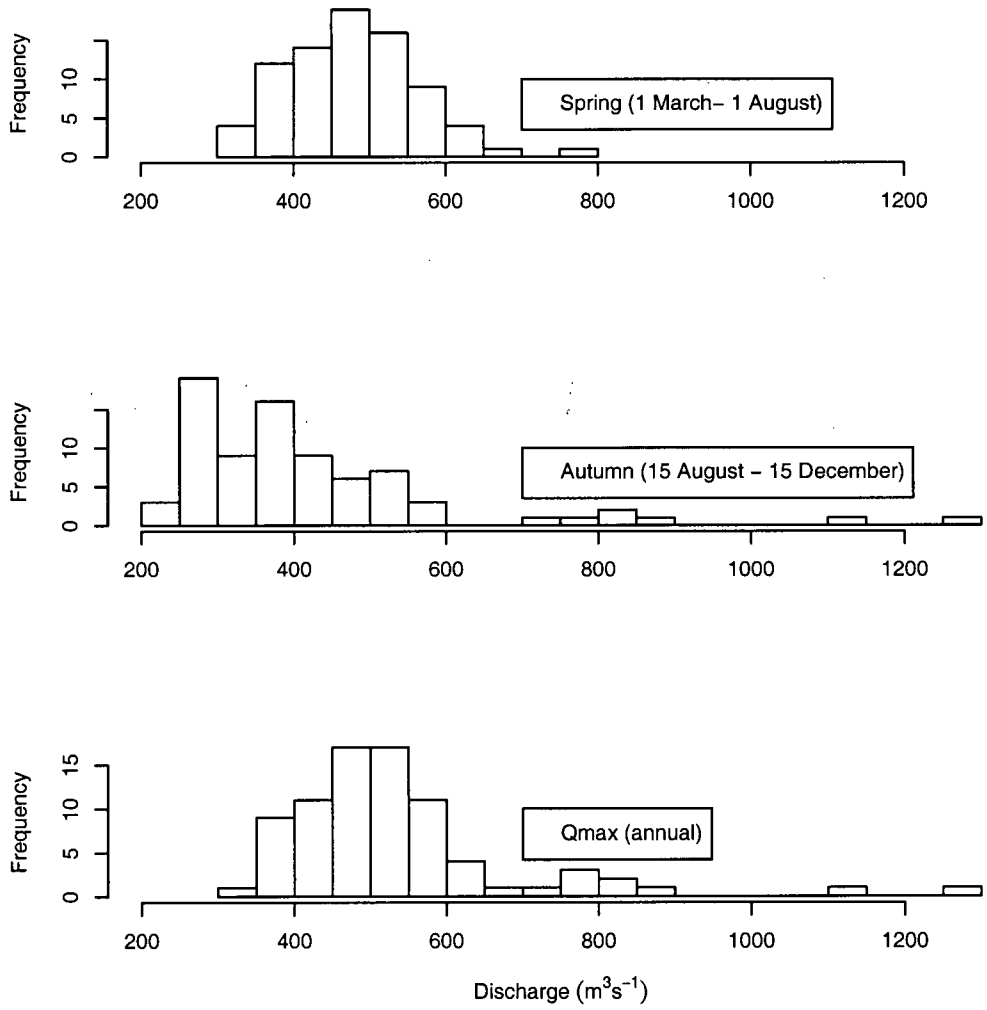

Figure 5.3: Q_{max}, Spring (3/1-8/1), and Autumn (8/15-12/15) Flood Distributions, Lillooet River Nival flood distribution more closely approximates a normal distribution compared to runoff events during the snow-free season. Differences in the underlying distribution of the forcing mechanisms for flooding (i.e. extremes in air temperature vs. rainfall intensity) are the most likely cause for such difference.

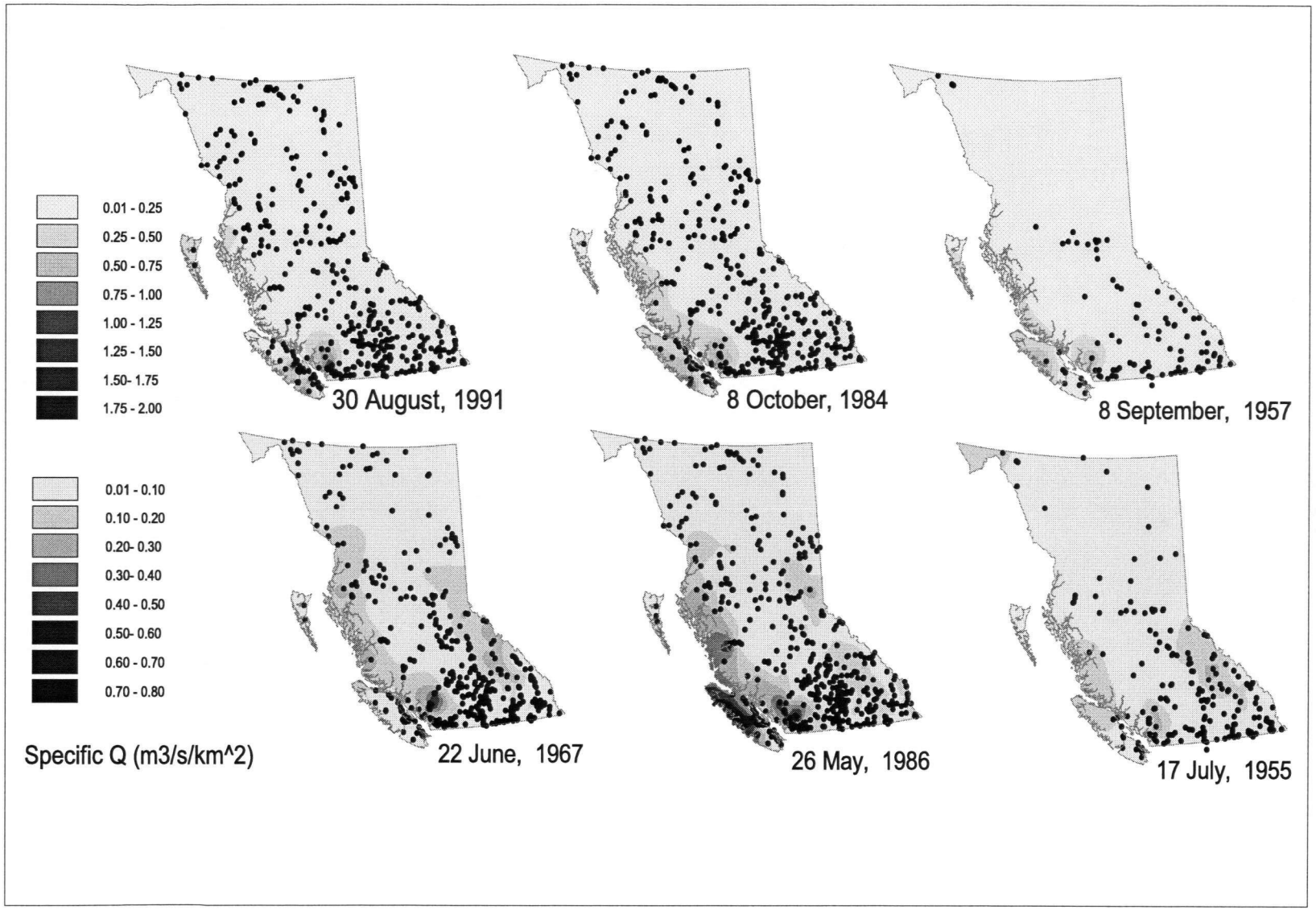

Figure 5.4: Spatial Distribution of Specific Flow ($m^3 km^{-2} s^{-1}$) When Lillooet River Discharge Exceeds 700 $m^3 s^{-1}$
Note that autumn runoff events (upper 3 panels) generate higher specific flow but are more spatially restricted than floods during the nival season.

The Q_{max} record fails a runs test ($n = 72$; $p < 2.2e^{-16}$) suggesting that floods within the Lillooet River Basin are not randomly distributed through time. Such memory is apparent in both annual flood time series and cumulative departure plots (figure 5.5). Inspection of the annual flood record and daily flow in excess of the long term mean (536 m^3s^{-1}) indicates a substantial increase of extreme events following 1970 (figure 5.5) and likely explains the notable increases in large sedimentation events in Lillooet Lake (Desloges and Gilbert, 1994b). Most of the floods following 1970 are R rather than S or ROS events. Between 1977-1998 the probability of Q_{max} events occurring during autumn (15 September-15 December) on the Lillooet River for any given year was 0.33 but decreases to 0.23 for the period 1923-1976. The flood record was broken into these two different periods to account for the abrupt change in northern hemispheric circulation patterns following 1977 which appear in a number of hydro-climatic time series from western north America (Ebbesmeyer et al., 1991).

Analysis of monthly meteorological data (e.g. autumn precipitation totals and temperatures) does not indicate any statistically significant increase in autumn precipitation totals. Similar conclusions were drawn for a more regional analysis of seasonal rainfall intensities (daily) and totals for southwest British Columbia (Stone et al., 2000) though the analysis was completed on pooled station data (10 in southern British Columbia) rather than on a station-by-station basis. An assessment of changes in maximum daily rainfall during autumn for several meteorological stations near the study area was attempted but practically all records have large gaps of missing, estimated, or incomplete data.

The increase in extreme runoff during autumn could conceivably be caused by increases in air temperatures as higher temperature could cause a decrease in the proportion of snowfall at higher elevations but notable changes in air temperatures during fall is not apparent. To test whether the increase of flooding was related to large-scale climate variability, Autumn (1 August -15 December) and Q_{max} events were compared to the seaonal and annually averaged atmospheric and ocean indices (PNA, ENSO, PDO). Neither Q_{max} nor autumn flooding showed any zero lag correlation to the indices but surprisingly, autumn floods are weakly correlated ($r = -0.39; p = 0.001; n = 70$) to ENSO (annual average of SOI index) the following year (figure 5.6). The significance of the correlation changes little if the discharge data are log transformed, by examining the association non-parametrically (Spearman Rank Test), or by investigating the correlation for subsets of the data (prior to and following 1977). Cumulative departure series of the SOI indicate, much like the flood time series, an abrupt change in the behavior of ENSO following 1977 when there was a greater frequency of years where eastern equatorial SST's were warmer than average (figure 5.6).

Though the correlation is significant, it is difficult to explain physically as it suggests that the intensity of the autumn flood for Lillooet River is a precursor for SST variability in the tropics. The correlation may simply arise from chance but as discussed in Chapter 2, a recent study demonstrated a similar lead relation between wintertime precipitation intensities during winter and ENSO conditions the following year in western North America (Higgins et al., 2000). Based on evaluation of NCEP data, the cause of the relation was hypothesized to result from teleconnections between the eastern and western Pacific regions prior to the onset of ENSO. Upper level moist air from large scale convection near Indonesia is advected into western North American regions by the jet stream and and appears to be more prevalent during ENSO events. Further work is needed to assess the significance of such a linkage within the study area and British Columbia given the importance of autumn precipitation events in controlling sediment transport within the study area (e.g. Desloges and Gilbert, 1994b) and elsewhere (Desloges, 1987).

5.2.3 Conclusion

Analysis of hydro-climatic datasets which are likely to be correlated with sediment production and the intensity of runoff events (glacial, nival and autumn) indicate the following: Long-term monthly records of temperature and precipitation anomalies indicate that prior to 1920, precipitation was similar to the long term (1890-1990) average but air temperatures were slightly cooler on average. Warm and dry conditions characterized the 1930-1945 period with temperature anomalies close to 2 °C between 1935-1945. Inter-annual to inter-decadal changes in temperature and precipitation appear to be most highly associated with inter-decadal changes in the PDO though cold and/or wet years occur during years of large ENSO variability. The frequency of floods within the study area is controlled both by rainfall intensities during autumn and the magnitude and timing of nival runoff. Autumn floods in the Lillooet River basin have become more frequent following 1977 and may be related to ENSO in a complex way. These results will allow an assessment concerning the percentage of climatic information which can be recovered from the sedimentary archives of the lake basins.

5.3 Analysis of Sedimentary Archives Within the Lake Basins

The six outlet lake basins differ in their size, overall morphometry and ability to preserve high resolution sedimentary records. Simple bathymetry characterizes Cheakamus, Duffey and Lower Joffre Lake basins while Glacier and Birkenhead Lakes are more complex and consist of distal and proximal basins (figures 5.7,5.8,5.9). Green Lake has the most complex bathymetry and it remains unknown whether this reflects underlying bedrock control. Sedimentary archives within the lake basins were detailed through recovery and analysis of sediment cores (see Chapter 3 and Appendix A). Sediment description and analysis are primarily limited to those sediments believed or verified to have been deposited within the last century. Analysis and discussion of the sedimentology and down core changes for sediments exceeding 100 years in age are considered in chapter 6.

Recovered lake sediments from the lake basins are inorganic (0.5-8 percent LOI) light grey (dry color), silty-clay to clayey-silts with negligible carbonates (1-2 percent; see Appendix A). Sediment density is variable (0.4-1.4 $g\ cm^3$) depending on core location or lake basin and density does not appear to be related to depth below the sediment-water interface. Coring-induced compaction of the under consolidated surface sediments (1-10cm) is a likely reason to explain this independence between depth and density (e.g Gilbert, 1975). In general, sediments are most clastic (i.e. low organic content, most dense) in Green, Cheakamus and Glacier Lake Basins, less so in Duffey and least in Joffre and Birkenhead Lakes. Smear slide analysis reveals that the coarse silt and fine sand size fraction of the sediments are largely comprised of angular quartz and feldspar grains, mica, and minor constituents of mafic-rich lithologies. The visible proportion of organic matter is comprised of terrestrial detritus (wood, conifer needles and pollen grains) and lower percentages of aquatic fossils such as diatoms and or chironomids. In short, sediment composition appears to be largely dominated by allochthonous sources which is common for oligotrophic lake environments (e.g. Souch, 1994; Leonard and Reasoner, 1999).

Representative samples of the sediment were embedded with low viscosity resin (Spurr), polished and examined under a low power (10-40x) dissecting microscope with illuminated light (see appendix A for details). Thin sections were made for those portions of the cores which were laminated to facilitate sediment analysis and for construction of varve chronologies. The uppermost (10-50cm) recovered sediments from the lake basins can be classified as massive, indistinctly-laminated, laminated sediments, and bedded sediments:

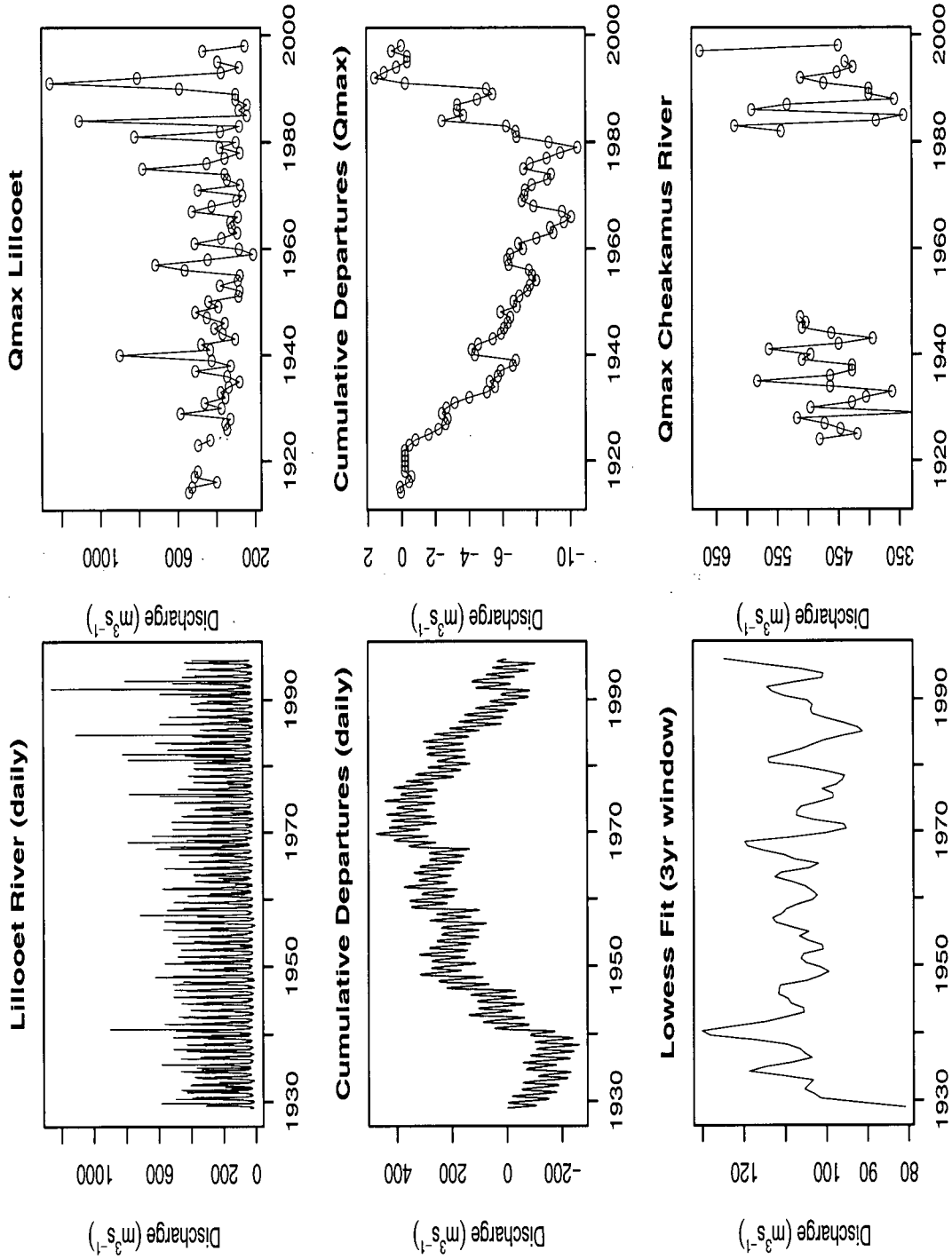

Figure 5.5: Daily and Annual Discharge of the Lillooet and Cheakamus Rivers
Long-term changes in discharge (m^3s^{-1}) are similar to variations in runoff experienced in other southern BC watersheds where a majority of the runoff is derived from snowmelt runoff. Anomalously high runoff around 1940 corresponds to a period when air temperatures were anomalously warm and precipitation totals were well below average (c.f. figure 5.1). The higher runoff is likely caused by enhanced glacial runoff during this period.

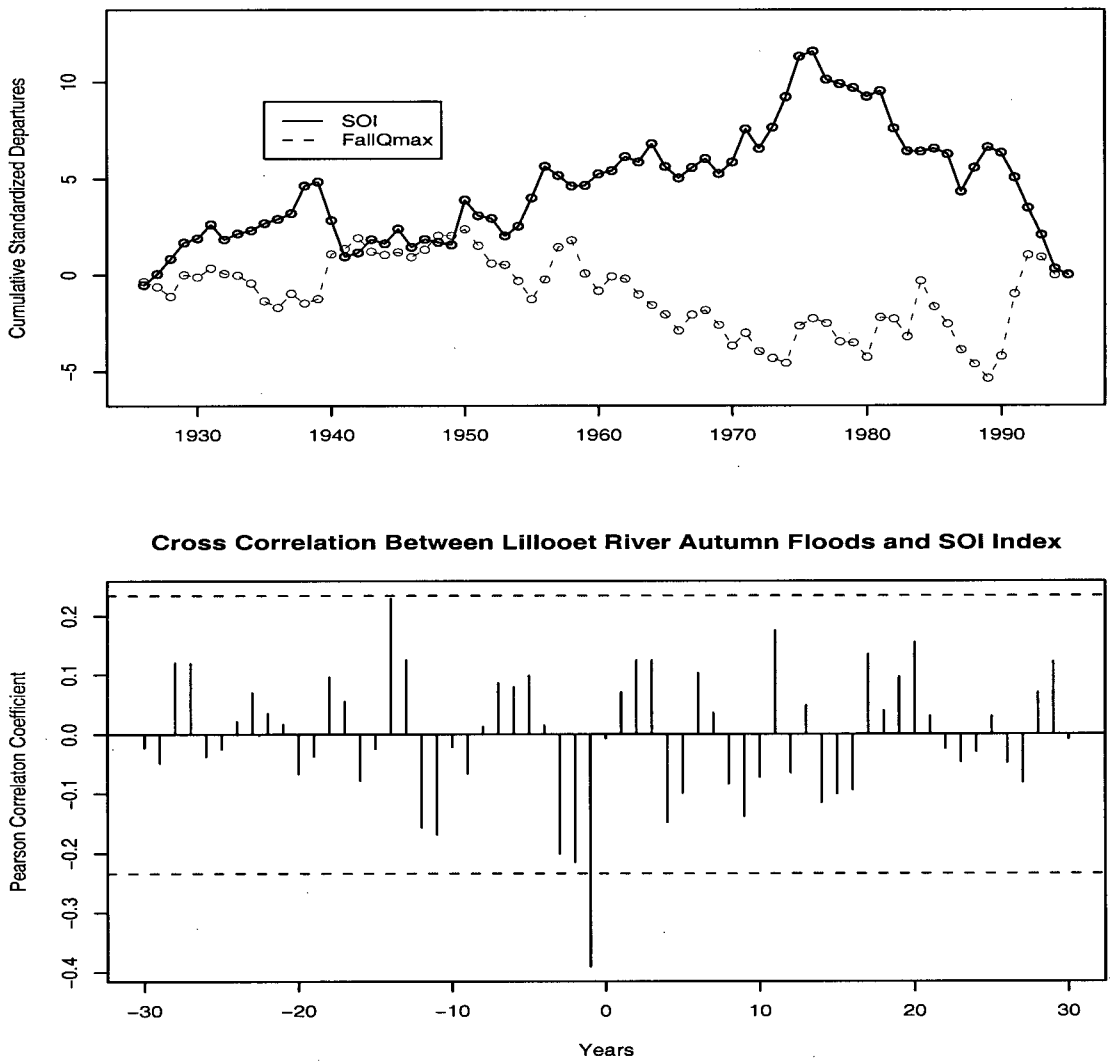

Figure 5.6: Cumulative Departures and Cross Correlation Between SOI and Lillooet River Autumn Flood Events

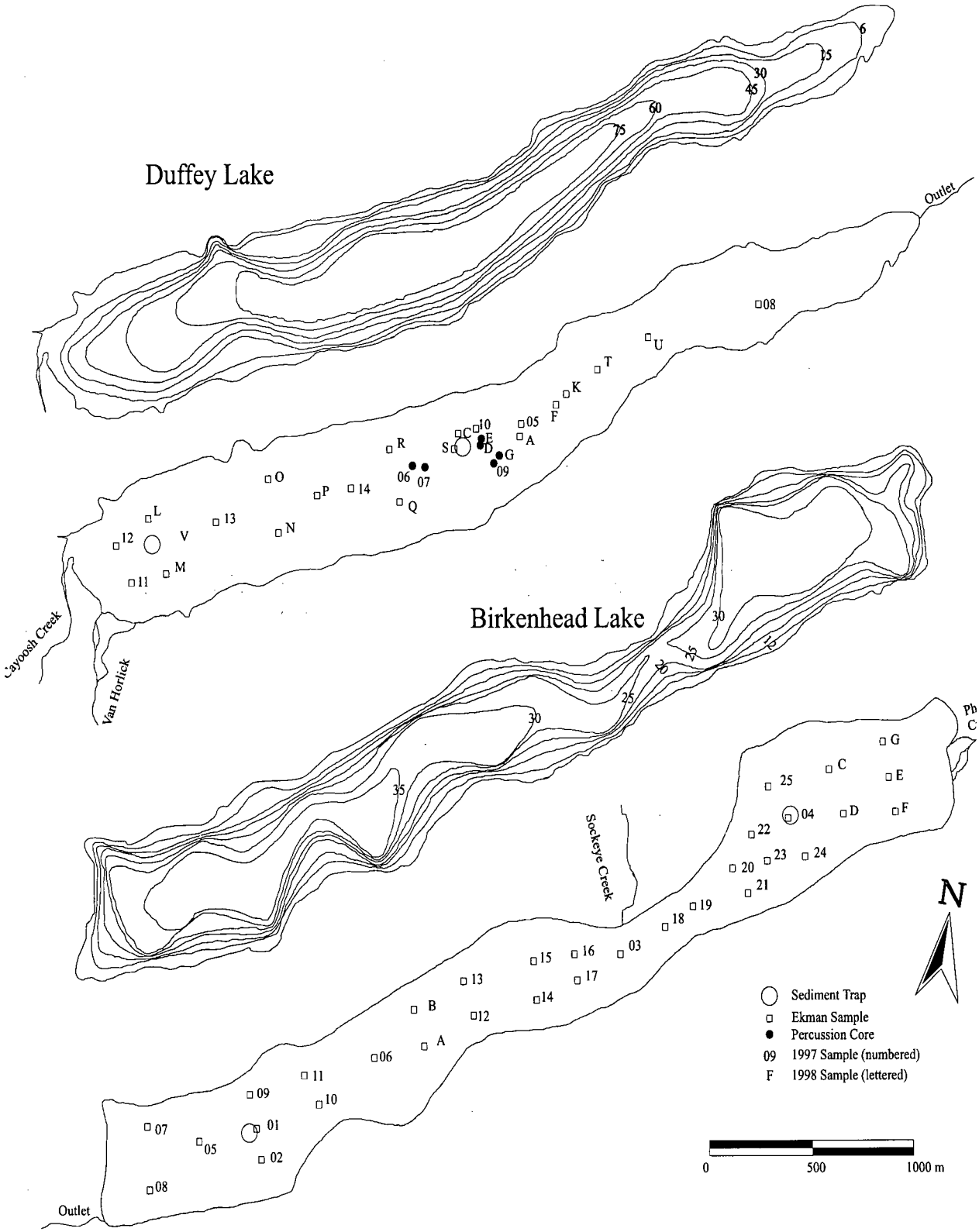

Figure 5.7: Bathymetry and Core Locations, Duffey and Birkenhead Lakes
Bathymetric data from Ministry of Environment, British Columbia. Isobaths in meters

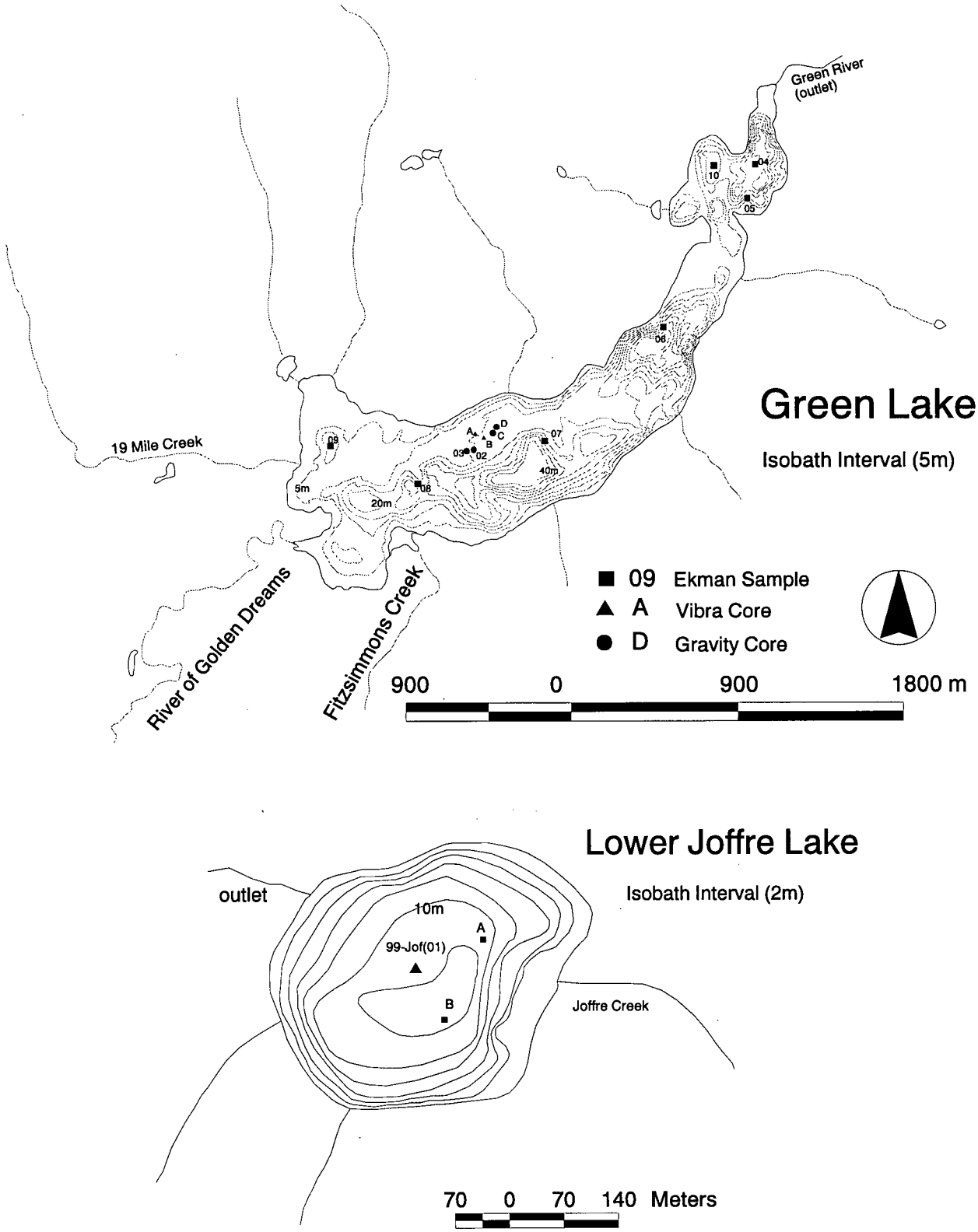

Figure 5.8: Bathymetry and Core Locations, Green and Joffre Lakes
Bathymetric data for Joffre Lake from Ministry of Environment, British Columbia. Green lake bathymetry provided by E. Schiefer (UBC Geography).

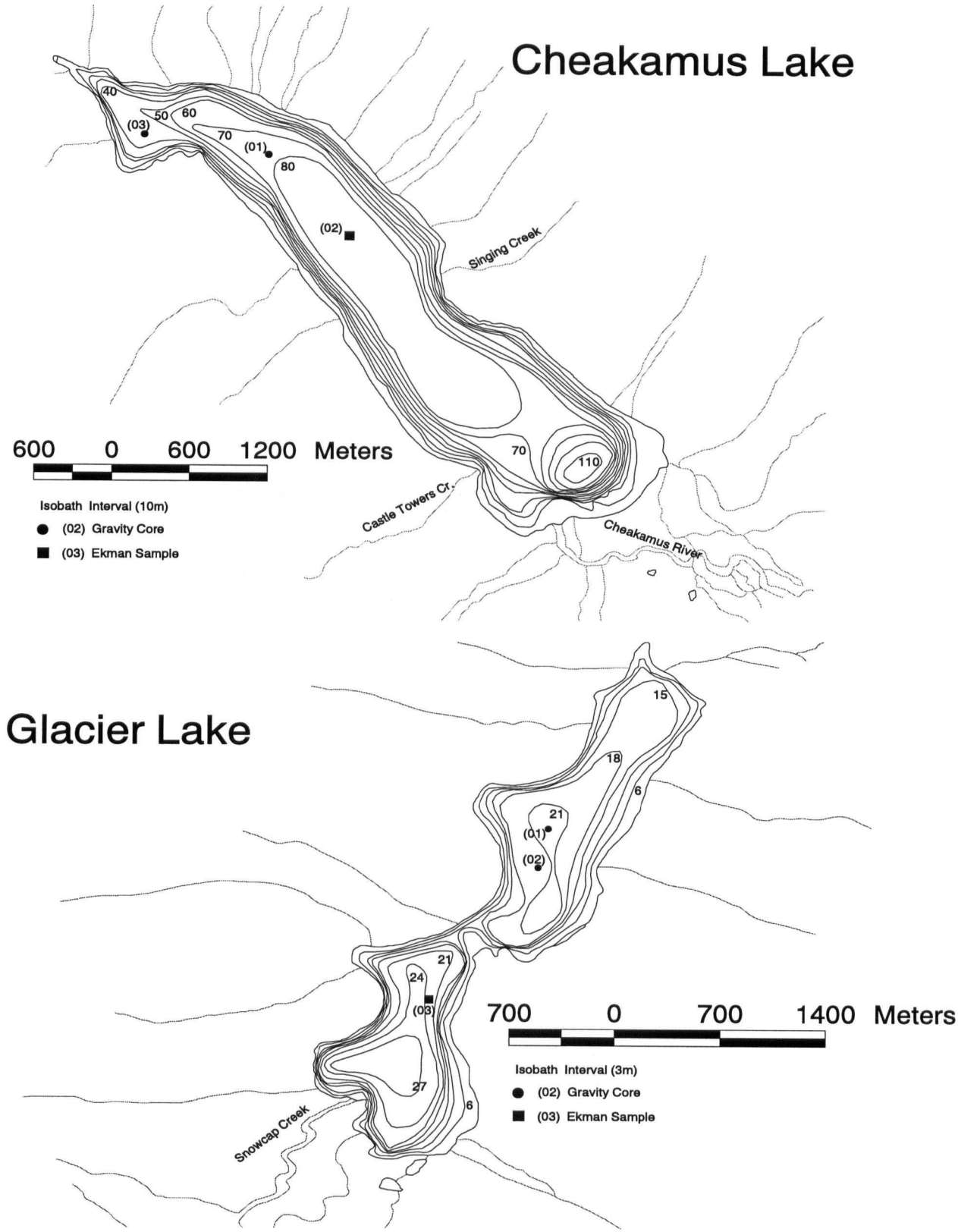

Figure 5.9: Bathymetry and Core locations, Cheakamus and Glacier lakes

5.3.1 Massive Sediments

Sediments which are described as massive are light grey (dry color) silty clay and characterized by lack of significant down core changes in color, texture or bedding. Such sediments were found exclusively in Joffre and Birkenhead Lake basins. Infrequent event beds are present in those cores taken close to major inflows or close to steep, unstable, sub-areal terrain. Sediment fabric is largely comprised of pelletized sediment (0.2-0.3mm) with little evidence for preferred orientation.

5.3.2 Indistinctly-laminated sediments

Indistinctly-laminated sediments were recovered from four of the six basins (Duffey, Green, Cheakamus and Glacier) and are classified according to primary structure and deposition environment. The first group of indistinctly-laminated sediments is comprised of silty-sand to sandy-silt found in deltaic environments and major inflows to the lakes. In Glacier Lake such sediments appeared to be isolated to the proximal basin whereas the extent of such sediment can be found further down-lake (up to 1.5km) for Duffey Lake. In Green Lake, coarser-grained, indistinctly-laminated sediments are found in proximal settings of the lake basin. Many overlying laminae have eroded into underlying sediment as evidenced by sole marks and tool structures. Textural variations between laminae are slight and contribute to their low, visual bi-modality (figure 5.10).

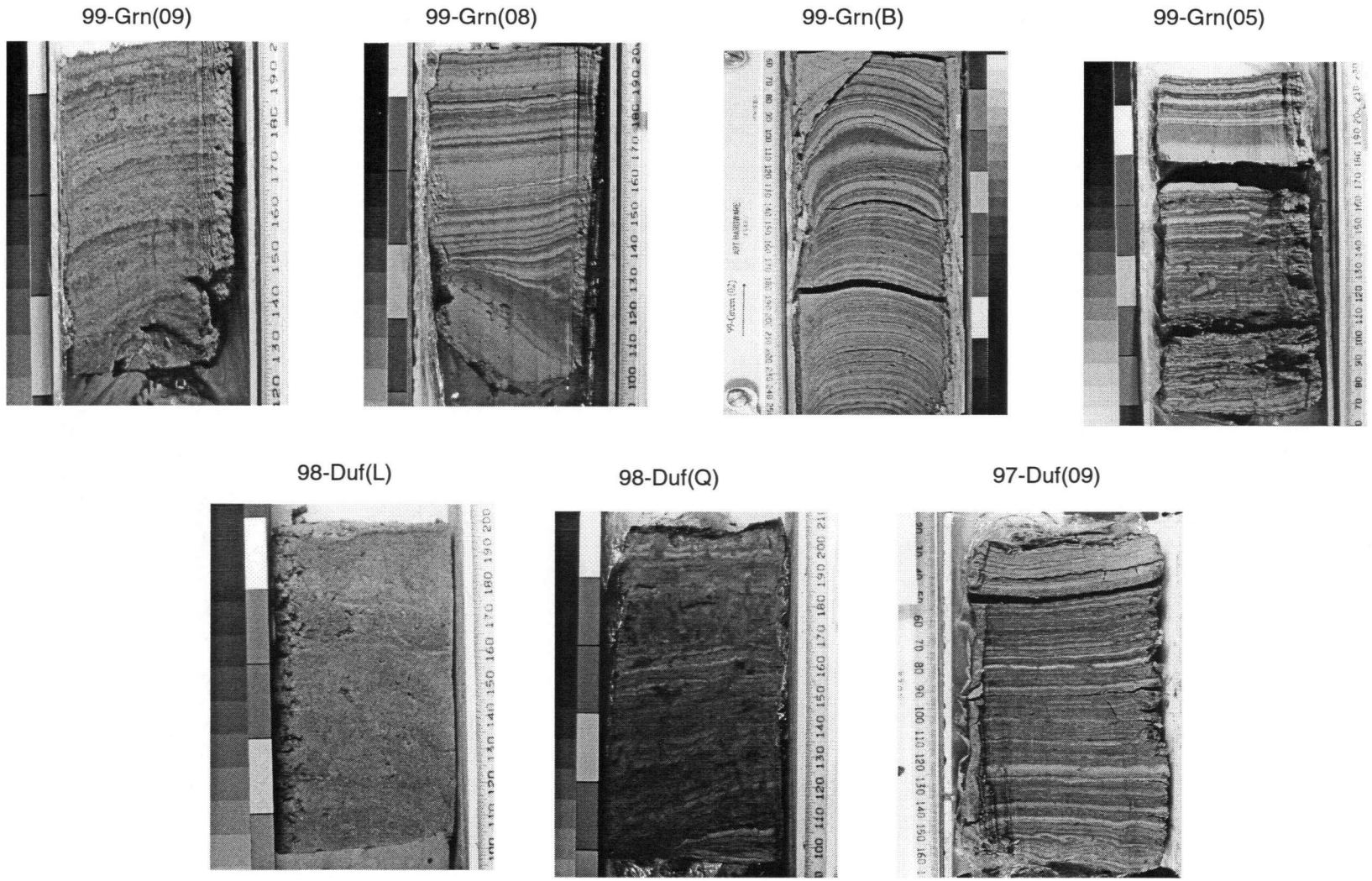

Figure 5.10: Representative Sediment Cores from Duffey and Green Lake Basins
Cores illustrate weakly (99-Grn(09); 98-Duf(L)) to well laminated (99-Grn(08)) sediments taken from proximal locations in the lake basins, bioturbated (98-Duf(Q)), finely laminated (99-Grn(09), 99-Grn(B)) sediments and laminae deposited in distal (99-Grn(05)) settings.

The second type of indistinctly-laminated sediments was recovered from shallow water environments (with respect to maximum depth) away from areas of major inflow. Laminae have higher visual bi-modality and are commonly mottled. Micro-analysis of the the mottling reveals that it is primarily caused by 1-3mm diameter, 5-10mm long linear features interpreted to be trace fossils. The visibility of such traces is accentuated by textural and color differences between the laminae; overlying, lighter colored sediment has filled in burrows within darker colored sediment. Traces are most recognizable in those sediments which are more organic rich, are less dense and largely limited to sediment cores recovered from Duffey Lake in water depths shallower than 80m (e.f. core 98-Duf(Q) in figure 5.10).

5.3.3 Distinctly-laminated Sediments

Sediments which are classified as distinctly laminated are predominantly comprised of silty-clay to clayey-silt couplets. Sand percentages are generally low (< 1 percent) except for sedimentary couplets of Duffey Lake where fine sand content occasionally is as high as 8% caused by the presence of inter-calated sand lenses. Distribution of finely laminated sediments varies according to lake basin. In Duffey Lake well laminated sediments are primarily restricted to deeper water (>70 m) but are well distributed in Green Lake where such sediment can be found in shallow water environments (10m). Based on Ekman samples recovered from Glacier Lake, distinctly laminated sediments are found throughout the distal basin but not in the basin closest to the major inflow to the lake. Incomplete sampling within the Cheakamus Lake basin prevents a comprehensive assessment of the spatial distribution of distinctly-laminated sediment within the lake. Distinctly-laminated sediments do exist in the distal environments of the lake.

Laminae within Duffey Lake are organized as 0.3-5mm thick clayey-silt couplets. Ungraded to weakly graded coarse silts to very fine sands are most often overlain by lighter colored laminae which abruptly terminate into a thin (0.2-0.5mm) light brown, very fine grained unit interpreted to be clay. The thinness of the unit prevents a quantitative assessment of its particle size characteristics. Contacts between individual couplets vary between sharp and continuous to contacts which are diffuse, wavy and occasionally broken by 0.2- mm diameter gaps which appear to be trace fossils (figure 5.10). There appears to be an association between these gaps and the presence of pelletized sediment below such breaks (figure 5.11). Clay layer thickness does not covary with thickness of the underlying lamina except for those couplets which are thicker than approximately 5mm. The sediments from Green, Glacier and Cheakamus lakes are well laminated silty-clay to clayey-silts. Individual laminae range in thickness from 0.5 to 20 mm and most laminae consist of simple couplets comprising a lower most, ungraded unit of coarse silts which grades into darker, clay rich unit (figure 5.10). The contact between the sediments of an underlying clay unit and overlying silts is most often sharp and uniform. Significantly thicker, graded laminae occur infrequently and most commonly overly coarser-grained laminae. Contacts between the underlying unit and overlying graded laminae are sharp and uniform. These laminae grade into fine clay which is proportional in thickness to the thickness of the lamina. Taken together they represent sedimentary triplets and are most common in the sediments of Green, Cheakamus and Glacier lake sediments. Particularly in Glacier Lake, graded laminae deposited over underlying, coarser grained sediments are easily differentiated by their reddish brown color in thin section compared to the greenish-grey color of the other laminae (figure 5.12).

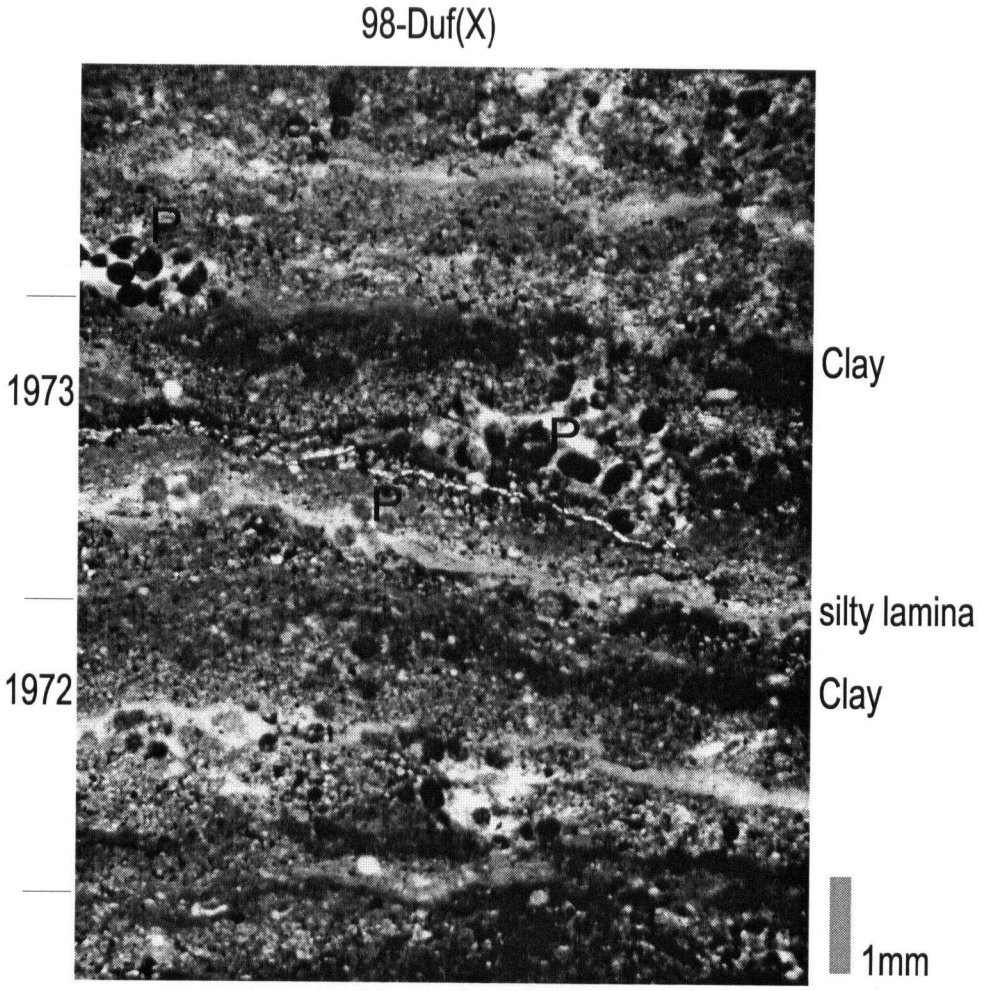

Figure 5.11: Photo-micrograph of Sedimentary Couplets from Duffey Lake
Note irregular couplet boundaries (denoted by lines on left of image) and presence of pelletized sediment. Couplet age estimated by varve counting. Despite the well-laminated nature of the sediments, the common occurrence of pellets (p in figure) suggests low intensity, infaunal growth.

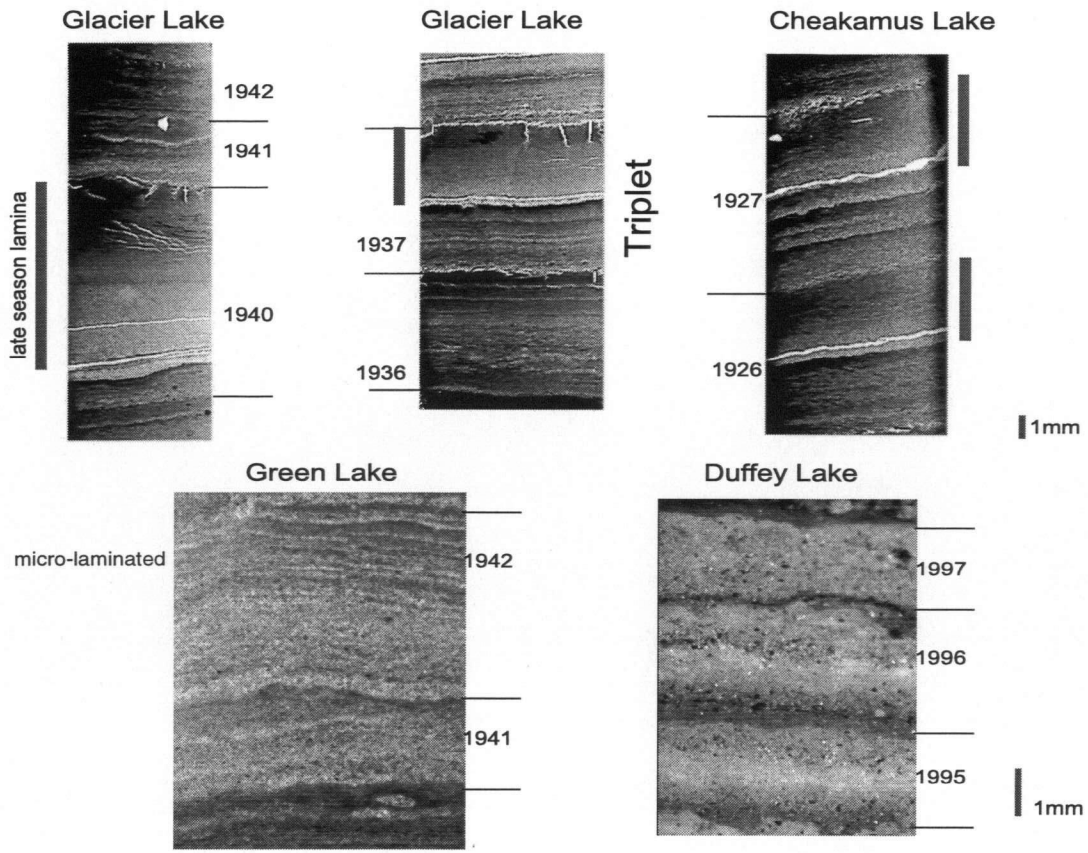

Figure 5.12: Photo-micrographs of Thin Section Samples from Cheakamus, Glacier, Green and Duffey Lakes
Numbers refer to calendar age based on varve counting. Note detailed stratigraphy evident within sediments from Cheakamus and Glacier Lakes (upper 3 photographs) and presence of sedimentary triplet. Micro-laminated couplets from Green Lake (lower left panel) deposited 1940AD and characteristic of couplets deposited in lake basin between 1920-1950AD. Photomicrograph showing uppermost 3 couplets (lower right) from Duffey Lake. Note lack of intra-varve detail and evidence for bioturbation.

Finely laminated, sediments recovered from Green and Duffey Lake basins are slightly coarser-grained ($D_{50} \approx 13\mu m$) than the sediments recovered from Glacier and Cheakamus Lake ($D_{50} \approx 7.5\mu m$) basins (figure 5.13). Particle size of the clay sized fraction probably does not represent true settling diameters as such fine grained material should exit the lake basins based on Stokes' Law. Flocculation by biologic activity (e.g. Smith and Syvitski, 1978) or by organic matter complexes (Haknson, 1981) is the most likely reason for the high proportion of fine clay in the lake basins.

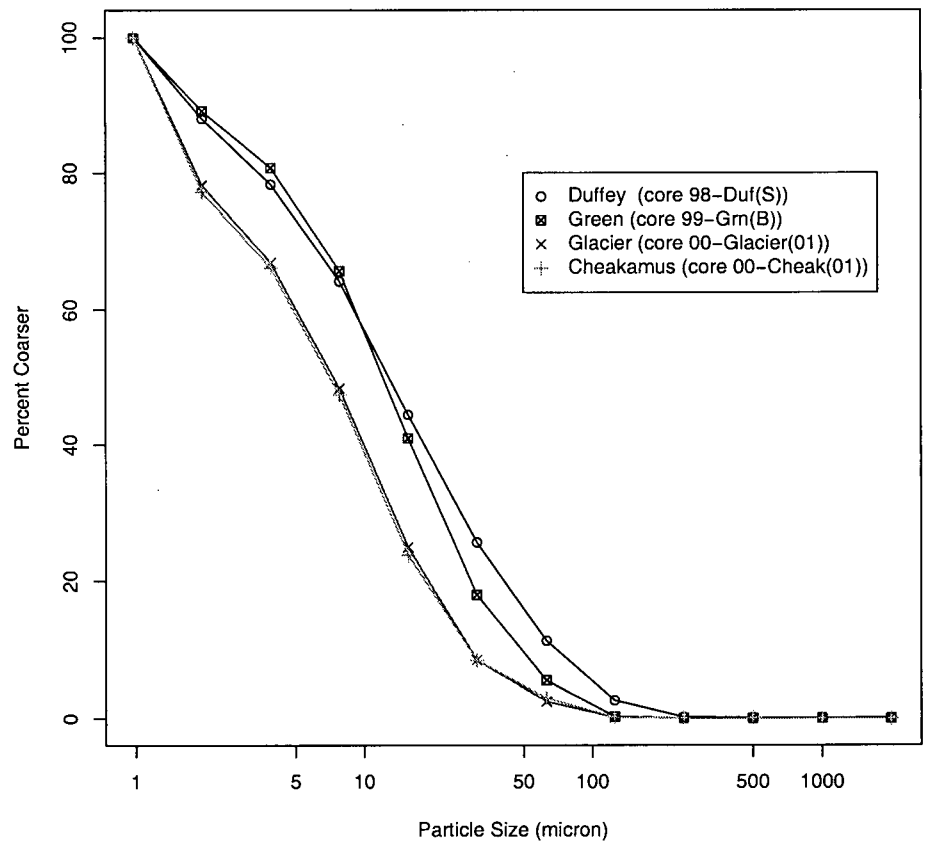

Figure 5.13: Particle Size Distribution of the Laminated Sediments
Averaged particle size distributions for the four lake basins. The number of averaged samples are 15, 4, 3, and 3 for Duffey, Green, Cheakamus, and Glacier Lakes respectively. The coarser-grained nature of the analyzed sediments from Duffey and Green are interpreted to arise from closer proximity to lake inflow (Green) and higher proportions of sediments reaching the coring site as underflow or grainflow events (Duffey).

5.3.4 Bedded Sediments

Coarser grained beds occur infrequently within the recovered sediments of Cheakamus, Glacier and Green Lake and most commonly in Duffey Lake. Most of the beds are normally graded, though several beds begin with finer grained, micro laminated sands which are then overlain by a coarser-grained (fine to medium sand), normally-graded unit. Such beds are largely confined to Duffey

Lake and were recovered from cores in deep water environments of the central basin. Often such beds begin as ungraded silty clay with matrix-supported terrestrial organic matter. These finer-graded sediments are then overlain by reversely-graded to graded silty beds and finally capped with a graded silt layer which terminates into clay. The organic detritus often comprises a significant fraction (up to 10 % in thin-sections) of material within the bed and is often graded in those cores taken closest to the lake margins. Moderate deformation (e.g. flute and tool casts, loading and de-watering structures) of underlying rhythmites occurs under the thickest and coarsest-textured graded units and current structures can often be found within such beds. Bioturbation is largely absent within such beds indicating such beds were deposited rapidly. The spatial distribution of beds within the lake basins appear to be primarily limited to those locations within the lake basins which are deepest and are most directly coupled (i.e. no sill) to contemporary inflows or to areas where hillslope instability is common.

5.4 Interpretation: Inter and Intra-lake Sedimentation Processes

Sedimentation rates and dominant ordering (non-laminated, indistinctly-laminated, laminated, and bedded) of the sedimentary archives within the lake basins, are interpreted to be a function of sediment supply, heterogeneous transport and spatial position within the lake basins. Differing mechanisms of sediment transport and sub-bottom characteristics are believed to influence the proportion of sediments delivered predominantly by high energy processes from those which occur more frequently and distribute sediments throughout the lake basins. High energy transport processes such as gravity flows (e.g. grain or debris flow, turbidity currents, and slump initiated surge currents) and turbidity currents deliver coarser-grained sediments to areas near contemporary inflow or those where the transport of such material is unhindered by bottom gradient. More commonly, sediments are transported within or near the epilimnion as interflows and overflows and comprise lower concentration events but occur with greater frequency. Observed stratigraphy, bathymetry and recognition of hillslope instability patterns in proximity to the lake basins is combined to infer which processes are most important for controlling patterns of sedimentation within the lake basins.

The bedded sediments (event beds) are interpreted to reflect sudden inputs of sediments to the lake either during high flow events or during slope instability surrounding the lake. Event beds are primarily located in the deepest sections of the lake basins and most are normally graded and have current structures and other features which indicate rapid deposition in a high energy environment (e.g. Smith and Ashley, 1985). The origin of the beds may originate from normal turbidity currents during periods of high runoff (e.g. Gilbert, 1973; Lambert and Hs, 1976; Lambert et al., 1976) surge currents generated by deltaic instability or slumping of sediment from steep side walls (e.g Smith, 1978; Smith and Ashley, 1985), or through sub-aerial rapid mass movement processes (snow avalanche or debris flow) on steep hillslopes adjacent to lake basins (e.g. Menounos, 2000). In general, such unconformable deposits are thickest and coarsest in the deepest areas of the lake basins or those regions closest to major inflows. Sediment distribution within Duffey Lake is characterized by both high and low energy processes which distribute sediments throughout the lake basin in a non uniform manner. Simple bathymetry of the lake basin allows sediment from the deltaic environment to be transported to the deepest portion of the lake basin some 2.5 km distant. Turbidity currents are believed to deliver the majority of sediments to the deepest portion of the lake basins during high discharge events, most commonly during snowmelt runoff. Such currents most likely occur in the other basins during high flow events but are restricted to low lying areas not separated from main inflows by a sill. Hillslope instability on the north side of Duffey Lake is the most likely source of coarse grained beds found within the sediments. Such activity is

likely to initiate instability of conformable sediments deposited along the margin of the lake and initiate surge currents as well as instability of sediments in deltaic environments. Inter-calated sand lenses within the laminated sediments of Duffey Lake may originate from grain flows and or traction currents from small creeks entering the south and or north side of the lake basin. For Duffey Lake, there is a lack of sedimentary evidence within the contemporary sediments which would indicate that the turbidity currents were powerful enough to erode underlying sediments within the deeper settings of the lake basin. As the summer progresses, the lake becomes stratified and interflow and overflow events become the dominant mechanism of sediment transport within the lake. Such an interpretation is in general agreement of lake sedimentation processes observed for Lillooet Lake (Gilbert, 1975) and for proglacial lake sedimentation in general (e.g. Smith and Ashley, 1985; Sturm, 1979). The significance and regularity of such bedding within the context of long sediment records is discussed in Chapter 6.

5.4.0.1 Factors Governing Bioturbation

Although transport by turbidity currents is an important and perhaps dominant process within Duffey Lake, laminated sediments can form in their absence as suggested by the presence of rhythmites in shallower and or sheltered environments of Glacier, Cheakamus and Green lake basins. In these lacustrine environments sediment transport through the epilimnion appears to have distributed clastic sediments in a more uniform manner. Such conformable sediments are likely transported throughout the lake basins as interflow and overflow events when the surface waters are well stratified (e.g. Smith and Ashley, 1985). It is somewhat surprising that well-laminated sediments are present in shallow environments of Green Lake (10m); the depth is sufficient to prevent erosion by wave scour while high sedimentation rates likely prevent severe or moderate biologic reworking.

Non-laminated sediments are believed to arise both from lower sedimentation rates and from active bioturbation. Though non-laminated sediments can form in anoxic environments where sediment type and supply patterns are constant (e.g. Grimm et al., 1996) the fluvial and lake-based monitoring indicate that sediment is supplied to the lake basins in a heterogeneous fashion largely controlled by the regularity of snowmelt and glacial runoff. In addition, the bathymetry, low dissolved and SSC content, and weakly stratified nature of the lake basins would limit anoxia to perhaps only a few months during winter when ice cover exists. Recent (2001) lacustrine monitoring (E. Scheifer, pers. comm.) indicates oxygen levels within Green Lake which are close to or above saturation levels (5-8 mgl^{-1}) for the observed temperature levels near the sediment-water interface. Biologic evidence for well oxygenated conditions within the lake basins include fossil chironomid head capsules (species unknown) within recovered sediments and live chironomid larva burrowing within the upper 1-2 cm of recovered sediment cores. Fecal pellets similar in shape and size to the pelletized sediment found in the polished, laminated slabs were produced from one chironomid specimen (Duffey Lake) after placement in ethanol. The pelletized nature of sediment from oligotrophic lakes is often attributed to copepod grazing (Smith and Syvitski, 1978) but chironomid egestion appears to represent an alternative mechanisms for aggregate development. Heterogeneity in the type and rates of sediment flux to the lake floors are believed to be the primary controls associated with laminae formation while minimal physical and biologic reworking allows their preservation (e.g. Grimm et al., 1996). It is commonly accepted that in clastic lacustrine environments biologic reworking is limited when sedimentation rates are high and when oxygen availability is low (c.f. Lamoureux and Bradley, 1996). Although low oxygen levels may explain some of the observed patterns of laminated sediments within this study, the presence of laminated sediments within shallow water environments of Green Lake argue against anoxia as a primary control. In addition, in all four lake basins many thin laminae (< 1mm) show little evidence for bioturbation and suggest an

additional factor which may limit biologic activity.

It is believed that temporally, varying patterns in bioturbation can be explained by changes in food supply directly controlled by glacial runoff to the lake basins. Chironomids appear to be one of the primary organisms responsible for reworking of the sediments within this study and much of their life cycle is spent burrowing into the uppermost sediments where they consume organic material (Walker, 1987). A large proportion of this organic matter originates from within-lake productivity and changes in its production in the photic zone will influence flux rates to the lake floor. Low levels of phytoplankton production have been shown to limit food supply of tubificids in other lake environments (e.g Cohen, 1984). Primary productivity in lakes is commonly assumed to be related to water temperature and or limiting nutrients such as phosphorus. Studies have demonstrated, however, that phytoplankton production (chlorophyll-a) is sensitive to ambient light levels within lake environments and sunlight within the eutrophic zone can be greatly attenuated by high turbidity levels caused by suspended sediments (Kirk, 1985). The lakes of this study become turbid during periods of sustained glacial runoff primarily because of increased delivery of fine sediments to the lakes but also because such runoff occurs during times when the lake are stratified. Studies within Alaskan lakes have demonstrated the inverse relation between chlorophyll-a concentrations and turbidity levels (caused by glacial inflow) (Lloyd et al., 1987) while controlling for complicating effects (available phosphorus). Evident within the lakes of this study is an association between the organic content of the lake sediments (an index of lake productivity) and intensity of bioturbation. Rates of primary productivity are often associated with lake temperature, but in this study such effects are unlikely as decadal scale changes in the intensity of bioturbation occur during times when air temperatures are coldest. Much evidence of bioturbation is found within sediments deposited during 1900-1920, 1945-1980 which are decades when air temperatures within the study area were colder than average (c.f. figure 5.1), and by inference water temperatures.

The proposed model of laminae preservation in these oligotrophic lake environments is fundamentally different from laminae preservation in ocean and productive lake environments where high organic matter availability tends to limit profundal oxygen levels by respiration effects and limits biologic reworking (e.g. Stott et al., 2000). The lack of laminated sediments within Joffre and Birkenhead Lake basins is believed to be caused by lower sedimentation rates and higher organic content of the lake sediments though the degree of independence between these factors is low in the study area (c.f. figure 4.9) and in other proglacial environments (e.g. Leonard, 1986a; Souch, 1994). Duffey Lake appears to be an environment close to the boundary for minimal requirements for laminae preservation. Well-laminated sediments during the contemporary period have been primarily restricted to the deepest portion of the lake basin where perhaps sediment focusing combines with lower oxygen levels to limit biologic reworking of the sediments. In short, the preservation of varves within the study area appears to be controlled by a complex interplay between fine-grained sediment delivery to the lake basins, sedimentation rates and perhaps oxygen levels. Delivery of rock flour during times of sustained glacial runoff likely reduces within-lake productivity limiting biologic reworking by chironomids or other organisms.

5.4.1 Decadal Scale Variations in Sediment Delivery to the Lake Basins

Down-core changes in the clarity of laminae within the lake basins sediment mirrors changes in sediment composition (figure 5.14). Those couplets which are most easily recognized are generally comprised of clay rich sediment which is denser, is less organic rich and there is less evidence for biologic reworking. These sediments can be shown to be more conformable (i.e. they can be found on steep side slopes) and are more uniformly distributed throughout the lake basins. Couplet thickness of such distinctively laminated sediments are generally thicker in Green, Cheakamus and

Glacier Lake basins but are thinner than coarser-grained (less distinctively laminated) laminae within Duffey Lake. For Duffey, the difference between the distinctiveness of laminae is attributed to both organic matter content and sediment texture of sediments delivered during non underflow events. Differences in grouped particle size for the upper (0-7cm) less distinctively laminated sediments of Duffey reveals a slight but insignificant decrease in median grain size (7.67 to 7.63μm) compared to lower (8-15cm) sediments. The presence of intercalated sand lenses within the lower most sediments is the most likely reason for non significant reduction in particle size and contrasts with significant changes in the bulk physical properties (e.g. water, density and organic matter) of the sediments from the lake basins.

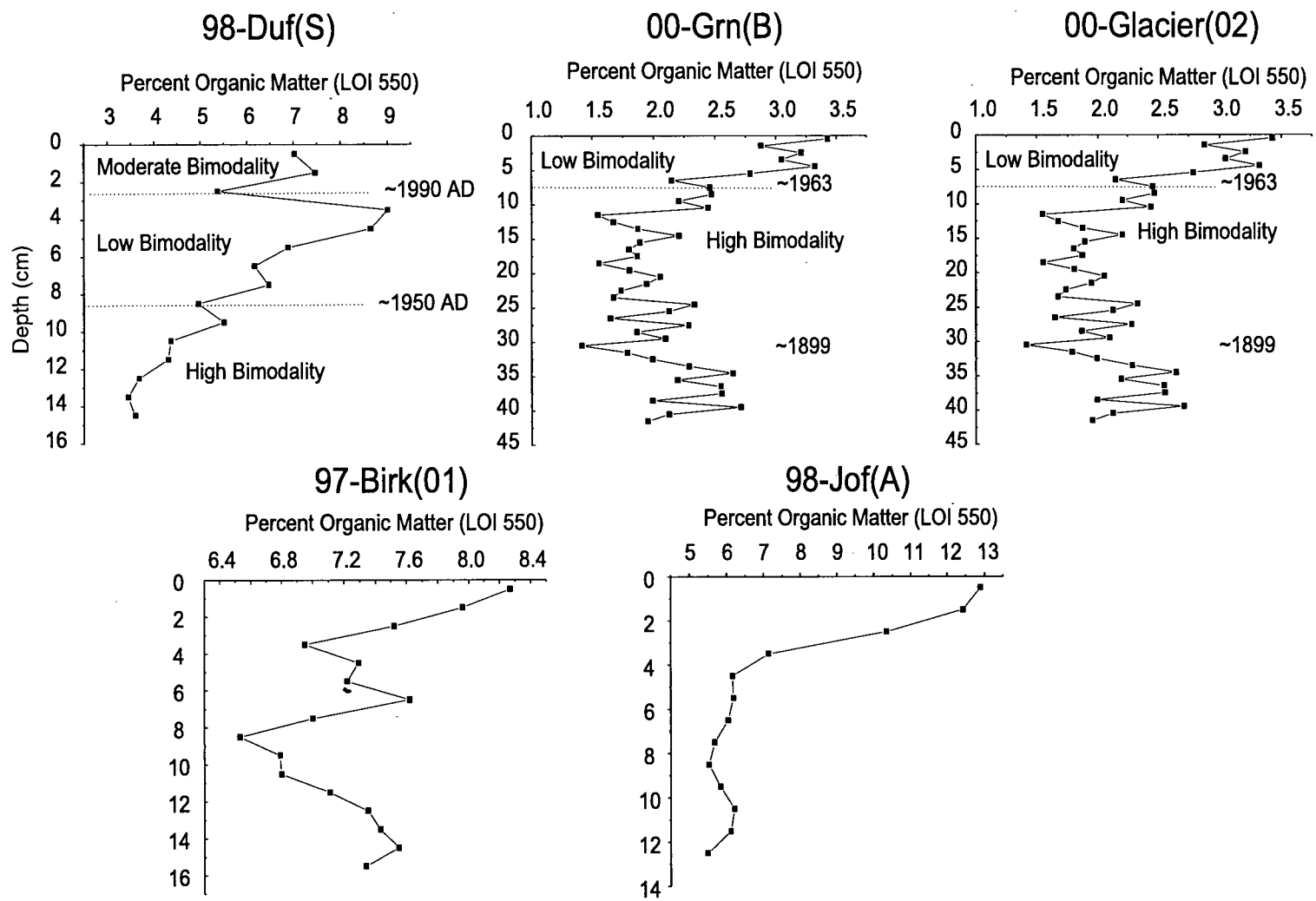

Figure 5.14: Organic Matter Content of Surface Sediments From the Lake Basins
Note the higher organic matter content for those sediments which are massive (Joffre and Birkenhead Lake Cores). Changes in the bi-modality of the sediments mirrors changes in the clastic nature of the sediments. Organic content trends are positively correlated with water content and inversely related to sediment density and magnetic susceptibility

These differences and observed micro stratigraphy within individual couplets are interpreted to reflect variation in both sediment source and transport processes to the coring site. The coarser grained, thicker couplets are indicative of mixed energy environments, both underflow and inter/overflow contributing to sedimentation during a given year. However, the distinctively laminated sediments are non-graded and there is less lake-wide variation in thickness indicative of processes which transport sediment in a more uniform manner (i.e. interflow/overflow). A complete record of laminated sediments for Duffey is only found within the deepest portion of the lake basin and lake-wide sedimentation patterns are restricted to decadal-scale estimates based on correlation of distinctive marker beds. Although time-varying changes in sediment type and laminae clarity may provide insight into major changes in sediment delivery and or sediment source, such a proxy should be used with caution as it may not reflect lake wide patterns of sedimentation (Lamoureux, 1999b). In this lake basin, couplet thickness of unconformable sediments which are distinctively laminated are generally thinner than those couplets which likely represent deposition by locally restrictive and conformable processes such as turbidity currents. Thus, a varve chronology developed from the central basin sediments may not provide as good an index of lake-wide sedimentation pattern as other sedimentation proxies which may be less spatially biased. These issues are considered in greater detail in Chapter 6.

5.4.2 Varve Interpretation of Finely-Laminated Sediment Archive

The laminae within Duffey, Green, Cheakamus and Glacier lake basins are believed to be clastic varves based on three independent lines of evidence: a) radiometric dating; b) recovery of subsequent cores through time; and c)statistically significant correlations between hydro-climatic variability and couplet thickness within the lake basins. A varve interpretation is strongest for Duffey and Green lake basins where all three lines of evidence can be used and lowest for Glacier and Cheakamus lakes where the conclusions are at present only based on (c).

5.4.2.1 Seasonal Recovery

Sediment core recovery began in the Duffey Lake basin in early spring 1997 and since that time, numerous surface cores have been collected (figure 5.7). A core taken in early summer 2000 reveals the addition of three couplets which are between 1-2 mm in thickness and sedimentologically similar to couplets deposited below them. Similar methods were used in Green Lake and reveal the addition of two, 5 mm thick couplets deposited between spring 1999 and summer 2001. The number of couplets and their physical similarity to underlying laminae interpreted to be varves suggest that the lakes are recording sedimentation events which can be resolved at the annual to sub-annual scale.

5.4.2.2 Radiometric Dating (^{137}Cs)

Radioactive fallout from mid century atomic weapons testing can be used to estimate the age of clastic sediments mainly because ^{137}Cs has a strong affinity to clay-sized particles which are commonly found in the sediments of oligotrophic lake basins. It may enter the lake directly from the atmosphere or during runoff events when fine-grained sediments enter the lake basins. Its short half life (30 years) provides dynamic changes of activity in environments with high ($>1mmyr^{-1}$) sedimentation rates and so the methodology is well suited for determining whether sedimentary laminae reflect true varves (e.g. Leonard, 1990; Desloges and Gilbert, 1994b; Lamoureux, 1999b). The method commonly compares the number of recovered couplets to the depth at which Cs^{137}

activity is maximum in the core and this level is considered synchronous with the peak in atmospheric fallout (1963) in the northern hemisphere. Success of cesium series dating is dependent upon sediment texture and history of reworking and or bioturbation as the technique gives the least ambiguous results when sediments are clay-rich and have undergone minimal post-deposition modification by water or organisms.

^{137}Cs levels were determined on two short cores from Duffey and Green Lake basin to test the varved interpretation of the sedimentary archives. The couplets are too thin to sample annually so onset (1954) and peak (1963) levels were bracketed by sub-sampling the sediment into 1cm thick slices. Average uncertainty (i.e. number of couplets per sample) introduced by the aggregation is ± 2 yr. Recovery of undisturbed sediment-water interfaces in both cores minimized the potential for loss of upper sediments from the cores (e.g. Leonard, 1990). A peak in ^{137}Cs activity is evident in the profiles obtained from both sediment cores and calendric ages assigned to the couplets by counting backwards from the sediment water interface to the level of maximum activity are within the uncertainty of the estimate (figure 5.15).

Though difference between onset and peak levels is often used as a means of inferring sediment age, the initial, non-abrupt increase of ^{137}Cs suggests that the 1954 datum is much less certain. It is likely that the 1.0 cm samples have integrated bomb and non bomb contaminated sediment. Other sources of profile smearing may include migration of ^{137}Cs and or mixing introduced by bioturbation. Minor bioturbation is evident within both cores though its effects have not obliterated the identification of varve boundaries within the sediment cores. Whatever its cause, the 1954 datum can not be precisely determined but the correspondence between the 1963 level estimated by the cesium profile and that obtained through couplet counts suggests that the laminated sediments within the two lake basins can be resolved at the annual to sub-annual scale.

5.4.2.3 Hydrologic Correlations

Perhaps the single-most important verification of a varve interpretation comes from the statistically significant correlations of varve thickness and hydro-climatic events. Such relations minimize the probability of accumulated counting errors over the interval of common overlap between the hydrologic records and the varve chronologies. Much like those results obtained from the contemporary monitoring program, a majority of sediment is mobilized and routed to the lake basins during infrequent, high flow events. Similar relations between sedimentation rates and the intensity of inflow event have been documented for other lacustrine settings (e.g. Page et al., 1994) and specifically for variations in varve thickness (e.g Granar, 1956; Desloges and Gilbert, 1994b) and those correlations are discussed below.

5.4.3 Spatial and Temporal Variations in Varve Thickness

Varve chronologies were developed for the four basins with an aim to examine the correspondence between observed climate variability and concurrent lake sedimentation for the last century. The chronologies consist of at least two sediment cores taken in portions of the lake where laminated sediments were most recognizable and from sites believed to be dominated by overflow/interflow rather than underflow processes. The exception to this is the chronology developed from Duffey Lake where the sediments are strongly bioturbated in shallower, more protective core settings . Chronologies were constructed from photographs of partially dried sediment cores, polished sediment slabs and thin sections (Appendix A). Varve thickness was defined by the sediments deposited between two clay laminae and cores were cross correlated using distinctive marker beds and and unique, sedimentary ordering of sub-laminae (c.f. Lamoureux and Bradley, 1996; Lam-

oureux, 1999b). An assessment of counting errors, between core variations in varve thickness, and the subjectivity of varve counting are considered in Appendix D.

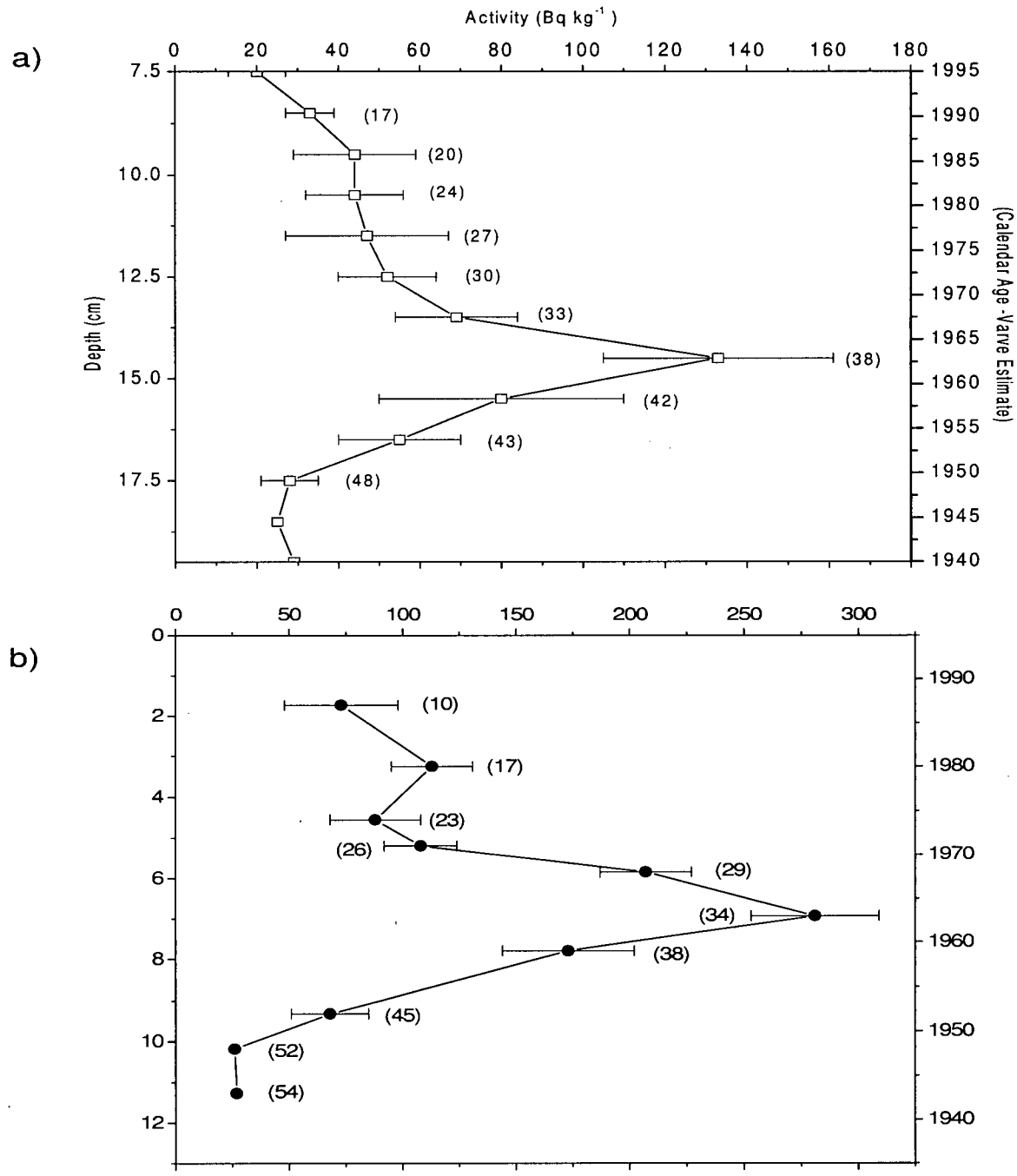

Figure 5.15: Cesium Profiles for Green and Duffey Lake Basins
a) Cesium activity Green Lake Core 00-Grn(D). Error bars ($\pm 1\sigma$) denote uncertainty of measurement. b) Activity level for Duffey Lake Core 97-Duf(10). Couplet numbers differ for this peak because dates of core recovery varied (1997 vs. 2000).

5.4.3.1 Spatial Patterns of Sedimentation

Yearly sedimentation determined from varves within the sediment cores reveal variations in varve thickness which are mainly attributable to distance from dominant inflow though because sediments can be delivered to the core sites through a variety of processes, some complexity is introduced to the relation. For Green Lake, couplet thickness averages 33mm some 300 m from the delta of Fitzsimmons Creek but declines to 2.4 mm (1999-1950) near the lake outlet (2.6 km from the delta). The proximal sedimentation estimate is only based on 3 couplets recovered in the Ekman sample so it represents a rough estimate of sedimentation at this site. In Duffey Lake, sedimentation 500m from the contemporary delta averages 8.6 $mmyr^{-1}$ (1998-1954), declines to about 1.85 $mmyr^{-1}$ 1 km down lake then increases slightly (2.25 $mmyr^{-1}$) in the deepest portion of the lake basin about 2.0 km down lake from the delta. Distal averages are not possible given the strongly bioturbated nature of the sediments from these locations. The slight increase is caused by a thicker and coarser-grained lower-most unit for those sedimentary couplets which can be traced sub-proximal and distal sites. Down-lake thickening is a common feature which is found in lakes where a significant proportion of sediment is transported by underflow and where bottom topography cause flow de-acceleration and coincident sedimentation (Gilbert, 1975; Lambert and Hs, 1976; Gilbert et al., 1997). Sedimentation (1984-1991) in the deeper (80m), distal setting of Cheakamus is approximately 9.5 $mmyr^{-1}$ and declines to 5.4 $mmyr^{-1}$ and 3.56 $mmyr^{-1}$ some 1.2 and 2.4km from the delta respectively (figure 5.9). Sedimentation rates for the central distal basin of Glacier Lake average 4.1±3.2 $mmyr^{-1}$ over the period (1991-1884) but an assessment of spatial variation is not possible as the recovered Ekman sample from the proximal basin of the lake was indistinctly-laminated.

5.4.3.2 Temporal Variability

Variations in varve thickness within the lake basins can be broadly summarized by two components; a) lower frequency variations where departures in varve thickness vary on inter-annual to inter-decadal time scales and; b) infrequent but large sedimentation events for a given year. Varve measurements from each core for a given lake were combined into master chronologies reflecting unweighted, average varve thickness. The chronologies reflect unweighted averages as most of the cores contributing to the chronologies were taken from localized portions of the lake basins were varves were continuous and between core average thickness were not statistically different. The upper (1-5 yr) surface sediments recovered from Glacier and Cheakamus Lake basins were disturbed during core recovery and or transport and absolute age was determined by cross correlating varve departures with the record of extreme discharge events recorded at Cheakamus River (1924-1948; 1982-1999). Exceptional floods occurred during autumn 1940, 1984 and late summer 1991. The number of couplets deposited between these thicker laminae are similar to the number of years between these major floods. This and statistically significant correlation between annual maximum daily discharge (Q_{max}) and varve thickness for these basins indicate that a calendar age can be given to these records.

For three of the varve chronologies (Green, Glacier and Cheakamus), the most notable feature in inter-annual to inter-decadal variations in lake sedimentation is the generally high sedimentation rates during the 1920's to 1940's which decreases rather abruptly until about 1990. The chronologies also indicate a reduction in inter-annual variability between the mid 1940's until about the early 1980's. A similar increase in exceptionally large varves occurs in the Lillooet Lake varve chronology following 1990. The trend for the fourth chronology (Duffey) indicates lower than average sedimentation rates from the 1920's to the early 1950's followed by thicker varves between

1950-1990 and a slight reduction in varve thickness following 1990 (figure 5.16).

5.4.3.3 Climatic Controls on Varve Departures

The contemporary monitoring indicated the importance of infrequent discharge events on controlling lake sedimentation within the study area primarily by increasing rates of sediment entrainment. Detachment effects may be locally important during the snow-free season. Other processes which control sediment availability are expected to influence sedimentation in the lake basins over periods exceeding the event scale. Because glacial cover appears to play an important role providing fine-grained sediment to stream channels within the catchments, their fluctuations may be expected to influence downvalley lake sedimentation as found in other mountain environments of the Canadian Cordillera (e.g. Leonard, 1986b, 1997), Thus, in addition to the timing of flood events, those climatic factors which may influence glacial mass balance (e.g. winter snowfall and/or temperature variability) may play an important albeit indirect role in controlling inter-annual to decadal scale patterns in lake sedimentation. Glacial retreat commonly occurs during times of prolonged wintertime drought and/or during summertime meteorological conditions favoring strong glacial melt.

Varve thickness data were normalized so that they could be statistically compared to hydro-climatic data. A log transform was the most easily interpretable transformation though only the Cheakamus varve chronology passed the Shapiro-Wilks test for normality after transformation. The chronologies (transformed and untransformed) were compared to hydro-climatic systems which are known or were assumed to influence the production and transfer of fine sediment within the study area. These included annual time series of precipitation and temperature (seaonal and annual averages), streamflow (mean and Q_{max}) ,variations in April 1 snow water equivalence (mm H_2O) measured at several sites in proximity to the study area (figure 3.1), variations in mass balance (1965-1999) for Place Glacier, and broad-scale indices of climate, namely those time series which explain the dominant modes of wintertime atmospheric (PNA) and ocean (PDO and ENSO) variability. High flow events were found to be the best predictor of inter-annual variations in varve departures though the importance of floods varies depending on the hydrologic season in question. For Cheakamus, Glacier and Green Lake basins, maximum daily discharge (Q_{max}) is most correlated to varve thickness while inter-annual variations in varve thickness appear to be controlled by high flow events during May and June ($Q_{max(mj)}$) for Duffey Lake (figure 5.17). There is some correspondence between the annual PDO index (October-September) and variations in sedimentation in Cheakamus and Glacier Lake basins though the correlations for the entire period of record are low but statistically significant (table 5.2). For Cheakamus Lake, the significance of the correlation increases significantly (r=0.56) when only the period 1900-1976 is considered.

5.4.3.4 Duffey

Although the correlation between varve thickness and spring floods is statistically significant, the proportion of explained variance is very low ($r^2 = 0.07; p < 0.026$) over the period of usable record from Lillooet River (1929-1998). The poor relation could arise from the complexities introduced between sediment inflows to the lake and transport processes to the coring site and were recognized in the contemporary lake sedimentation monitoring program (c.f. figure 4.8). Other possibilities for the poor relation include errors in varve identification and or counting. Many of the varves deposited between 1950 and 1970 are diffuse and inter-calated with thin sand lenses and inconsistencies were noted between varve counts of different cores. Such inconsistent varve counts were observed more commonly from photographs of partially dried sediment cores (Appendix D) but also in thin

section and polished slabs. The possibility of false or missing varves was examined by splitting the chronology in half and examining cross correlation plots at various lags. In addition, 'missing' varves were randomly inserted or deleted but did not improve the runoff-thickness relation. A third possibility for the poor relation and one which agrees with recognizable changes in physical properties (and couplet type) is a change in sediment source during the contemporary period. Cumulative departures of varve thickness and spring runoff events, indicate that prior to 1950, trends in varve thickness are *inversely* correlated to spring runoff. Varves deposited prior to 1950 are comprised of inorganic silty-clay, are generally thin (1-2mm) and more uniformly distributed throughout the lake basin (c.f. figure 5.10 core 97-Duf(10) lower-most sediment). Following 1950, nival runoff intensity and varve thickness track one another until about 1990 when they diverge again and the sediments become less organic rich and denser and varve thickness is much less variable. Although there remains much noise, correlation of varve thickness and $Q_{max(mj)}$ between 1950-1989 increases ($r = 0.46\, p < 0.003$).

The complexities associated with inter-annual variations in varve thickness for Duffey Lake may also represent a change in the dominant transport process to the coring site. From 1950 to about 1990, sediments reaching the central basin are believed to originate from fluvial sources and likely reached the central basin by underflow (turbidity currents). An underflow interpretation is partially supported by sedimentologic features of couplets deposited during this time which are similar to those expected in surge or turbidity dominated glacial lake environments (e.g. Smith and Ashley, 1985). Such features are particularly evident for couplets deposited during the mid to late 1960's which, consequently was period when large nival floods were common in the Lillooet River Basin. Between 1930-1950 and following 1990, sediments reaching the lake basin were finer-grained and interpreted to have been more effectively distributed throughout the lake basin by interflow and overflow events.

5.4.3.5 Green, Cheakamus and Glacier Lakes

Varve thickness for Glacier, Green and Cheakamus varve chronologies are most highly correlated to Q_{max} for the Cheakamus River (1924-1948, 1982-1998) and less so for Lillooet River for the period 1914-1998 (table 5.2). The break in the Cheakamus River data reflects relocation of the gauging site some 5km downstream from the former gauging site but the relocation does not significantly increase the contributing area of the basin. Residuals from the regressions between Q_{max} events (Cheakamus) and varve thickness variations were examined for trends and or behavior which would indicate poor fits between the records of annual flood and varve thickness. Patterns in the residuals often indicate that important explanatory variables have not been considered or in the case of this study, that climate-fine sediment cascade linkages may have changed. Several hydro-climatic time series were correlated with varve departures from a given basin (table 5.2) though multiple linear regression models did not significantly change the proportion of explained variance for any basin. In addition to flood events, sedimentation rates in Green Lake are weakly correlated to variations in annual air temperature and to the SOI in the following year. The correlation with the SOI suggests that the relation between autumn flood events on Lillooet River and ENSO is likely real but its influence on controlling sediment delivery to Green Lake is not strong and the regional significance of the relation is tenuous as it does not appear to control sedimentation in the other lake basins.

Examination of the residuals from the regression models between Q_{max} events (Cheakamus) and varve thickness variations (Green, Cheakamus, and Glacier) indicate that Cheakamus and Glacier varves are thicker than expected (residuals are consistently positive) and are generally thinner (residuals consistently negative) between 1982-1998. Green Lake varves are anomalously thick between 1935-1945 and again following 1990. Regression models based on annual temperature

fluctuations (PC1temp) indicate similar behavior. The largest discrepancies between lakes were noted between Green and the pattern of sedimentation in Cheakamus and Glacier Lakes where higher than average sedimentation began following 1920 but did not occur in Green Lake until the mid 1930's. The cause of the differences is unknown but may indicate sediment source limitations in Green Lake prior to large temperature anomalies during this time (figure 5.1). In general, all of the chronologies appear to become less sensitive to hydro-climatic changes following 1950.

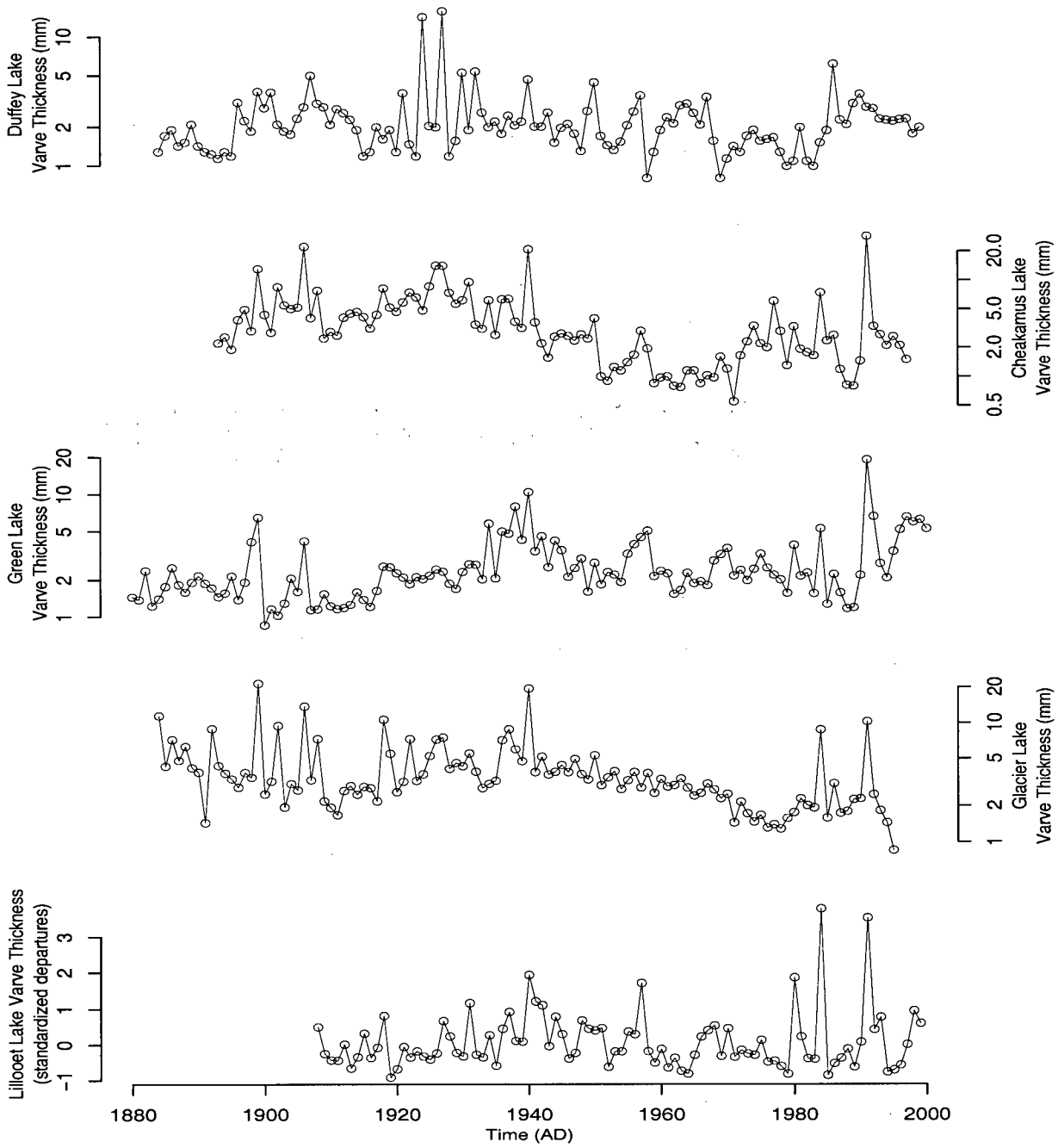

Figure 5.16: Varve Thickness Departures
Abscissa scale in log units for Duffey, Green, Cheakamus, and Glacier and standardized units for Lillooet Lake Data. Lillooet Lake chronology is a compilation of data from Desloges and Gilbert (1994b) and varve measurements from surface cores (n=3) taken in summer 2000. Standardized units used because original varve thickness measurements were not available. Varve departures for data for Lillooet Lake (1912-1989) were provided by J.R. Desloges.

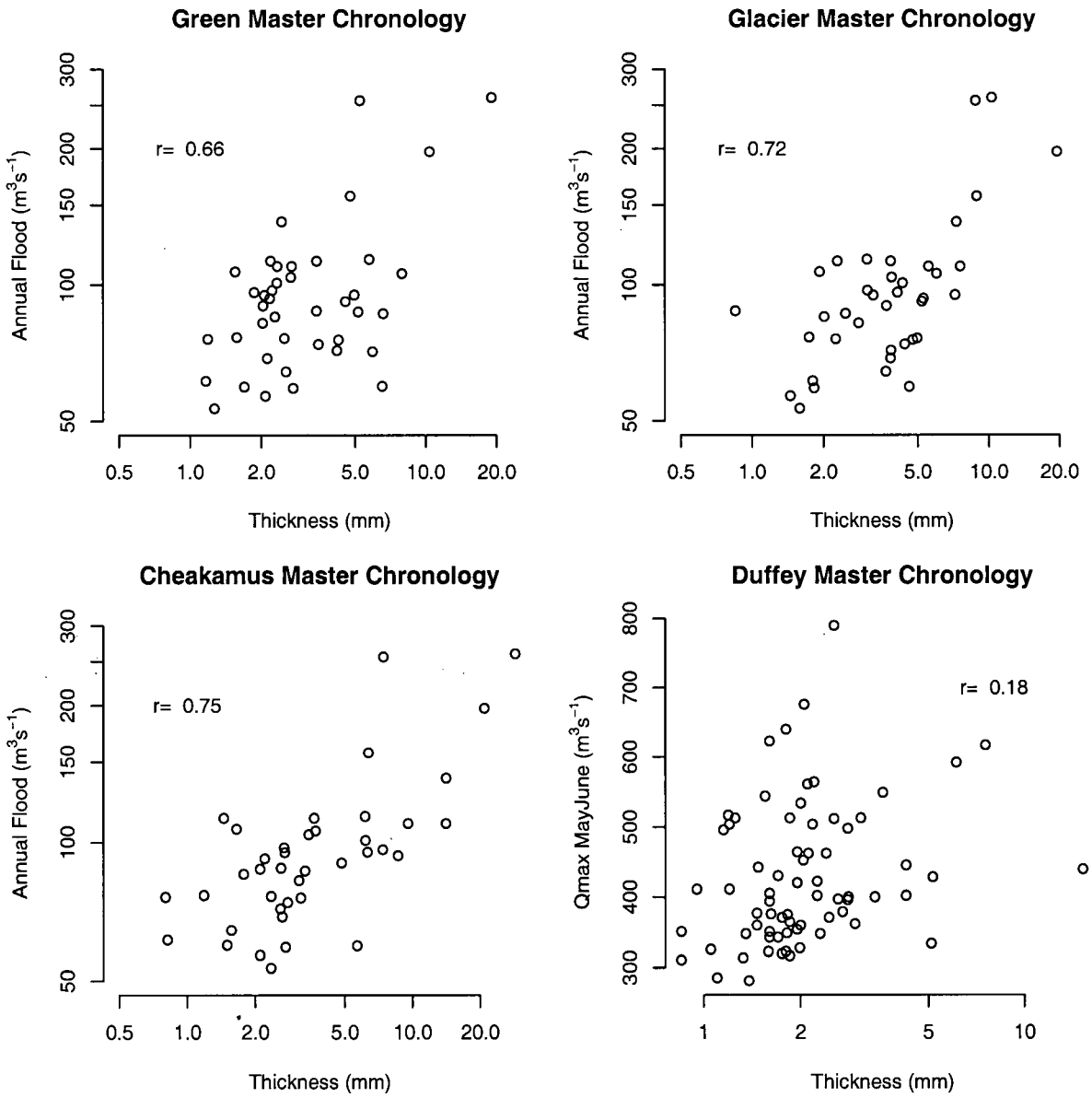

Figure 5.17: Varve Thickness-Q_{max} Relations
The scatterplots (Cheakamus, Green, Glacier) are based on log-log transformed varve thickness (mm) and annual flood for Cheakamus River (08GA072). Nival floods ($Q_{max(MJ)}$) for Lillooet River did not require a transformation and are only weakly related to varve thickness from Duffey Lake. Correlation to Q_{max} events for Lillooet River gave less significant results

Lake	Cheak	Green	Glacier	Cheak(Q_{max})	Lillooet(Q_{max})	PDO	SOI	PC1(temp)
Cheak	-	n=103	n=103	0.69	0.46	0.33	ns	ns
Green	0.30($p = 0.003$)	-	n=103	0.55	0.49	ns	-0.27($p = 0.02$)	0.36
Glacier	0.61	0.43	-	0.67	0.36	ns	ns	ns
				n=41	n=78	n=95	n=82	n=103

Table 5.2: Pearson Correlation Coefficients for Varve Records
Significance levels below $p < 0.001$ unless specified. SOI, PDO, and PC1temp are annual averages (Jan-Dec). The PNA and monthly departures in precipitation (PC1 ppt) were not correlated to the chronologies at zero or other lags.
[a] Annual average of SOI in following year. Zero lag correlation not significant

5.4.4 Extreme Sedimentation Events and Seasonality

A sizable proportion of the overall variance in the varve chronologies for three of the four basins can be explained the timing of infrequent, high discharge events to the lake basin. As observed in Chapter 3, flood generating mechanisms vary across the study area primarily caused by the topographic barrier imposed by the Coast Mountains. Despite the significance of the correlations between flood magnitude and varve thickness, there remains a considerable proportion of variance which remains unexplained. Some of this complexity appears to be produced by seasonal to inter-annual scale hysteresis in sediment supply and the timing of exceptional runoff events. Four floods (3 late summer-autumn and 1 snowmelt) provide good examples of the importance of runoff generating mechanisms and sediment availability in controlling sediment transport within the watersheds. Three of the floods (1940, 1984, 1991) were generated by rainfall events during late summer-Autumn while the fourth (1986) represents a rain-on-snow event.

The 1986 flood followed a prolonged period of warm weather in mid May. Discharge on the Lillooet River remained below 100 m^3s^{-1} until 20 May when warm weather elevated streamflow by snowmelt runoff. The passage of a low pressure system 24-25 May generated moderate precipitation totals near Whistler (31mm- 2 day total) and temperatures remained mild (minimum temperature was 8 °C) allowing for runoff generation from melting snow and precipitation. Little evidence for significant channel change and or hillslope instability in those basins which lie to the west of the Coast Mountain divide is evident from air photos but the flood apparently caused significant channel change on one of the tributaries (Van Horlick) to Duffey Lake (figure 5.18).

The 1986 varve (Duffey Lake) is comprised of silty-clay sediments with an inter-calated coarse silt to fine sand layer. The sand likely originates from proximal environments of the lake as the unit can be traced towards the delta where it is 40mm thick (98-Duf(V)). At this coring site, the unit consists of ungraded fine sands and much terrestrial organic material (needles and pieces of conifer wood) is present. In contrast to Duffey, the 1986 couplet in the other three lake basins is slightly larger than average (figure 5.16). Differences in sediment delivery between Duffey and the other three lake basins is interpreted to reflect the larger importance of fluvial sediment availability within the Duffey Lake catchment (Van Horlick) during snowmelt runoff compared to more seasonally restricted sediment sources (e.g. hillslopes and glaciers-glacial forefields) of the other watersheds.

The 1991 rainstorm produced the flood of record for Lillooet River (08MG005) and for several of the gauged stations between Elaho Valley and Lillooet River. Maximum daily discharge exceeded 1260 m^3s^{-1} for Lillooet River and sequential air photos before and after the event (1990, 1994) indicate significant channel change in channels east of Lillooet River (figures 5.19 and 5.20). The event was preceded by an 800 m^3s^{-1} flood on 9 August 1991 and both events likely contributed to observed channel change. Within the Green Lake basin, the second flood initiated hillslope instability on side slopes (valley fill) adjacent to Fitzsimmons Creek where a landslide was believed to have temporarily dammed the creek and elevated instantaneous discharge of the event following dam collapse (Golder Associates, 1992). Vertical change in the channel following initial aggradation and later scour exceeded 5m in several locations (Ward and Skermer, 1992). Recurrence interval estimates for the rainstorm vary depending on analyzed rain gauge network and inferences of underlying distribution but indicate that the event had a moderate (20-50 yr) return interval (Golder Associates, 1992; Ward and Skermer, 1992). However, this estimate is based on all 24-hr precipitation events irrespective of season and the significance of the event is closer to a 100-yr event for maximum recorded 24hr precipitation in summer (Golder Associates, 1992).

The flood appears to have been most significant in the Green Lake watershed where the event delivered an estimated 40,000 tonnes of sediment to the lake. This is a minimum estimate as it does not account for outflow losses or sediment deposited in deltaic environments. The 1991 event

is easily recognized within the sediment records of Cheakamus and Glacier Lake chronologies where it is the 2nd and 4th thickest varve within the composite records respectively (figure 5.16). Despite the significance of the event in those basins which lie to the west of Lillooet Lake, the event did not appear to deliver exceptional quantities of sediment to Duffey Lake. The 1991 couplet begins as ungraded coarse silts which are overlain by a conspicuous light-brown lamina but couplet thickness is not anomalous in the context of the contemporary record (figure 5.16).

The 1984 flood event occurred on 8 October following 3 days of heavy precipitation. The precipitation resulted from the passage of an intense low pressure system and total precipitation,

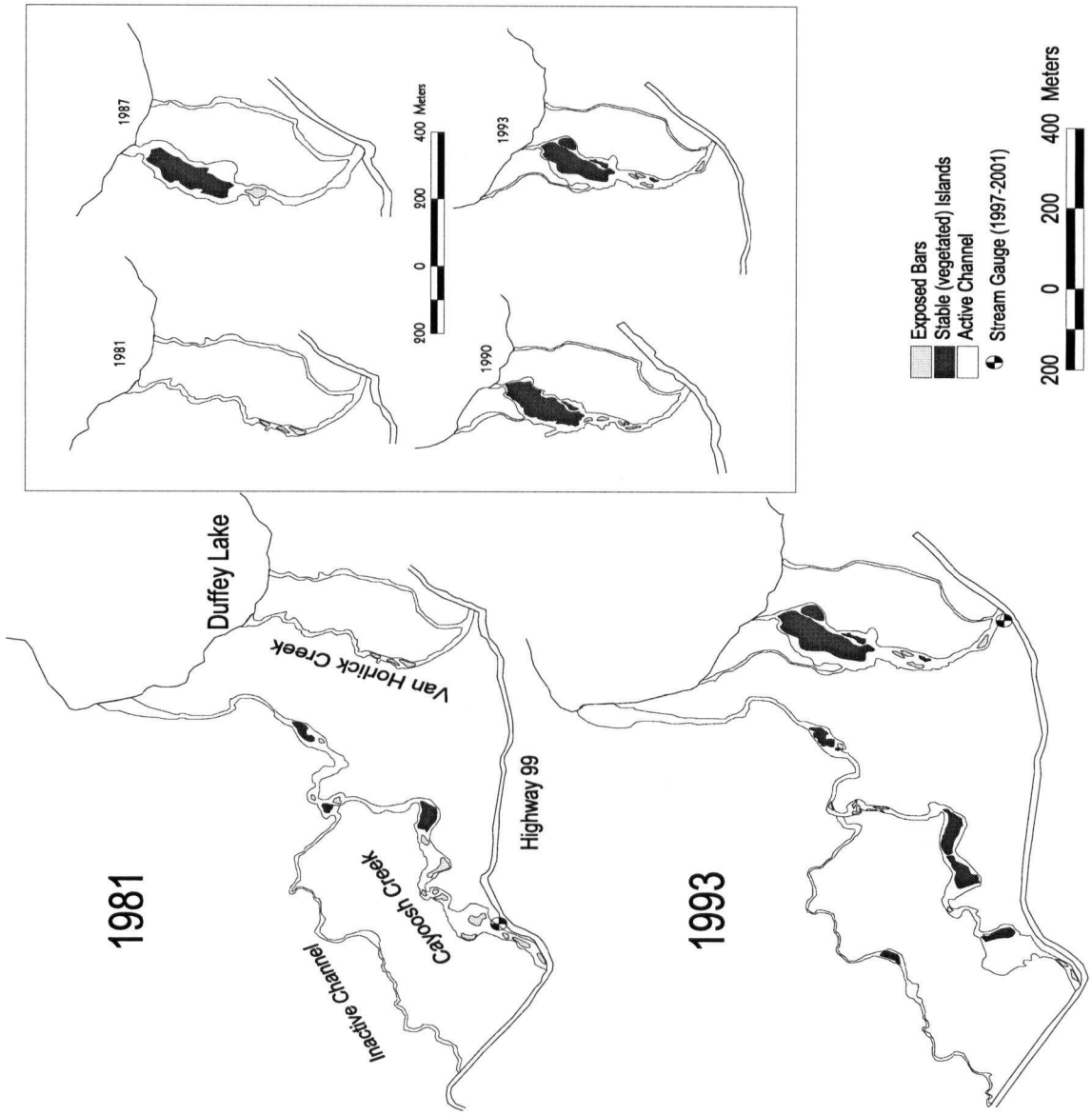

Figure 5.18: Channel Changes of Cayoosh and Van Horlick Creeks, Duffey Lake Basin
Note the contrasting histories of channel change for the neighboring sub-basins. Channel stabilization characterizes Cayoosh Creek near the delta while increasing complexity (increases in channel bars and active channel width) is observed for Van Horlick from 1981 to 1993. Channel patterns mapped from rectified air photos (RMS error < 5m).

much like annual totals varied widely across the study area with close to 150mm in Squamish, declining to 100mm in Whistler and only 2.4 mm recorded near the town of Lillooet. Temperatures remained moderate (10 °C) over the course of the event and both precipitation totals (daily) and temperatures were not dramatically different from the 1991 event. Evidence for the flood is present in all of the lake basins but its signature is not exceptional in the recovered lake sediment cores (figure 5.16). Much like the 1991 event, there is only minor evidence in the 1984 varve from Duffey Lake where thickness of both varves is comparable.

Precipitation amounts (3 day) and temperatures for an autumn flood in 1940 (19 October) were

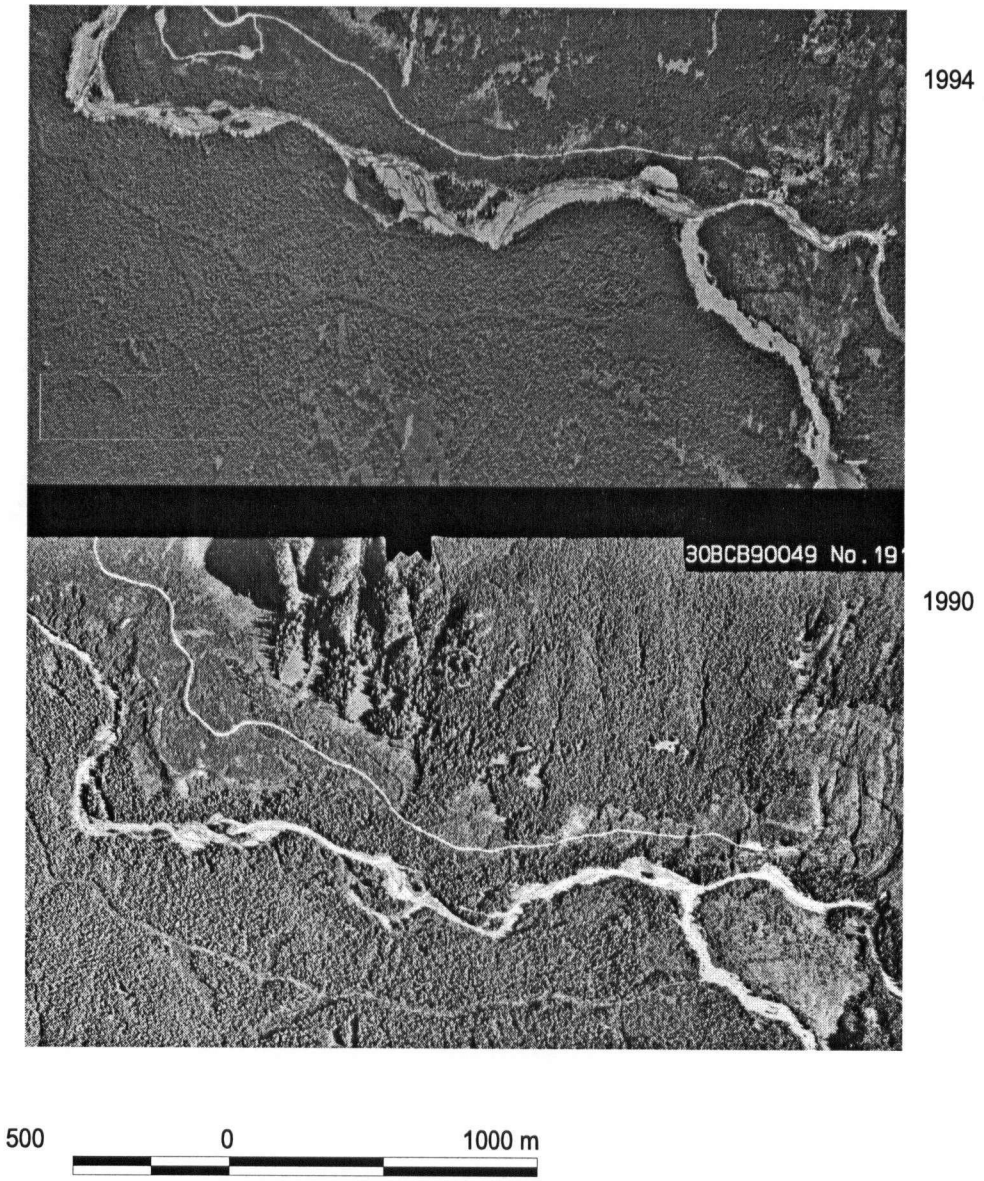

Figure 5.19: Channel-change Following 1991 Flood (Lower Cheakamus River)
Air photos (both at approximately 1:15,000 scale) showing channel before (30BCB90049:191) and after (30BCC94116:147) 1991 flood where maximum daily flow exceeded 260 m^3s^{-1} and was the flood of record (n=43) for Cheakamus River (08GA072) 5 km downstream from photo. Outlet of Cheakamus Lake is 500m to the right of the photo.

very similar to those observed for the 1984 event, but the quantity of sediment delivered during the event for Cheakamus, Glacier, and Green basins was considerably higher than that delivered during the 1984 event. In most sediment cores (except Duffey) recovered from the lake basins, the sediments entrained during the flood can be easily recognized as a normally graded lamina deposited late in 1940 and comprise between 40-60 percent of the total thickness of the 1940 varve. The 1940 event is also clearly recognized in the varves of Lillooet Lake (Gilbert, 1975; Desloges and Gilbert, 1994b). Although the thickness of the autumn flood deposit is appreciable, a significant proportion of the couplet appears to have been deposited prior to the flood. The micro-laminated structure of such sediment suggests that it was deposited in the lake basins over numerous rather then infrequent inflow events (e.g. figure 5.12).

5.4.4.1 Discussion

Differences in fine sediment response of the basins both across the hydrologic divide of the Coast Mountains but also within a given watershed over the contemporary period suggests that despite the statistically significant relation between lake sedimentation and runoff magnitude, seasonality

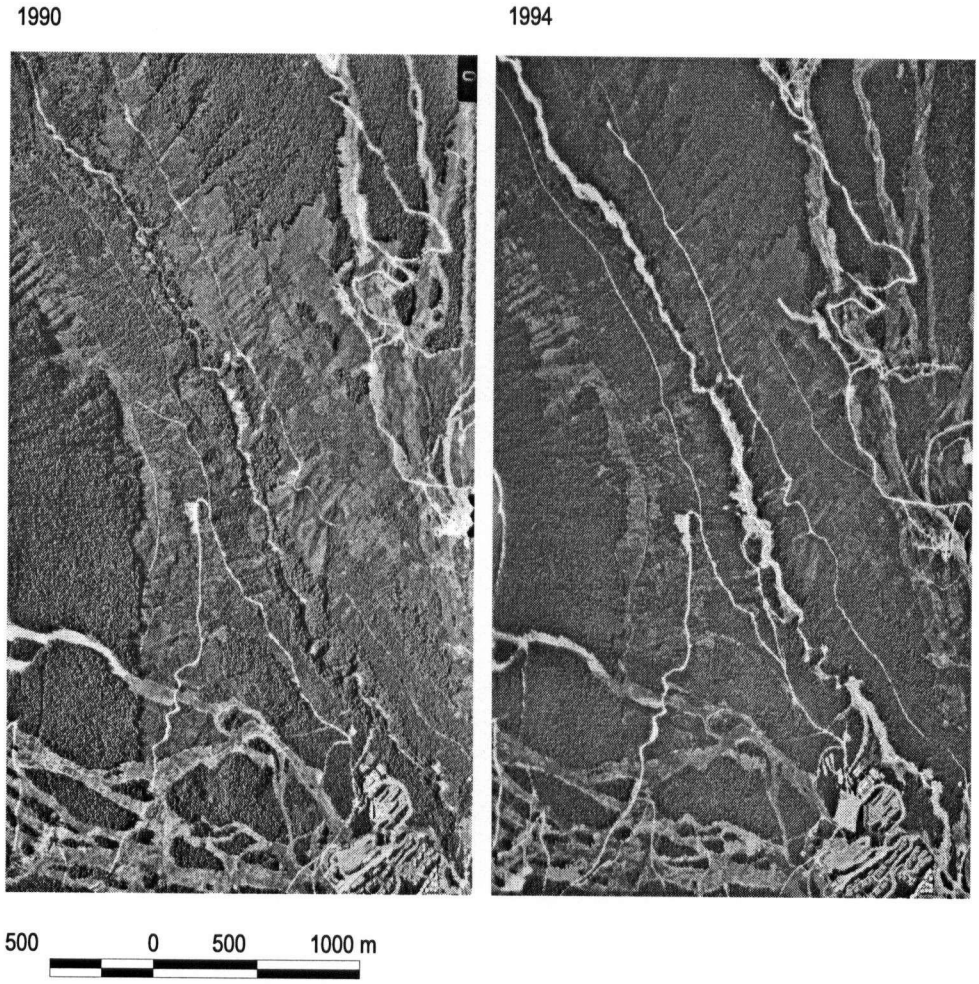

Figure 5.20: Channel-change of Fitzsimmons Following 1991 Flood
Same flight lines as photos in figure 5.19. Lower ski trails of Blackcomb ski resort can be seen in lower left-hand portions of the photos.

of runoff and changes in sediment supply introduce considerable complexities into the runoff-fine sediment response system of the watersheds. Seasonality or timing of the runoff event controls the sediment availability for a given rainstorm while longer term changes in sediment supply may alter the slope of the relation between the magnitude of runoff event and sediment transport. It is believed that both seasonality and the precursor precipitation event in early August contributed to the exceptional signature of the 1991 varve in Cheakamus, Glacier, and Green lake basins. The 1991 event occurred during late summer when most of the precipitation would have occurred as rainfall and during a time when glacial runoff was active. Such conditions are hypothesized to have contributed to the exceptional quantity of sediment mobilized during the event. It is possible that rain falling on glaciers during the event was effectively routed from supra-glacial to sub-glacial regions, elevating subglacial water and sediment discharge. Other glacial sediment sources for the event most likely included glacial deposits and forefield areas absent of vegetation.

The contrast between sediment delivery during 1984 and 1991 is surprising given the exceptional sedimentation which occurred during 1984 for Lillooet Lake during the same flood (Desloges and Gilbert, 1994a). It is likely that the differences between the sedimentologic response of the basins results from the following; a) the lower elevation of the Lillooet catchment which allowed most of the 1984 precipitation to fall as rain. This scenario would allow for higher rates of runoff and increase the proportion of the catchment which could contribute sediment during the event; b) similar varve thickness for the 1984 and 1991 couplets within Duffey compared to those basins lying in a more maritime setting where presumably, the 1991 event was likely to have produced larger instantaneous runoff peaks.

5.4.5 Sediment Source Changes Indirectly Related to Climate: Changes in Glacial Extent During the 20th Century

Recognized within the varve chronologies of the lake basins and variations in the bulk physical properties of the lake sediment archives is the lower frequency component of sedimentation within the lake basins. Such low frequency trends could arise from changes in the intensity or frequency of extreme discharge events. Changes in the intensity of runoff events were recognized for the Lillooet River basin but most of the change occurred following 1970 (figure 5.5). The low frequency components (Cheakamus, Green, Glacier) show similarity to inter-decadal fluctuations of air temperature in the study area and it is not unreasonable to speculate that such climatological effects are important for controlling ice extent in the study area since air temperature represents one of the primary controls on glacial mass balance within most mountain environments of the world. Numerous studies both within the Canadian Cordillera (e.g. Souch, 1994; Leonard, 1997; Leonard and Reasoner, 1999) and elsewhere (e.g. Karln, 1981) have demonstrated the importance of glacial cover on influencing downvalley sedimentation rates.

To examine the relation between ice cover changes in lake sedimentation, decadal scale variations in glacial cover were evaluated over the contemporary period through mapping from air photos and compilation of documentary records. Glacial extent within the southern Coast Mountains during the 20th century have been documented in much less detail than in other environments of the Canadian Cordillera (e.g. Luckman and Osborn, 1979; Luckman, 2000). Prior evidence for 20th century glacial extent for the study area comes primarily from studies conducted in Garibaldi Park (Mathews, 1951). In order to extend (in both space and time) these earlier results, sequential mapping of contemporary ice limits was completed on several glaciers within the study area.

Documentary evidence for glacial extent prior to 1931 is limited to verbal records of climbing parties (Heaney, 1912) and through several oblique photographs taken in Garibaldi Provincial Park (Mathews, 1951). Photographs and a field map of glaciers in proximity to Garibaldi Lake taken in

1912 (Heaney, 1912) reveal that most glaciers were only slightly (100-200m) retracted from moraines inferred to be 'Little Ice Age' in age (Mathews, 1951). Little change in downvalley position of two of these glaciers (Sentinel and Sphinx) is revealed in a oblique photo taken in June 1920 (Hardy et al., 1978). By 1928, many of the glaciers in the western portion of Garibaldi Provincial Park were photographed by A.J. Campbell (Ministry of Lands and Environment) from ridges and peaks in Garibaldi using a large format camera. Those photographs were combined with survey data to compile the first base map of Garibaldi. Large scale (1:15,000) air photos become available by 1931 and sequential photos for many of the glaciers exist for 1946(9), 1969, 1980, and 1986(7). A summary of methods is given in appendix B.

Based on the mapping, it appears that those glaciers for which air photo coverage was available were responding in a more or less similar fashion over decadal time scales for the period 1929(31)-1993 (table 5.3). The period between 1929(31)-1946(9) was characterized by rapid rates of retreat and there is little evidence of recessional moraines or other features which may indicate reduced rates of glacial ablation. Many of the termini are irregular in plan form and thin over steep, exposed bedrock interpreted to reflect stagnating and or retreating ice. For the larger glaciers of this study, reductions in length between 1929(1931)-1946(9) are on the order of 200-300m (figure 5.21).

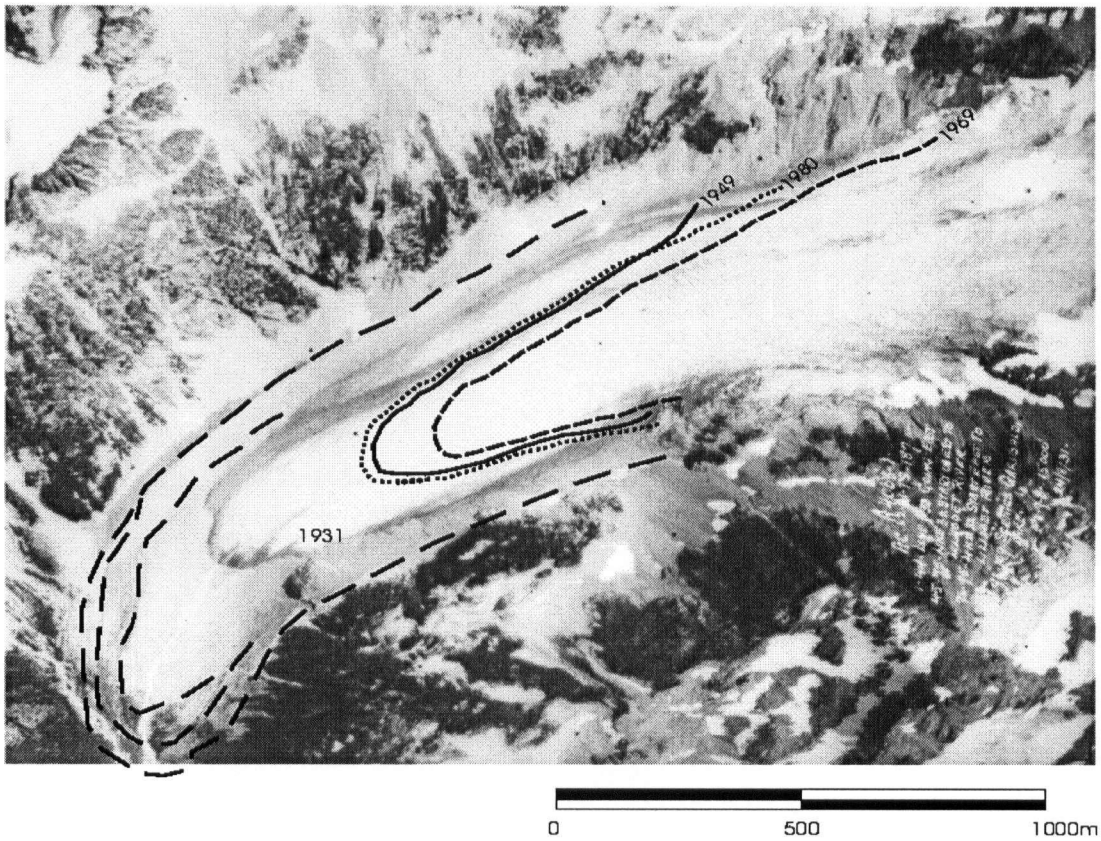

Figure 5.21: Contemporary record of terminus fluctuations, Fitzsimmons Glacier
Federal air photo (A 4068-1) taken 24 August, 1931 showing terminus of Fitzsimmons Glacier and downvalley positions in 1949, 1969 and 1980. Inferred ages of outermost three moraines are ≈ (1900-1910), 1840 and 1700AD based on photographic record (Heaney, 1912) and environmental reconstruction (Mathews, 1951) of glacial fluctuations near Garibaldi Lake.

Changes in ice extent between the late 1940's and 1960's are characterized by continued glacial

retreat but rates are significantly slower than recession during the 1930's and early 1940's. Bands of supra-glacial debris which do not appear to be medial moraines become more pronounced in the ablation areas of many glaciers and are interpreted to reflect stagnant ice conditions where net deficits of ice have accumulated debris at the surface of the glacier (Drewry, 1986; Menzies and Shilts, 1996).

Between 1969 and 1980 several of the glaciers within or near the study areas showed no net change in areal or downvalley extent and many of the glaciers underwent minor re-advances (table 5.3). Additional glaciers, based on air photo analysis, were more extensive in 1980 but could not be mapped due to large errors caused by relief displacement. Termini became more convex in cross section in those glaciers which experienced a renewed phase of growth and most advanced close to their 1946(9) downvalley positions. The two major glaciers within the Green Lake watersheds (Fitzsimmons and Overlord) thickened and termini advanced some 200m between 1969-1980 and the largest glaciers within the Van Horlick basin (Duffey Lake) built small moraines sometime between 1946 and 1993. The moraines are not large and are interpreted to be correlative with the observed glacial advances in the Green Lake catchment during the 1970's. Evidence for other minor scale glacial advances have been reported for other glaciers within the study area (Ricker, 1978; Ricker and Tupper, 1978). Thunderclap and Griffin Glaciers (Glacier Lake watershed) underwent similar scale advances ($\approx$100m) during this time. Place Glacier experienced several years of positive mass balance, apparently the result of high snowfall rates during the late 1960's and early 1970's followed by cooler summer conditions between 1970 and 1975 (figures 5.1, 5.2). Such climatic conditions were large in spatial extent as glaciers within the mid Coast Mountains (Desloges, 1987), the Canadian Rockies (Luckman and Osborn, 1979) and the Pacific Northwest (Spicer, 1989) were behaving in a similar fashion. Slow glacial retreat characterizes their behavior following 1986.

Glacier	Watershed	area (km^2)	1912	1928[a]	1931	1946 (9)	1952	1969	1980
w. fork Van Horlick[b]	Duffey	0.48	-	-	0.760 (+300)[c]	0.517 (+30)	-	-	-
Hidden Glacier[b]	Duffey	0.52	-	-	-	no change	-	-	-
Fitzsimmons	Green	1.95	-	-	2.15 (+315)	no change	1.44 (no change)	1.81 (-360)	1.97 (+360)
Overlord	Green	3.10	-	-	-	no change	2.73 (-90)	3.09 (-150)	3.12 (+150)
Helm	Garibaldi	1.41	4.06 (+825)[d]	3.85 (+825)	-	2.27(+340)	-	-	-
Sentinel	Garibaldi	3.01	4.06 (+1730)	3.78 (+1520)	-	3.37 (+830)	3.53 (+860)	3.20(+320)	-
Spinx	Garibaldi	4.76	5.98(+1910)	5.79 (+1650)	-	-	4.85 (+230)	no change	-
Warren	Garibaldi	5.33	10.5 (+2515)	9.59 (+1700)	-	6.21(+945)	7.18 (+980)	5.56(+410)	-
Diavolo	Cheakamus	3.29	-	-	-	3.64 (+1600)	3.32(+60)	2.93 (-55)	3.42 (+210)
Naden	Cheakamus	1.16	-	-	-	-	-	1.08 (-290)	1.20 (+50)
Thunderclap	Glacier	3.21	-	-	3.91 (+780)	-	-	no change	-
Grinnel	Glacier	2.51	-	-	2.98 (+925)	-	-	2.49 (-125)	-

Table 5.3: Changes in Areal and Downvalley Extent of Glaciers Within or Near Study Basins During Contemporary Period Planimetric changes relative to TRIM mapping datum (1986/1987). Sign denote length changes more (+) or less (-) extensive than 1986-1987.

a. Co-registered survey data (1928) from provincial map (mapping from oblique 1928 photography)

b. Un-official names (Glaciers are not named on NTS map sheets)

c. Change in area and length (m) from TRIM mapping project (1986/1987 air photos 1:70,000).

d. Larger uncertainty of 1912 estimate as areas estimated from oblique photographs and from maps with less ground control

5.4.5.1 Discussion

Over decadal time scales, there appears to be a general correspondence between low frequency climate variability and glacial fluctuations during the contemporary period. Rapid recession of the glaciers within the study after 1931 until the mid 1940's was following by conditions favorable for small glaciers to experience no net change in balance or experience slight advances during the 1970's and appears to be the result of both precipitation and temperature anomalies (of opposite sign) during this time (figure 5.1). Such departures closely mirror the secular trend in the Pacific Decadal Oscillation (PDO) during this century (figure 5.2). Additional evidence for high rates of glacial recession centered around the early 1940's is provided by low frequency (3 yr) variations in runoff from the Lillooet River Basin (figure 5.1) and the significance of the anomaly becomes larger if only late summer variations in flow (e.g. 15 August-15 September) are considered.

The length-scale response of most of the glaciers within the study area is less than that predicted by theory (e.g. Jhannesson et al., 1989a,b; Bahr et al., 1998). Desloges (1987) noted a similar, short term response of glaciers within the middle Coast Mountains which did not appear to be scale dependent for glaciers smaller than 10 km^2 . Similar findings have been reported for glaciers in other mountain environments (e.g. Spicer, 1989; Patterson, 1994). One possibility for such rapid response is a decoupling between terminus fluctuations and true internal adjustments of the glacier to mass balance variations experienced in the accumulation area. Although it would be expected that maritime glaciers experience significant ablation at the terminus each year, deep insulating snowpacks of the Coast Mountains may severely limit melt in the ablation zone. Such conditions were observed at Place Glacier late in the ablation season (September) of 1999 where ice at the terminus was mostly covered by snowfall from the previous year. Such a wintertime surplus of snowfall could conceivably cause length scale changes over small time scales (1-2 years) because any mass advected to the ablation area by normal glacial flow would tend to lengthen the glacier under such conditions. Adjustments of the glacier to increases in mass as caused by increases in winter snowfall may be expected to take considerably longer than these minor-scale adjustments at the terminus and in this case should scale to equation 2.1 which would be on the order of decades. It is possible then, that glacial response times of the study area are comprised of a shorter scale response primarily controlled by climatological conditions of the terminus and a longer term response related to the residence time of the ice within a particular glacier. The apparently lower than predicted response time of the study area glaciers minimizes the filtering effects commonly imposed by the mechanics of glacial flow. Such results provide direct and useful information regarding the behavior and severity of one of the important geomorphic filters discussed in Chapter 2.

5.4.5.2 Glacial Activity and Lake Sedimentation

In those watersheds where sediment sources appear to be dominated by immediate (rockflour) glacial sources, patterns of increased lake sedimentation appear to coincide with phases of glacial retreat. Receding ice exposed fine-grained sediments which were routed to the lake basins by higher rates of runoff. Highest sedimentation rates are observed between 1920-1950, a time of rapid glacial recession though there are important differences between the watersheds. For example, highest sedimentation rates occurred in Green Lake around 1935-1945, coincident with maximum air temperature and discharge (Lillooet River) anomalies. In contrast, maximum sedimentation within Cheakamus and Glacier lakes appeared to occur a decade earlier, corresponding more with precipitation (negative) rather than temperature (positive) anomalies (figure 5.1). Such a lag may indicate a larger temperature component controlling glaciers within the Green Lake catchment or perhaps geomorphic differences in the rates of sediment production or transport. It would,

however,be expected that sediment delivery from Cheakamus and Glacier would lag behind Green given their size, active flood plains, and larger percent glacial cover. Causality for the differences remains unknown.

Varve clarity is poorest during those periods when glaciers within the study area were either advancing or show little change in downvalley extent. Such a relation is particularly evident for Green Lake for the early 20th century (1900-1920) where varves are poorly defined in an area close to the lakes' major inflow. Despite the inferred downvalley extent of the glaciers within the Fitzsimmons Creek basin during this time (inferred from the position of glaciers near Garibaldi Lake), delivery of clastic sediments to the lake basin was minimal. Though lower sedimentation rates are observed for Cheakamus and Glacier lake basins, the varves are more easily recognized and may relate to the higher percentages of glacial cover within these catchments. Secular trends in varve thickness for the fourth lake basin (Duffey Lake) appear to be related to general periods *favoring* periods of ice growth as varve departures are believed to reflect the intensity of underflow events, most common during snowmelt within this watershed. Dominant sediment sources for this catchment appear to be the fine-grained sands which comprise the channel of Van Horlick Creek. There is minimal opportunity for permanent storage of these sediments between contemporary ice bodies and the lake basin. Despite the poor relation between glacial retreat and varve thickness, changes in the bulk physical properties (e.g. organic matter content, density) of the sediments from the central basin of Duffey Lake do appear to record changes in glacial cover. Most easily recognized varves and those which are less bioturbated characterize sediments deposited between 1930 and 1950. Such data suggest that changes in the bulk physical properties of the Duffey Lake sediments may provide a more representative index of lake wide sedimentation patterns than do changes in varve thickness recorded in the central basin sediments of the lake.

In contrast to these results, studies in the Canadian Rockies have indicated that high rates of lake sedimentation within proglacial lake basins can occur during time of ice growth and/or when glacial ice is more extensive (e.g Leonard, 1986b, 1997). Such conclusions were made for the period preceding the contemporary period and were based on isolated terrestrial evidence for glacial activity. During the contemporary period, variations in varve thickness in Hector Lake are most strongly correlated with inter-annual variability of summer air temperatures, which appear to control the intensity of glacial runoff (Smith, 1978; Leonard, 1986b). Analysis of century-scale records of lake sedimentation, combined with climate-proxy data in Chapter 6 will test the robustness of the conclusions drawn here. Changes in contemporary ice cover were not considered to be a major contributor to 20th century variations in sedimentation within Lillooet Lake (Desloges and Gilbert, 1994b) which is in contrast to the observations made in this study. Such a conclusion is surprising given the moderate proportion of the catchment which is ice covered (14 percent), the general lack of intervening lakes between the lake and contemporary ice cover and the terrestrial evidence for glacial recession during the 20th century. A re-inspection of the varve chronology for Lillooet Lake does indicate a general pattern of above average sedimentation between 1935-1945AD (figure 5.16).

5.4.5.3 Climatic Controls on Sediment Source Variability: Limitations for Environmental Reconstruction

Variations in sediment availability and the importance of extreme runoff events in sediment entrainment impose significant difficulties in using the sediment archives to reconstruct hydro-climatic variations within southwest British Columbia. For portions of the records (1900-1977), varve thickness variations do show correspondence between variations in annual temperature fluctuations and more integrative indices of climate, namely the PDO (table 5.2) . However, like the residual anal-

ysis after controlling for flood intensity, the sensitivity of the watersheds to record such variations declines significantly following 1945. In all of the lake basins, sedimentation within the last 50 years appears to be primarily controlled by the frequency and intensity of flood events rather than temperature variations or inter-decadal variations in the PDO. Thus, it is believed that following early 20th century recession, the importance of glacial sources for the lake basins decreased at the expense of those sediment sources that can be eroded and entrained during high flow events. The lack of a simple, stable relation between a particular hydro-climatic forcing (e.g. nival runoff, rainfall events or glacial runoff) is likely to introduce considerable difficulty in inferring hydro-climatic variability from varve thickness alone. The instability of the proxy-sediment response relation with be assessed in the following chapter with the use of multiple climate proxy records over considerably longer time scales.

5.4.6 Internal Controls on Sediment Delivery: Land Use and Natural Diversions

Although it appears that changes in sediment availability are primarily controlled by glacial fluctuations in the catchments, effects of recent land use within two of the basins (Duffey and Green) may have altered the natural fine sediment cascades within these watersheds. As discussed in Chapter 3, a diversion within the Glacier Lake catchment may have likewise altered sediment availability.

Effects of land use as recorded by the sediments of Green Lake appear to be slight and the only conclusive evidence for such change exists in the increased terrestrial organic matter within the sediments of the most distal basin. Two short Ekman cores (99-Grn(04, 05)) recovered in 1999 reveal sediments that are finely laminated and low organic content characterizes the sediments deposited between 1952 and 1991. Varves deposited between 1951 and 1959 contain small, fibrous wood particles which make varve counting and measurements impossible prior to 1951. Air photos from 1946 indicate the presence of log booms in close proximity to the core sites near the former township of Parkhurst. The booms were presumably storage sites for logs before milling and or shipment by rail. Thus, the fibrous woody debris within the cores is likely the result of wood storage within the lake. Lack of longer and more uniformly distributed cores from the lake prevent an evaluation concerning the spatial significance of the event. The inferred change of sedimentation rates and potential sediment source change following the flood of 1991 is significant. In contrast to earlier evidence for floods within the sediments, the laminae deposited after 1991 are light brown to reddish in color (wet sediment) and micro laminae within varves become more common. The 1992 varve is an exception; its color is similar to the event of 1991 and its thickness (10mm) is also significantly thicker than average couplet thickness ($2.93 \pm 2.32mm$) over the contemporary period (1880-1999). Varve boundaries become more difficult to recognize which appears to result from a lower bi-modality of the sediments (with respect to grain size variations) following 1991.

It is likely that following the 1991 flood, dominant sediment sources for the lake basin switched from predominantly glacial in origin to glacial/valley fill. Much evidence for continued instability with the Fitzsimmons Creek valley is visible today and fine sediment can enter the channel through detachment during rainstorms and/or material routed directly to the channel during small scale rapid mass movement. Additions of fine-grained material within the lower confines of the channel were likely introduced during gravel extraction within the channel following the 1991 flood as a means of increasing channel capacity. Between 1991 and 1999 over 2.5 x 10^5 m^3 of sediment was removed from the floodplain of Fitzsimmons Creek above the lake (Sigma Engineering). Unfortunately, most of the sediment found within the valley fill of Fitzsimmons is minerologically identical to those lithologies near or presumed under the main glaciers of the watershed so that differentiating fluvial/hillslope from glacial source using geochemistry and/or magnetic properties is not

possible. It remains unknown to what degree logging contributed to the hillslope instability within Fitzsimmons Creek valley. The valley was clearcut in the 1950's but such effects were believed not to contribute to the observed hillslope/channel instability (Golder Associates, 1992). Air photos from 1946 and 1969 indicate only minor evidence for former instability. Dominant sediment sources during that time appeared to be the Fitzsimmons and Overlord Glaciers and their forefields.

Of particular importance is the "memory" introduced to sediment transport following 1991 (figure 5.22). Prior to the flood, varve thickness following large floods (e.g. 1940, 1984) showed little autocorrelation but this increased following 1991. A likely cause for such effects would be for increases in the proportion of fine grained sediments originating from exposed till surfaces or from fluvial storage sites elevating overall sediment availability. Such effects may also explain the apparent declining trend observed in the SSC-Q relations in Chapter 4 over the two years of contemporary monitoring. Residuals from Cheakamus and Glacier Lake basins do not show such consistent positive departures. Evidently, the effect of the 1991 event was most severe in the Green Lake basin.

Evidence for disruptions of the normal sediment cascade for the Duffey Lake catchment is limited to 1-3 years following initial construction of the Duffey Lake road. Evident within the recent varved sediments from the lake basin is the presence of thin (< 2mm) ungraded silty laminae within the varves deposited between 1970 and 1973 (figure 5.11). The laminae are within the lower-most sediments of the couplets and decrease in thickness from 1970 to 1973. Their presence in the lower-most unit of the varves is important as it suggests that the material was delivered early versus late in the hydrologic season. The laminae deposited between 1970 and 1973 may represent minor contributions to the lake during the primary construction phase of the Duffey Lake road which began in 1970. Their deposition in the lake basin early in the season suggests that they do not represent material delivered to the lake during glacial runoff. Provenance determination based on mineralogy was not attempted because the sediments used to construct the road (quartz diorite and granodiorites) are similar to the rock type found near contemporary glaciers. If the sediments indeed derive from land use, it suggests that such effects were relatively minor in altering sediment supply to the lake basin and that the effects were short lived. The minimal evidence for such disturbance may reflect the overall minimal impact of land use within the catchment (10 percent of the watershed was logged) but also confirms the suspicion that sediment transport within the watershed is event rather than supply limited as much of the contemporary sediment storage of glacially derived sediments exists in the Van Horlick Creek. Thus, at least for the contemporary period, fluvial sediment sources to the lake basin appear to be un-limited.

The final example of lake sedimentation patterns which may have been affected by internal geomorphic factors is the diversion of streamflow within the Glacier Lake catchment. Based on air photo interpretation, the diversion is known to have occurred prior to 1931 (Ricker, 1978). Before the diversion, Snowcap Lake was tributary to Glacier Lake contributing an additional $20km^2$ of land surface (5 percent glacial cover) to the lake basin. Based on the varve chronology from the lake basin, the effects of the diversion, if it occurred between 1880 and 1931 was slight. The most notable change in sedimentation occurs following the early 1940's when varve thickness is appreciably lower than before this time. In addition to climatic conditions not favorable for high glacial runoff (figures 5.2, 5.1), sediment storage sites (proglacial lakes) within the Glacier Lake basin increased following rapid recession during the 1930-1940's and most likely contributed to reductions in sediment supply. Nevertheless, similar reductions in sedimentation were observed in Cheakamus and Green Lakes suggesting a more regional signal of reduced sediment delivery to the lake basins following the second half of the twentieth century.

To conclude, the evidence for effects of land changes and land-use in influencing rates of sediment delivery to the basins (Green and Duffey) is tenuous at best. Within the Duffey Lake sediments

the effects are short lived and decline rapidly (3 years) following road construction. In Green Lake sediment delivery to the lake basin following the 1991 flood is significantly different from pre-event rates. It remains unclear whether forest removal within the the Fitzsimmons Creek basin elevated the natural thresholds of instability, although the 1991 represents the flood of record. Sedimentation rates following the 1991 event in the other two hydrologically similar watersheds (Cheakamus and Glacier) returned to pre-event levels. This observation lends support for the theory that forest removal (or continued gravel extraction and river engineering following 1991) within the Fitzsimmons basin may have contributed to the general instability found there. Analysis of extreme events within the longer sedimentary archives of Green Lake will help to put the 1990's into a longer perspective.

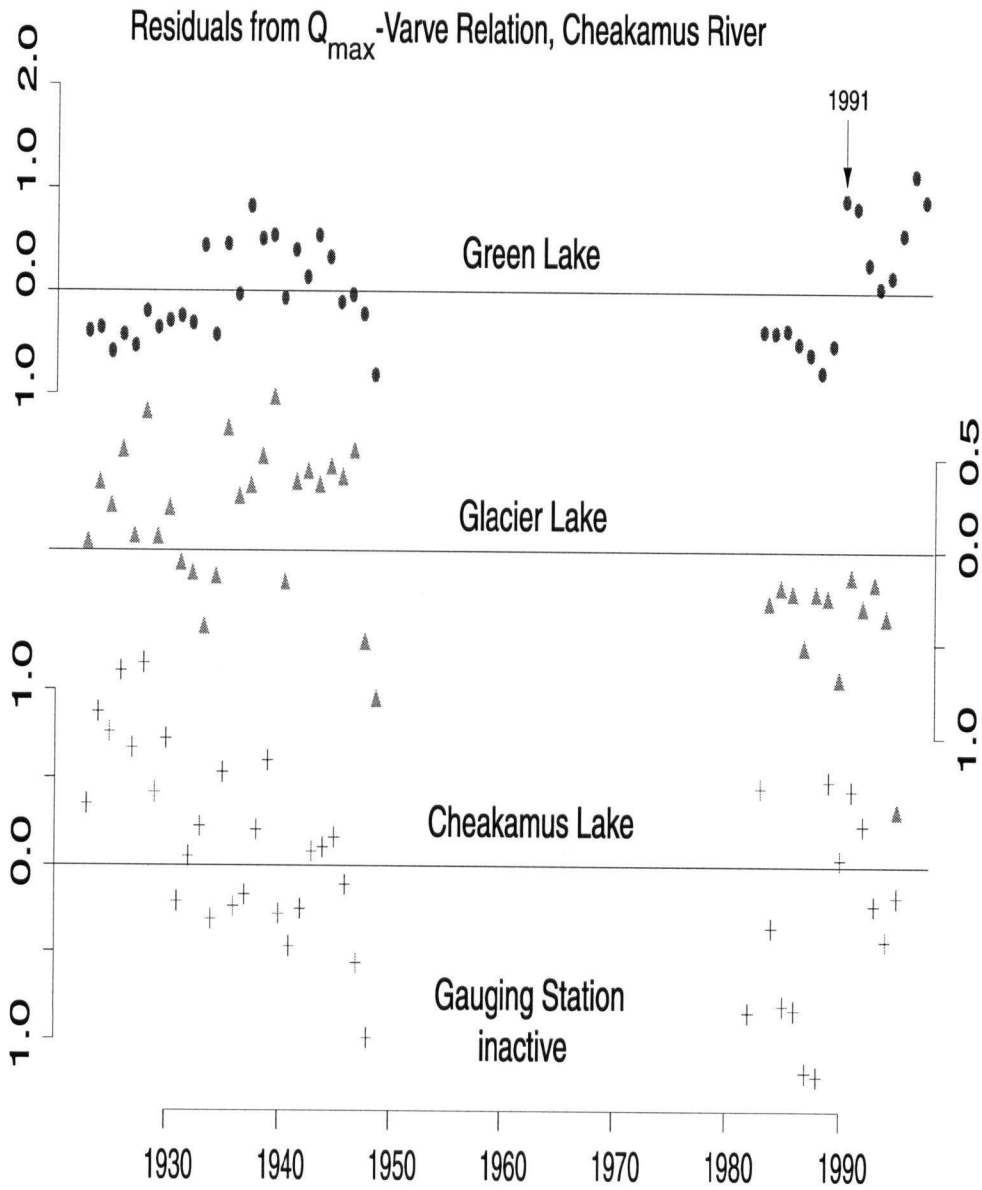

Figure 5.22: Residuals of Varve Thickness From Green Lake After Controlling for Flood Intensity Residuals from linear model between log transformed varve thickness and Q_{max} (n=43) for Cheakamus River (08GA072). Note consistent positive residuals in Green Lake chronology following 1991.

5.5 Lake-Based Sediment Yield Estimates

Lake-based sediment yields were estimated for the basins in this study (Green, Duffey and Birkenhead) where a sufficient number of surficial cores was recovered. Comparisons between lake and fluvial based estimates of sediment transport were also made. Bias introduced by analyzing variations in sediment delivery to the lake basins from those isolated areas where varves are continuous and most apparent was also assessed. Because of hydrologic and biologic reworking, sediment yield estimates could only made at the decadal scale for Birkenhead and Duffey Lake basins.

Procedures follow those outlined in Evans (1997) where sediment mass (after removal for organic and carbonate fraction) is determined for a given time interval within a lake core and multiplied by that fraction of the lake basin it represents. The estimate requires the correction for outflow losses which is often estimated by determining the residence time of the lake water (e.g. Heinemann, 1981). Results from such methods may deviate considerably from true trapping efficiencies due to particle size characteristics of the sediment, thermal stratification of the water body, and wind stress (e.g. Sundborg, 1992). A significant component of the clastic load may be transported across and through the epilimnion and out of the lake if sediment inflow occurs when the lake is thermally stratified. Such effects can be found in Cheakamus and Green Lakes where the thickness of late summer/early autumn flood deposits in distal setting are considerably thick and indicate that a large fraction of sediment exited the basins during the event. Because data necessary for outflow correction based on thermal characteristics are not available, correction for outflow losses is not estimated. The severity of the error (underestimate) is likely to increase substantially during exceptional inflow events, especially during seasons when the lakes are strongly stratified and sediment sources are predominantly fine grained.

Estimates for sediment yield from Birkenhead Lake require an estimate of sediment age or at the very least, an estimate of average sedimentation for the recovered sediment as the contemporary sediments of the lake are massive. Though trends in bulk physical properties can be traced throughout the lake basin, the lack of unique and spatially contiguous marker horizons prevents a sub-division of the sediment record into specific time intervals. Trends in the measured bulk physical properties of the cores were combined with lake sedimentation rates estimated from three alternative methods to estimate yields for the period 1937-1997 AD. Average sedimentation within the distal basin of the lake (figure 5.7) is provided by sediment fluxes determined during the lake monitoring program, an estimate provided by ^{210}Pb dating and a longer estimate obtained from an AMS ^{14}C age (1070 ± 90 ^{14}C yr BP; table 6.7) presented in Chapter 6. Estimates for the proximal basin are provided by the sediment trap data. A constant rate of supply (CRS) model was used with the slope between sediment depth (cm) and ^{210}Pb activity ($dpgs^{-1}$) giving an estimate of average sedimentation. The CRS model is the most applicable as the results from the other lake basins indicate high inter-annual variability in sedimentation. Slumping and or reworking of ^{210}Pb-depleted lake sediment was unlikely given the absence of sedimentary beds in the core (97-Birk(01)) analyzed for unsupported ^{210}Pb. Sedimentation rates estimated from the trap data (figure 4.8) were calculated from :

$$\frac{u}{\rho_{0-1cm}} \tag{5.1}$$

where u is the average, yearly sediment flux ($g\ cm^{-2}\ yr^{-1}$) to the lake floor and ρ_{0-1cm} is the density (gcm^{-3}) of the uppermost sediment collected within the surface cores sub-sampled from the Ekman dredge and ranged between 0.35-0.55 $g\ cm^{-3}$. The trap-based method provides an estimates of $2.1 \pm 0.6 mmyr^{-1}$ for the proximal and $1.1 \pm 0.4 mmyr^{-1}$ for the distal basin respectively. The uncertainty (1 σ) reflects variations in seasonal trap flux rates. The trap-based estimates for

lake sedimentation in the distal basin agrees rather closely with longer-term estimates provided by the ^{210}Pb dating ($1.1mmyr^{-1}$) and the AMS ^{14}C age ($0.7mmyr^{-1}$). Overall, the results indicate a two-fold reduction in sedimentation down lake, interpreted to reflect the increasing distance from main inflows but may also result from the uplake direction of prevailing winds during summer. The estimates of sedimentation rates also help to confirm the suspicion that the absence of sedimentary laminae within the lake basin does not result from low sedimentation rates. These estimates are comparable to sedimentation rates in the central area of Duffey Lake. Lack of laminae preservation is interpreted to result from shallower water environments (more O_2) and lower turbidity of the lake water resulting from smaller contributions of fine grained sediments from glacial sources.

Sediment yields to Duffey Lake could be estimated on a decadal scale as several laminae could be traced throughout the suite of lake sediment cores. Intervals at which the yield estimates were calculated depended entirely on the presence of marker horizons rather than selected epochs. Multiple estimates provide some indication of the reliability of the estimate, though an assumption regarding general climate stationarity has to be made over the 1937-1998 period which, based on the previous results is probably not entirely valid. The mass data were used in conjunction with the varved record from the central basin to estimate sediment delivery on a decadal basis. Estimates with greater uncertainty are provided by Ekman samples from Green Lake (for the past 10 years). Greater error in the Green Lake estimate arises both from the comparatively shorter length of record but also the limited spatial coverage of the Ekman samples.

Decadally-based estimates of sediment delivery to Duffey Lake do not show significant variations through time but generally higher yields (though not statistically significant) are observed for the earliest interval (1937-1946). The lack of decadal variability is undoubtedly caused by the the aggregation of highly variable, yearly sedimentation (c.f. figure 5.16). Varves deposited within the lake during 1937-1946 are thinner but denser and more uniformly distributed throughout the lake basin. The average yield over the 1937-1998 period is $0.069 \pm 0.01Mgkm^{-2}day^{-1}$ and the agreement between this estimate and that ($0.089 \pm 0.06Mgkm^{-2}day^{-1}$) obtained from the fluvial methods (combined fluvial yield estimated for Van Horlick and Cayoosh Creeks normalized to the Duffey Lake catchment) differs by 22%, which is close considering that outflow losses have not been accounted for and the coring program did not recover sediments deposited in deltaic environments. The lake ($0.096Mgkm^{-2}day^{-1}$) and fluvial ($0.20 \pm 0.21Mgkm^{-2}day^{-1}$) estimates differ by 50% for the Green Lake catchment. They are within the range of fluvial-based variability observed during the two years of study. Bedload transport studies completed in the Green Lake catchment (Pepola, 2001) indicate that the fine grained fraction (silts and clay) within the delta is low ($\approx$1%). Estimates based on the more spatially restrictive sediment cores which comprise the varve chronologies of both basins over the 1937-1998 period gave average yields of $0.089Mgkm^{-2}day^{-1}$ and $0.13Mgkm^{-2}day^{-1}$ for Duffey and Green Lake respectively. A single estimate $0.052Mgkm^{-2}day^{-1}$ is provided for Birkenhead Lake based on the entire 1937-1998 period.

5.5.0.1 Discussion

The results indicate that a lake-based, sediment yield approach can provide an alternative method of estimating sediment delivery from watersheds (e.g. Foster et al., 1988, 1990; Evans, 1997; Hassan et al., 2000). The method is likely to be more reliable than fluvial-based yield estimates as it can provide longer and less temporally biased estimates of yield in environments where most of the sediment is transported infrequently (e.g. Church et al., 1989) and is likely to be missed in monitoring programs. The influence of the extreme event is well illustrated by the quantity of sediment delivered to Green Lake during 1991, which is comparable to the mass of sediment deposited in the lake during the previous decade. As most clastic yields in Canada are derived from interpolation

rather than rating curve procedures, the magnitude of error posed by inadequate representation of such events is at the very least, severe. The similarities between estimated yields from the spatially restrictive coring sites where long varve chronologies were developed and those based on lake-wide and fluvial methods indicate that, outside of major changes in sedimentation patterns within the lake, the varve records will provide a gross estimate of yield to the lake basins. Changes in sedimentation pattern have been observed in other lake studies (e.g. Lamoureux, 1999b). Because Duffey is a fjord-type lake basin with simple morphometry and inflows while the coring sites in Green are elevated, and only sediments delivered by interflow and overflow processes are recorded, sedimentation patterns may be hard to compare.

The results indicate that most sediment entering the lake basins appears to originate from specific points within the watersheds rather than reflecting a more diffuse contribution from upland areas. The conclusions are drawn from the seemingly minor contribution from land surfaces not drained by Fitzsimmons Creek in the Green Lake watershed and the very small contribution of sediment from Cayoosh Basin to Duffey Lake. However, when examined at the slightly large scale (i.e. the convergence of the sub-basins) the yield estimates conform to the regional model of sediment yield for British Columbia. Based upon the limited morphometric analysis of the watersheds presented in Chapter 3, proximity to the Coast and percent glacial cover appear to be the dominant explanatory variables controlling contemporary sediment discharge within the study area and agree with a larger dataset for the Coast Mountains (Desloges and Gilbert, 1998). The above results confirm the importance of distinguishing spatial scale effects in sediment yield and the recognition of emergent properties of basins at different scales.

5.6 Conclusions

The following conclusions concerning climate-fine sediment linkages during the 20th century are drawn from contemporary sedimentation patterns in Duffey, Green, Cheakamus and Glacier Lake basins. At the annual time scale, fine-grained sediment transfers appear to be directly related to the intensity of floods but the combination of sediment source location and differences in runoff generating mechanisms varies across the study area. Sediment delivery to Cheakamus, Glacier and Green lake basins occurs during summer and autumn floods while most sediment is delivered to Duffey Lake during nival runoff events. The linkage between ENSO and autumn runoff for Lillooet River suggests that some of the temporal changes in extreme events may be caused by large-scale ocean atmospheric processes, specifically regime shifts in ENSO or the PDO. Additional (i.e. regional hydrologic analysis) is required to substantiate the ENSO-autumn runoff relation.

At the decadal time scale, the influence of variable sediment supply becomes clear. Based on sediment source identification, glaciers appear to be the primary mechanism of such sediment source changes. Prior to 1945, a moderate proportion of the variance within varve thickness from the lake basins (excluding Duffey) can be explained by variations in annual air temperature which control the intensity of glacial runoff. Analysis of meteorological data indicates that glaciers responded rapidly to warm and dry conditions between 1923-1945AD, a period when sedimentation rates are high within those basins where varve thickness is likely a surrogate for lake-wide patterns of sedimentation. The exhaustion of these glacial sediment sources following ice retreat is rapid indicating that most proglacial sediment reaching the lake basins likely originates from sub-glacial sources or during melting of debris-laden ice. The data indicate that a general lack of stability between lake sedimentation and hydro-climatic forcing exists within the records and that the source of the complexity results from changes in sediment availability. Some of the complexity may be minimized by controlling for long-term variations in the intensity of glacial runoff. The degree to which large-scale variations in ice cover have influenced downvalley lake sedimentation is considered

in Chapter 6.

Chapter 6

Century to Millennial Time Scales: Variations in Sediment Production and Delivery

This chapter evaluates the climatic and geomorphic controls of fine-grained sediment transport within the study area over time scales that significantly exceed the contemporary monitoring program. The primary goal is to isolate major modes of climate variability from climate-proxy records so that this "climatic variance" can be controlled for within long proxies of sediment yield. The analysis and removal of climatic effects is primarily limited to the last 600 years, a period where suitable spatio-temporal coverage of tree ring sites exists and consequently, where most direct evidence for former ice limits is available within the Canadian Cordillera (e.g. Mathews, 1951; Ryder and Thomson, 1986; Osborn and Luckman, 1988; Clague and Mathews, 1992; Luckman et al., 1993; Smith et al., 1995; Smith and Laroque, 1996). Major changes in ice cover are reconstructed by mapping from air photos and analyzing the data in a GIS. These data are important to this study as changes in ice cover are hypothesized to affect the intensity and hence, volume of fine-grained sediments available for transport during the Holocene. The climate signals of the last 600 years are recovered from long-term, regional-scale patterns of tree growth from climatically sensitive regions in North America. Major modes of variability extracted from the tree ring network are then calibrated against instrumental data from southwest British Columbia. Finally, causes of millennial-scale variations in sediment discharge are evaluated by first examining the correspondence between sediment yield proxies developed for the lake basins and the terrestrial record for Holocene glacial advances in the North Pacific and Canadian Cordillera region. The sediment yield indices are then compared to and evaluated against proxies of atmospheric circulation and air temperature variability preserved within the Greenland ice cores (GRIP and GISP2).

The chapter begins by describing the terrestrial evidence for former glacial positions within the study area and those changes in precipitation and temperature required for such change. Climate indices are then recovered from the tree ring data and compared to the varved records from Duffey and Green Lake basins. An attempt is made to remove these climatic signals so that changes in sediment production independent of climate can be analyzed. The remainder of the chapter examines lower frequency changes in sedimentation, evaluated primarily through changes in bulk physical properties of the recovered lake sediment cores, and assesses the covariance between these records and climate-proxy records from the cores.

6.1 Changes in Sediment Production-Glacial Fluctuations during the last 600 Years

Over the contemporary period (1880-2000AD), glacial cover is an important control on sediment discharge within the watersheds of this study but the exact relation is complex (e.g. Hallet et al., 1996; Leonard, 1997) and modulated by factors such as the intensity of inter-annual to inter-decadal climatic conditions favorable for glacial melt. The largest and most abrupt period of sediment transfers over the instrumental period occurred between 1920-1950AD when anomalously warm air temperatures coincided with a period of below average winter accumulation. Such anomalous sedimentation during the early 20th century was observed by Leonard (1997) in Hector Lake though in that case the amplitude of these sedimentation patterns was similar to those observed during

the 18th and 19th centuries, coinciding with the height of the 'Little Ice Age'.[1]

The previous six centuries provide a unique opportunity to detail the significance of variable glacial extent on influencing the timing and amplitude of sediment export. This is because most terrestrial-based evidence for Holocene glacial fluctuations within the Canadian Cordillera indicate that advances during the past 600 years were generally the largest over the Holocene (e.g. Mathews, 1951; Luckman and Osborn, 1979; Ryder and Thomson, 1986; Osborn and Luckman, 1988; Smith et al., 1995; Luckman, 2000; Luckman and Villalba, 2002). The timing of such advances can be dated using dendrochronologic methods (e.g. Luckman, 1993; Smith et al., 1995). Because most temperate glaciers lose mass by ice melt within the ablation area, the elevation of the terminus and the equilibrium line altitude of a given glacier is often related to average temperature or precipitation anomalies. Consequently, the elevation of former ice limits can be used to reconstruct former ice positions and make inferences concerning former precipitation or temperature departures when the deposits were constructed. This technique has proved useful for estimating temperature and precipitation changes during the late Pleistocene (e.g. Porter, 1977), over the Holocene (e.g. Dahl and Nesje, 1996) and for a smaller collection of glaciers in a more spatially restricted portion of the southern Coast Mountains (Evans, 1993).

Within the Canadian Cordillera, three main phases characterize glacial fluctuations during the last millennium: a) a period of ice growth beginning sometime after 1000AD which continued until the early 15th century with possible standstill or recession (e.g. Luckman and Osborn, 1979; Ryder and Thomson, 1986); b) subsequent re-advance of glacial ice with most glaciers experiencing most extensive advances of the Holocene during the early 18th century or mid 19th century advances; and c) retreat thereafter. Evidence from the Coast Mountains indicates that glaciers did not experience significant retreat until the the beginning of the 20th century, apparently the result of cool and wet conditions during the beginning of the 20th century (e.g. Mathews, 1951; Desloges, 1987; Smith and Laroque, 1996). Based on limited photographic evidence, several glaciers built recessional moraines during the early 20th century in Garibaldi Provincial Park and were only slightly more restricted than LIA positions. It remains unclear whether early to mid 18th century glacial advances were more extensive than advances during the mid 19th century (Smith and Desloges, 2000) though it is to be expected that site characteristics are responsible for local variability given that both advances appear to be of relatively equal magnitude.

LIA Deposits and Probable Climatic Departures

Given the importance of contemporary ice cover in influencing sediment production and transport in the watersheds, maximum extent of glaciers during the 'Little Ice Age' was mapped for 76 glaciers located within the study area (Appendix B). Several of the glaciers and glacial forefields were visited with an aim to collect detrital wood which could be used to provide minimum or maximum-age estimates of moraine age (c.f. Ryder and Thomson, 1986) but no wood which could be stratigraphically related to downvalley ice position was located. The stratigraphy at several fluvial sites on the Van Horlick Creek system (Duffey Lake) was detailed as access was easy and the reaches were locations which were characterized as large (valley wide), active sediment sources. Two sites in particular were excavated and the stratigraphy was detailed as they recorded abrupt changes in fluvial sedimentation. The site relevant to the LIA is a large (200-300m wide), sandur-like fluvial deposit approximately 2km downstream from one of the most active glaciers within the

[1]Though the timing of the "Little Ice Age" was previously considered vague and possibly an event which was not global in scope, there exists simply too much evidence for its occurrence in the western Cordillera of North America to ignore its significance. The similarity in timing of the events between North America and Europe suggests that the event is synchronous. This study uses Bradley's (1999) definition for its timing (1510-1850AD).

watershed. The stratigraphy of 1.5m excavated soil pit dug 20 m away from the contemporary channel revealed approximately 60cm of unweathered, weakly stratified silty sediments overlying a vegetative mat (mostly *Carix* stems). Weakly stratified, oxidized silty sands occur below the sedge and overlie woody debris. An AMS age from the uppermost *Carix* stems (180±45 ^{14}C yr BP; table 6.7) provides a minimum-limiting date for the inception of the (overbank ?) sedimentation event. The 2σ calibrated age range of this ^{14}C age is large (1645-1951), though air photos (1946) reveal that the sampled site was vegetated and not much different than today indicating that the latter two calibrated ages (1942 and 1946AD) for the event are unlikely (table 6.7). Thus, the interval of abrupt sedimentation at the site is interpreted to have occurred sometime between 1670-1800AD.

Based on prior work in southern British Columbia (Mathews, 1951; Ryder and Thomson, 1986; Smith and Desloges, 2000)it is most probable that the moraines which are fresh and commonly most extensive were constructed between ca. 1700-1850 AD within the study area. Photographic evidence from Garibaldi Provincial Park (Heaney, 1912) indicates that smaller recessional moraines positioned 100-200m upvalley from these deposits record ice positions at ca. 1912AD and based on the instrumental record, the glaciers were most likely responding to cooler annual temperatures. Similar conditions and recessional moraines are found in the Canadian Rockies (e.g. Luckman et al., 1997).

Based on vegetation, weathering characteristics and downvalley position, the glacial deposits within the study area can be classified into three groups and include:

1) Vegetated moraines or moraine fragments lying 1-2km downvalley from contemporary ice masses. These deposits are rare (they can be found in proximity to contemporary ice in $< 5\%$ percent of the total glaciers examined). Their subdued morphology, vegetative cover and soil development suggests that they are old ($>$ 500 years) landforms. Such deposits appear to be slightly more prevalent in the northern section of the study area and it is unknown whether the distribution is an artifact of lower rates of weathering or vegetative cover. Prominent moraine fragments can be found in the Joffre Lakes basin where they are situated immediately (10-100m) outside fresh, unweathered moraines and also appear to have impounded uppermost Joffre Lake (figure 6.1). These deposits can be found in several other sites within the Duffey and Birkenhead Catchments.

Soils on these deposits are well developed but no evidence of tephra (Bridge River or Mazama) could be found. It is likely that high weathering rates do not allow preservation of tephra in such deposits[2] . The ages of these glacial deposits are unknown; based on their downvalley position they could be correlative with early LIA (prior to 1500AD), early Neoglacial (ca. 3300-1900 ^{14}C yr BP) or late Pleistocene-early Holocene glacial advances.

2) Unweathered, well defined trim lines, lateral and terminal moraines 1-2km downvalley from contemporary glaciers. These deposits are the most extensive within the study area. In the southern wetter, section of the study area the average maximum downvalley elevation of such deposits is (1370±220m; n=29) some 300m lower than downvalley positions (1670±190m; n=60) of contemporary ice masses.The difference in elevation between contemporary ice margins and these deposits is less (minimum elevation of such deposits 1940±135m; n=24 and minimum elevations for contemporary ice cover is 2020±120m; n=18). Average ELA (60:40 AAR) depression for those glaciers within the study area with a well-defined contemporary terminus is 125±75m; n=33. This value was determined by calculating the mean difference observed between contemporary and LIA ELA (133m). Based on their downvalley positions, and their overall lack of weathering, these deposits

[2]Tephra (Bridge River) was found in only one terrestrial site (a fluvial deposit in the Duffey Lake catchment) of this study. Here the deposit was located at 54cm depth and was 1 mm thick. A charred twig taken 1cm below the tephra yielded an age of 2230±60 ^{14}C yr BP (table 6.7).

are believed to be those which were constructed during the later phase of the 'Little Ice Age' (ca. 1700-1850AD).

3) Sequences of moraines which lie inside deposits of group 2. They appear to be less common in front of steeper ice masses. The photographic evidence suggests that these deposits were emplaced in the 20th century.

An opportunity is afforded to estimate changes in winter precipitation or temperatures using the contemporary and former positions of the glacial deposits interpreted to be LIA in age. To do so, two procedures were utilized. The first and simplest procedure estimates the difference in air temperatures which would be required to lower ELAs to their observed values. Assuming a wet environmental lapse rate (.006 °C m^{-1}) an annual temperature decrease of 0.75±45 °Cwould be

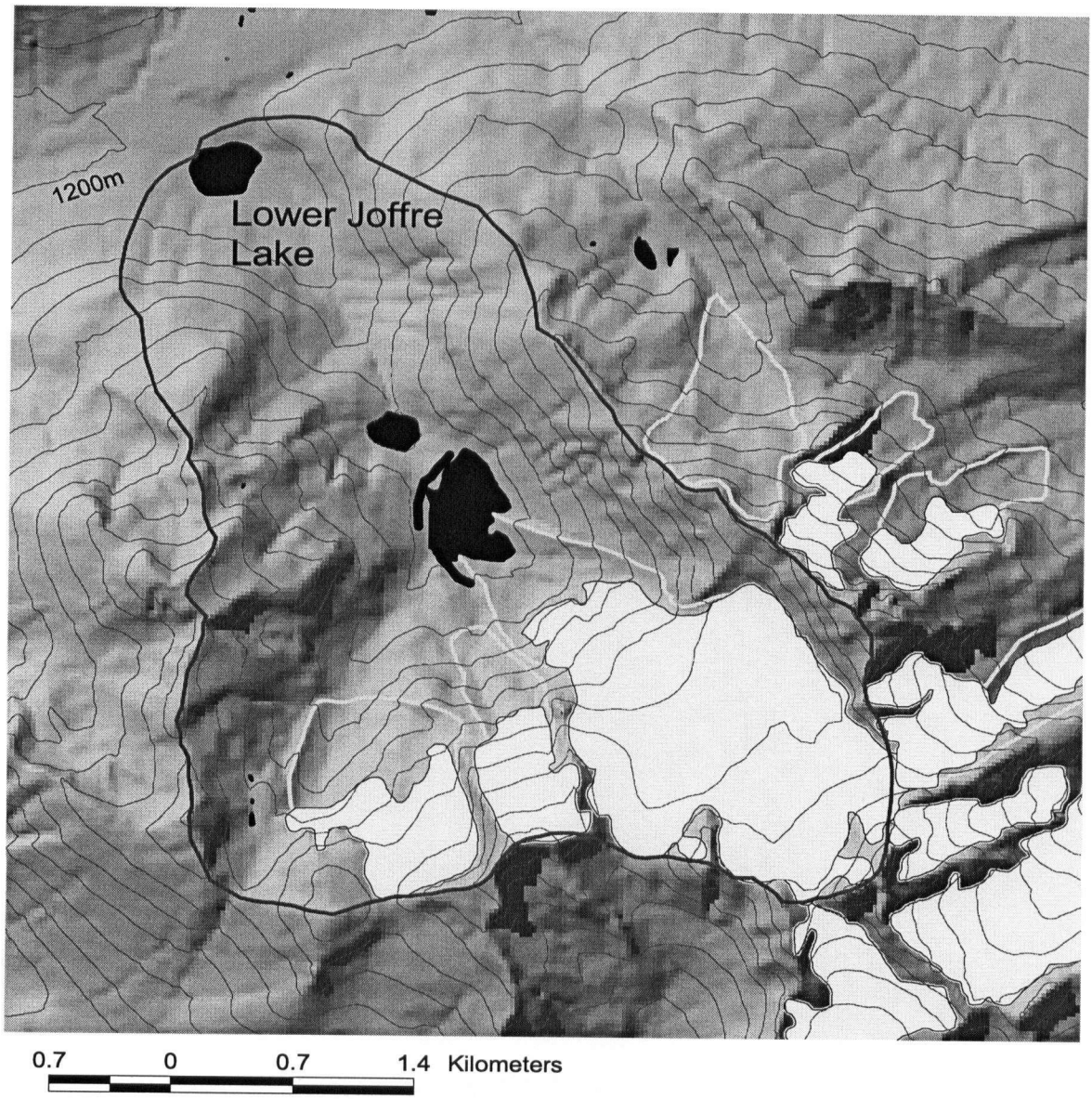

Figure 6.1: DEM and Moraine Record near the Joffre Lakes Basin
Contour interval is 100m. Contemporary and LIA ice limits shown as solid (light blue) and outlined (light green) polygons respectively. Older moraines (black line) impound uppermost lake.

required to cause the observed ELA depression within the study area during the period when glaciers were at their furthest downvalley positions. To estimate probable changes in winter precipitation, a transfer function was developed between average April 1 snow water equivalence (SWE) and glacial ELAs. A large precipitation gradient across the study area allows such an approach to be employed. Glaciation levels mirror this trend, rising from west to east across the Coast Mountains (Evans, 1990). Porter (1977) employed a similar technique but used average temperature and precipitation totals from nearby meteorological stations. A period of common overlap was not used as it would severely limit the number of contributing stations. Inspection of the data indicated that there are no gross step-jumps which would introduce errors into the analysis except the well documented reductions in April 1 SWE following 1977 (Moore and McKendry, 1996; Moore, 1996). Average April 1 SWE does not differ statistically between the two periods suggesting that such factors probably contribute less error than the overall lack of station coverage.

The glaciers of the current study (figure 6.2) appear to follow the elevational trend noted by Evans (1990) though there is an apparent break in the slope of the data approximately 50km from the coast, between Whistler and Pemberton, BC. Median elevation was used to define the trend because it can be calculated simply with a GIS whereas the determination of the ELA is more difficult. The latter requires the the determination of hypsometry for each glacier. Median elevation differs slightly from ELA (figure 6.2 upper right panel) but the difference does not appear to be statistically significant and both measurements show a moderate degree of covariation ($r = 0.66$).

A splined surface was generated from the April 1 SWE station data to produce an estimate of SWE across the study area as a function of spatial position. The resulting grid (2.5km resolution) was then clipped to glacial coverage to estimate April 1 SWE for a given glacier in the study area. Sources of error include the gross-scale resolution of the grid and interpolation errors, significant additions of mass to a given glacier by snow avalanching or wind re-distribution, and increases in snow accumulation not accounted for by the snow course network resulting from orographic effects. Despite these effects, there appears to be a moderate amount of covariation between April 1 SWE and contemporary ELA (figure 6.2). Using the linear relation between April 1 SWE and observed contemporary ELA positions, estimates concerning probable increases in wintertime precipitation causing the 'Little Ice Age' within the study area can be made. For example, in the northern section of the study area (2000m contemporary ELA) a 16 % increase in 1April SWE ($\approx 200 mm\ yr^{-1}$) averaged over time could cause glaciers to expand to their LIA positions. The estimate does not reflect actual wintertime precipitation totals as April 1 SWE is also controlled by air temperature variability within the study area (Moore and McKendry, 1996; Moore, 1996).

The estimated values for average ELA depression (125±75m) and change in temperature (0.75 °C) are consistent with an earlier study which determined ELA (114m) and temperature depressions (0.8 °C) within a smaller sub set of the study area (Evans, 1993). Both studies agree with tree-ring based reconstructed temperature departures in the Canadian Rockies during the LIA (Luckman et al., 1997). The break in slope in the relation between ELA and longitude (figure 6.2) was not observed by Evans (1993) and is interpreted to reflect a major precipitation divide separating the westward maritime glaciers from those where inter-annual variations in net mass balance are also heavily controlled by summer air temperatures (e.g. Moore and Demuth, 2001).

6.2 Decadal-to-Century Scale Climate Variability and Sediment Transfers

In an effort to understand how decadal-to-century scale climate variability might influence sediment production and transport within the study area, dominant spatio-temporal patterns were evaluated in long time series of tree growth (ring width) from North America. Though prior studies have reconstructed large-scale climatic patterns in western and Pacific North America from tree-ring (e.g.

Blasing and Fritts, 1976; Fritts, 1991) and ring density (e.g. Briffa et al., 1992) networks, there are several reasons why a reanalysis of the ITRDB data would prove advantageous. First, significantly more sites have become available in the past decades increasing the spatial and temporal degrees of freedom. In addition, major modes of climate variability which were poorly documented or understood (e.g. the PDO) are now recognized and have been shown to be particularly well recorded by variations in tree growth (Gedalof and Smith, 2001). Finally, continual rehabilitation of precipitation and temperature datasets provides a means of developing stable and error-reduced

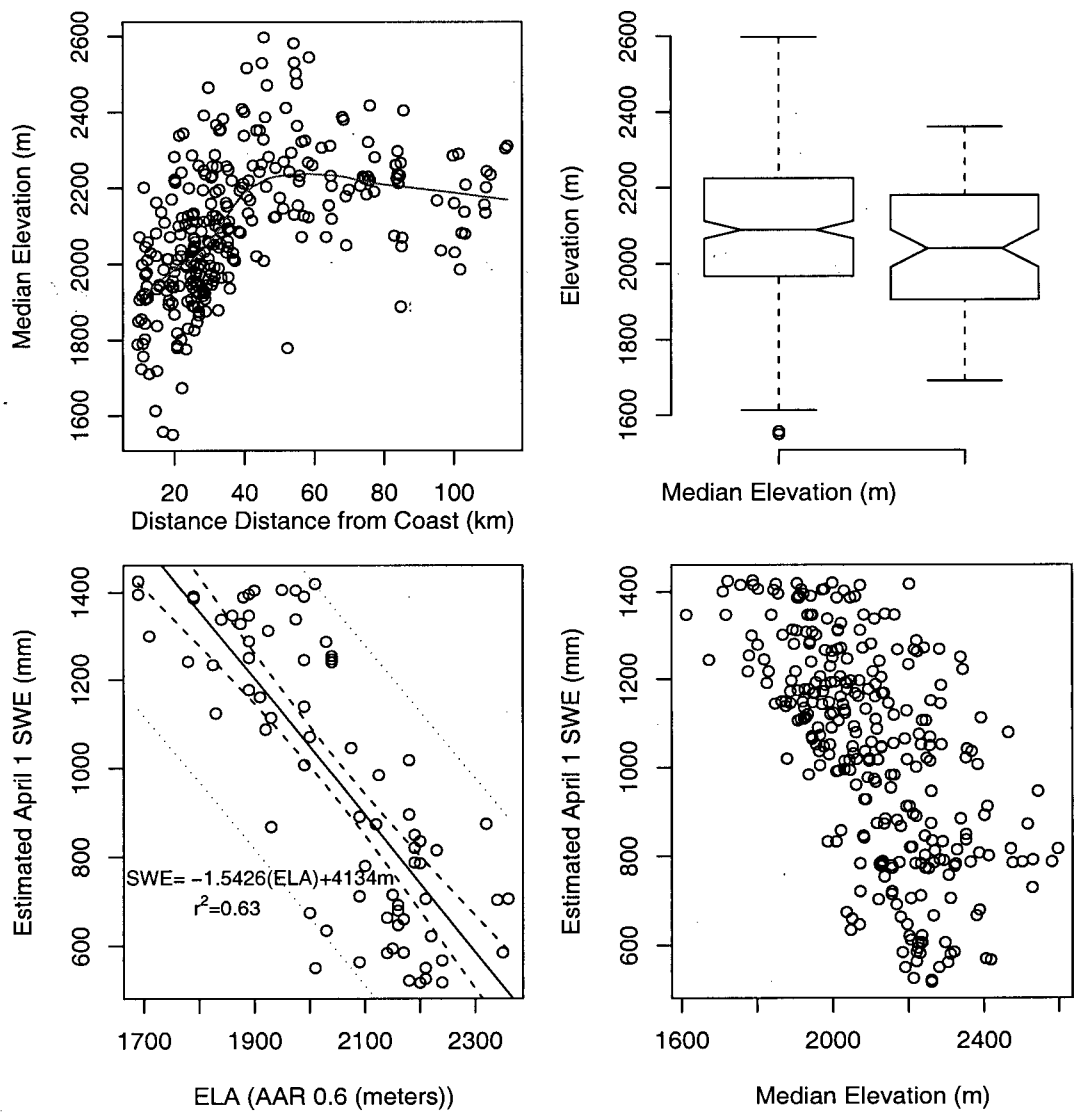

Figure 6.2: Observed Trends in Glaciation Levels and Relation to April 1 SWE
Upper left panel shows data and lowess fitted trend as a function of distance from the Coast (km). Kink in trend occurs near Whistler, BC. Upper right panel demonstrates close correspondence between measured ELA (n=76) and median elevation (n=306) of glaciers within study area. Lower panels demonstrate relation between April 1 SWE and ELA (lower left) and median (lower right) elevation.

transfer functions between tree growth and variations in temperature and precipitation. Though the datasets and implications of the analysis may be relevant for reconstructing climate variability across North America the primary goal of this study remains: developing climate proxies for southern British Columbia so they can be evaluated against annual indices of sediment delivery.

The climate signal archived by natural systems such as trees or lakes is commonly small in magnitude compared to the fraction of variance attributable to non-climatic factors such as growth response, changes in sediment supply or random, unpredictable stochastic events. The approach used in this study is to increase the signal to noise ratio and to determine the spatio-temporal covariance structure between stations (i.e. climate stations or tree-ring sites). This information is then used to reduce the dimensionality of the system by recovering the majority of the total variance in a much smaller number of principal modes and is commonly referred to as factor or empirical orthogonal function analysis (EOFA).

Two important elements make the use of EOFA useful in this study. The first is that it can recover underlying spatio-temporal structure in large datasets by reducing the overall noise and the majority of the variance can be explained by relatively few EOFA (appendix C). The second utility of EOFA is that, by definition, it reproduces dominant factors (eigenvectors) within the data set that are uncorrelated and this allows the construction of stable "predictors" which can be used to develop linear regression models. Because they are orthogonal, the predictors are uncorrelated and do not suffer from multicollinearity which can cause large confidence limits and instability within the prediction models (Hocking, 1996). These predictors can then be used to reconstruct climate variability and is the chosen method for reconstructing climate variability within the study area.

With respect to the tree ring data, the current study examines ring width variations over a larger region (North America) than the study area for the following reasons: a) the density of existing tree-ring sites within British Columbia is low; b) many of the local chronologies were developed from trees in environments where the tree growth is not limited by extremes in precipitation or temperature so that ring width series are complacent; c) non-sensitivity of local sites or tree species to large-scale climatic variability (e.g. ENSO) which is known to affect temperature and precipitation fields in the study area. Teleconnections within the climate system may allow distant tree-ring sites to archive climatically-relevant information which can be used to reconstruct temperature and precipitation variability within the study area. This can occur even though local tree-ring sites fail to capture such variability.

The ring-width records were obtained from the web-based International Tree Ring Data Bank (ITRDB), a collaborative effort to provide a database which is open for public use and re-analysis (Contributors of the International Tree-Ring Data Bank, 2001). The records reflect common patterns of ring-width variation within a given site where errors due to false or missing rings have been corrected (cross dating) and where non-climatic factors such as normal tree growth patterns, competition, disease or insect infestation have been reduced (standardization). Uncertainty in calendar age for a given year and absolute errors are generally very low (¡¡ 1%), and cross-dating methods are more or less consistent between studies (e.g. Holmes, 1983, 1992). Unfortunately, standardization procedures vary widely between studies and relate to *a priori* knowledge of the growth response of a given tree species to increases in age, disease, or competitive stresses. Essentially, standardization removes low frequency variations thought not to be related to moisture or temperature stress; subsequently their removal reduces a significant proportion of total variance within the data. Unfortunately, some unknown fraction of the low frequency variability is due to climate. Recovery of low frequency climatic data from tree rings is also problematic in very long tree ring records because the lowest recoverable frequency depends on the longest, continuous segment of ring-width indices contributing to the chronology (e.g. Cook et al., 1995). For these reasons extraction of low frequency information from the extracted ITRDB is not possible without reanalysis of the data on

a site-by-site basis. Low frequency variability over century to millennial time scales and its linkage to changes in sediment delivery will be assessed with ice core records.

6.2.1 Data Retrieval, Analysis, and Calibration

The entire network of tree-ring sites recovered from the ITRDB consists of over 1200 sites distributed over the United States and Canada (figure 6.3). There is a significant lack of northern sites within the 1800-1979AD chronology and this spatial bias increases considerably for the 1600-1979 and 1400-1979AD chronologies. A computer program was written to extract the archived tree-ring data from the ITRDB and combine sites over a common period, irrespective of site elevation, tree species or location (figure 6.3). Such a network will likely capture both temperature and precipitation patterns given that many tree species and site characteristics suitable for moisture or temperature stresses are distributed throughout the network (Fritts, 1991, e.g.). A weakness of this approach is that the clarity and robustness of major climate modes will be compromised in the spatial domain but the temporal information is preserved. Consequently the time-varying patterns in growth are regarded as the more important data type for this study.

After inspection of beginning and ending years three individual networks were constructed to encompass 1400, 1600, and 1800-1979AD. This last year of the networks results from the dramatic reduction (spatially and temporally) of sites after 1979 (Mann et al., 1998). For example, the requirement that a given site begins prior to 1600AD but ends after 1990AD reduces the number of available sites from 250 (1598-1979AD) to 70 (1598-1990AD).

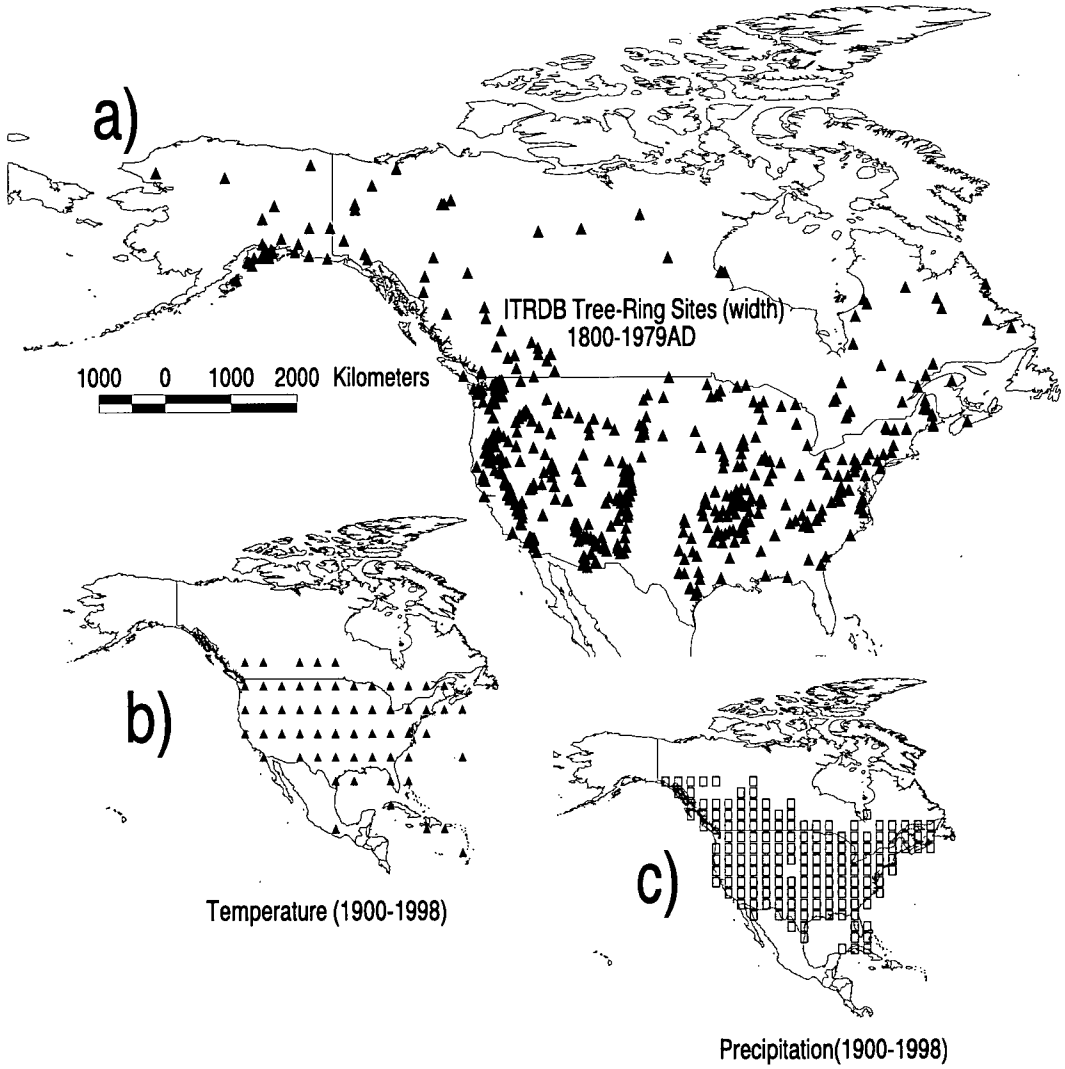

Figure 6.3: a) North American (1800-1979AD) Tree-ring Network Recovered From the ITRDB
b) Monthly Gridded Temperature (5 °) for 1900-1998AD; c) Monthly precipitation (2.5° latitude x 3.75° longitude) from 1900-1998AD. Only grid points with no missing data were used in the analysis

Much like contributing trees within an individual site, the number of contributing sites decreases as a function of age, reducing the strength and statistical reliability of extracted spatio-temporal patterns of climate (e.g. Fritts, 1991). Three time periods (≈1800-1980AD, 1600-1980AD, 1400-1980AD) were chosen for analysis and the data matrix (M sites with N years of contributing data) was subject to EOFA (C). Unlike gridded climatological datasets, tree-ring sites are non-uniformly distributed which, without correction for representative areas or re-sampling, can produce erroneous spatial patterns for a given eigenvector if the data are clumped (Buell, 1978). Such error can be minimized by reducing the dataset to reflect a more uniform area distribution, resampling onto a grid or derivation of weighting factors for each station depending on the area it represents in 2-D space (Meko et al., 1993). All of the methods have their weaknesses but a compromise was met by deriving a quadrature power-law weighting scheme (C):

$$w_i \propto a_i^{0.1} \tag{6.1}$$

where w_i represents the weight for station i with areas a_i. Correction of a_i was chosen to penalize those tree-ring sites which were not well represented (areally) in the station network. Determination of the power coefficient was chosen to produce a distribution of weights which reflected these trade-offs between representativeness (number and area) and use of normally-distributed weighting coefficients. The 1400-1980AD network is much too sparse to recover meaningful spatial patterns so stations were not weighted and only qualitative estimates concerning similarities in the spatial loadings of a given eigenvector (for the nth principal component) can be made. The distribution of weights calculated by equation 6.1 passes a normality test (Shapiro-Wilks). The spatial patterns obtained by the EOFA on the ITRDB data are used to estimate qualitatively the correspondence between the dominant spatial temperature and precipitation modes against those extracted from the tree ring data. The non-gridded nature of the tree-ring data prevents the appraisal of this similarity with standard statistical methods (i.e. canonical correlation analysis). Tree ring data are most commonly represented as departures from some mean value without standardization for variance. The data were standardized (e.g. zero mean and unit variance) before EOFA in order to account for the differences in overall sensitivity between sites (e.g. Fritts, 1991) and to prevent a few stations with disproportionate variance dominating the overall spatial structure.

6.2.2 Calibration Datasets: Temperature and Precipitation

To understand large-scale temperature and precipitation patterns and how they may relate to tree growth during the period of common overlap, gridded temperature and precipitation anomalies for the 1900-1998AD period for North America (Hulme, 1992; Jones, 1994; Parker et al., 1994; Hulme et al., 1998) were subject to EOFA. Only those grids with no missing data over the 1900-1997AD period were used in the analysis. Spatial resolution of the temperature dataset is 5° and reflects merged surface temperatures from the land and ocean, though over the 1900-1997AD period there are no ocean grids with complete data so the results pertain to surface temperature variations over land (figure 6.3b). Spatial resolution of the monthly precipitation is 3.75°Lat x 2.5°Long and the estimates of either field for a particular grid point reflect spatially averaged anomalies from meteorological stations closest to a given grid point. The precipitation data have been checked and corrected for gross outliers and inconsistencies but especially in high latitude regions, under-catch during winter may underestimate total precipitation (Hulme, 1992; Hulme et al., 1998). These inaccuracies should not greatly affect the results of this study as the data are used for recovering dominant spatio-temporal patterns and potential centers over southern British Columbia. Details concerning the datasets and their reliability are described elsewhere (e.g. Hulme, 1992; Jones, 1994; Parker et al., 1994; Hulme et al., 1998).

6.2.3 Results-Temperature and Precipitation

The EOFA on both temperature and precipitation datasets indicate the following: The first 5 EOFs extracted from the temperature dataset (EOF_{temp}) explain over 78 percent of the cumulative variance while a much lower percentage of overall variance (42 percent) is explained by the dominant precipitation (EOF_{ppt}) EOFs (table 6.1). The patterns associated with EOF_{temp} are spatially unique and appear to be robust in terms of temporal sub sampling (table 6.1). The smaller proportion of variance explained by the first principal $EOFs_{ppt}$ is expected within spatial precipitation datasets. Meso to local-scale precipitation is influenced by topographic effects. Similar, small-scale structure is evident in spatial patterns of monthly streamflow variability for the US (Lins, 1997) confirming the greater heterogeneity associated with precipitation and runoff processes compared to air temperature variability.

Lack of spatial stability of the dominant $EOFs_{ppt}$ is also a characteristic of the lower overall variance explained by the principal mode of precipitation. This instability is revealed when subsets of the the dataset are re-sampled (table 6.1). Both principal $EOFs_{temp,ppt}$ have same-sign loading over the domain of the datasets, a common feature that illustrates the spatial distribution of secular trends within the data (e.g. Richman, 1986). In the case of the temperature dataset, when this EOF is projected onto the temporal data (i.e. the PC), it mirrors the well illustrated secular trend in global temperature through the 20th century (e.g. Mann et al., 1998; Jones et al., 1999). $EOF2_{temp}$ recovers approximately 22 percent of the overall temperature variance within the data and has principal areas over the Pacific Northwest and southeastern United States. Consequently, $EOF2_{temp}$ is interpreted to be the temperature manifestation of the PDO because $PC2_{temp}$ is negatively correlated ($r = -0.27$) to monthly anomalies of the PDO (1900-1998AD). In addition, the spatial pattern associated with $EOF2_{temp}$ is similar to the observed correlation between wintertime temperature anomalies (Nov-March) and the PDO (e.g. Mantua and Hare, 2002).

This correlation remains highly significant after correction for autocorrelation (appendix C). $EOF3_{temp}$ is interpreted to be the result of ENSO as monthly SST anomalies (Nino12) are positively correlated ($r = 0.24$) to $PC3_{temp}$ but with an approximate 5 month lag. This lag is a common feature observed in ENSO temperature-precipitation variability in North America where SST anomalies of ENSO commonly begin in early summer and the effects in temperature and precipitation fields do not occur until the following winter. Analysis (not shown) based on seasonally-averaged data indicate that, as expected, wintertime (November-March) precipitation anomalies contribute the majority of the variance to the raw monthly data and when the dataset is subject to EOFA, it produces modes of variability with several principal centers over the study area.

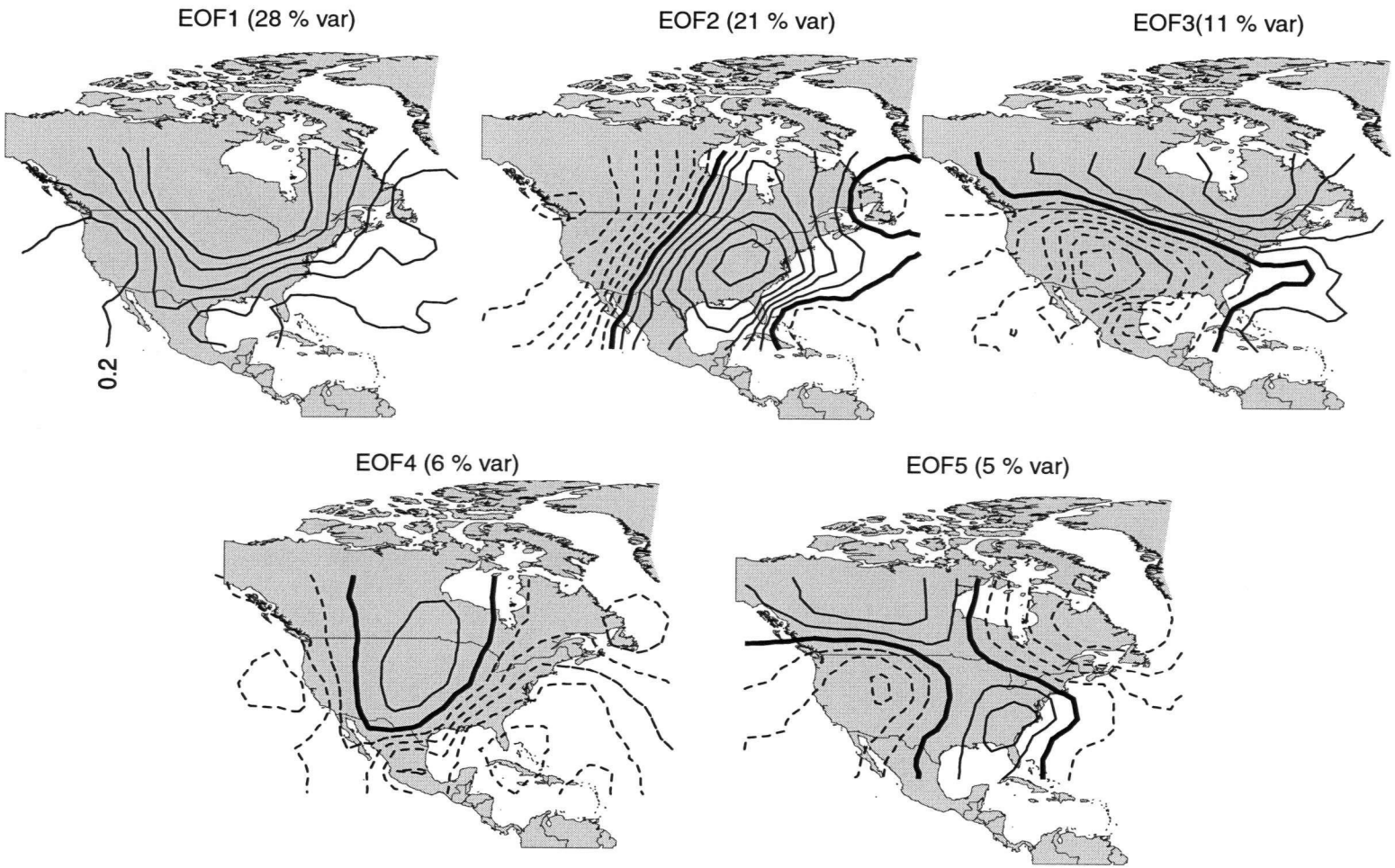

Figure 6.4: First 5 EOFs of Monthly Temperature Anomalies (1900-1998AD)
Correlation plots showing positive (solid), negative (dotted) correlation between EOF and time series at a given gridpoint and illustrate the spatial patterns of a given EOF, its amplitude, and correlation with the instrumental data.

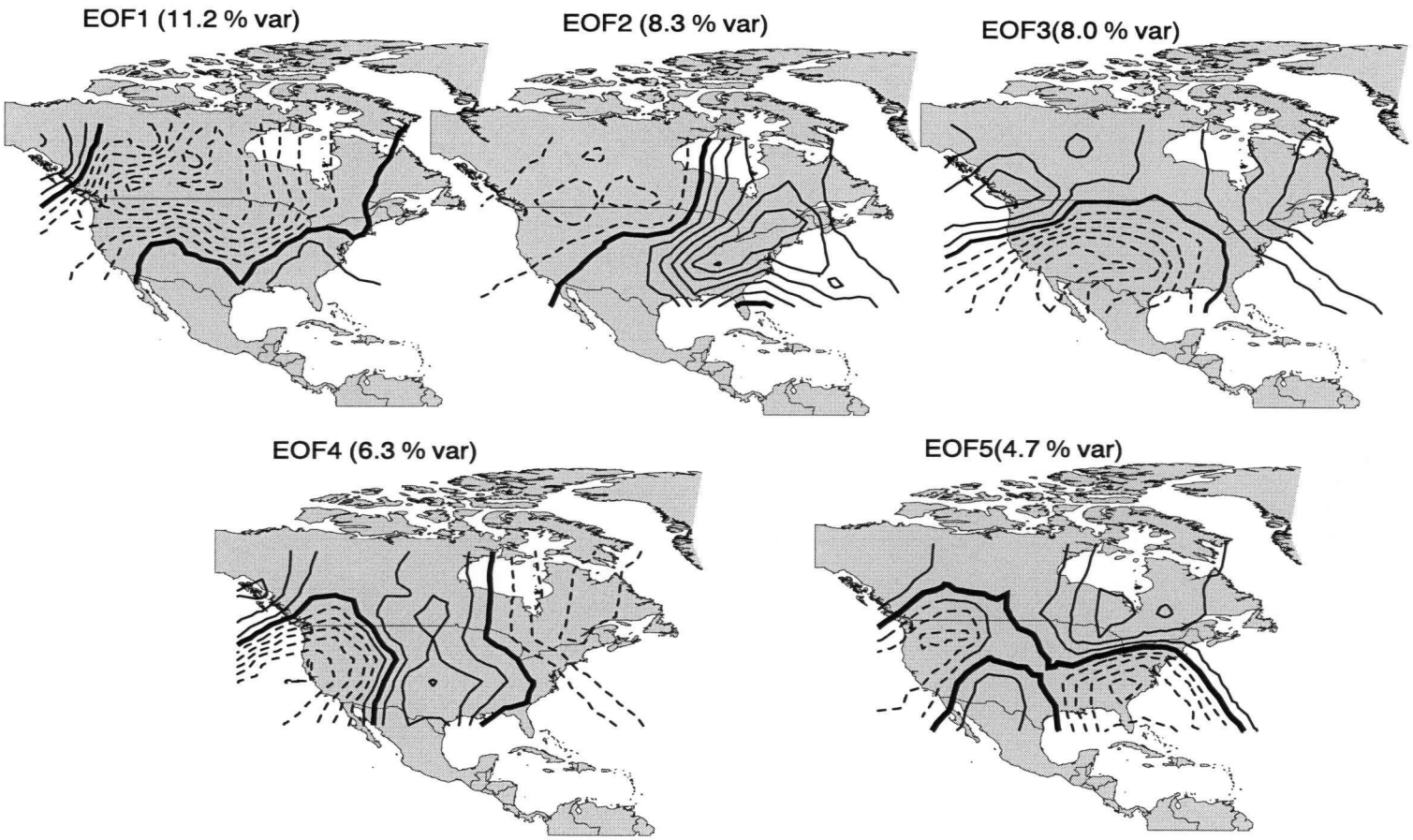

Figure 6.5: First 5 EOFs of Monthly Precipitation Anomalies (1900-1998AD)
Plots organized same as figure 6.4

The precipitation EOFs are not as clearly linked to SST variability as those associated with the air temperature data. Based on cross correlation analysis, only $EOF3_{ppt}$ appears to be linked to SST variability as both are weakly correlated both to the PDO ($r = 0.14$) and Nino12 ($r = 0.12$) at zero lag. The covariance between tropical and extra-tropical SST variability complicates the strength of an isolated ENSO or PDO precipitation signal within the study area (Dr. Dan Moore, pers comm) and elsewhere (e.g. Bonsal et al., 2001; Gershunoz and Barnett, 1998; Gershunov et al., 1999).

The spatial patterns associated with the first three EOFs of this study (both temperature and precipitation) compare favorably to results presented by Fritts (1991) though the sign of the loadings associated with the principal EOF of temperature anomalies was negative in that study. The sign change undoubtedly arises from the absence of late 20th century data in that study (1900-1970AD) where average North American temperatures have increased substantially following 1977 (e.g. Jones et al., 1999). Taken together, the 5 leading EOF's are interpreted to explain the dominant spatio-temporal patterns of annual precipitation and temperature for North America on annual time scales. Important for this study is the amplitude and spatial coherence of these precipitation and temperature EOFs. In addition to the well-observed di-pole precipitation pattern in western North America (e.g. $EOF3_{ppt}$), there appears to be a significant east-west pattern in temperature anomalies (e.g. $EOF2_{temp}$) during the period of instrumentation. These large-scale patterns in the instrumental data suggest that it may be possible to use distant tree ring sites to reconstruct temperature and precipitation patterns for the study area. An important assumption but unfortunately, one that can not be tested, is that the large-scale spatial patterns of temperature and precipitation seen in the period of instrumentation are stationary.

	Precipitation					Temperature				
	Eigenvalue[a] (λ)	EV[b]	NT[c]	CTeofs[d]	r^e	Eigenvalue	EV	NT	CTeofs	r
PC1	12.13	11.17	0.90	0.99	-0.27	11.12	27.75	1.35	0.99	0.62
PC2	9.03	8.37	0.67	0.95	-0.24	8.32	20.77	1.00	0.99	0.56
PC3	8.64	7.96	0.64	0.81	-0.44	4.40	10.97	0.51	0.99	-0.11
PC4	6.81	6.27	0.51	0.83	-0.15	2.52	6.28	0.33	0.98	-0.16
PC5	5.04	4.64	0.37	0.84	-0.26	2.17	5.41	0.24	0.98	-0.34
	171 gridpoints			$N = 1176$	$N_{eff} = 362^f$	65 gridpoints			$N = 1176$	$N_{eff} = 360$

a PCA completed on standardized ($\frac{(x_i - \overline{x_i})}{\sigma}$) dataset after removal of monthly climatology (1900-1998AD) from series

b Percent variance accounted for by PC

c Degeneracy values approximating standard error of a given eigenvalue (North et al., 1982)to evaluate to statistical independence of spatio-temporal modes (Appendix C).

d Congruence statistic to determine reliability of EOF pattern based on Monte Carlo (e.g. Richman, 1986) sampling of dataset. Surrogates (n=100) used first 10 EOF's using all grids points with length of $\frac{n}{2}$.

e Pearson correlation coefficient of PC and closest grid point over 1900-1998 period

f Effective degrees of freedom after correction for autocorrelation (Appendix C)

Table 6.1: Summary Statistics of RPCA Analysis of Gridded Monthly Temperature and Precipitation Analysis

6.2.4 Results-Tree Ring Patterns and Correspondence to Temperature, Precipitation Fields, and Large-Scale Climate Indices

The number of contributing sites decreases notably with increasing age (table 6.2) and prior to 1800AD there is a significant bias in the data set towards tree-ring sites in the US rather than Canada. This bias also occurs in the US where there is a higher density of site in the southern US, a region where tree-ring cambial growth is sensitive to moisture variability (e.g. Fritts, 1991; Meko et al., 1993). Temperature-dependent, densitometric data sets are currently being made public at the ITRDB and subsequent analysis may help to reduce the northern bias within the ITRDB data.

Network	*Contributing Sites* (n)	$\rho^a_{\Delta 1}$	MS^b	N_{eff}
1800-1979AD	678	0.37	0.21	81
1596-1979AD	266	0.32	0.24	199
1400-1979AD	91	0.29	0.27	318

[a] Lag1 autocorrelation averaged across the network

[b] Mean Sensitivity (Fritts, 1976) of time series $\frac{1}{(n-1)}\Sigma_{t=1}^{t=n-1}\left|\frac{2(x_{t+1}-x_t)}{(x_{t+1}+x_t)}\right|$

Table 6.2: Statistics of Tree-Ring Networks

Unlike the temperature and precipitation fields, principal modes extracted from the 1600-1979 and 1800-1979AD tree ring networks indicate that only the first few principal modes appear to represent unique and spatially coherent patterns of variability (table 6.3). The mixed nature is apparent in the instability in temporal sampling and overlapping eigenvalues based on estimated standard errors of the eigenvalues when corrected for effective degrees of freedom. This correction is based on mean autocorrelation, averaged across a particular network and does not include estimates based on modeling spatial independence within the dataset. To understand the principal spatial patterns within the most complete dataset, the first four EOFs from the 1800-1980AD network are shown (figure 6.6).

The first EOF from the 1800-1980AD tree ring network explains 8 percent of the variance common to 679 individual tree ring sites distributed across North America. Positive loadings of the eigenvector are centered in the central, southern United States declining outward in magnitude (figure 6.6). Consequently, its PC is inversely correlated to $PC2_{temp}$ positively correlated to $PC4_{temp}$. The second EOF from the 1800AD network appears to be linked to $EOF2_{ppt}$ as the spatial patterns are similar and the PC's from the respective fields are correlated. The third EOF extracted from the 1800AD network is spatially most coherent (figure 6.6) consisting of an opposing west-east pattern. This pattern is most similar to $EOF2_{temp}$ and $EOF2_{ppt}$ though its PC is most highly correlated with the first principal component of precipitation.

These results indicate that a simple one-to-one mapping between EOFs derived from temperature and precipitation datasets and those of the tree ring networks is not possible. In terms of spatial structure, the non uniqueness associated with the tree ring network likely arises from a number of factors including: a) mixed tree species and overall sensitivity to environmental stress; b) spatial distortion of the loading structure imposed by the dimensions of the network (e.g. non-gridded structure); and c) a much higher fraction of non-uniform variance (e.g. trends) imposed by differing standardization procedures and growth patterns. Such complexities have been recognized by others (e.g. Fritts, 1991) using multi-species tree-ring networks distributed over large spatial scales and much of the spatial complexity of this study may have arisen from the use of

non-gridded data (Meko et al., 1993) or a quadrature weighting algorithm which was too low.

The first 20 EOFs capture between 53-55 percent of the variance within all three networks. Monte Carlo sampling (c.f. table 6.1) of the data indicates, however, that only the first few principal modes are robust with respect to temporal sub-sampling (table 6.3). Taken together, these factors are interpreted to indicate that recovery of coherent, large-scale climatic patterns in the spatial domain is not possible due to degeneracy of the eigenvectors and the major spatial modes of variability are effectively mixed within the dominant EOFs. Given the complexities associated with tree growth and its response to climate, the different site characteristics and tree species contributing to any of the networks, it would be rather surprising if the majority of the variance within the datasets were explained by only a few principal modes. Some of the complexity in the spatial structure may arise from the use of non-gridded data and a reanalysis using gridded data may prove more successful. From the current analysis, however, it would be unwise to infer large scale atmospheric dynamics from the EOF's outside of perhaps, the first 2 principal modes. It does not, however, indicate that the network is useless for climate prediction because linear combinations of several EOFs are likely to account for significant proportions of covariance between many different sites and or tree species. Linear combinations of the EOFs are utilized in this study to develop statistical models (Orthogonal Linear Regression) to reconstruct inter-annual to inter-decadal changes in temperature and precipitation within the study area. To reinterate, the large-scale, spatial patterns recovered from the instrumental data suggests that such an analysis is warrented despite the lack of tree-ring sites in close proximity to the study area. Other methods (e.g. canonical correlation) can be employed to recover the total fraction of variance in the instrumental records by developing linear relations between the principal climate and tree ring EOFs (Fritts, 1991). Using such an approach over 60 percent of the total variance in the first five temperature or precipitation EOFs fields can be explained with the first 20 EOFs retained from the tree ring network. Because simpler methods (OLR) can be employed to meet the objectives of this study, they will be used to estimate precipitation and temperature variability within the study area.

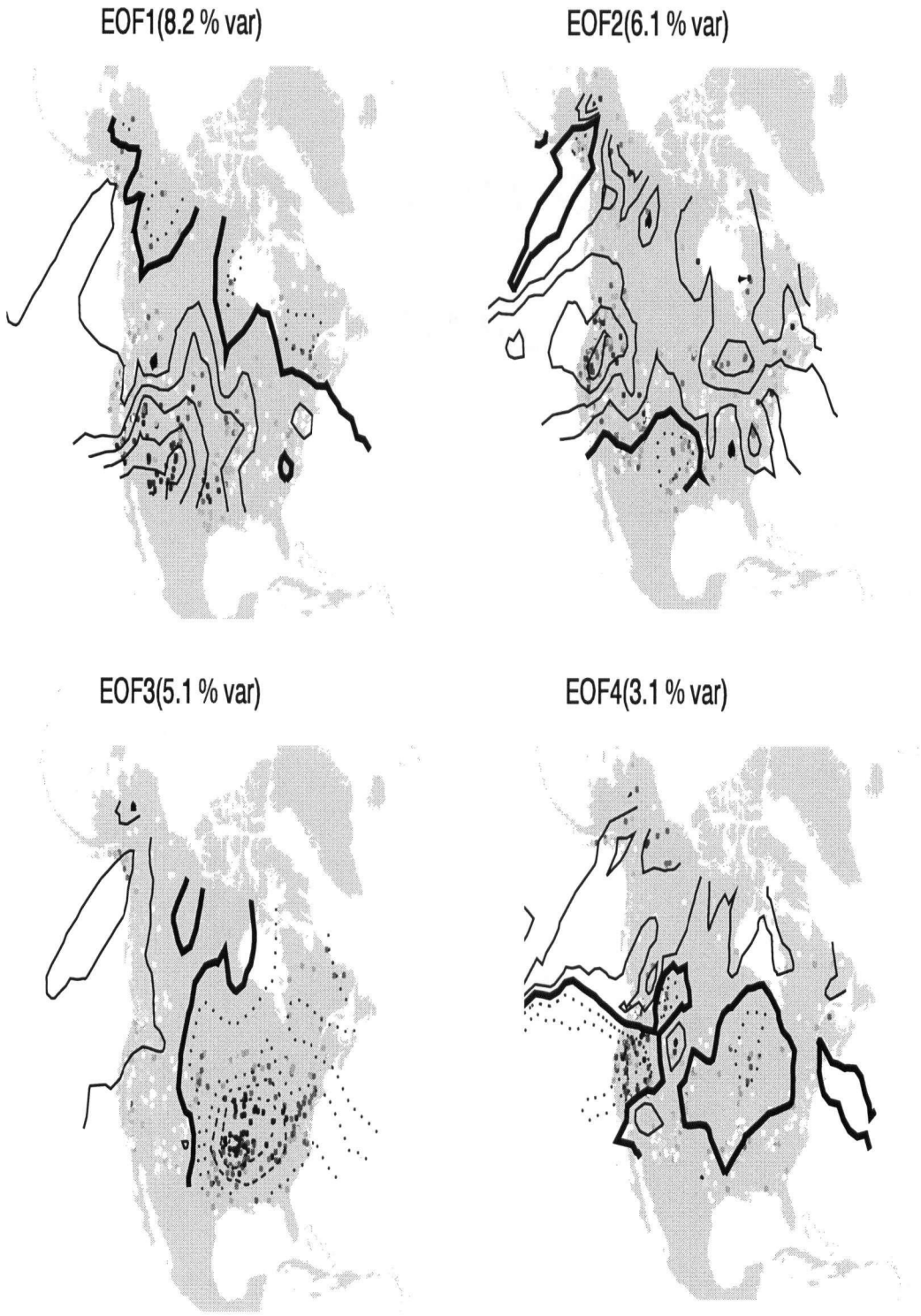

Figure 6.6: Amplitudes and Spatial Loadings of the First 4 EOFs From the 1800-1980AD (n=678) Tree-Ring Network
Contouring similar to figures 6.4 and 6.5. Dots denote tree ring sites within network.

Network	1400-1980AD				1600-1980AD				1800-1980AD			
	Eigenvalue (λ)	EV[a]	NT	CTeofs	Eigenvalue(λ)	EV	NT	CTeof	Eigenvalue (λ)	EV	NT	CTeof
EOF1	10.0	11.36	0.79	0.99	23.31	7.41	2.27	0.96	21.46	8.22	2.15	0.93
EOF2	6.26	7.12	0.50	0.92	17.92	5.70	1.75	0.91	15.81	6.06	1.58	0.71
EOF3	5.36	6.09	0.31	0.91	14.69	4.67	1.43	0.90	13.28	5.09	1.33	0.61
EOF4	3.92	4.46	0.27	0.89	11.31	3.60	1.10	0.80	9.18	3.52	0.92	0.45
EOF5	3.39	3.85	0.26	0.70	9.74	2.76	0.95	0.64	8.21	3.14	0.82	0.51
	$\Sigma_{i=1}^{i=20}$	55				53				55		

Table 6.3: EOF Statistics From the Tree-Ring Network

[a] Same as for table 6.1

6.2.4.1 Orthogonal Linear Regression (OLR)

Climatic reconstructions commonly employ canonical correlation or similar techniques (Briffa et al., 1992) to estimate the proportion of explained variance over a spatial domain which is similar to the tree-ring network utilized. For this study, the analysis is simplified because only temperature and precipitation over southern British Columbia need to be considered. Reconstructing large-scale, ocean-atmospheric indices (e.g. ENSO and the PDO) are also considered as they were shown to be linked to precipitation and temperature variability in the previous section and in Chapter 2. They are important for this study given their influence on controlling glacial mass balance within the study area (e.g. Hodge et al., 1998; Bitz and Battisti, 1999) and thus, the intensity of glacial runoff. The PNA was not modeled because its time series is much too short (1948-1979AD) to examine stability of the models employing standard approaches (e.g. calibration and verification).

A requirement when using EOF analysis for statistical prediction is an arbitrary decision on the number of principal modes to retain. For standardized data, a sensible rule is to retain those EOFs with eigenvalues greater than 1.0 (Preisendorfer, 1988, e.g.) as they explain more variance than any single predictor. This rule was combined with an arbitrarily-imposed requirement that over 50 percent of the original variance within the tree ring networks be retained for climate reconstruction. Using both requirements, the first 20 EOFs from each network were retained, re-standardized and defined a new basis set for the linear regression models. Individual models were constructed using a stepwise regression algorithm which was run in both directions (i.e. first entering then removing variables). EOFs that did not statistically improve the explained variance (by maximizing the explained variance of the model using Akaike Information Criterion) were omitted from the final model. Model stability was assessed by splitting the time series in half, and examining the percentage of variance predicted during calibration (1900-1939AD) and verification (1940-1979AD) periods. Goodness of fit of a given model is evaluated with an adjusted R^2 to account for the number of predictors within the model as well as a reduction of error (RE) statistic (Lorenz, 1977):

$$RE = 1.0 - \frac{\Sigma_{i=1}^{i=n}(\widehat{y_i} - y_i)^2}{\Sigma_{i=1}^{i=n}(y_i^2)} \tag{6.2}$$

where $\widehat{y_i}$ is the standardized, estimated value of the predictand and y_i is the standardized, predictand. The sign of the statistic gives an immediate index for whether the model is a useful predictor as an $RE > 0$ implies the model performs better than the mean of the dependent data (Fritts, 1991).

6.2.4.2 Results

Using linear combinations of the first 20 EOFs from the tree ring networks, annual temperature variability in the study area can be predicted with a moderate degree of success and the simplicity of the models increases only marginally with increasing spatial degrees of freedom (figure 6.4). The simplicity, however, increases at the expense of explained variance with a 5% reduction between the 1400-1980AD and 1800-1980AD networks. Calibration and verification statistics are most stable for the 1400-1980AD network and because it resolves the greatest proportion of variance, it will be chosen for temperature reconstruction purposes. The explained variance of the model (46 %) is similar to the proportion of variance explained by a densiometric study reconstructing half-year temperature (April-September) across western North America (Briffa et al., 1992) though that study used slightly longer records of temperature variability (1881-1982AD). Its performance is only marginally better than an earlier study reconstructing annual temperature variations in the

western US (Fritts, 1991). To examine the effects of the areal weighting, the EOFA was completed on the unweighted network but it did not appear to significantly alter the results (it slightly reduces spatial clarity) or increase the predictive capabilities of the orthogonal regression models.

In contrast to annual temperature variability, precipitation models for the study area resolve a considerably smaller proportion of variance (table 6.4). The recoverable variance is considerably less for wintertime precipitation (Nov-March) models (not shown). Verification period models (1940-1979AD) for the 1600-1980AD and 1800-1980AD networks are not significant at ($p = 0.05$) when the number of predictors are taken into account though the RE statistic is positive for all models. These results indicate that although OLR models for annual and wintertime precipitation variability are statistically significant, they are unstable and the fraction of variance they resolve is low for prediction purposes. Similar difficulties in estimating precipitation totals for the Pacific Northwest were observed by Fritts (1991) using a more restrictive (in time and space) tree ring network though this study recovers slightly more (5%) of the total variance. A more recent analysis reconstructing large-scale patterns of drought from a 248 site network (1705-1979AD) also reported generally poor results of reconstructing inter-annual changes in precipitation in the Pacific Northwest (Meko et al., 1993). It is also likely that some of the difficulties in estimating inter-annual changes in precipitation totals is due to the underlying characteristics of the proxy and instrumental datasets. Annual precipitation datasets commonly have significantly less memory or autocorrelation than those of annual temperature changes or tree ring variations. For example when tested against a white noise model, the lag1 autocorrelation for the precipitation data ($\rho_{\Delta 1(ppt)}$) is only marginally significant compared to $\rho_{\Delta 1(temp)}$ which is 0.58. The temperature time series is autocorrelated out to $\rho_{\Delta 8(temp)}$ and such memory reduces the overall statistical significance of the linear regression models.

Network	Model		Calibration	Verification
	Annual Temperature (Jan-Dec)	*1900-1979AD*	*1900-1939AD*	*1940-1979AD*
1400-1980AD	$temp_{ann} = (5, 6, 8, 12, 13, 14, 18, 19, 20)$ [0.31][a]	0.46[b]; 0.31[c]	0.51; 0.58	0.49; 0.55
1600-1980AD	$temp_{ann} = (2, 3, 4, 6, 10, 16, 19, 20)$ [0.40]	0.44; 0.52	0.35; 0.39	0.40; 0.44
1800-1980AD	$temp_{ann} = (2, 3, 7, 19, 21)$ [0.41]	0.41; 0.34	0.48; 0.47	0.15; 0.01
	Annual Precipitation (Jan-Dec)	*1901-1979AD*	*1901-1939AD*	*1940-1979AD*
1400-1980AD	$ppt_{ann} = (6, 7, 14, 15, 20)$ [303]	0.24; 0.08	0.34; 0.3	0.14[d];0.004
1600-1980AD	$ppt_{ann} = (2, 4, 10, 12, 14, 16, 20)$ [311]	0.25;0.13	0.32; 0.33	0.18[d]:0.14
1800-1980AD	$ppt_{ann} = (4, 5, 6, 13, 14, 16)$ [302]	0.30; 0.18	0.34; 0.33	0.25;0.14

Table 6.4: Summary Statistics from multiple regression models

[a] Standard Error of the estimate

[b] Variance (fraction) explained after correction for number of independent variable (r^2_{adj})

[c] Reduction of Error statistic (equation 6.2)

[d] Not significant at ($p = 0.05$)

Models developed using data from closest grid point from gridded temperature and precipitation datasets.

6.2.4.3 Temperature and Precipitation Reconstruction (1400-1979AD)

Using the 20 retained EOFs from the 1400-1980AD tree ring network, precipitation and temperature were reconstructed for the 1397-1979AD period. Unfortunately a true verification of such a regression model is limited to the period of instrumentation and can be viewed as extrapolation. Any time varying changes in tree-growth response to precipitation and temperature will cause extrapolated values to be in error. Despite this limitation, such models are used for lack of better methods of reconstructing temperature and precipitation back in time. The reconstructions are based on the 1400-1980, 1600-1980, and 1800-1980 networks.

The degree of recovered precipitation variance during the period of instrumentation is so low that trends in reconstructed precipitation should be viewed with caution. In general, the reconstructions using all three networks show similar low frequency trends over the period of overlap but there are significant departures at the decadal scale. All three regression-based estimates of annual temperatures reconstructed cooler (ca. 0.75 °C) temperatures during most of the 19th century, which is largely consistent with reconstructions of growing season temperatures in western North America (e.g. Fritts, 1991; Briffa et al., 1992), the Canadian Rockies (Luckman et al., 1997)and multi proxy based reconstructions from the northern hemisphere (Mann et al., 1998). This estimate is also consistent with estimated temperature depressions based on paleo-ELA positions within the study area. The tree-based reconstruction also indicates cooler conditions during the early 1400's and the mid 1600's. The early 1400s is the coolest period with the 1400-1450AD interval close to 1.0 °C below the instrumental average (1900-1979AD). Despite the large number of contributing sites (91 individual sites), however, it is also based on the fewest trees so the absolute magnitude of the deviation is subject to the greatest uncertainty. The timing of this cooling is considerably different from the mid 1400s cooling event which is well replicated in tree-ring based temperature reconstructions for western North America and the northern hemisphere (e.g. Mann et al., 1998). Rapid, early 20th century warming is particularly prevalent in this study and appears to reflect an anomaly which is global in scope (e.g. Jones et al., 1999). However, in contrast to a tree-ring based temperature reconstruction from Washington (Graumlich and Brubaker, 1986), the departure within the study area does not seem to be anomalous when viewed against the 600 year record (figure 6.7). Reconstructed temperatures during the early to mid 1500's is similar in magnitude to the early 20th century anomalies in the instrumental record. Several sites in the Canadian Rockies recorded higher than present treeline during the early to mid 1500's (e.g. Luckman, 1993, 1994) and these data are taken to reflect warm conditions during that time (Leonard, 1997). Consequently, these observations provide some independent verification of the reconstructed, early to mid 1500 warm period.

Several significant differences exist between temperature reconstructions from linear regression models developed for the three networks which are also evident in tree-ring derived temperature estimates made during earlier studies. Surprisingly there appears to be greatest correspondence between the 1400-1980AD and 1800-1980AD networks and least similarity between the annual temperature estimates from the 1600-1980AD network. The largest differences occur around 1600AD and 1700AD; the 1600AD-1980AD network reconstructs annual temperatures which are, on average 1.0 °Ccooler than those estimated from the 1400AD chronology. The degree to which these differences reflect smaller sample sizes associated with the 1600-1980AD network is unknown but a large percentage of tree ring sites in North America begins around 1600AD. These observed differences are also noted in the previously discussed summer (e.g. Briffa et al., 1992; Luckman et al., 1997) and annual temperature reconstructions from North America (Graumlich and Brubaker, 1986; Fritts, 1991).

Interpreting changes in annual precipitation using the regression models of this study should be

viewed with caution as only approximately one quarter of the variance is recoverable with any of the models. The reconstructions indicate that there is considerably less persistence in precipitation variability (especially following the early 1600's) and that drought-like conditions occurred in the early 1400s the early 1600's and during 1920-1930AD. That similar scale persistence occurs in the contemporary records of precipitation from the study area is a promising result. The coincidence of drought-like conditions in the study area and warmer than average temperatures during the early 20th century appears to be unique within at least the last 600 years. Such conditions are interpreted to have played a major role in causing such rapid retreat of glaciers within the study area during this time. The data do not indicate any particular period in which precipitation departures could have sufficiently depressed ELAs to those calculated in the beginning of this chapter. This is taken as a first order approximation that the LIA within the study area was most likely caused by consistently cool temperatures rather than dramatic increases in precipitation totals. The low resolved variance, however, limits any refinement of the estimate using the current tree ring data.

6.2.4.4 Large-scale, climate indices

To extend the time series of ENSO, the ocean manifestation (SST variability) rather than atmospheric effects (e.g. the SOI index) was chosen as an ENSO index. Long (1857-1979AD) time series of tropical SST variability between 0-10° S and 80-90° W (NINO12) were used to extend the length of the atmospheric (SOI) signal of ENSO. SST variations in NINO12 are well correlated to SOI over the period of common overlap. Values of NINO12 were averaged over the Nov-March period for each year as ENSO has the largest amplitude during these months and effects on large-scale hydroclimatic variability are most pronounced. The strength of ENSO does not appear to be estimated reliably using the OLR models. Explained variance varies from 14 % for the 1400-1980AD network to 27% for the 1800-1980AD network. Calibration and verification periods are similar though the low explained variance of the models is not encouraging for prediction purposes.

The OLR were used in an attempt to extend a 1600-1900AD PDO reconstruction using Mountain Hemlock (*Tsuga mertensiana*) from maritime environments of Pacific North America (Gedalof and Smith, 2001) back to 1400AD. That model (first EOF of growth pattern from 6 sites) explains a moderate proportion ($r^2 = 0.30$) of covariance between ring width and the spring phase (March-May) of the PDO. Based on the EOF analysis of monthly precipitation and temperature fields noted in this study large areas in North America appear to be influenced by the PDO and tree-ring sites away from the North Pacific may be useful for developing a more robust and potentially longer PDO reconstruction. To examine this possibility, OSL models were developed from the 20 retained PC's and monthly PDO time series aggregated according to season and year. Yearly data were aggregated into Nov-Oct estimates, as it was believed that by November, radial growth at most sites would be complete. The best and most stable regression model for the PDO was developed from 13 EOFs recovered from the 1400-1980AD network (table 6.5).

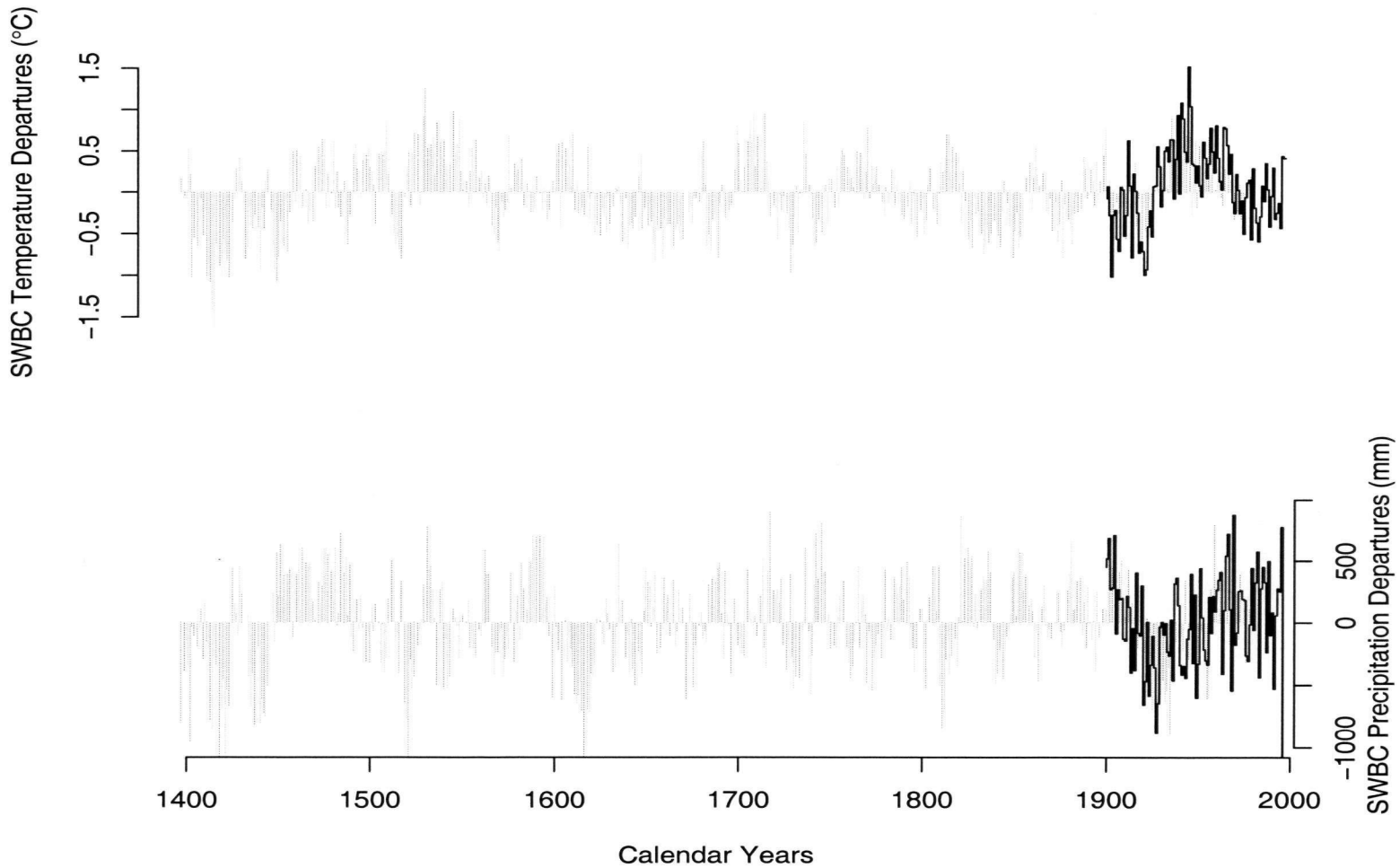

Figure 6.7: Reconstructed Annual Temperature and Precipitation Variability for the Study Area
Reconstructions based on linear regression models developed from 20 EOFs from 1400-1980AD tree ring network. The temperature model explains over 45 percent of the instrumental variance (grey line) over the period of common overlap (1900-1979AD) while the precipitation model performs much more poorly (table 6.4). Precipitation variability are departures (mm) from instrumental period (1900-1997AD; $2483 mmyr^{-1}$)

The residuals from the regression are stable throughout the period of overlap (figure 6.8) and are uncorrelated in time (i.e. $\rho_{\Delta 1}$ is not significant when tested against a white noise model). Such characteristics and consistent model performance during calibration and verification periods are indicative of a stable regression model adequate for reconstruction estimates of the PDO.

Model:	$PDO_{nov-oct} = f(2-6, 8, 11, 13-19)$	SE_{est}	RE
	$r^2 = 0.63$; $r^2_{adj} = 0.56$; $p = 7.28e^{-10}$	0.48°C	0.59
Calibration	*(1900-1939AD)*		
	$r^2 = 0.64$; $p = 0.002$	0.44°C	0.69
Verification	*(1940-1979AD)*		
	$r^2 = 0.72$; $p = 0.001$	0.51°C	0.61

Table 6.5: PDO Model, Verification, and Calibration Statistics

Four of the EOFs are not significant ($p = 0.05$) in the regression when subject to partial correlation but they contribute to the overall quality of the model and appear to stabilize the variance. The residuals of the model are uniformly distributed throughout the period of tree ring-PDO overlap and similar regression coefficients indicate the overall robustness of the model (figure 6.8). The number of contributing EOFs to the model is large and is interpreted to indicate that although the region of greatest influence of the PDO is centered in the north Pacific region, its influence on tree growth is widespread throughout North America. This large spatial domain of the PDO was recognized in the analysis of the dominant spatial modes of temperature and precipitation variability within the North American gridded datasets (e.g. $EOF2_{temp}$) and agrees with a recent analysis examining the spatial influence of the PDO (Mantua and Hare, 2002). Gedalof and Smith (2001) suggest that fluctuations in the PDO explain more of the variance in tree growth patterns than atmospheric indices of climate variability perhaps because many of the atmospheric indices they considered (e.g. NPPI, SOI) are manifestations of SST variability. However, it is equally likely that the better fit arises from the highly autocorrelated structure within the tree ring and PDO data compared to the instrumental data.

The 1900-1979AD model was used to reconstruct the contemporary record of the PDO back to 1400AD (figure 6.8). The overall behavior of the reconstructed PDO time series is comprised of both low and high frequency variability. The time series is significantly correlated ($r = 0.33$; $p < 6.6e^{-16}$) to the reconstructed annual temperature time series (figure 6.7). Based on analysis of the instrumental data in Chapter 5, such a positive relation should be expected. Much of the coincidence for the reconstructed series arises because both models share many of the similar EOFs. Spectral power is primarily distributed within a 100-400 year window but given the non -uniform standardization practices associated with the ITRDB data it remains unknown to what degree this power is related to climate. When low frequency variability (> 100 yr) is removed from the record, there is a significant spectral power at inter-decadal (≈25yr) frequencies. Similar power is observed within a circum-Pacific tree ring network (Minobe, 1997) and climatic reconstructions of summer temperature within southern British Columbia and the Pacific Northwest (Briffa et al., 1992). The reconstructed PDO series shows moderate similarities to the Gedalof and Smith reconstruction and the reconstruction of the PDO by Biondi (Biondi et al., 2001).

An appraisal is now made concerning the correspondence between these indices of climate and sediment yield proxies developed from Green and Duffey Lake basins.

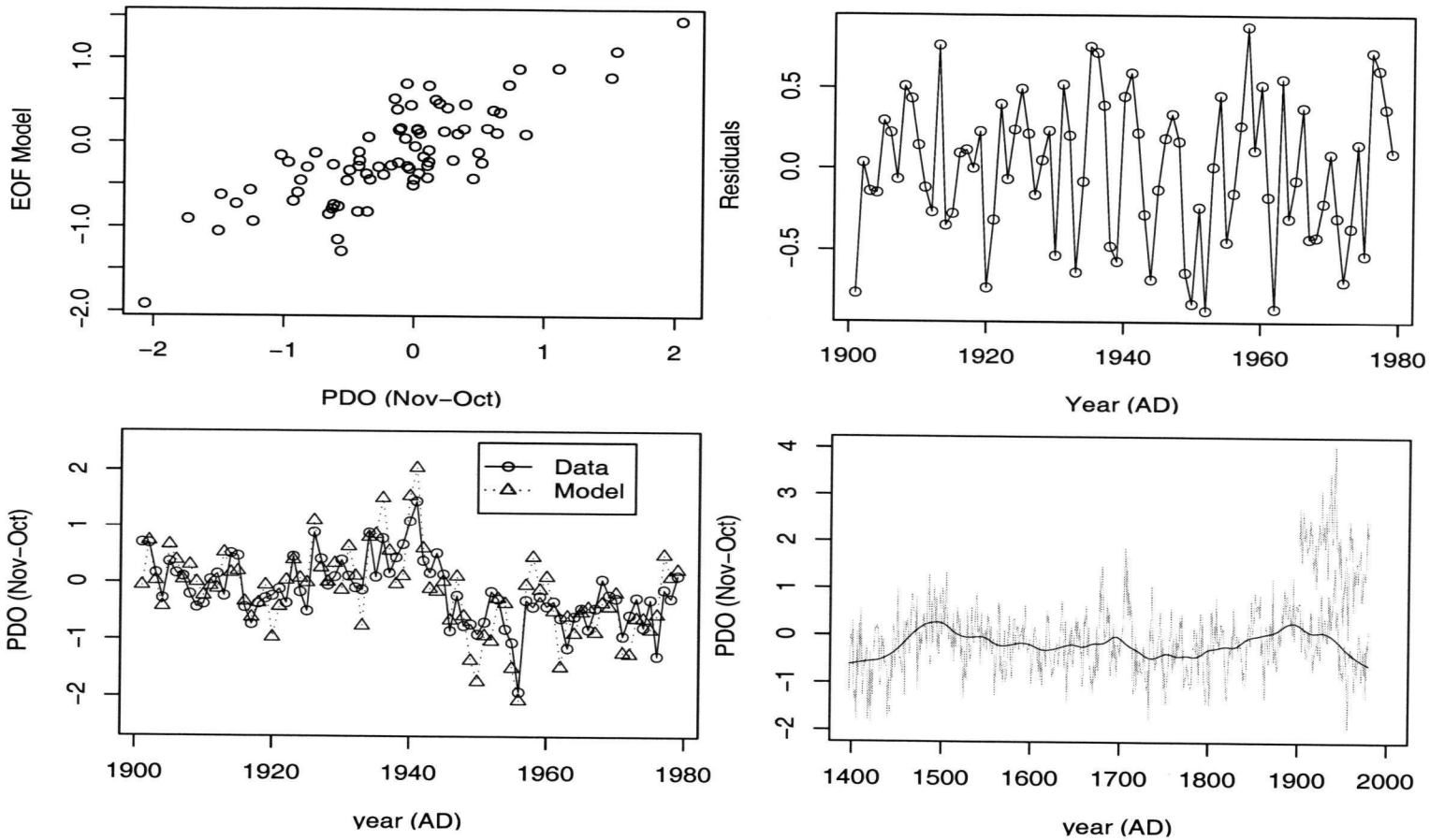

Figure 6.8: PDO Model
Upper left plot shows observed vs. predicted fit based on the 1400-1979AD chronology. Upper right panel are residuals from the fit though time. Lower left panel is the reconstructed vs. observed annual PDO time series and the lower right panel show reconstructed (1400-1979AD) and observed series. Observed series offset by 2.0 °C for clarity. Thicker line is lowess fit to the data (window length =58 years).

6.3 Climate-Sediment Transport Linkages over the past 600 years: Varve Chronologies From Green and Duffey Lake Basins

Varve chronologies were constructed for two lake basins (Duffey and Green Lake) to evaluate annual sedimentation rates over periods which considerably exceed the contemporary monitoring program. The chronologies were developed from multiple sediment cores to reduce uncertainties in age and varve thickness measurements. To summarize, the quality and reliability of the chronologies differ considerably between the lake basins; the chronology developed from Green Lake appears to be sensitive and uncertainties in age in the last 600 are considered low while the record from Duffey is considerably noisier and more subject to uncertainty in true age.

The chronologies were developed employing methods outlined in Chapter 3 and Appendix D. These entailed combining thickness measurements obtained from photographs of partially dried sediment cores and measurements made from embedded sediment slabs and thin section measurements. Thickness variations between the contributing cores were not significantly different at ($p = 0.05$) so they were combined into an unweighted average. Overall errors in counting and varve identification were considerably less (~1.7 percent) for the Green Lake chronology than for the varves of Duffey Lake (over 5 percent). The difficulties associated with Duffey Lake include difficulties in varve identification, the presence of erosive turbidites and event beds within the lake records, and intervals of strongly bioturbated sediments even in cores obtained from deep (> 80m) water settings. Despite the recovery of multiple cores, the errors associated with these factors could not be minimized and the chronology can not be considered to be accurate by varve standards (e.g. Leonard, 1995; Lamoureux and Bradley, 1996; Lamoureux, 1999a).

6.3.0.5 Results-Green Lake

A continuous, multiple core varve chronology was constructed for Green Lake back to 1387AD. Below the 1387AD couplet, the varves become intensively bioturbated for approximately 5cm in all of the recovered cores. The sediments within this interval are more organic rich than older or younger sediments and the temporary rise in organic content appears to be partly caused by small fragments of poorly-preserved charcoal. Based on average varve thickness (1.25 $mmyr^{-1}$) for couplets in the vicinity of the interval, 40 varves were added to the chronology below this depth. With the addition of these "missing" varves, the estimated varve (880±20AD) and calendric $AMS\ ^{14}C$ age (648-865AD) obtained from 241 cm depth (table 6.7) can not be shown to differ at 2σ . Similar results indicate that the varve chronology appears reasonable to at least 342cm or approximately to 365AD (appendix D). In order to make meaningful comparisons to the climate reconstructions, varve thickness was transformed to normality by converting thickness measurements to their natural logarithms.

The distribution of varve thickness for Green Lake differs considerably from a normal distribution (figure 6.9). The distribution could not be transformed to normality with a Box-Cox transformation (i.e. no suitable λ could be found) for either a subset (1387-1999AD) or complete (n=2960) distribution of varve thickness. Nevertheless, the data were log-transformed to better approximate a Gaussian distribution. The normality requirement is necessary for statistical comparisons between the normally-distributed, reconstructed precipitation and temperature data. In addition, an assumption of normality is required for least squares regression analysis and for the determination of confidence limits in time series analysis (Hegge and Masselink, 1996).

The highly skewed nature of varve distributions from clastic environments is a commonly observed phenomenon (e.g. Hughen et al., 2000a; Lamoureux, 2000; Rittenour et al., 2000) indicating that large magnitude sedimentation events occur infrequently. In the case of many of these

chronologies, such events are turbidites (c.f. Lamoureux and Bradley, 1996) and they are subsequently removed from the record. No turbidites were found in the long sediment records from

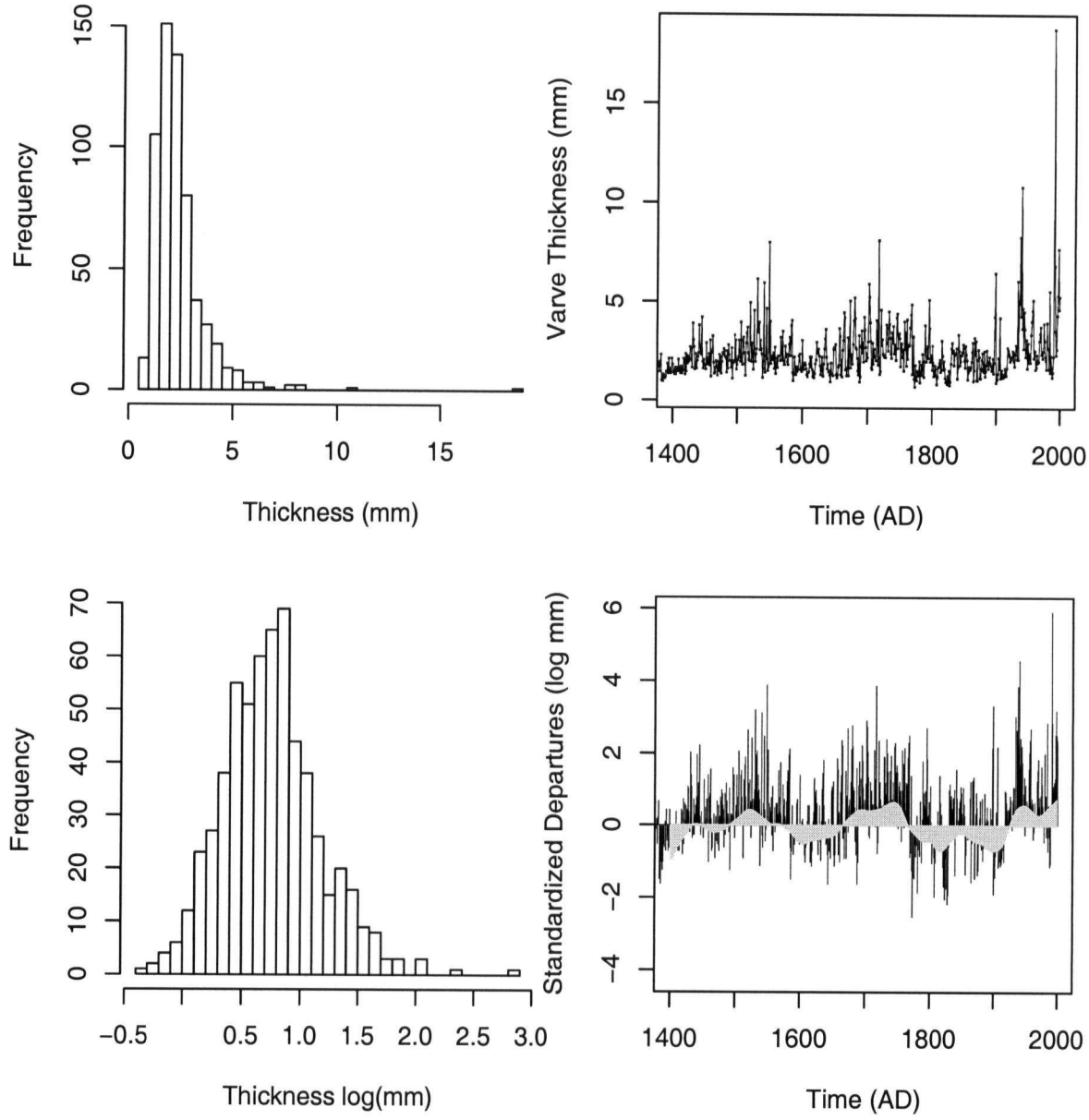

Figure 6.9: Raw and Standardized Varve Thickness, Green Lake (1387-1999AD)
Histograms showing distribution of varve thickness for the raw and transformed (log) data for the 1387-1999AD record of varve thickness. Standardized departures were calculated by log-transforming the data and averaging deviations across year in question. Lowess smoothing (53 yr window) on the standardized, log-transformed data (light grey) indicates two main periods of enhanced sedimentation centered on 1500 and 1700AD.

Green Lake, a rare occurrence for varved sediment sequences; the unique bathymetry of the lake basin prevent any underflows from reaching the core site (c.f. figure 5.8).

An analysis of varve-thickness variability reveals the following: The 1991 varve (18.9 mm) is thicker than any preceding event within the last 3000 years within the record. Its extreme nature remains if compaction effects (determined from porosity and density measurements of the sediments) are taken into account while the second thickest varve within the chronology was deposited during 1940AD. Other, thick varves occur infrequently throughout the 1387-1999AD chronology. Varve thickness varies considerably over the 1400AD -1980AD period (figure 6.9). Notable increases in average thickness are centered around the early to mid 1500s, the mid 1600s to the mid 1700s. The rather abrupt and consistent positive anomalies of varve thickness during the late 1920's to mid 1940's is also evident. Other abrupt shifts in the record occur in the late 1700s where varve thickness remains lower than average until the late 1920s.

Low frequency variations within the 1387-1999AD varve chronology share some similarities with annual reconstructed temperature departures (figure 6.10). Low frequency (29 yr lowess window) departures indicate negative anomalies in the the early 1400s, the early 1600s and throughout the 1800s while positive departures are observed for the mid 1500s, the very early 1700s and again during early to mid 20th century. Cross correlation on the unfiltered records (figure 6.10) indicates a maximum correlation of $r = 0.22$ at a 14 yr lag though the Pearson correlation coefficient at lag3 is 0.2. Approximate[3] verification for the relation between air temperature and varve thickness over the 1387-1979AD period is provided by a multi-proxy based temperature reconstruction (Mann et al., 1998) which indicates a near zero lag between the records. The overall strength of the correlation increases in time, mainly caused by abrupt, zero lag increase in varve thickness and temperatures during the early 20th century (figure 6.11). For example, the correlation between the 1800-1980AD records is $r = 0.42$, but drops to $r = 0.25$ when comparing 1700-1980AD and then becomes fairly constant $r \approx 0.2$ thereafter. Without the 20th century signal, the correlation between the two records becomes close to statistically insignificant.

6.3.0.6 Results-Duffey Lake

Although it appears that clastic varves have formed in the lake since at least 3700 cal. yr BP, a continuous varve chronology could only be developed for the past 530 years. The difficulties which limit the extension of a continuous sediment proxy include several intervals of bioturbated sediment common to all cores, the common presence of erosive turbidites, debris flow and snow avalanche deposits. The master chronology is only comprised of a single core for much of the 19th century and half of the 15th centuries. Where replication is available, between-core varve measurements are highly correlated and mean thickness can not be shown to differ between cores. The lack of replication for these intervals resulted from too many intervals of bioturbated sediments or erosive events. Below the 1465AD varve, there were simply too many erosive deposits which were common in all of the cores except one core taken in shallower (75m) water settings 97-Duf(09). Unfortunately, the sediments from this core are often strongly bioturbated. The most probable uncertainty associated with the varve chronology is on the order of 5 percent. A derivation of this uncertainty estimate can be found in appendix D. The large (by varve standards) error associated with the chronology does not allow strong conclusions to be made concerning the inter-annual to inter-decadal sediment transport-climate linkages over the last 500 years. The error associated with inferring lower frequency variations (decadal to century) are proportionately lower and verified by agreement between varve age and independently-derived ages using $AMS\ ^{14}C$ dating.

[3]Both records contain data from the ITRDB so they are not strictly independent

A considerably noisier record of annual sedimentation is recorded in the varved record from Duffey Lake (figure 6.12). Much of this noise originates from turbidites and event beds within the record. Their frequency appears to be random through time and because they do not appear to contribute any meaningful information concerning basin-wide changes in sediment delivery, they were replaced by the mean of the series (without such events). Most laminae interpreted to be the products of surge currents generated by slope or deltaic failures could be immediately identified within the records and commonly exceeded 5mm in thickness. This is close to the thickest varve recorded in any of the cores and is close to a natural scale break in varve thickness when the data are visually compared to random log normal variates with similar location and scale statistics. Using the 5mm boundary, 22 couplets were removed from the chronology and replaced by the series mean.

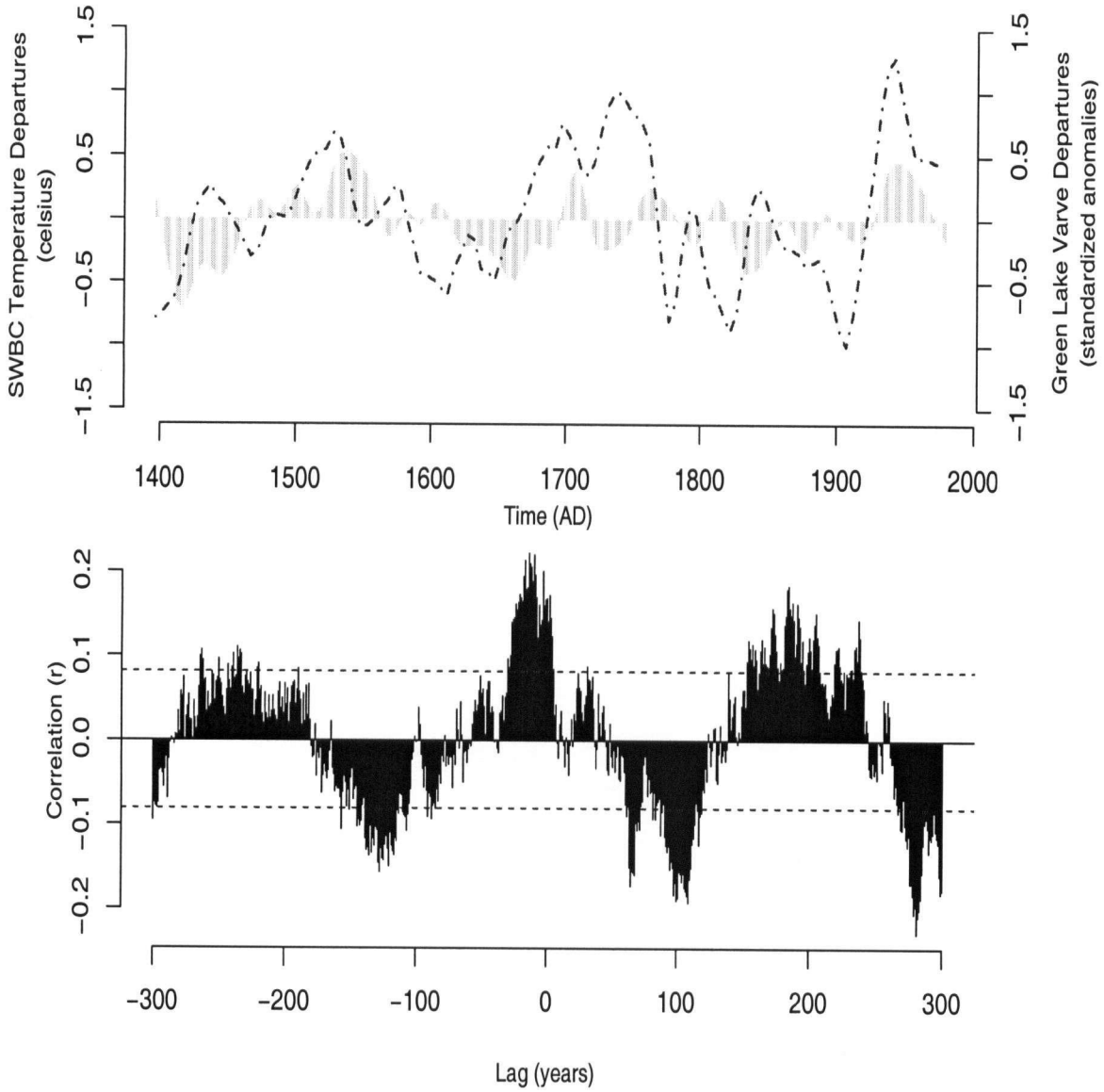

Figure 6.10: Reconstructed Annual Temperature and Green Lake Varve Departures
Upper panel: Reconstructed annual temperature (solid line) and varve thickness (dotted) time series. Lower panel: Cross correlation plot between the two series.

Departures in varve thickness from Duffey Lake show little low frequency structure following ca. 1700AD (figure 6.12). Prior to this, the varves are thick in the early portion of the record (the late 1400s) and consequently, the chronology has good replication (n=3,4) because varves are easily identified and have undergone minimal bioturbation. Sedimentation rates become low during the 1500s and the late 1600s, almost opposite to the trends observed in Green Lake (figure 6.13). Cross correlation between the original time series (not smoothed) indicates that the varve chronologies are inversely correlated with positive varve departures from Duffey Lake occurring some 37 years after negative anomalies in sedimentation occur in Green Lake. The significance of the correlation is moderate but overall covariance between the records is low ($r = 0.18$; $p = 3.4e^{-05}$; $df = 518$). Repeating the analysis by halving the series and testing the strength of the correlation

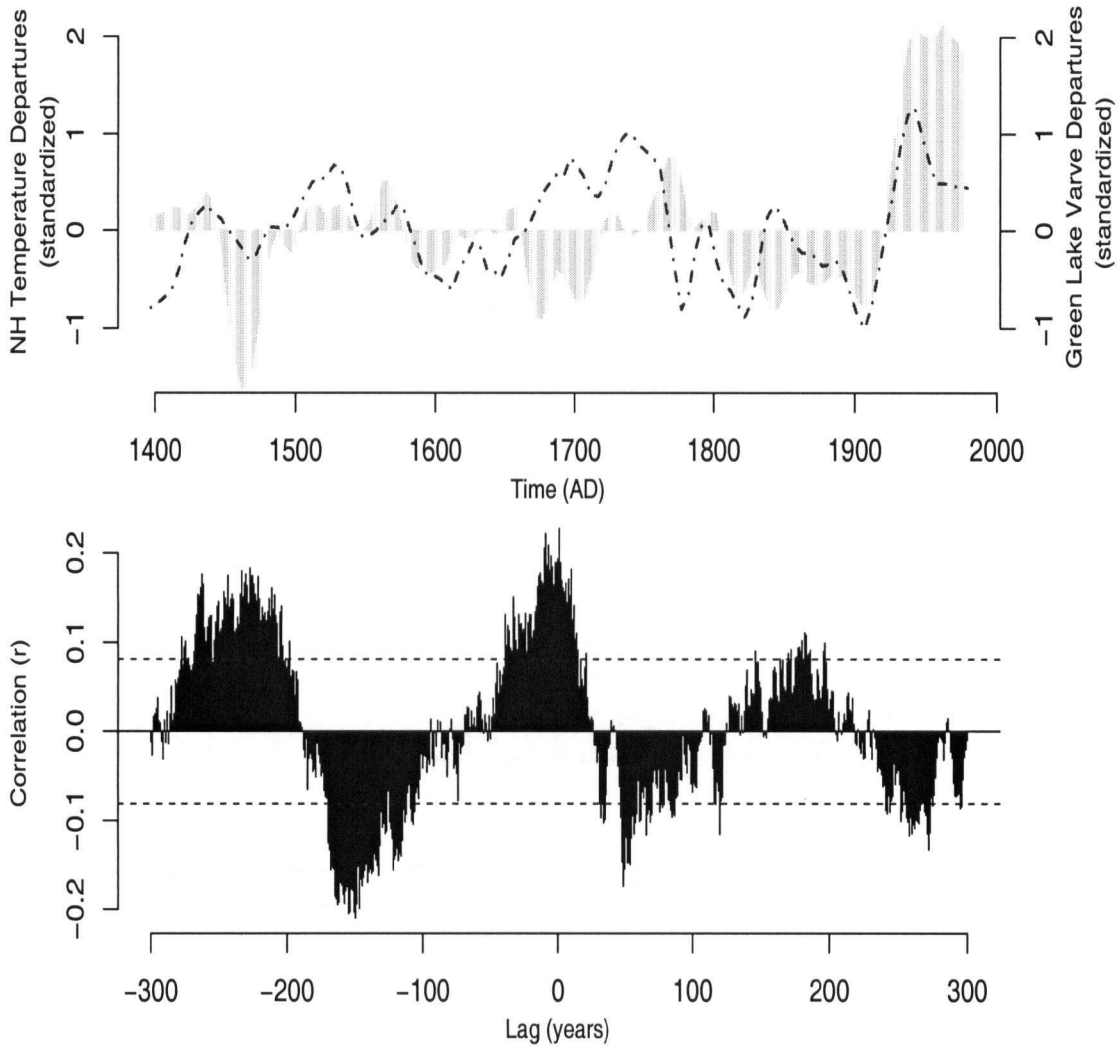

Figure 6.11: Northern Hemispheric Air Temperature and Green Lake Varve Departures
Upper panel: Reconstructed annual NH temperature (solid) and varve thickness (dotted) time series. Lower panel: Cross correlation between the two series.

and stability of the lag produced similar results. Autocorrelation in both chronologies is low ($\rho_{\Delta 1(green)} = 0.41$; $\rho_{\Delta 1(duffey)} = 0.38$) indicating that the statistical significance does not simply arise from comparing autocorrelated time series. Cross correlation between Duffey Lake varve record and the temperature and precipitation reconstructions indicates a poorer fit to either time series than the Green Lake chronology. The best agreement between the records is a weak, positive association ($p = 0.19$; $p = 4.3e^{-05}$; $df = 467$) between varve thickness and reconstructed annual air

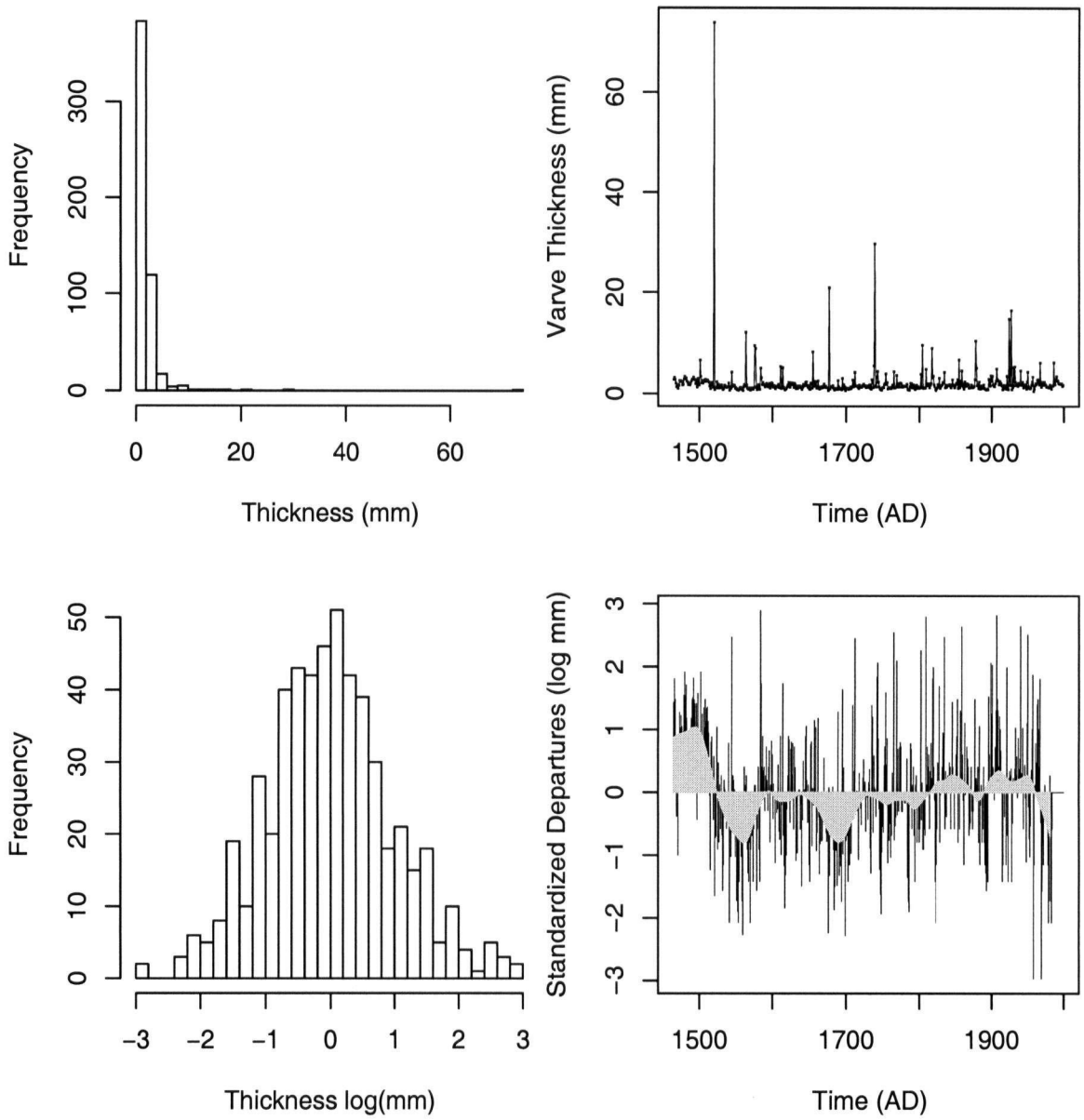

Figure 6.12: Raw and Standardized Varve Thickness, Duffey Lake (1465-1999AD)
See figure 6.9 for explanation of key. Laminae > 5mm were removed in the lower two panels.

temperature variability at a lag of 47 years.

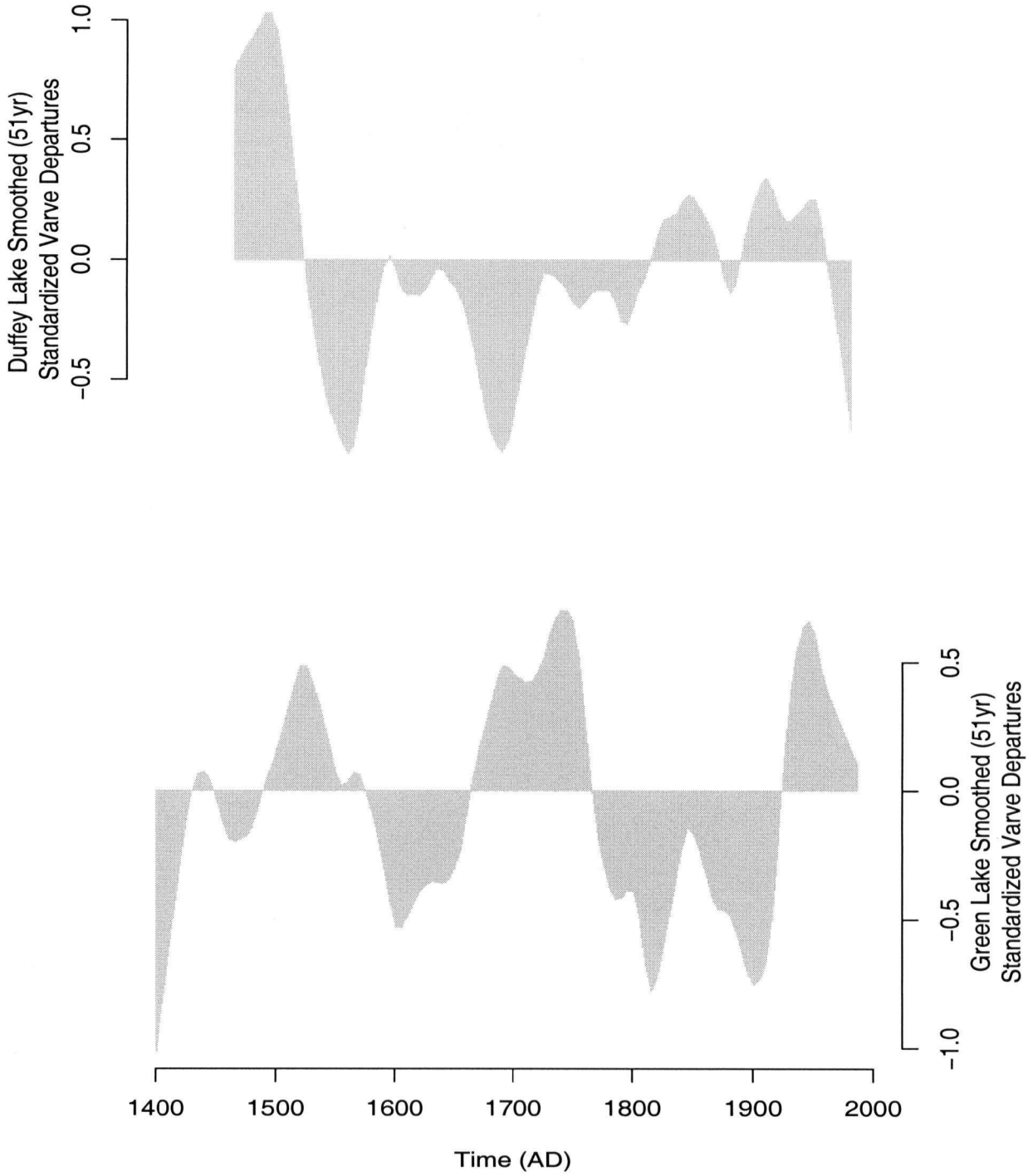

Figure 6.13: Smoothed (lowess-53yr) Varve Departures, Duffey (top) and Green (bottom) Lakes

The negative and lagged correlation between the chronologies could arise from a number of factors, several of which have no particular geomorphic or climatic significance. It is possible that a statistical error (a type 1 or α error) was committed where the null hypothesis (H_o: $\rho = 0$) was

incorrectly rejected. The significance level of the correlation, however, implies that this probability is low. The lag may also arise due to the potential error (especially Duffey) of the varve age. Taking the average uncertainty into account (2σ), the two time series could conceivably be anti-correlated at zero lag though if the lag was due to counting errors one would expect the lag to increase as a function of age. Such effects were not apparent and because the two series exhibit similar lead-lag relations for varve departures in the 20th century (where the records have been dated using ^{137}Cs), the lag is taken as real and caused by a physically-based phenomenon. Based on the temperature reconstructions and multi-proxy reconstructions of northern hemispheric air temperature, there appears to be little (6yr or less) lag between air temperature variability and lake sedimentation in Green Lake. Such zero lag relation between observed climate variability and the Green Lake varve record suggests that the offset between the records, if real, occurs within the Duffey record. A physically-based explanation for such a lag would be the time scale to route fine-grained sediments from sites of production to ultimate deposition in the central basin of the lake. Most of the fine grained sediments entering the lake during contemporary time appear to originate from the Van Horlick stream system (26 km) and ultimately, from headwater glaciers. Although speculative, an annual velocity of the sediment slug ($700myr^{-1}$) is estimated for the system and appears to be within the range ($10^2 - 10^3myr^{-1}$) of reported natural sediment wave velocities (e.g. Lisle, 1997; Lisle et al., 1997). The value reflects an average velocity over a given year as most sediment waves and bedload move considerable distances during flood conditions (e.g. Gilbert, 1917). Similar short-scale dependence on transport rates was observed in the contemporary monitoring portion of this study (see Chapter 5) where the majority of suspended sediments are transported over 1-2 days. When the proposed sediment wave velocity is rescaled for transport over such times the velocity ($700 - 350mday^{-1}$) is consistent with a recent flume study investigating transport distances of coarse sands (Dr. Hassan, UBC, pers comm).

6.3.1 Removal of Temperature Signal from the Green Lake Varve Chronology

Leonard (1997) observed a relation between sediment delivery and ice cover which was time scale dependent. At century and longer time scales, a good relation was observed between glacial extent and sedimentation in Hector Lake where enhanced delivery accompanied more extensive ice cover. At decadal time scale the relation became more complex and he attributed the complexity to sediment delivery which could occur when glaciers were advancing, were more extensive, or during phases of retreat. Without controlling for climate variability at these time scales, however, it remains unknown whether this complexity is due to variations in sediment production or its ability to be delivered downstream. By controlling for inter-annual variations in air temperature, the relation between sediment production and glacial extent at decadal time scale may become more clear.

Two approaches were adopted to control for climatically-driven fluctuations in sediment transfers. The first approach examines the standardized residuals produced from differencing reconstructed temperature variations over the study area (SWBC) and the Northern Hemisphere (NH) time series (Mann et al., 1998). The second procedure uses the tree-ring derived EOFs to model 20th century variations in varve thickness in an attempt to develop a regression model using the 20th century data as a "training set" for the expected covariation between tree-ring variability and varve thickness prior to 1900AD. This model is then used to reconstruct "expected varve departures" independent of any changes in ice cover. A comparison between the actual and reconstructed time series is then evaluated and compared to the record of glacial fluctuations during the 1400-2000AD period.

6.3.1.1 Temperature Model Residual Analysis

Cross correlation analysis of the varve chronology from Green Lake and the SWBC and NH time series indicated that varve thickness and air temperature covary at lags of zero-to 10 years. To highlight decadal and lower frequency variations, the time series were smoothed with a 15-year Gaussian filter to give highest weights to observations closest to the center of the filter window. Such filters are useful for noisy time series and do not cause temporal offsets introduced by standard moving averages (boxcar shaped filters). Comparison of the filtered temperature and varve time series indicate several regions where the series trends diverge. The divergence within the NH-varve comparisons is appreciable in the early (the early 1400's) and late (early 1900's) portions of the records where varves are consistently lower than expected if air temperature variability were the primary control (figure 6.14). Consistently higher rates of sedimentation occur for about a century between the mid 1600's to the mid 1700's. Cumulative departures of the differenced series show these trends more clearly (figure 6.14) and highlight important times where the runs of the residuals change sign. Evident within the cumulative departure plot of the differenced NH varve time series is the termination of consistently larger than expected residuals at ca. 1760AD and dramatic decline in expected sedimentation rates following 1940 (figure 6.14).

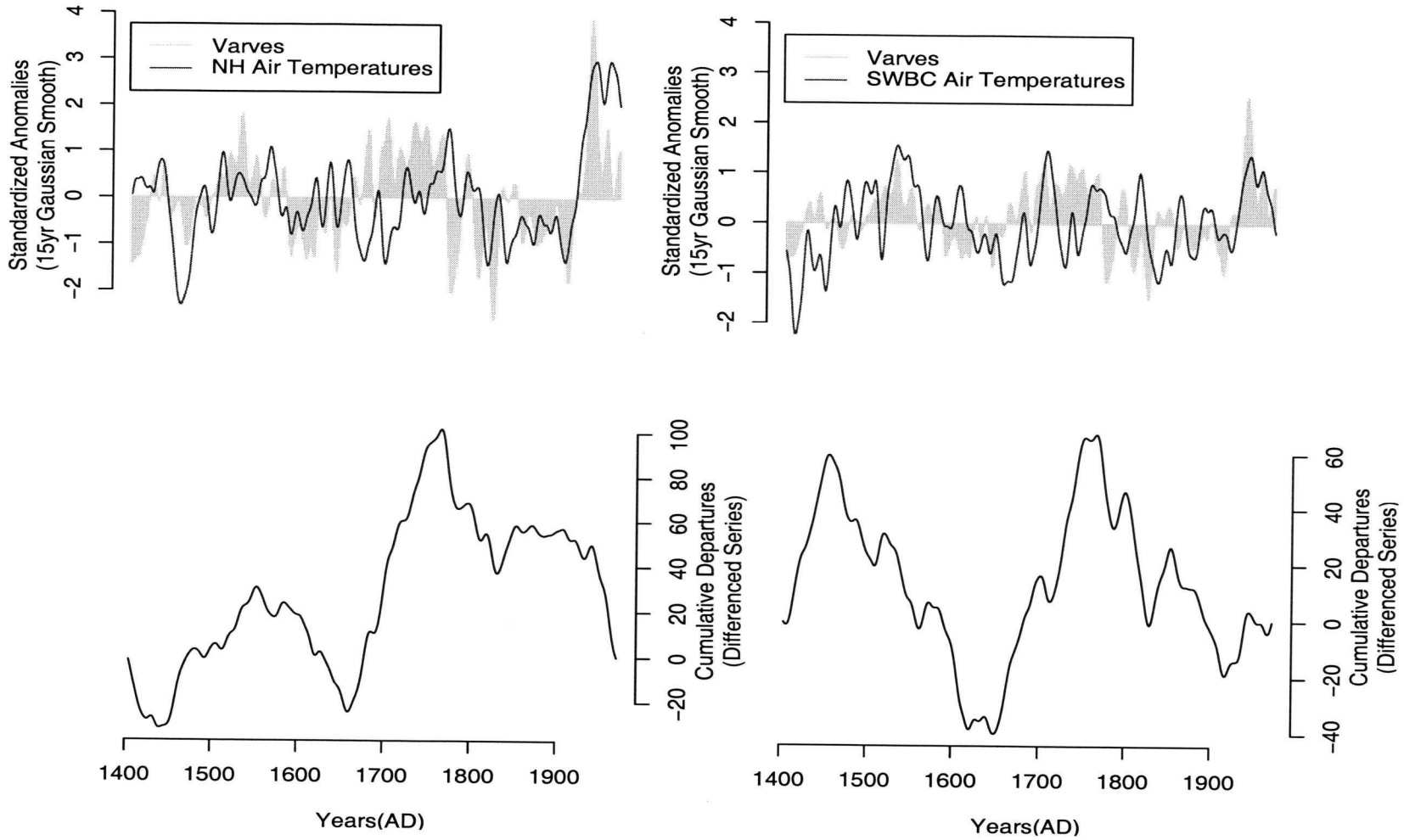

Figure 6.14: Reconstructed Temperature and Varve Thickness Variations
Upper two panels: Low frequency trends within the reconstructed SWBC and NH time series and those from Green Lake. Lower panels: Cumulative departures of low frequency, differenced series (varves-temp).

The SWBC temperature, varve series agree more closely and similarly indicate a larger than expected sedimentation between ca. 1710-1740AD. In contrast to the NH series comparison, the SWBC-varve differenced departures for the early 20th century do not show an abrupt decrease in sedimentation anomalies but do indicate a consistent reduction from 1740AD towards the present.

6.3.1.2 Reconstruction of Varve Thickness

A multiple linear regression model was developed from the 20 tree-ring EOFs to reconstruct expected varve thickness back in time. Variations in varve thickness during the 20th century were used to "train" the model. Similar to the PDO reconstruction, the developed model of varve thickness is complex though its predictive capabilities are impressive both over the entire 1900-1979 period but also during calibration and verification periods (table 6.6). Residuals from the model are well behaved though there is a slight tendency to underpredict large sedimentation events (figure 6.15). The under prediction may arise because of the failure to transform the varve data into normal variates though it could also arise because extreme sedimentation events often reflect short-lived flood events and it is unlikely that tree-based climate reconstruction models can control for such short -term variability. Significant autocorrelation within the contemporary record of varve thickness departures ($\rho_{\Delta 1} = 0.53$) decreases the effective degree of freedom within the record to df=7. The reduction significantly reduces the probability of chance correlation to ($p = 0.02$) but the model remains significant at the chosen significance level ($p = 0.05$).

Model:	$Varves = f(6-9, 11, 13-15, 17-20)$	SE_{est}	RE
	$r^2 = 0.76$; $r^2_{adj} = 0.64$; $p = 1.1e^{-12}$	$0.76(log\ mm)$	0.66
Calibration	*(1900-1939AD)*		
	$r^2 = 0.81$; $p = 8.7e^{-07}$	$0.82(log\ mm)$	0.80
Verification	*(1940-1979AD)*		
	$r^2 = 0.66$; $p = 7.0e^{-04}$	$0.77(log\ mm)$	0.63

Table 6.6: 20th Century Varve Prediction Model

Differences between the expected vs. observed varve departures indicate a primary mismatch between 1700-1750AD where modeled varve thickness is lower than the observed data (figure 6.15). A second and less significant deviation between the two records is noted for the early to mid 1400s. These differences are interpreted to reflect higher than anticipated fluxes of clastic sediments to Green Lake than can be explained by variations in climatological conditions responsible for tree growth.

6.3.2 Discussion

The correlation between air temperature and varve thickness for Green Lake suggests that fine-grained sediments are supplied to the lake basin during years which are warmer than average. This is similar to observation of early 20th century varve thickness departures and air temperature variability discussed in Chapter 5 though shallower snowpacks (April 1 SWE) are also associated with years which are warmer on average. Shallow snowpacks combined with years with warm summers would tend to prolong the glacial runoff season thereby controlling the quantity of fine-grained sediments reaching the lake basin. Similar, positive relations between varve thickness and the principal controls on glacial mass balance (summer air temperature and winter precipitation) have been observed in other lacustrine environments (e.g. Perkins and Sims, 1983; Leonard, 1986b; Leemann and Niessen, 1994; Ohlendorf et al., 1997). The lack of a stronger relation between

the reconstructed PDO time series and varve thickness departures for the varve chronologies was surprising because based on this study and that of Mantua (1997), the PDO is positively associated with air temperature variability and negatively with winter precipitation anomalies in the North Pacific over the period of instrumentation (1900-2000AD).

Much of the unresolved variance within the Green Lake varve chronology is likely caused by other factors which influence the quantity of fine grained sediments reaching the lake basin during flood events. Unfortunately, reconstructing the annual record of high flow events within the immediate study area is not possible with the current data set. This unpredictability of reconstructing flood events is scale dependent. Floods in larger, snowmelt-driven watersheds are commonly the result of wintertime anomalies in precipitation which are often related to large scale climate-variability. Using the EOFs of this study (analysis not shown), approximately 50 percent of the variance in Fraser River floods can be recovered over the period of instrumentation (1916-1979AD).

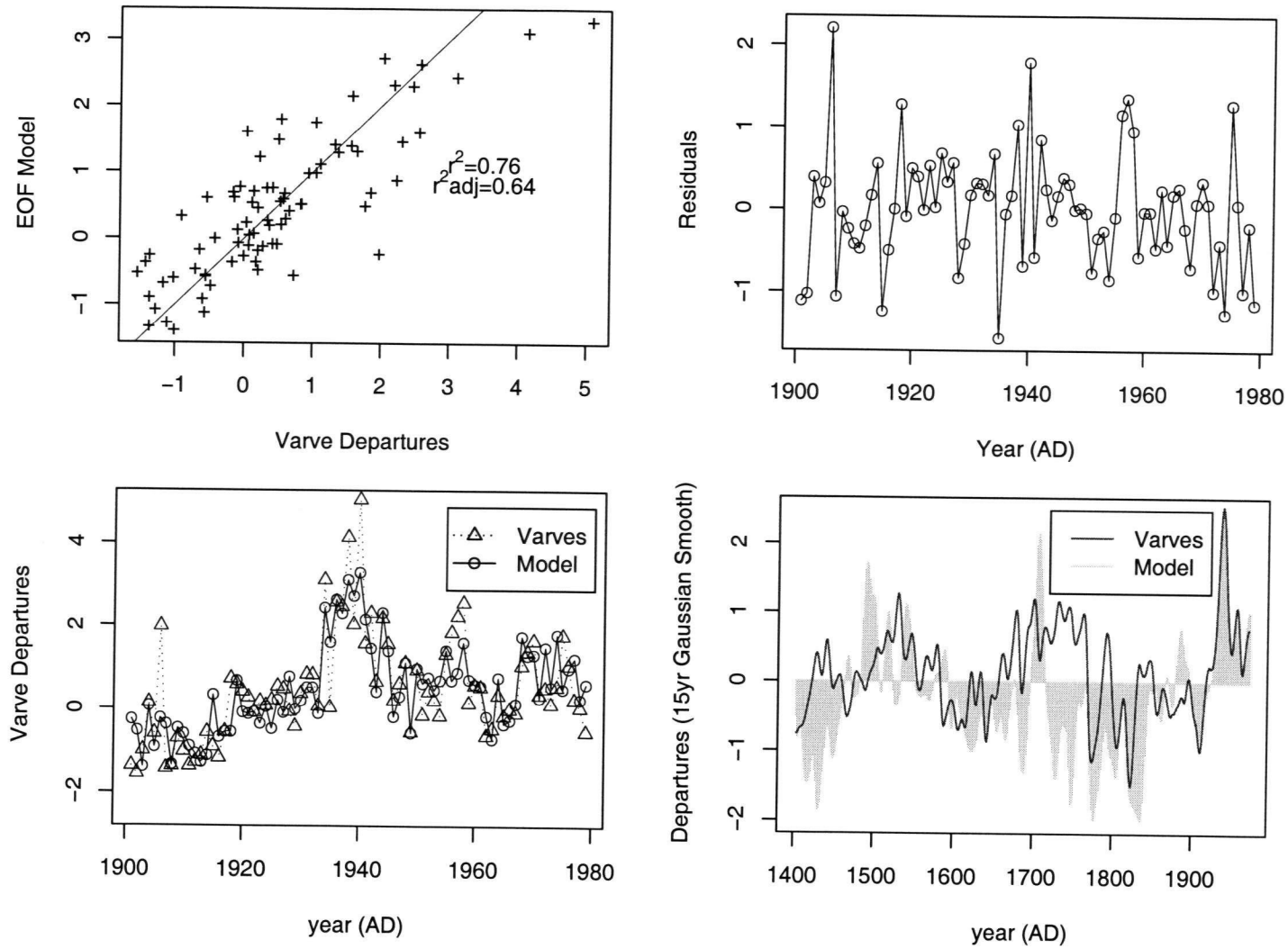

Figure 6.15: Modeled Versus Observed Varve Thickness

Given the mixed nature of flood generating mechanisms within the study area and its much smaller areal extent, a large proportion of the total variance within the Green Lake varve chronology can not be effectively controlled for using the tree ring data. The significance of flood events within the contemporary record of sedimentation in Green Lake is apparent and suggests that land-use effects (road construction and or deforestation) were partly responsible for the wide-spread channel change and hillslope instability noted in Chapter 5. Although other extreme sedimentation events occur within the varve chronology, the 1991 event is exceptional.

Based on the reconstructed indices of lake sedimentation and their comparisons to reconstructed climate indices for the study area, the following generalizations can be made. It appears that inter-decadal to century-scale variations in lake sedimentation are related to fluctuations in air temperature for at least the past 600 years but only a minor fraction of the total variance within the chronologies can be explained by inter-annual to inter-decadal temperature variability. This is not surprising as glacial fluctuations, among other things, will introduce non-linearities into the system through changes in sediment availability. The relation of varve thickness to inter-annual changes in air temperature is interpreted to reflect the intensity of glacial melt as annual changes in temperature in maritime environments of the Coast Mountains can influence total snowpack accumulations during winter (Moore, 1996) and the strength and duration of glacial runoff. Over long (e.g. century) time scales, growth and demise of glacial ice affect overall sediment availability within the catchments.

The explanatory power of air temperature does little to predict zero lag changes in sedimentation in the central basin of Duffey Lake. The complexity may relate to a number of factors, the most interesting but also most speculative is that a time lag (40-50yr) is introduced by fluvial storage between sites of sediment production (glaciers and glacial forefields) and the lake basin. It is hypothesized that following a period of significant glacial recession, it takes approximately 40-50 years for sediments originating from these glacial areas to propagate through the fluvial system. Based on the contemporary monitoring, Van Horlick Creek appears to be the major contributor of fine-grained sediments to the lake. The estimated sediment wave velocities are consistent with the contemporary characteristics of the channel, its availability of glacial sediment, and the low specific discharge observed during major sediment transporting events. Such conditions are absent in the Green Lake basin where the major river contributing glacial sediments is steep and the distribution of flow is highly skewed. Such conditions probably do not allow fine grained sediments originating from active glaciers to be stored in the channel for any appreciable amount of time. Similar lag effects between sediment production and ultimate deposition have been suggested for other high resolution sediment archives. Analysis of autocorrelation structure within the varved sediments of the Santa Barbara Basin (Soutar and Crill, 1977) revealed an apparent 7-year lag between precipitation maxima and sediment response. This lag was interpreted to reflect transitory storage of clastic sediment within the fluvial or near-shore shelf settings after flood event before final delivery to the core site. Similar short term (5-10year) memory effects appear to be common in varved sediments from Nicolay Lake, Nunavut (Dr. S. Lamoureux, Queens' University, pers. comm.), an environment where earth flows and detachment from exposed minerogenic surfaces during summer rainstorms are the principal source of clastic sediments for the lake basin. The lag in Nicolay catchment is believed to be caused by fluvial sediment storage effects. Much longer lags (20-30 years) were observed by Gilbert (1917) for near-shore sedimentation rates following export of sediment slugs introduced to the fluvial system following large scale mining.

In contrast to this study, Desloges (1999) noted a positive, lagged correlation between varve thickness at Moose Lake and variations in ring width from a nearby high elevation site in the Canadian Rockies. His results show Moose Lake varve thickness **leading** (25 yr) departures in ring width and interpreted the covariation (r=0.68) as resulting from similar climate forcing but that

trees experienced a longer response time associated with such change. It is somewhat difficult to envision such a slow response of the trees (*Pinus Albicaulis*) to climate variability and appreciably slower than sediment delivery (believed to originate primarily from glaciers) from a large (1640 km^2) watershed. The actual strength of the relation remains uncertain as the correlation was completed on filtered (and hence on highly autocorrelated time series) time series.

6.3.2.1 Sediment Residuals and their Relation to Glacial Extent

After explicitly controlling for air temperature, the time series of annual sedimentation to Green Lake reveals low-frequency trends which are likely controlled by other factors influencing sediment yield (figure 6.14). Changes in precipitation totals and/or the changes in the frequency or intensity of late-summer or autumn rainstorms may account for such trends, an evaluation of such effects must await more robust reconstructions of precipitation for the study area. Monitoring data from this study suggested that sediment yield is positively correlated with percent glacial cover, an observation made by others for lake-based sediment yield reconstructions in the Canadian Cordillera (Desloges and Gilbert, 1998). It is possible that those periods in which sedimentation rates can not be explained by changes in air temperature are taken to reflect conditions where glaciers were more extensive. The major period in which this occurs is centered between the late 1600's to the mid 1700's. As a first approximation, the record of cumulative departures between the air temperature and varve series (e.g. figure 6.14) is interpreted to provide an index of ice movement; the slope of the departures is positive with ice advance and negative with ice retreat.

The changes in sedimentation observed in Green Lake are largely consistent with terrestrial-based reconstructions of glacial fluctuations during the past 600 years in the Canadian Rockies (e.g. Luckman and Osborn, 1979; Osborn and Luckman, 1988; Smith et al., 1995) and the Coast Mountains (Mathews, 1951; Ryder and Thomson, 1986; Desloges and Ryder, 1990; Smith and Laroque, 1996; Smith and Desloges, 2000). In the Coast Mountains (using dendrochronologic and lichenometric methods) most evidence suggests that glaciers reached their maximum downvalley Holocene positions in the mid to late 1800's (Luckman and Villalba, 2002). In contrast, evidence from the Canadian Rockies indicates that most glaciers reached their maximum downvalley positions about a century earlier (Osborn and Luckman, 1988). Moving Glacier (Vancouver Island) overrode a forest around 1718AD and reached its maximum downvalley position sometime after 1818AD (Smith and Laroque, 1996). These two advances appear to be particularly well expressed in middle Coast Mountains where lichenometric and dendrochronologic ages are available for the two advances (ca. 1700AD and 1850AD) the former slightly more extensive than the later (Smith and Desloges, 2000). Using lichenometric dating, outermost terminal moraines of three glaciers (Borealis, Deer Lake and Fyles) near Bella Coola were deposited at ca. 1715, 1760 and 1760AD (Desloges, 1987; Smith and Desloges, 2000). Dendrochronologic data from Garibaldi Provincial Park indicates that 2 glaciers (Lava and Sphinx) reached their maximum downvalley positions at ca. 1725-1750AD while a third (Helm) was most extensive at ca. 1850AD.

Those periods in which the Green Lake sedimentation residuals are consistently positive are similar to the inferred dates for the period of major moraine construction within the Canadian Cordillera. In particular, the cumulative departures plots indicate that following 1600AD, sediment delivery in excess of that predicted by temperature begins in the mid 1600s and reaches its maximum values at about 1750AD (figure 6.14). A smaller sediment pulse which can not be attributed to air temperature occurs ca. 1850AD in the cumulative departures from the differenced SWBC-varve series but the amplitude of the signal is much less in the NH-varve data. If the magnitude and timing of these residuals are correct it suggest that glaciers within the Green Lake catchment probably reached their maximum downvalley positions sometime between 1725-1750AD. This estimate is

comparable to the most probable calibrated age range (1670-1800AD) associated with rapid over bank sedimentation in the Duffey Lake catchment discussed in the beginning of this chapter. The lacustrine evidence for the overbank sediments, however, is more tenuous as sedimentation in the central basin of Duffey lake is relatively low during this time. Varves deposited during 1670-1800AD are clear, least bioturbated and finer grained and is interpreted to reflect sediments which were deposited as inter/overflow events. Such sedimentological evidence may indicate a higher sediment delivery to the lake basin despite thinner couplet thickness. Such conclusions agree with the results of Chapter 5 and suggest that varve thickness in the central basin of Duffey Lake is a poor predictor of total sediment discharge to the lake.

To summarize, by using an independent proxy record of air temperature, inter-annual to inter-decadal changes in downvalley sedimentation related to climate could be controlled for and removed from long records of annual lake sedimentation. The residuals from such records can then be evaluated for structure which appears to provide insight into variations in ice cover. The removal of climate variability from the records is required to assess properly the true relation between glacial cover and sediment yield. For example, without the corrections, the above average departures in varve thickness during the mid 1500s would be taken to indicate that glaciers were possibly more extensive during this time. Reconstructed annual temperatures, however, indicate that the period was characterized by warmer than average conditions. Equally important, the coincident behavior of both proxy records provides independent verification for periods which are reconstructed to be warmer (cooler) than present.

6.4 Millennial-Scale Changes in Sediment Delivery

6.4.1 Bulk Physical Properties and Dating Control

Sediment yield proxies exceeding the contemporary varve records or where varve counting was uncertain (due either to intervals of bioturbated sediment and or event beds) were developed through analysis and construction of bulk-physical property time series from three of the six watersheds examined in this study. A short (1m) core was recovered from the distal basin of Birkenhead Lake and although the core was analyzed for changes in bulk physical properties, those data are not discussed in detail primarily because of the young basal date from the core (table 6.7).

Age control is provided by 22 AMS ^{14}C dates and two volcanic tephra recovered in the sediment cores (table 6.7). The tephra are believed to be Bridge River (2360 cal. yr BP) and Mazama (7710 cal. yr BP) air fall based on their stratigraphic consistency with the suite of AMS^{14}C ages. Petrographically, the samples are similar to published descriptions (e.g. Mathewes and Westgate, 1980; Reasoner and Healy, 1986; Souch, 1990). Details concerning sediment analysis and sampling strategy are summarized in chapter 3 and appendix C.

AMS ^{14}C Radiocarbon Ages

Lab ID	Field ID	Material Dated	**Duffey Watershed**	*AMS age* (yr BP)	Calendric Age *Range* ($\pm 2\sigma$)	Comments
TO-7312	98-Duf(E); 54cm	Conifer Needles	Lake	90 ± 100	1645-1958AD (1710)	(1711 AD –varve age)
TO-7313	98-Duf(E); 78cm	Conifer Needles	Lake	300 ± 60	1450-1675AD (1637)	(1587 AD –varve age)
TO-7041	98-Duf(E); 135cm	Conifer Needles	Lake	970 ± 50	990-1210AD (1029)	
TO-7585	98-Duf(E); 257cm	Conifer Needles	Lake	1240 ± 60	660-895AD (776)	
TO-7314	98-Duf(E); 318cm	Conifer Needles	Lake	2460 ± 70	800-390BC	Older than BRT at 538cm; slump ?
TO-7584	98-Duf(E); 410cm	Leaf (*Alnus*)	Lake	2190 ± 60	390-85BC (347, 321, 227, 223, 204)	
AA-33497	98-Duf(E); 585cm	Conifer Needles	Lake	2555 ± 65	828-411BC (787)	
TO-7583	98-Duf(E); 626cm	Conifer Needles	Lake	3020 ± 80	1436-1004BC (1289, 1281, 1262)	
TO-7042	98-Duf(E); 770cm	Conifer Needles	Lake	3390 ± 60	1878-1521BC (1687)	
AA-35515	E.fork Van Horlick	*Carex*. Stems	Soil (64cm)	180 ± 45	1645-1951AD (1673, 1777, 1800, 1942, 1946)	Buried O (Ob)
TO-7581	W.fork Van Horlick	Twig (charred)	Soil (58cm)	2230 ± 60	400-118BC (357, 286, 258, 243, 234)	Charcoal layer above 1mm thick ash layer
TO-7580	Cayoosh Terrace	Wood (conifer)	Fan Surface	9520 ± 70	9209-8628BC (9087, 9080, 8796)	50m above Cayoosh Floodplain (2m below fan surface)
			Birkenhead Watershed			
TO-7582	98-Birk(V); 92cm	Leaf (*Alnus*)	Lake	1070± 90	733-1162AD (984)	
			Joffre Watershed			
AA-33501	99-Jof(01); 120cm	Conifer Needles	Lake	2260±65	406-169BC (377, 266, 264)	
AA-33499	99-Jof(01); 200cm	Conifer Needles	Lake	3375±55	1864-1520BC (1684, 1666, 1664, 1645)	
AA-33500	99-Jof(01); 373cm	Conifer Needles	Lake	6700±100	5767-5475BC (5623)	
AA-33502	99-Jof(01); 469cm	Conifer Needles	Lake	8780±65	8201-7603BC (7937, 7932, 7915, 7901, 7870, 7861, 7828)	
AA-33502	99-Jof(01); 469cm	Duplicate	Duplicate	8705±70		
AA-33498	99-Jof(01); 496cm	Conifer Needle	Lake	8560±180	8202-7144BC (7584)	
AA-33503	99-Jof(01); 559-561cm	Conifer Needles	Lake	9380±160	9216-8268BC (8686, 8674, 8630)	
AA-35512	99-Jof(01); 1084-1097cm	Rootlets	Lake	9150±270	9214-7598BC (8292)	
			Green Watershed			
AA-38704	00-Grn(B); 241cm	Conifer Needles	Lake	1302±45	648-865AD (688)	(920AD –varve age)
AA-38705	00-Grn(B); 342cm	Conifer Needles	Lake	1864±50	5-317AD (130)	(365AD –varve age)
AA-38706	00-Grn(B); 619cm	Conifer Needles	Lake	3231± 45	1617-1411BC (1516)	(1090 BC estimated varve age)
AA-38707	00-Grn(B); 800cm	Conifer Needles	Lake	5035±50	3961-3703BC (3890, 3883, 3798)	
AA-38708	00-Grn(B); 962cm	Twig (sp.?)	Lake	7935±45	7056-6645BC (6977, 6973, 6891, 6885, 6819, 6785, 6774)	

Table 6.7: Radiocarbon Ages Used in This Study

6.4.2 Duffey Lake

Representative cores were collected from Duffey Lake to characterize downcore changes in physical characteristics of the lake sediments and to estimate sedimentation rates over long time scales. These cores were initially collected to construct a basin-wide varve chronology for the lake but as discussed, bioturbation and the presence of large, erosive event beds within the sediment cores precluded any reliable chronology exceeding 500 years in length. Acoustic profiling (3.5 kHz) of the lake basins in the summer of 1998 indicated the the sediment comprised both conformable and unconformable sediments which are at least 3-5m thick and distributed throughout the lake. Acoustic facies can not be determined below this depth, interpreted to be caused by wide-spread, coarse grained event beds (discussed below) or trapped methane and or CO_2. Unconformable sediments are primarily located in the deeper, central setting of the lake basin while conformable sediments are concentrated on the steeper side walls of the lake and over large (50-100m) sub-aqueous mounds located near the proximal, north side of the lake. Such features appear to be primarily located under contemporary snow avalanche paths. Despite the steep side walls, evidence of slumped sediments is largely absent.

Six long cores (3.5-8m) were recovered from the lake basin and transported to the laboratory. They were subsequently split, photographed, logged and bulk physical properties were analyzed in detail (5 cm sampling interval; 2.5 cm for LOI) for two long cores (97-Duf(09) and 98-Duf(E)) where disturbance by event beds was least severe.

The sediments from these cores vary between indistinct to distinctly-laminated, silty clays. The laminae are thin (1-3mm) sedimentary couplets with sedimentological characteristics similar to those of the surface (see Chapter 5). There is an association between the clarity of the couplets and the bulk physical properties of the sediment; couplets which are most distinctive are lighter colored, less organic and denser (figures 6.17 and 6.16). The correspondence between couplet thickness and clarity is more ambiguous as some of the most distinctive, least bioturbated couplets are thin (1mm). Such laminae are considerably finer-grained in thin section than thicker couplets.

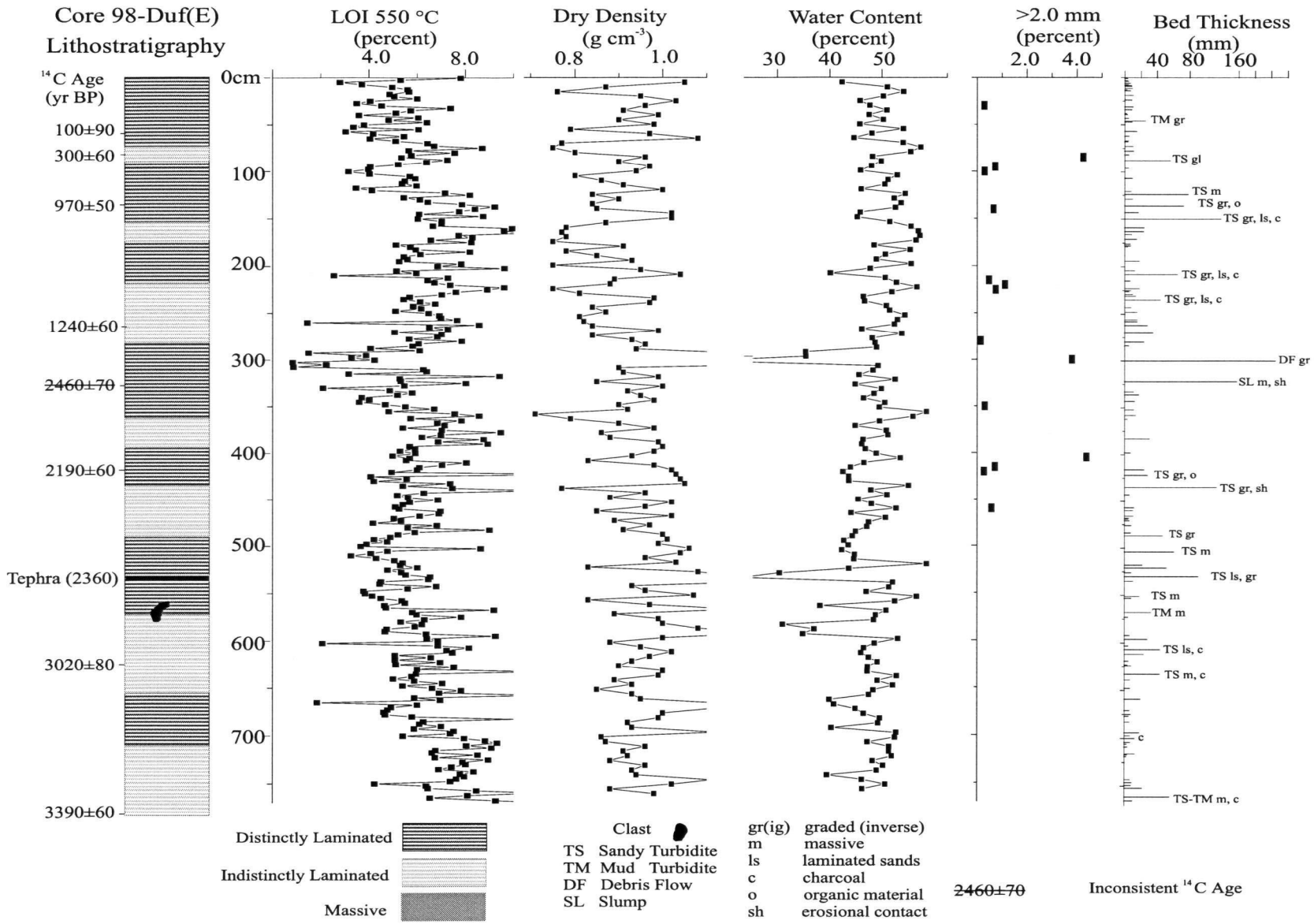

Figure 6.16: Lithostratigraphy and Bulk Physical Properties of Core 98-Duf(E)

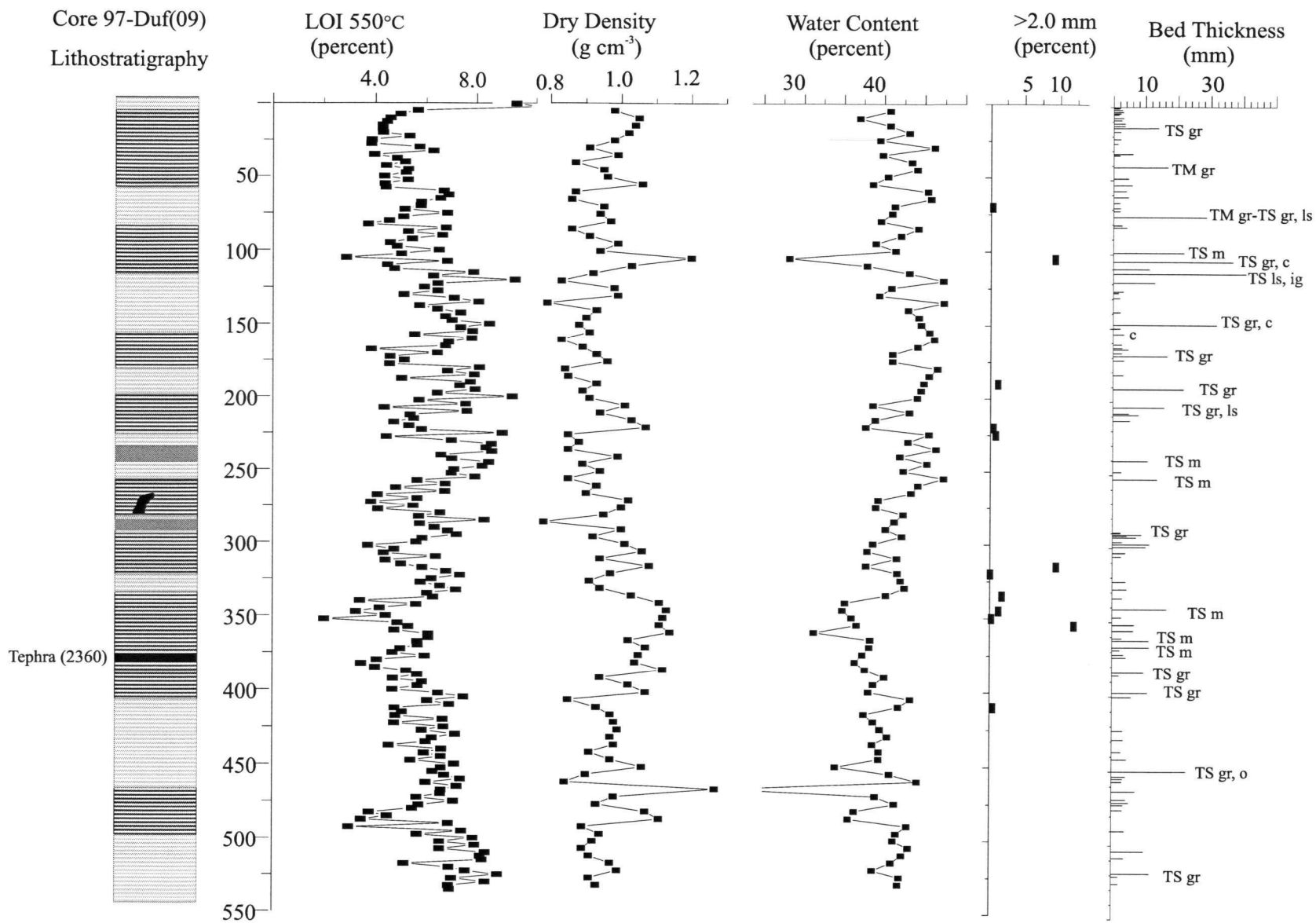

Figure 6.17: Lithostratigraphy and Bulk Physical Properties of Core 97-Duf(09)

Coarser grained, graded beds are common within the sediment archives (table 6.8) and their distribution and thickness with depth appears to be random (figures 6.17, and 6.16). Organic content ranges between 3 to 12 percent (LOI); the minimal values often coinciding with the presence of normally graded event beds (c.f. figures 6.17,6.16). These event beds can often be traced throughout the deepest reaches of the lake basin. Grading structure and bed thickness decline away from the north and proximal side of the lake basin. Cumulative thickness of the event beds (12 %) is considerably less in core 97-Duf(09) which was recovered from shallower (75 m) water environments and considerable (1km) distance from the north side of the lake basin (table 6.8). The presence of the beds significantly influence average sedimentation rates for the deeper cores where 23 percent of core 98-Duf(E) is comprised of event beds and this fraction increases slightly for cores 98-Duf(B) and 97-Duf(07). Distinctly-laminated portions of the cores are lighter-colored, clayey-silts to sandy-silts which are denser and more inorganic than indistinctly-laminated sediments. Angular, clastic material (> 2mm) is often found within portions of the cores which are distinctly laminated. On average, distinctly-laminated sediments and coarser grained event beds have a higher magnetic susceptibility (normalized for mass) than indistinctly laminated portions of the sediment cores.

Many of the event beds recovered in the sediment cores exceed 10 cm in cores recovered from the deepest portion of the lake basin (table 6.8). Small gravel (4-8mm) comprises several of the thicker, graded beds from those cores taken closest to the north side of the lake (table 6.8).

			97-(07)		98-(E)		97-(09)		98-B		Comments
event #	deposit type	Direction	Depth (cm)	Thickness (cm)	Depth	Thickness	Depth	Thickness	Depth	Thickness	
1	Turbidite	?	NA	NA	8.5	5	11	5	3.5	6	Deposit has erosive base in 98-Duf(B)
2	Turbidite	?	16.5	22.5	12	12	13.5	17.5	8.5	5.5	
3	Turbidite	?	19	8	13.5	6.5	17	3	10.5	6	
4	Debris Flow	w. of E	27.5	30	23.5	8.5	24.5	2.5	19	7.5	sandy, pebbles in 07
5	Debris Flow	w. of E	34	20	29	10	28.5	5	23	11.5	sandy, pebbles in 07
6	Turbidite	?	52.5	27.5	43.5	28	39.5	15.5	36.5	11.5	~1740AD
7	Turbidite	east of E	68	14	56.5	14	47.5	7	46	34	Coarsest in core B
8	Turbidite	?	73	8.5	61	4.5	51.5	6	53	4	
9	Turbidite	w. of e	81.5	17	67	4	56.25	1.5	57.5	1.5	grades from v. coarse sand to thin unit w to e
10	Turbdite	?	82.5	6	68.5	4.5	56.5	4.5	58.5	4	flood ?? constant thickness '
11	Turbidite	w of E	88	5	75	9.5	63.5	0.5	63.5	5	
12	Turb-Avalanche	e. of E	90.5	16.5	77	12	66.5	4.5	65	40.5	Terrestrial macros in B
13	Debris Flow	w. of E	105	195	85	52	72.5	37	75.5	37.5	Internally Laminated
14	Turbidite	w. of E	145.5	39	122	43.5	97	19	103.5	35	
15	Debris Flow	w. of E	153	19	129	8	101	2.5	110	7	Coarse sands in core 07
16	Debris Flow	e. of E	155.5	50	133	63.5	102.5	34.5	114	210	15 cm of Gravel in core B
17	Debris Flow	w. of E	164	36.5	141.5	14	109	11	140	19.5	Coarsest (vc. Sands) in 07
18	Debris Flow	w. of E	167	201	144	208	111.5	61	142	49	Gravel base in 07
19	Turbidite	?	198.5	4.5	170	12	125	4	160.5	7	Non graded
20	Turbidite	?	216	7			133	2			Non graded
21	Avalanche	e of E	223	41	204	61	146	36	188	81	Grades from B , charcoal in 09, E
22	Avalanche	?	End of	Core	231.5	56	168	19	215	32	Charcoal in 09, E
23	Debris Flow	?			267	40	190.5	27	246	39	
24	Debris Flow	?			289	172			265.5	17	Gravel in base of deposit in E, at core break in core 09
25	Slump	?			314.5	123	203	28	274.5	70.5	Slump – inconsistent 14C age
26	Avalanche	?								197	Grades from core B 5x10 cm (sheared) conifer wood (B) massive to very indistincly laminated seds above bed
27	Turb-Avalanche	e. of E			428.5	110	298.5	34.5	394.5	84	Grades from B (grain size and thickness)
28	Avalanche	e. of E			485	44	340	22	428	36	Grades from B (grain size and thickness)
29	Avalanche	e. of E			500	53.5	349.5	10	428.5	39	Grades from B (grain size and thickness)
30	Avalanch	e. of E			527	32	361	37	438.5	42	Grades from B (grain size and thickness)
	Tephra				538	11.5	376.5	10	466	10.5	Bridge River Tephra (ca. 2360 cal. yr BP)
	Percent Event	Beds		**34**		**23**		**12**		**25**	

Table 6.8: Bedded Sediment Characteristics, Duffey Lake

These event deposits thin laterally and in more distal cores, correlative events begin as coarse sands capped with a poorly sorted, clayey-silt to silty sediment. The unit is often enriched with abundant terrestrial macrofossils such as leaves, twigs and conifer needles. Laminae overlying and underlying these units are often convoluted and laminae are often disturbed by gas or water escape structures.

An age of 3390 60 yr BP was obtained from terrestrial macrofossils within laminated sediments from basal sediments in core 98-Duf(E). Supplemental dating control is provided by 7 additional radiocarbon ages determined throughout the core (table 6.7) and a thin (2-4mm) layer of white, coarse-grained tephra. The tephra is believed to represent air fall from the Bridge River (BRT)for the following reasons: a) Duffey Lake is within the reported ash plume of the Mount Meager eruption (Mathewes and Westgate, 1980; Clague et al., 1995); b) the recovered tephra is similar in textural and petrographic properties to published descriptions of Bridge River Tephra recovered in lake sediments and c) the assumed BRT age is consistent with the depth age curve calculated with the ^{14}C ages only. One radiocarbon date (TO-7314) obtained from conifer needles collected from an event bed appears to be anomalously old as its stratigraphic position makes it older than the tephra believed to be BRT and its depth-age relation is inconsistent with the other ^{14}C ages for the core (figure 6.16, table 6.7). A reanalysis of the sedimentology of the bed from which the macrofossils were collected for the date, indicates that the material comprising the bed is likely from a slump; the sediments are poorly graded, organic rich and somewhat oxidized in color.

6.4.2.1 Interpretation

Two principal deposition regimes characterize the recovered sediments from Duffey Lake. The first and most common is the annual or low frequency component of sedimentation and reflects those processes (e.g. underflow and interflow-overflow events) controlling laminae formation discussed in Chapter 5. Consequently, the laminae are interpreted to be clastic varves based on those arguments presented in Chapter 5 and independent dating (AMS ^{14}C). The clarity (and commonly but not always thickness) of varves appears to alternate over depth scales of 5-20 cm or over period of 20-80years. These intervals are interpreted to reflect periods when inorganic, finer-grained sediments were entering the lake basin predominantly as interflow and overflow events. Based on the contemporary monitoring, such conditions are commonly encountered during periods of sustained glacial melt. Although a detailed analysis of particle size would help to support such an interpretation, the presence of inter-calated turbidites within the sequence makes such an analysis difficult. In short, the distinctly laminated portions of the sediment cores are interpreted to reflect sediments originating from glacial sediment sources but given the undocumented history of the glaciers within the catchment, the exact relation between glacial dynamics and sediment delivery to the lake basin remains poorly understood (e.g. Leonard, 1997).

The second sedimentological regime recognized in the cores occurs infrequently and is characterized by episodic sedimentation events which are short lived. These events most likely originate from a combination of hillslope instability or surge-generated turbidity currents caused during high river inflow events, slumping of sediments on over-steepened sidewall locations or through hillslope instability adjacent to the lake basin. The thicker (>25mm) graded beds (with sandy to gravel bases) are believed to originate from snow avalanching and hillslope instability concentrated on the north side of the lake. Snow avalanche paths are common features on both sides of the lake basin though the source areas on the north side are larger. During numerous visits to the study site during winter, avalanched snow was observed on top of the lake ice though the deposits contained very little clastic and vegetative debris. Eyewitness accounts by BC Highways personnel indicate that on at least one occasion a large snow avalanche on the north side of the lake basin had fractured

over a third of the lake ice cover radiating out from a large snow avalanche path on the north side of the lake. Here numerous curvilinear, cuspate, and parabolic-shaped landforms can be found in both sub-areal and sub-aqueous environments and are interpreted as avalanche plunge pools (e.g. Corner, 1980; Fitzharris and Owens, 1984). However, because snow avalanches and debris flows often initiate from similar source areas (e.g. Luckman, 1992; Blikra and Selvik, 1998), it is probable that the graded units recovered within the cores represent a mixture of both snow avalanching and debris-flow activity. The presence of charcoal within many of the beds deposited between 1500-1000 cal. yr BP suggests that forest fire activity may have been an important control in influencing the delivery of hillslope-derived sediments to the central basin. The presence of isolated clasts within distinctly laminated sediments most likely represent dropstones (Luckman, 1975) resulting from low-intensity snow avalanching onto the lake ice or directly into the lake. The presence of dropstones and graded event beds is common in lacustrine environments which are directly coupled to active hillslopes (e.g. Desloges and Gilbert, 1994b; Dirszowsky and Desloges, 1997).

Morphometric controls may play a part in influencing the magnitude of snow avalanches on the north side of the lake. Here the slope profile is moderately steep (35-45°) with a slight increase of slope at the footslope. The slightly over steepened gradient of the footslope does not allow the inertia of avalanched snow to decrease before it impacts the ice cover or water surface (c.f. Corner, 1980; Fitzharris and Owens, 1984). The impact forces produced by the snow could eject or initiate failure of clastic and organic material accumulated below such slopes ultimately causing failure of sub-aqueous slopes and generation of surge-generated turbidity currents. This type of instability likely accounts for some, but certainly not all of the recognized turbidites in the sequence as coarse grained turbidites may also form in the absence of unstable hillslopes and are especially prevalent near high energy inflows in lacustrine environments (Desloges and Gilbert, 1994b; Lambert and Hs, 1976). However, given the considerable distance (2-3 km) from main inflows to the lake, the gentle slope gradients of the lakes' thalweg ($< 1°$), and the presence of coarse sands to gravel sized clastic matter within the thickest of the beds, it is likely that such thicker, coarser grained beds have a more proximal origin. The presence of much unsorted organic detritus within many of the units also indicates that there was little opportunity for hydraulic sorting suggestive of local sediment sources.

6.4.3 Green Lake

Four sediment cores (2 percussion, 2 vibracore) were recovered from Green Lake to construct indices of sediment delivery to the lake basin. Based on the unique bathymetry of the lake and prior analysis of the Duffey Lake sediment archive, coring sites were chosen in shallow (12-15m) water environments to minimize the difficulties introduced by turbidites. Although the coring site is proximal to the delta, it appears to receive the majority of sediments from inflow and overflow events rather than bottom-hugging currents. Such morphometry will help to minimize changes in sedimentation caused by deltaic instability and channel avulsions (e.g. Lamoureux, 1999b). Preliminary acoustic surveys of the lake (not shown) suggest that the total postglacial fill of the lake basin is between 12-15m. Acoustic facies within the Holocene sediments can be traced throughout the lake basin except in the deepest basins, where it is interpreted that coarser-grained sediments, in addition to decomposing terrestrial organic material, attenuate the return signal.

Severe disturbance within one of the cores (99-Grn(03)) prevented meaningful laminae thickness measurements to be made on this core. This disturbance is comprised of severe coning or downwarping of laminae likely the result of high clay content (70-80 percent), the use of a core catcher, and small diameter (7.62cm) core barrel. The core was, however, sampled for bulk physical properties near the center of the core with a $1cm^3$ syringe. Bulk physical property trends are nearly

identical to those trends measured for 2 vibracores [00-Grn(A,B)] taken 50m apart. A continuous record (11.7m) of post-glacial (Pleistocene) sedimentation appears to have been recovered in Core 00-Grn(B) but based on the stratigraphy of the core any significant post-glacial (paraglacial) phase was not recovered. Over-penetration caused the loss of the uppermost 20cm of sediments from 00-Grn(A) so a continuous record of bulk physical properties was constructed by combining measurements taken from portions of both vibracores. Bulk physical properties were measured in the uppermost 10m of 00-Grn(B) and combined with measurements from the lower most 2m of core 00-Grn(A). The cores were oversampled (20cm above and below) a thick (2cm) graded bed which was used as tie point and the overlapping trends in both cores were identical.

Recovered sediments from the core site are predominantly laminated silty-clay to clayey-silts and, with exception of the basal sediments, the sediments are non sandy ($< 1\%$ by weight). The lowermost 10cm of sediments from core 00-GRN(A) are sandy silts (> 5 percent sand content) and contain isolated clasts (figure 6.18). These sediments are overlain by 1m of thick, inorganic laminae which are strongly bi-modal and show a complete absence of bioturbation. Laminae are bundled as sedimentary couplets and the thickness of the clay unit is proportional to the lower-most silty unit. Initially, the couplets are thick (> 1cm) but decline non-linearly to an average thickness of 5mm (figure 6.19). Despite attempts to date the basal sediments of the core, insufficient organic material could be found even with the small mass requirement of AMS ^{14}C dating.

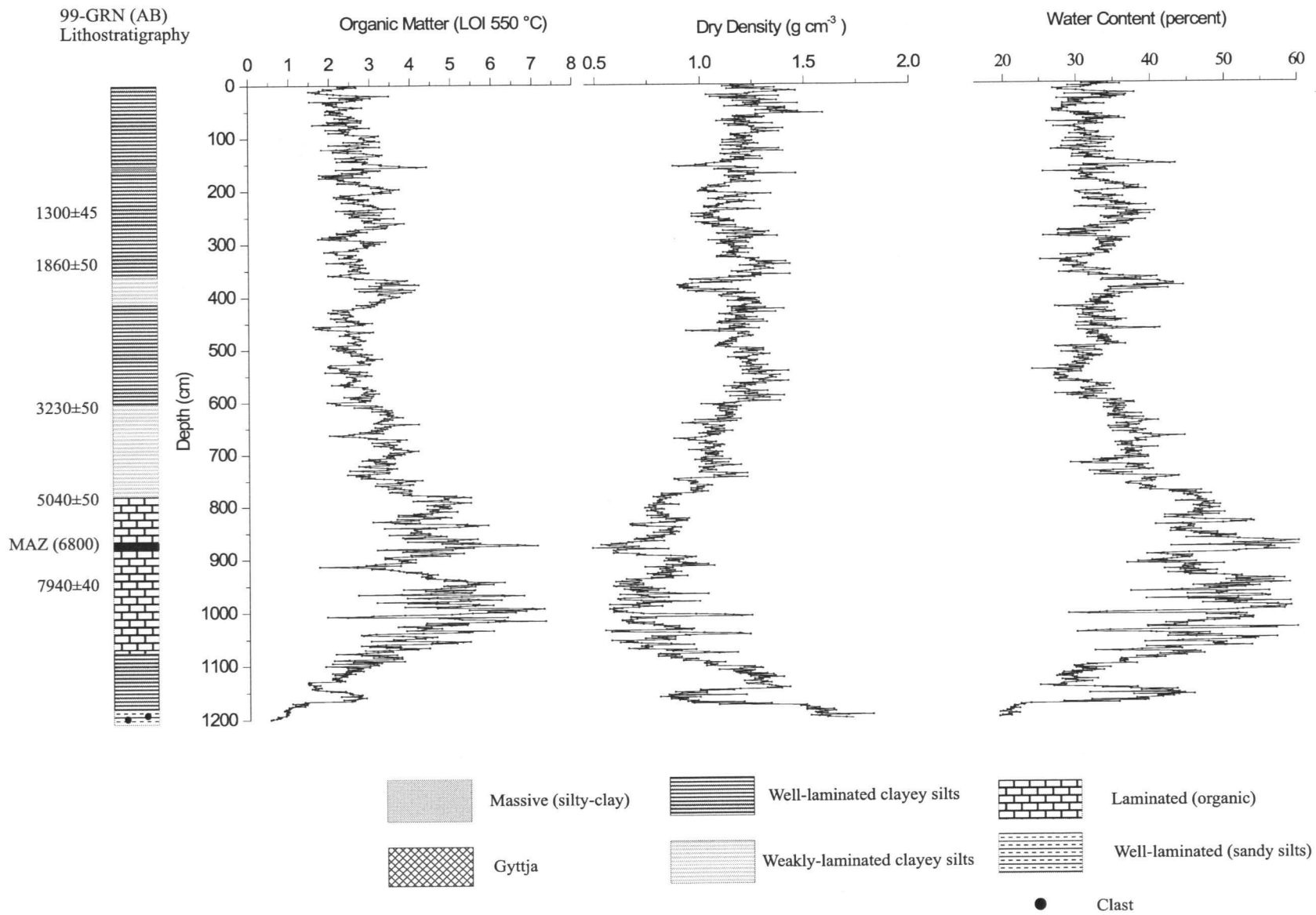

Figure 6.18: Lithostratigraphy and Bulk Physical Properties of Cores 00-Grn(AB)

A transition to laminated, silty-clay organic sediments (up to 8 percent LOI) occurs at 10.7m and the organic sediments continue to 8m. Macrofossils recovered near this contact (table 6.7) provide an age estimate (5040 50 ^{14}C yr PB) for this uppermost contact. Additional chronologic control (table 6.7) is afforded by an AMS ^{14}C age of 7940 50 ^{14}C yr PB from a small twig at 9.6m and from Mazama tephra (8.9m). Laminations are irregular where inorganic, clastic sediments are inter bedded with wavy organic bands. Localized white blobs of sediment can be found within the most organic rich sediments which turn to light blue when oxidized.In several regions between 10.7 to 8m, the sediments become inorganic, and lighter colored. The most evident of these intervals is centered around 9m, some 10cm below Mazama tephra (figure 6.18).

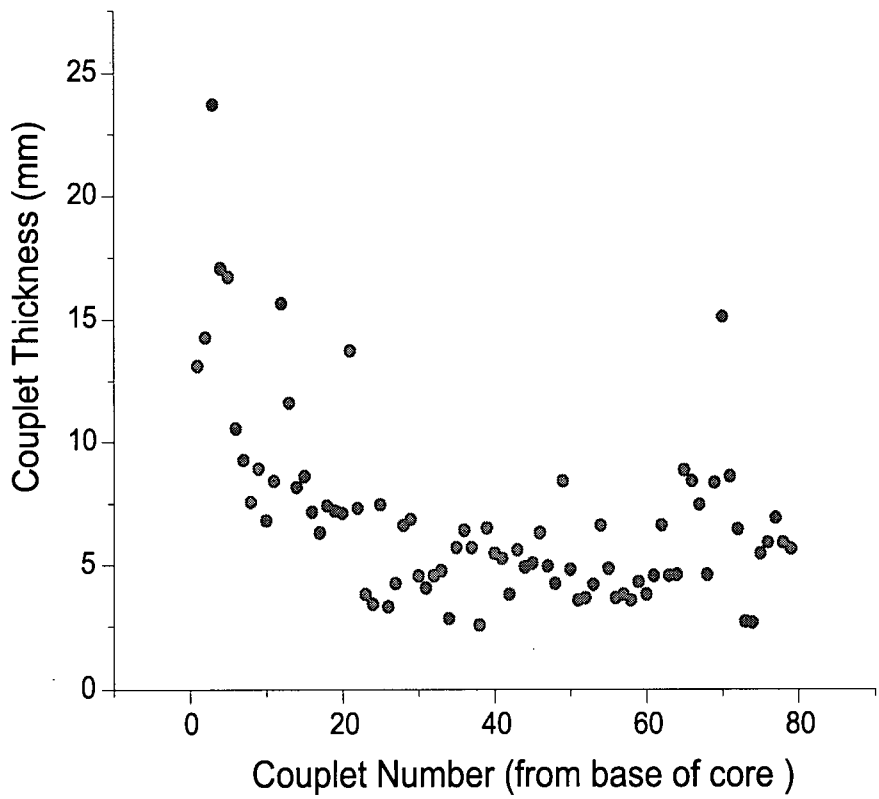

Figure 6.19: Couplet Thickness, Green Lake Core (00-Grn(A))

Above 800 cm, the sediments are inorganic silty-clay. Bimodality of the laminae increases up-core and the sediments become distinctively laminated above 600cm. Terrestrial macrofossils from this contact provide an age of 3230 50 ^{14}C yr PB for the onset of contemporary sedimentary environments for the lake basin. Laminae preservation and bi-modality of these uppermost sediments covaries with the bulk physical properties of the sediments; laminae within those sediments which are denser and less organic rich are clearest and show the least evidence of infauna growth. Two radiocarbon ages (1860 50 ^{14}C yr PB ; 1300 44 ^{14}C yr PB) help to constrain sedimentation rates and timing of events for these uppermost sediments (table 6.7). The sediments become very diffusely laminated to massive in three minor (3-10cm) intervals centered at ~150cm, 250cm and 140 cm where evidence for infauna growth is prevalent.

6.4.3.1 Interpretation

The recovered sediments from Green Lake record dynamic and time-transgressive changes in sediment availability which partly control the type and regularity of laminae during the Holocene. The lowermost sediments are interpreted to reflect a sedimentary environment where sediment supply is largely unlimited and controlled primarily by the intensity and duration of inflow to the lake basin. The coarse-grained nature of the lowermost 10cm of sediments probably reflects the last sequence of sediments from a high-energy environment characteristic of recently de-glaciated terrain (e.g. Wolfe and Teller, 1993; Gilbert, 1997). The lowermost couplets are believed to reflect high-sediment supply conditions but based on the proportionate thickness of the silt and clay unit within a couplet, formation occurred primarily by overflow and interflow events (Smith and Ashley, 1985). The thickness of the couplets indicates that sediment delivery to the lake basin was high though it appears to have stabilized to a constant rate of delivery rather quickly (figure 6.19).

The early Holocene sediments of Green Lake appear to reflect significantly reduced clastic delivery and moderate lake productivity. The light blue specks and blobs are likely vivianite, a phosphoric element which is commonly formed from diagenesis of phosphorus-rich organic matter under reducing conditions. The major clastic interval centered at 9m is interpreted to reflect a temporary return to an environment where clastic sediment availability was high. Through time, the proportion of clastics within the sediments increases following 9.0m, though in reality, the transition to modern flux rates occurs at abrupt transition points such as at 8.0m and 6.0m, (see dry density trend in figure 6.18). By 6.0m the sediments have become finely laminated and consist of sedimentary couplets interpreted to be clastic varves. They appear to define "modern" environmental conditions at the site; an ample supply of clastic sediments is delivered to the lake basin each year.

6.4.4 Joffre Lake

A single 11m vibracore was recovered from lowermost Joffre Lake (figure 6.20). The core appears to be comprised of two dominant facies; the lowermost recording sedimentation in a high energy environment, while the second reflects sedimentation in a sheltered lake environment with increasing proportions of clastic sediments reaching the lake basin through the Holocene. The lowermost 10cm of recovered sediments consist of gravel (figure 6.20). Rootlets (species unknown) were sieved from a 15cm thick sequence of sediment and provided an age of 9150 270 ^{14}C yr PB for the sediments approximately 20-30 cm above the base of the core (table 6.7). Over 6m of inorganic laminated clayey-silts with moderate (> 10 percent) percentages of fine sand overlie the basal gravels in the core (figure 6.20). Many individual laminae exceed 10cm in thickness and they appear to be roughly organized as sedimentary couplets consisting of a lowermost, coarser grained unit which is abruptly overlain by a thinner finer grained (fine silt to clay) unit. This upper unit is commonly graded and occasionally thin (1mm) coarser grained units can be found within it. Contacts between the couplets are often poorly defined and erosional contacts are common. The poor distinction between contacts and convoluted structure (coring-induced disturbance ?) prevents any systematic attempt at measuring variations in thickness though there is an apparent declining trend in thickness upcore. An abrupt change in sediment type occurs near 600cm depth where organic rich sediments (gyttja) overlie the lower, inorganic couplets (figure 6.20). Poorly preserved, conifer needles provide an age estimate (9380 160 ^{14}C yr) PB for the transition to organic sedimentation in the lake basin. The two lowermost radiocarbon ages from the core overlap at 1σ, and can therefore be considered to be statistically equivalent ages suggesting high (ca. 1-2 $cmyr^{-1}$) sedimentation rates for the laminated sediments.

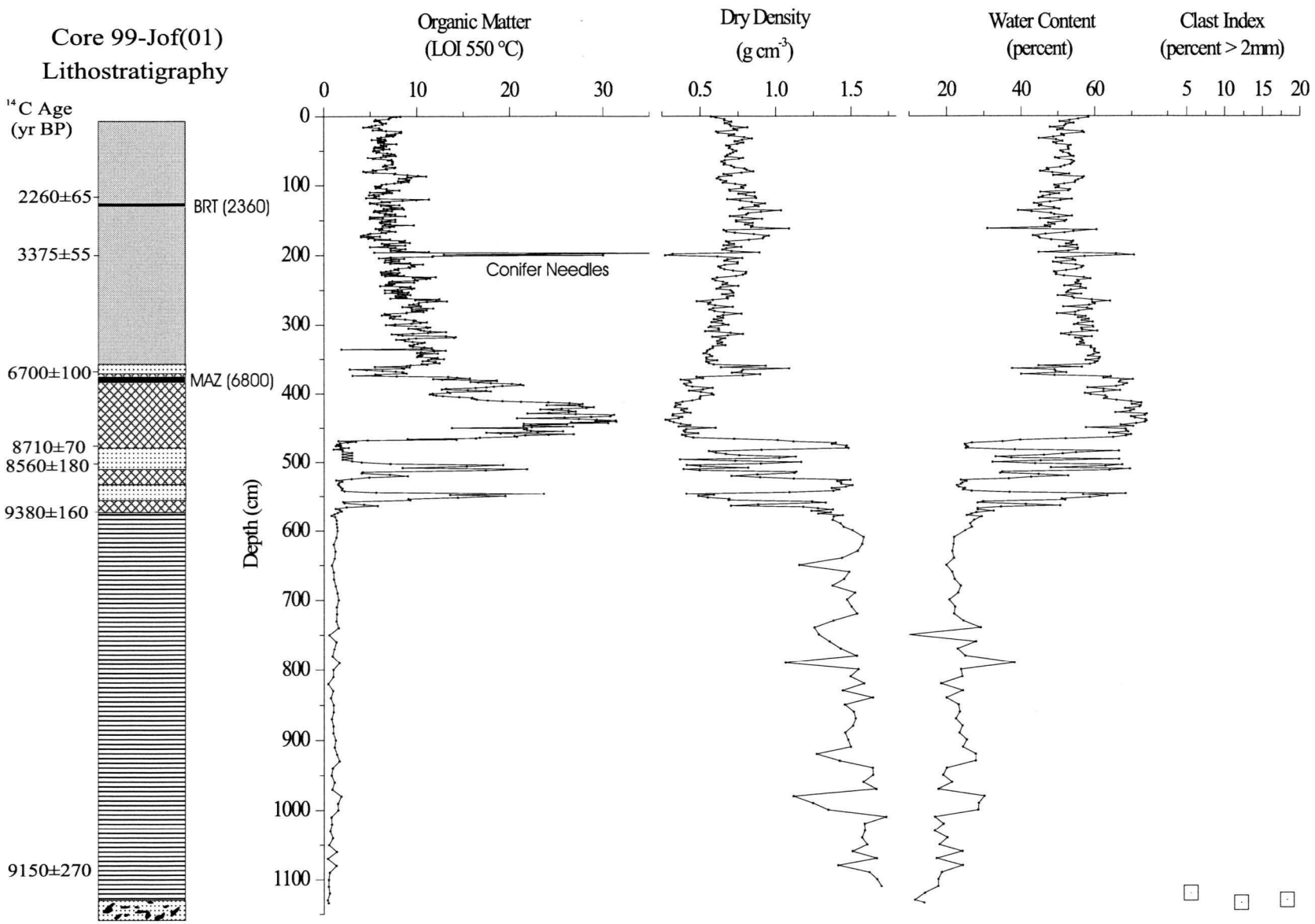

Figure 6.20: Lithostratigraphy and Bulk Physical Properties of Core 99-Jof(01)

Organic sedimentation is interrupted by two clastic intervals between 450 and 550 cm (figure 6.20). Bulk physical properties of the sediments return to pre-organic conditions and the timing associated with the two clastic events is bracketed by 2 AMS ^{14}C dates (8710 70 ^{14}C yr PB and 9380 160 ^{14}C yr PB). The uppermost clastic interval (490cm) consists of coarse-grained (sandy silts) sediments interbedded with layers of conifer needles. Following 8710 70 ^{14}C yr P, the sediments consist of dark gyttja with organic content close to 30 percent (LOI). Above 450 cm, the bulk physical properties of the core appear to reflect a non-linear increase in the proportions of clastic material comprising the sediments. Superimposed on the trend is a higher frequency (ca.. 10cm) component of clastic variability which reflects both an increased and decreased clastic component to the sediment record (figure 6.20). Two of the most significant, short-term departures occurred immediately before and following the deposition of a 1cm thick tephra interpreted to be air fall from Mt. Mazama. Following the deposition of Mazama ash, the sediments from lower Joffre Lake become more mineral rich with background clastic fluxes established by approximately 3500 14C yr BP (figure 6.20). Century-scale variations in clastic delivery to the core site are superimposed on this non-linear trend and the sediments become notably more clastic rich at ca. 5500, 3100, 2300, 1500, 700 and 300 cal. yr BP (figure 6.20).

6.4.4.1 Interpretation

The sedimentary environment of lowermost Joffre Lake appears to record a continuous record of sediment flux from the basin through the entire Holocene Epoch. The record is comprised of unique sedimentary facies which appear to record how sediment export from the watersheds has responded to changes in ice cover over century to millennial time scale. These facies are interpreted to reflect ice proximal, unstable to minimal ice cover, and ice growth to modern environmental conditions.

Facies1 Ice Proximal and or ice wastage: The physical properties and characteristics of the couplets deposited between 6 and 11m are similar to descriptions of clastic varves deposited in high energy, glacial environments (e.g. Smith and Ashley, 1985; Wolfe and Teller, 1993; Gilbert, 1997). The stratigraphic inconsistency of the two lowermost radiocarbon ages would be problematic if the inferred sedimentation rates for the lowermost 6m of sediments were low. However, many of the individual couplets are thicker than 10cm and indicate very high sedimentation rates. The rhythmites are interpreted to record ice proximal conditions within the catchment following retreat and/or wastage of Pleistocene ice. The minimum radiocarbon age from the core (9380 160 ^{14}C yr PB) is consistent with age (9520 70 ^{14}C yr PB) inferred for deglaciation of the nearby Duffey Lake Catchment (table 6.7 and discussion in Chapter 3). Both agree with estimated deglaciation ages (9500-10100 ^{14}C yr BP; n=7) of sites close to contemporary glaciers in the Canadian Cordillera summarized elsewhere (Osborn and Luckman, 1988) but are considerably younger than the estimated age of deglaciation (12 255 $\pm$770 ^{14}C yr BP) for the Kwoiek watershed located 100km to the southeast of the study area (Souch, 1994). The large uncertainty of the radiocarbon age from Kwoiek, however, overlaps those of this study at 2 σ so it remains unknown whether these differences are real (e.g. early meltout at edge of Coast Mountain Ice Cap) or reflect dating uncertainty.

Facies2-3 Unstable and Minimal Ice Growth: Organic rich sediment (gyttja) was deposited during the early Holocene (9300-6800 ^{14}C yr BP) with three periods of elevated fluxes of minerogenic matter to the lake basin (figure 6.20). In general, however, the sediments deposited during the early Holocene appear to reflect within-lake productivity. Lake productivity was facilitated by warmer water temperatures and reduced turbidity. High

rates of productivity are inferred because sedimentation rates during this time are comparable to those observed during the late Holocene when a greater percentage of clastic sediments reached the lake basin. Three notable intervals of clastic sedimentation are interpreted to reflect ice re-growth or climatic conditions favoring production and or entrainment of clastic sediments. Two of the larger events occur ca. 8700 ^{14}C yr BP while the third is bracketed by Mazama tephra (6800 ^{14}C yr BP) and a ^{14}C age of 8700 ^{14}C yr BP (figure 6.20).

Facies4-5 Ice Growth and Modern Conditions: Following the deposition of Mazama ash, the clastic component of the lake sediment increases moderately until ca. 3500 cal. yr BP when modern sedimentation rates and bulk physical property characteristics are established (figure 6.20). Such time-transgressive changes appear to be common in clastic sedimentary archives from the region (e.g. Souch, 1989, 1994) and from other mountain environments of the Canadian Cordillera (e.g. Leonard, 1986a; Reasoner and Hickman, 1989; Reasoner et al., 1994; Leonard and Reasoner, 1999). The century scale variability is interpreted to reflect episodes of enhanced (reduced) sediment delivery to the lake basin as the result of ice growth and demise within the catchment. Similar to Duffey Lake, the clastic content of the sediments is slightly higher between 2360-3375 ^{14}C yr BP than during the last 500 years of the record. Similar alternating sequences of inorganic/organic sediment facies were recognized in glaciolacustrine sediments to the east of the study area (Dirszowsky and Desloges, 1997). In that study, however, such sequences of enhanced sedimentation (more clastic rich, laminated sediments) occurred over shorter (decadal) time scales and were interpreted to reflect periods favorable for ice melt.

6.4.5 Depth-Age Sedimentation Models

Millennial-scale changes in lake sedimentation are assessed primarily through the analysis of changes in bulk physical properties of the lake sediments from Green, Joffre and Duffey Lake basins. In order to evaluate temporal correspondence between the records and to assess the proportion of variance which can be explained by climatic variability, depth-age models of lake sedimentation were developed for representative lake cores. Over these time scales chronologic control is provided by radiocarbon ages and by tephrochronology. An evaluation of the covariance between the clastic and the ice core records requires conversion of tephra and radiocarbon ages to calendric ages to develop a suitable depth-age model for the core in question. Though the conversion to calendric age is facilitated by the well known relation between ^{14}C activity and calendar age for tree ring samples (e.g. Stuiver and Reimer, 1993), variations in ^{14}C production within the atmosphere create non-unique calendric ages for the number of ^{14}C atoms for a given sample. The calendric age after conversion from the ^{14}C scale reflects both the uncertainty in the radiocarbon determination as well as the presence of significant "plateaus" in ^{14}C production and hence the "true" calendric age is unknown but can only be expressed in probabilistic form[4]. These age distributions are usually non-normal and do not allow confidence limits calculated using normal parametric methods. Fitting an appropriate depth-age model introduces additional uncertainty into estimating the calendar age for sediments at a given depth and does not allow correspondence to be assessed statistically between lake sediment cores or to climate-proxy records. In sum, the total error (ε_t) in an age estimate for

[4]A "single" calendric age for a given ^{14}C date can be obtained from calibration curves (i.e. where it intersects the calibration curve) but such a method only allows an error range to be put on the date rather than expressing the uncertainty as a continuous function

a given sediment depth is:

$$\varepsilon_t = \varepsilon_{14C(counting\ error)} + \varepsilon_{14C(calibration\ curve)} + \varepsilon_{(depth-agemodel)} \tag{6.3}$$

A non-parametric approach incorporating Monte Carlo (MC) sampling was used to estimate confidence limits for a given depth-age model for a given lake sediment core. MC approaches are particularly useful for estimating uncertainty in situations where the underlying error model is poorly known or the data are non-normally distributed (e.g. Press et al., 1986; Davison and Hinkley, 1997). Modeling the total uncertainty associated with a given depth-age model consisted of the following steps:

1) Calendric age ranges were determined for a given radiocarbon sample by using the counting errors (2 σ) of the ^{14}C sample and determining the maximum range that a ^{14}C age occurs for a given calendric age. Such methods were also employed on the two volcanic tephras (Bridge River, and Mazama) recovered in the sediment cores and incorporating ^{14}C age and 2σ ranges for the eruptions reported in the literature (e.g. Clague et al., 1995; Hallett et al., 1997);

2) calendric probability distributions (n=10,000) were generated over this range for a given radiocarbon sample and the process was repeated to construct calendric-age distributions for each radiocarbon sample for a given sediment core;

3) the distributions were then randomly sampled (n=1000) with replacement, and combined with the depth data;

4) an appropriate depth-age model (1 to 9th order polynomial) was determined for the surrogate bi-variate data using linear least squares regression and the model which gave the best fit (the smallest χ^2 statistic for a given polynomial model) was used as the surrogate model;

5) the model was used to generate age as a function of depth for the surrogate data and steps 3-5 were repeated to generate an ensemble (n=1000) of ages for a given depth;

6) the age data for a given depth were sorted and from this, the estimated age (median) and 68 and 95 percent confidence limits could be determined for a given depth-age model. The MC method allows average and maximum uncertainty to be placed on depth sedimentation models and more importantly, it allows an evaluation of probable error as a function of depth. Such error functions are useful when testing the statistical correspondence between bulk physical property trends between basins and to climate-proxy records derived from ice core records. It should be highlighted that the MC approach as developed in this context provides no indication of an important fourth source of error, ($\varepsilon_{absolute}$), namely the difference between true age of the sediments and that age estimated by radiometric methods. Such error could arise by obtaining radiocarbon ages from bulk sediments (old carbon effects) and such effects were minimized by only dating small, fragile terrestrial macrofossils such as conifer needles. Independent sediment age evaluation provided by varve counting (Green and Duffey) and through tephrochronology (Mazama tephra in Joffre) indicates that, on average, this source of error is not great ($\approx$100 years).

6.4.5.1 Results

Depth-age models developed for the three lake basins with associated error ranges indicate that uncertainty in sediment age for a particular depth within the sediment archives varies through time and for individual lake basins (figure 6.21). Sedimentation rates for Duffey and Joffre Lakes appear quasi-linear over the range of data while sedimentation rates appear to change considerably for Green Lake basin. A likely reason for the linear behavior for the Duffey Lake depth-age model is that the long-term trend in clastic sediment delivery to the lake basin has remained fairly constant throughout the last 3700 cal. yr BP which is not surprising as it is generally believed that modern climatic conditions within the Southern Coast Mountains were established by this time

(e.g. Hebda, 1995). Depth-age models for Green and Joffre Lakes over the last 9000 years differ in their shape with approximate linear sedimentation rates for lower Joffre Lake over the Holocene while sedimentation rates in Green Lake increased non-linearly until ca. 3500 cal. yr BP (figure 6.21). The linear nature of the depth-age model for Joffre lake is surprising considering that glacial sediments represent the major contemporary source of clastic sediments to the lake basin and at first evaluation may suggest that glacial cover during the early Holocene was as extensive as during modern (ca. 3500-present) times.

Heightened sedimentation rates during the early Holocene were likely caused by increased productivity within the lake water. The early Holocene sediments from Joffre Lake are primarily gyttja with organic content reaching 30 percent (c.f. figure 6.20). Higher lake productivity would result from a combination of warmer conditions and increased photic zone of the water column caused by smaller contributions of glacial rock flour introduced to the lake basins during the glacial runoff season. Increased clastic delivery during the middle to late Holocene apparently compensated for lower productivity rates within the water column. Such compensation, however, is not observed within Green Lake where sedimentation rates during the early to mid Holocene are considerably lower than modern conditions (figure 6.18). Differences in lake volumes between the lakes (e.g. Hkanson and Jansson, 1983) may account for generally lower productivity for Green Lake during the early to mid Holocene.

Lowest overall errors are observed for Duffey Lake where the maximum range of uncertainty (95 percent) is less than 300 years and average uncertainty is less than 200 yr (figure 6.21). The uncertainties (average and max) increase twofold for Green and Joffre lakes, firstly because they are longer records and utilize portions of the radiocarbon in the middle Holocene with fluctuating ^{14}C activity levels but also because the depth-age model for Duffey is constrained by a greater number of radiocarbon samples. Uncertainties reach a local minimum for Joffre and Green Lake depth-age models near 8000 cal. yr BP and increase considerably (> 400 yr) prior to 8000 cal. yr BP (figure 6.21).

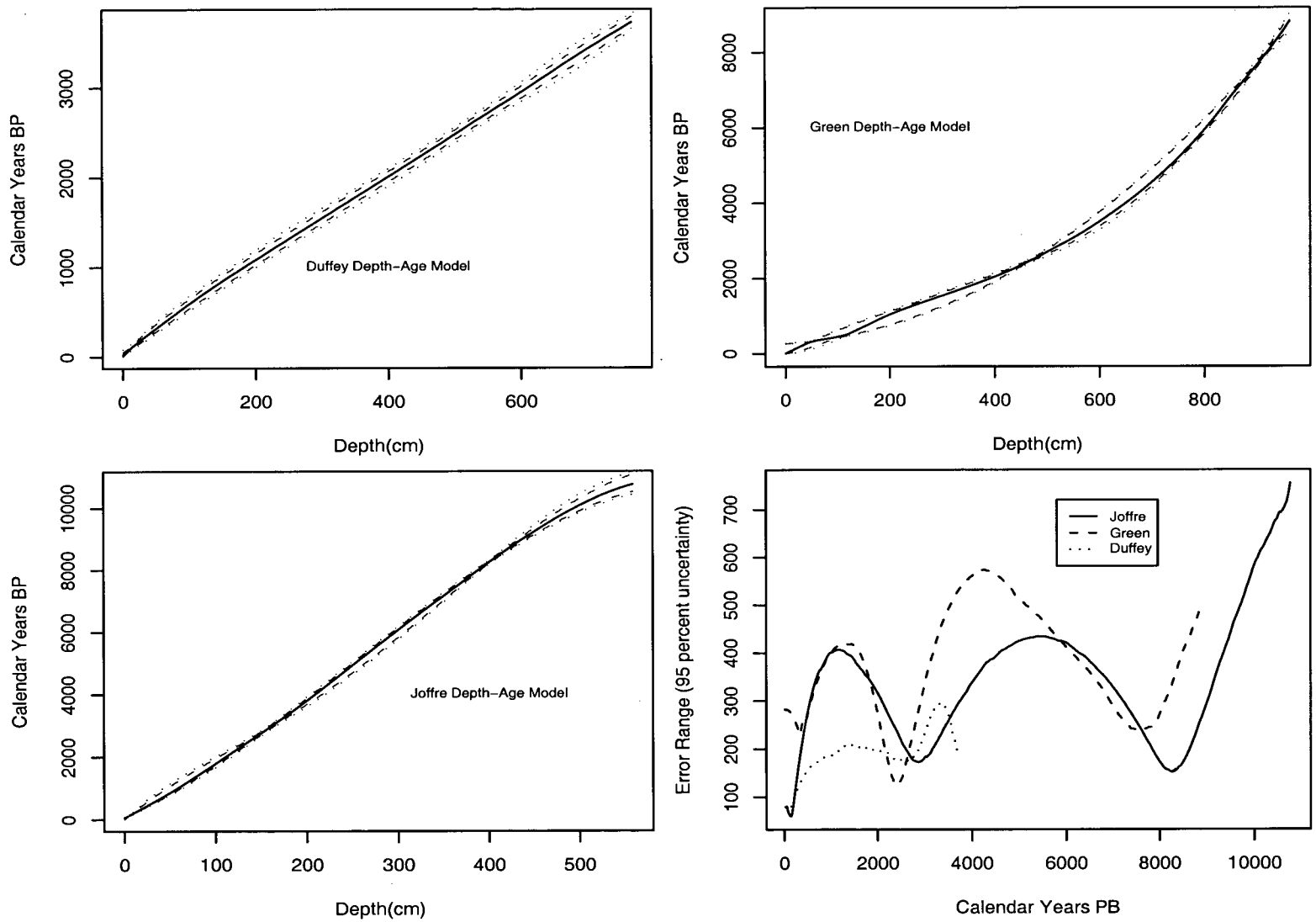

Figure 6.21: Depth-Age Models and Uncertainties
Median (solid), 68 (dashed), and 95 (dotted) percent age ranges determined by Monte Carlo sampling methods

6.4.5.2 Sedimentation Indices

Bulk physical property measurements from Green, Joffre and Duffey lake basins were combined with Monte Carlo derived depth-age models for the sediment cores. Souch (1990; 1994) developed such indices from organic matter variability within lake sediment cores through time using the assumption that sedimentation rates and organic matter are inversely related in linear fashion. Indeed, her data suggested that such assumption was valid for the contemporary portions of her sediment cores which were interpreted to be varved and agrees with earlier work in other glacierized watersheds (e.g. Karln, 1976, 1981; Leonard, 1986b,a; Karln, 1988). However, the organic content of lake sediment may not always be a good indicator of sedimentation rates especially if lake productivity has not remained constant, which appears to have occurred for Joffre Lake during the early Holocene. In addition, the density of the sediments is a very important parameter to determine especially if calculation of sediment flux through time is desired (Evans, 1997).

Because bulk physical properties of lake sediments are often highly highly correlated (e.g. Menounos, 1997), the dimensionality can be reduced through EOFA (e.g. Dean, 1993). Such an approach was used on the dry density, organic and water content trends for the master (dated) core from each basin to develop clastic indices. Non-regular sampling of particle size magnetic properties of the sediment limits their use in the current analysis. The first EOF explained over 90 percent of the variance for each lake basin and was interpreted to reflect the percentage of minerogenic matter reaching the core site through time. Comparison (not shown) of the EOFs with minerogenic flux (i.e. mass of clastic component) reveals that the two series are closely related though the EOF approach is more conservative in that it resolves the fraction of variance common to all bulk physical parameters.

The clastic EOFs indicate that for Joffre and Green Lakes, clastic delivery to the lake basins has increased steadily through the Holocene (figure 6.22) though superimposed on this trend are significant departures many of which, based on modeled error ranges, appear to be coincident between basins. Though early Holocene fluxes are generally below average, there are notable, large amplitude loadings to the lakes at ca. 9500 cal. yr BP (Joffre) and between 7500-8500 cal. yr BP (Green and Joffre). Although bulk physical properties were measured which are stratigraphicaly older, ambiguous radiocarbon ages and or lack thereof (c.f. figures 6.18, 6.20) does not allow their calendar age to be modeled. Both records (Green and Joffre) indicate a transition to clastic loading rates above the Holocene average near 4500 cal yr BP. Following 3500 cal. yr BP, all three records indicate two principal periods of higher than average (late Holocene) proportions of clastics between 3500-2000 cal yr BP and 1050AD to the present. The large positive anomaly centered at 1500 cal. yr BP within the Duffey Lake record is caused by a large event bed (table 6.8) and represents clastics from hillslopes rather than fluvial or glacial sources.

6.4.5.3 Green Lake Varve Index

Based on the method used in section 6.3, a single-core varve chronology was constructed for Green Lake which is over 2963 years in length. Unfortunately, comparison of varve age to the inferred age of the sediments using radiocarbon dating can be only completed up to 340cm or at ca. 1700 cal. yr BP. With the addition of 40 'missing' years into the chronology to account for bioturbation at 150cm (see 6.3 and appendix C) the varve based and radiometric ages overlap at 2σ. Much more uncertainty in the varve-based estimate of sedimentation is likely to occur prior to 340 cm as a large interval of poorly laminated sediments occur at 400cm depth. Varve boundaries in this interval were poorly defined and replicate counts produced errors exceeding what is considered acceptable (> 5 percent) by varve standards but still considerably lower than the uncertainty of radiocarbon-based

ages at this depth (figure 6.21). Additional uncertainty in age and thickness occurs because the measurements are based on one core, though a large fraction of the potential error in varve age is reduced because the counts were completed on thin sections and polished sediment slabs (appendix C). The last varve measured in the sequence occurs at ca. 600cm depth and the best estimate of its age is 3003BC $\pm$ 60 yr (including the additional 40 "missing varves" inserted at 150cm into the chronology). Below 600cm the sediments are too bioturbated to count and based on average sedimentation rates near this boundary ($1mmyr^{-1}$) the estimated sediment age at 619cm is 3190$\pm$ 60 yr. This age does not overlap (2 σ) the ^{14}C estimated calendric age range 3680-3400 cal. yr BP for a terrestrial macro fossil recovered at this depth (table 6.7) and suggests that varve-based ages may be in error prior to 342cm. The most probable source of the errors originate from poorly preserved varves near 400cm.

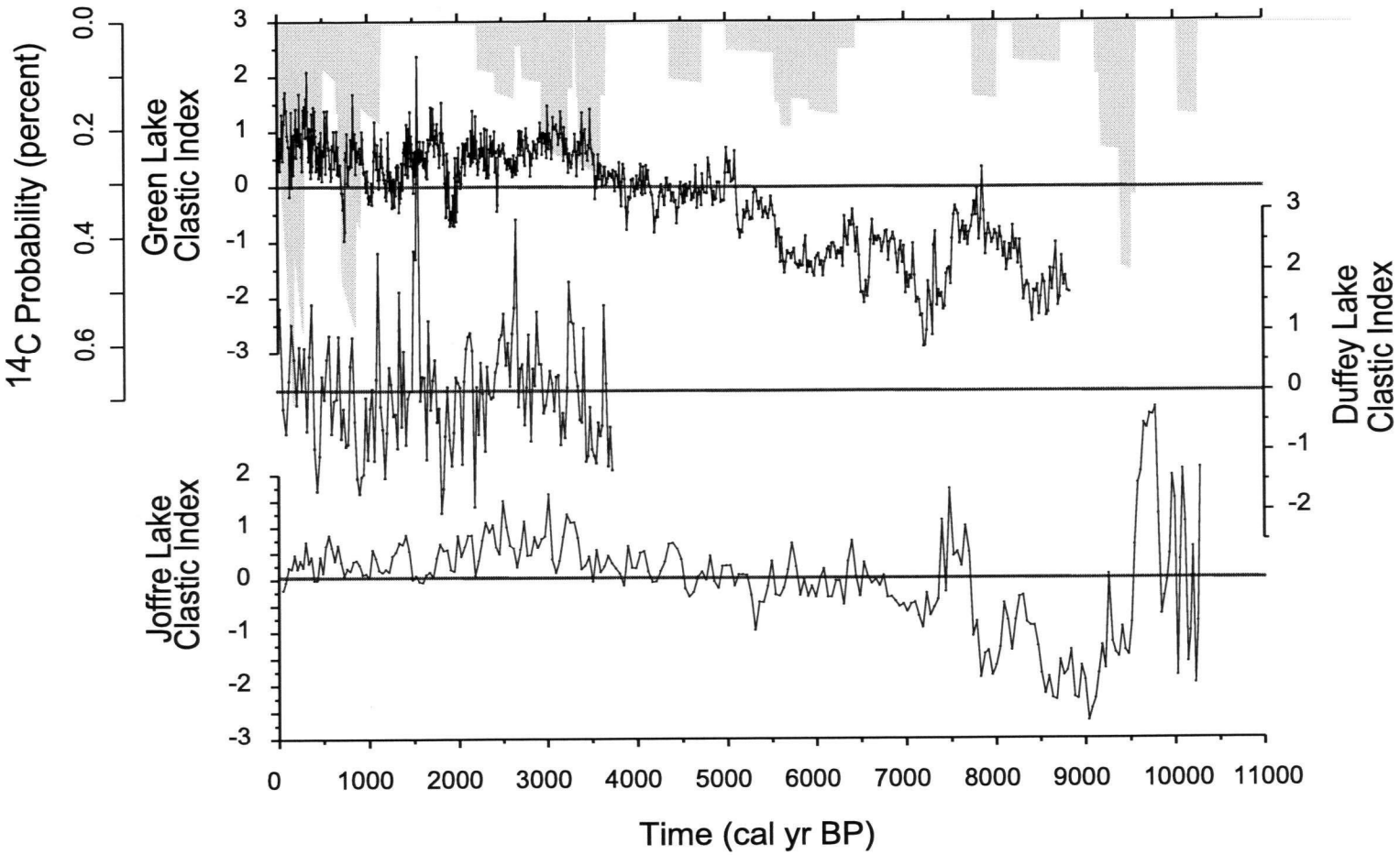

Figure 6.22: Clastic Sedimentation Indices and Terrestrial Evidence for Glacial Advances in the North Pacific
Indices (EOF1) of bulk physical properties from the lake sediment cores (lines) compared to^{14}C dated glacial advances in the North Pacific Region (Alaska, BC, Washington) and Canadian Rockies. Depth-age models for the cores constructed using Monte Carlo methods. Radiocarbon ages (shaded bars) represent probabilities (normalized for sample size) of 27 ^{14}C ages from *in situ* stumps overridden by glaciers or organic material from within moraines interpreted to date moraine formation (Denton and Karlen, 1973; Beget, 1981; Ryder and Thomson, 1986; Luckman, 1993; Luckman et al., 1993; Heine, 1998; Thomas et al., 2000). Clastic indices are standardized to zero mean and unit variance.

This event is particularly ubiquitous throughout the recovered cores of this study and well illustrated by the high organic matter content (ca. 90 cm in figure 6.20, 380 cm in figure 6.18, 240cm in figure 6.17) and is interpreted to reflect a period of prolonged drought-like conditions. Thus, there is the potential for an additional 100-200 year uncertainty in the chronology prior to 300AD.

Variance in the varve chronology from Green Lake indicates both low and high frequency changes in observed sedimentation at the core site (figure 6.23). Highest sedimentation rates occur from 2700-2300 cal. yr BP and again from 500 yr to present. The overall trend in the record is consistent with the trends noted in the clastic indices from the lake and from Joffre and Duffey lake basins where highest rates of clastic delivery occur at ca. 2500 cal yr BP and during the last 500 years. Varves from Duffey Lake are the thickest immediately preceding the deposition of Bridge River Tephra (ca. 2400 cal yr BP). Given the consistent behavior of this late Holocene trend between the basins of this study, it is interpreted to reflect changes in sediment supply which are apparently not modulated by internal geomorphic controls.

Comparisons of the Green Lake varve chronology to varve chronologies developed in other lacustrine environments highlights several important differences between the sediment-yield proxy records (figure 6.23). The decadal resolution record from Hector Lake (Leonard, 1986b, 1997) indicates generally decreasing sedimentation rates from ca. 1700 cal. yr BP until approximately 700 ca. yr BP when sedimentation rates increase. Above average sedimentation rates occur primarily between 2500 and 1500 cal. yr BP though less significant than the past 400 years (figure 6.23). Long-term sedimentation from Moose Lake (Desloges and Gilbert, 1995; Desloges, 1999) over the past millennium appear to be opposite to that trend recognized in Hector Lake though more agreement is recognized in the records prior to 1500 cal. yr BP.

6.4.6 Discussion -Glacial fluctuations and Changes in Sediment Supply

At the century to millennial time scales, growth and demise of glaciers through the Holocene is interpreted to be the primary sediment source for "non event" sediments reaching the lake basins. This belief is primarily based on the temporal agreement between published records of Holocene glacial variations in the Western North American Cordillera and periods of clastic sedimentation of this study (see reviews by Denton and Karlen, 1973; Ryder and Thomson, 1986; Davis, 1988; Osborn and Luckman, 1988; Luckman, 1993). Other evidence includes paleo-botanical data (e.g. Hebda, 1995; Pellatt and Mathewes, 1997) which indicates warm and dry conditions following wastage or recession of late Pleistocene ice in the early Holocene with a gradual decrease (increase) in annual temperatures (precipitation). Taken together the data indicate early climatic conditions not favorable for sustained nourishment of ice within the study area. Following the early Holocene, palynological data from the Coast Mountains indicate a steady and transitory change from warmer and drier environments to those which are more characteristic of modern environmental conditions. Consequently, such changes were the most likely reason for the increased clastic delivery to the lake basins and the glaciers are inferred to be the sediment sources.

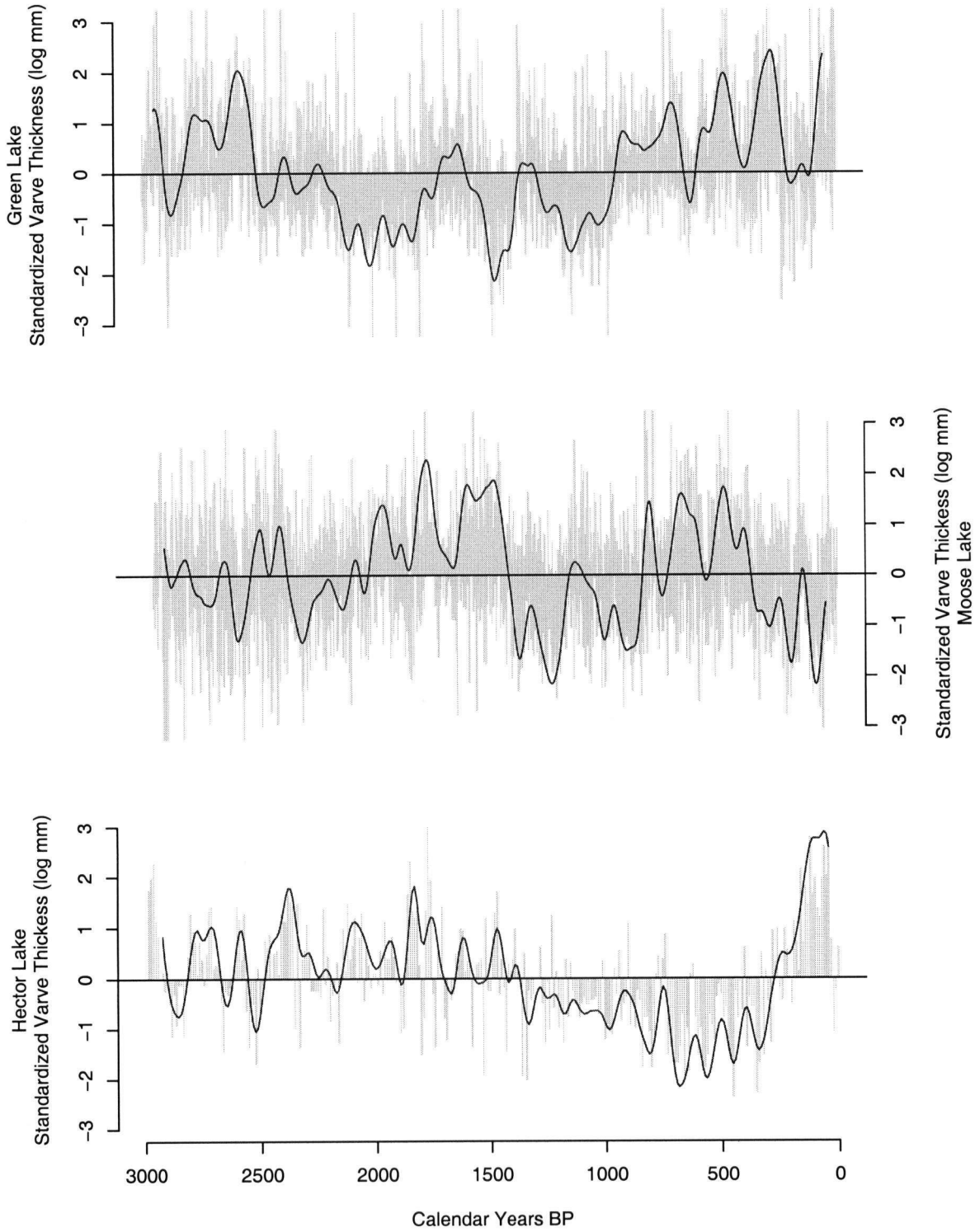

Figure 6.23: Comparison of Green (upper), Moose (middle), and Hector (lower) Lake Varve Chronologies

Departures and low frequency trends (101 yr Gaussian filter) reflect standardized (log transformed) varve measurements and are annual for Green and Moose Lakes and decadal for Hector Lake. Moose and Hector Lake varve data provided by Drs. Joe Desloges and Eric Leonard respectively.

At the lowest frequencies, the sediment-yield proxies (figure 6.22) indicate increasing clastic delivery to the lake basins through the Holocene and are largely consistent with reported changes in proglacial sedimentation rates in other glacierized catchments (e.g. Souch, 1994; Leonard and Reasoner, 1999). Consequently, the sampling detail and temporal constraint afforded in this study allows a more detailed assessment between between terrestrial evidence of glacial advances and clastic sediment delivery to the lake basins than was previously possible prior to the Neoglacial period.

6.4.6.1 Early Holocene Glacial Advances (?)

There has been continual debate concerning the evidence of early Holocene glacial advances in the Canadian Cordillera and the western North American Cordillera (e.g. Davis, 1988; Heine, 1998; Thomas et al., 2000; Reasoner et al., 2001). Based on the presence of clastic intervals within lacustrine sediments taken immediately downvalley from a series of moraines in cirques around Mt. Rainier, Heine 1998 suggested that Holocene glaciers underwent a moderate re-advance ca. 9800-8950 ^{14}C yr BP. The radiocarbon age was determined on terrestrial organic matter (twig) and is probably a reliable age for the clastic sediment sequence though its relation to the emplacement of the moraines upvalley is open to interpretation (e.g. Reasoner et al., 2001). Additional terrestrial evidence for glacial fluctuations during the early Holocene come from moraines on Mount Baker (Thomas et al., 2000) and from cirque deposits in the north Cascades (Beget, 1981). These studies use the spatial arrangement of moraines which have been dated with radiocarbon and tephrochronology to infer that glaciers underwent expansion sometime between 7400 to 8400 ^{14}C yr BP. Because the glacial moraines which date to early Holocene time are downvalley from 'Little Ice Age' (LIA) deposits, both studies infer the advance(s) were caused by cooler and or wetter conditions than during the LIA.

One of the principal reasons that the terrestrial evidence for proposed, early Holocene glacial advances has been so scrutinized is that glaciers would be advancing during a period from which there is ample paleo-botanical evidence for warm and dry conditions (e.g. Clague and Mathewes, 1989; Hebda, 1995; Pellatt and Mathewes, 1997). Inferred warmer and drier conditions for the North Pacific region are in general agreement with calculated summer insolation values at this latitude using orbital variations of the earth (Berger, 1977, 1978, 1988). Nevertheless, climate variations at shorter time scales are also driven by internal factors such as ocean circulation and such factors could conceivably cause short-term climate deterioration in the North Pacific and elsewhere. For example, the largest Holocene cold event (inferred from $\delta^{18}O$ variations in the GRIP and GISP2) recorded at Summit, Greenland occurred around 8.2kyr ago and similar scale departures have been recognized in disparate climate-proxy records around this time (Alley et al., 1997a). A recent study (Barber et al., 1999) suggests that the origins of the 8.2 kyr event may lie in the North Atlantic region where normal ocean circulation responsible for redistribution of heat from lower to higher latitudes (Broecker, 1994, 1997) was temporally altered. Such evidence suggests that despite the overwhelming paleo-botanical evidence for a warmer and drier early Holocene, high amplitude, climate variability on century time scales can not be ruled out. The absence of cooler and/or wetter conditions in pollen or macro vegetation -based climate reconstructions may be an artifact of the methodology as it is unlikely that vegetation can respond to such rapid and short-lived climate variability (e.g. see discussion in Bradley, 1999). The short response time of the glaciers observed in this study (see Chapter 5) and high sedimentation rates within the lakes suggests that signals of such rapid climate change could conceivably be transmitted to the lake basins during periods of prolonged or reduced sediment delivery resulting from glacial activity.

Evident within the early Holocene records from Lower Joffre and Green Lake are the presence

of clastic intervals which reflect temporary increased sediment delivery to the lake basins. Two intervals of inorganic sediments are recorded in sediment core from lower Joffre Lake and based on bracketing radiocarbon they were deposited at ca. 8700 ^{14}C yr BP. Large magnitude, short term variations in the clastic content of the Green Lake sediment cores occur prior to 8000 ^{14}C yr BP, but given the lack of radiocarbon control their age remains uncertain. Both lakes record a significant clastic event centered around 7700 ^{14}C yr BP or ca. 8400-8000 cal. yr BP. The timing is similar with a clastic event recorded in proglacial lakes in the Canadian Rockies though its amplitude appears to be considerably smaller than the event in this study (Leonard and Reasoner, 1999). Although the amplitude of the event is considerable (figures 6.20, 6.18), the absolute proportion of clastic matter which reached the basins during this time is considerably less than during modern conditions (3500-present). If the clastic events reflect contributions of sediment delivery during or shortly after a glacial advance it suggests the 8400-8000 cal yr glacial advance was less extensive than later advances during modern conditions. The timing of the clastic interval agrees rather closely with the timing of the '8.2 kyr' recognized in north Atlantic region (Alley et al., 1997a) and lends support for an earlier suggestion of a short-lived global cooling event during the early Holocene (Beget, 1981). In contrast to this study, Thomas et al., (2000) argue that moraine evidence for early Holocene glacial advances on Mount Baker indicates that glaciers advanced prior to the 8.2 cal yr BP and from this they conclude that the '8.2 kyr' event "...did not cause a glacial advance in the northwestern US". The absence of preserved moraines, however, does not preclude the event because the terrestrial evidence would be destroyed if a subsequent advance (such as the LIA) was more extensive. Thomas et al., (2000) infer that their glacial deposits are probably correlative with early Holocene advances near Mount Rainier which apparently occurred between 9000-9800 ^{14}C yr BP (Heine, 1998). Based on temporal similarity, and the radiocarbon evidence for other early Holocene advances within the North Pacific region during this time (figure 6.22), it is believed that existing glaciers within the Joffre Lakes catchment underwent a re-advance between ca. 8560-9480 ^{14}C yr BP. Based on the magnitude of the clastic event, (figures 6.22, 6.22), ice was probably more extensive than during the final phases of the 'Little Ice Age'. Perhaps coincidentally, it is within the Joffre Lake basin where vegetated moraines lie downvalley 100-300m from LIA-age glacial deposits and impound the uppermost lake of the basin (figure 6.1). Future work is planned to recover distal sediment cores from the upper basin in an attempt to derive minimum-limiting ages for the formation of the uppermost lake.

6.4.6.2 Middle Holocene Glacial Advances

There is unequivocal evidence which suggests that glaciers during the middle Holocene (7000-4500 cal. yr BP) were less extensive than during the late Holocene. There are no dated sites in North America which indicate ice extent more extensive during the middle Holocene than during the final phases of the Little Ice Age. A large number of sites also indicate that contemporary ice extent today is less than during the mid-Holocene as 20th century recession has exposed detrital and *in situ* wood in many glacial forefield locations. Based on *in situ* stumps, it appears that glaciers in Garibaldi Provincial Park were advancing between ca. 6500-5000 cal yr BP (Lowdon and Blake, 1975) but it appears that the advances may have been limited to more maritime environments. Most data for downvalley ice positions come from North Pacific environments (e.g. Denton and Karlen, 1973; Ryder and Thomson, 1986) rather than those mountain ranges to the east. The degree to which this difference reflects changes in winter precipitation remains unknown but may explain the disparity. Lacustrine records from the region do appear to record increased clastic flux (Souch, 1990, 1994) but not in those proglacial environments to the east (e.g. Leonard and Reasoner, 1999). Based on the clastic indices from Green Lake, it appears that clastic sedimentation

increased moderately and is most apparent at ca. 5500 cal yr BP when the change in the clastic index is most abrupt and coincident with maximum-limiting, radiocarbon dates of glacial advances (figure 6.22). Fluxes to Joffre Lake do not record such variability so the evidence for increased clastic sedimentation resulting from mid-Holocene glacial advances within that watershed remains ambiguous.

6.4.6.3 Late Neoglacial Advances and the Inception of the 'Little Ice Age'

Late Neoglacial (ca. 5500-present) clastic records of this study appear to be comprised of both low (millennial) and high (century) frequency variations. Centennial-scale variations are recognized in the cores of this study with heightened delivery of clastics centered at approximately 4500, 3200, 2500, 2100, 1500, 800, and 300 cal. yr BP (figure 6.22). In Duffey Lake, varves are thicker and clearly visible within these intervals of the cores where the organic carbon content is below average. Approximately similar scale departures and timing can be recognized in the sedimentary records of Green and Joffre lake basins (figure 6.22). Above average varve thickness is observed in Green Lake near 2500, 1600, and from 1000 cal. yr BP to the present. These intervals are taken to reflect periods when sediment delivery to the lake basins was higher than average. Dating control is inadequate to discriminate phases of ice growth, standstill or recession. More importantly, however, it suggests that glaciers were responding in a dynamic fashion and century-scale periods of glacial advance were separated by equal intervals of retreat. The following summarizes the terrestrial evidence for glacial activity within the Canadian Cordillera.

Several sites within the Canadian Cordillera record glacial advances between 3800 and 1500 cal. yr BP but the chronologies differ slightly from Coastal and Interior regions. Ryder and Thomson (1986) provide evidence for advancing ice at two glaciers (Gilbert and Tiedemann) in the Southern Coast Mountains (about 300 km to the northwest of the study area) between 3345 to 1300 ^{14}C yr BP. They suggest that Neoglacial activity within the Coast Mountains culminated ca. 2300 ^{14}C yr BP but in general, appreciable recession of these glaciers did not occur for almost two millennia. A period of regional climate that favored glacial expansion between 2800-3000 cal. yr BP is recorded in the northern Coast Mountains by a well constrained unit of glacio-lacustrine sedimentation within now-relict Tide Lake (Clague and Mathews, 1992; Clague and Mathewes, 1996). Unlike the Coast Mountains, Bugaboo glacier (300 km to the east of Duffey Lake) apparently underwent a glacial recession between a 3390-3090 cal. yr BP glacial advance and a later phases of ice growth (Osborn and Karlstrom, 1986; Osborn, 1986; Osborn and Luckman, 1988).

Localized channel aggradation is inferred to have begun following ca. 2400 cal. yr BP along the Van Horlick Creek (west fork) based on an excavated fluvial sequence. The stratigraphy consists of well oxidized, individual gravel facies below 60cm and overlain by a weakly developed soil sequence at 58cm depth. A charred twig overlying a thin (5mm) tephra unit provided a maximum-limiting age (2230 ± 60 ^{14}C yr BP) for the inception of significant overbank sedimentation (table 6.7). Overlying the soil are moderately stratified, oxidized gravel and sand lenses. The tephra is likely Bridge River based on its physical characteristics and the radiocarbon date. The stratigraphy from the sequence is interpreted to reflect channel aggradation following 2230 ± 60 ^{14}C yr BP. Aggradation appears to have been more or less continuous with little evidence (e.g. soil development) for prolonged periods in which sedimentation abruptly terminated. The overall channel, floodplain and valley morphology of the Van Horlick is interpreted to indicate channel aggradation following 2230 ± 60 ^{14}C yr BP. The most likely sources for such sediments are contemporary glaciers and glacial forefields and transfers to the channel system occur during or immediately following major glacial advances within the Van Horlick headwaters.

The terrestrial evidence for ice growth between 2000 and 1500 cal. yr BP within the Canadian

Cordillera is limited. Gilbert Glacier (Coast Mountains) is interpreted to have reached a size comparable to that at its late Neoglacial maximum ca. 2000 cal. yr BP (Ryder and Thomson, 1986) and advancing ice on Mount Baker, Washington (200 km to the south of Duffey Lake) sheared trees ca. 1900 cal. yr BP (Fuller et al., 1983). A glacial advance at Peyto Glacier is estimated to have commenced between 1560-1460 cal. yr BP based on two ^{14}C dates obtained from logs embedded within lateral moraine material (Luckman, 1994). Other wood found within the moraine yielded a calibrated radiocarbon age between 1750 and 1600 cal. yr BP. A second phase of glacio-lacustrine sedimentation began at Tide Lake between 1650-1450 cal. yr BP but a minimum-limiting age for this phase is not known (Clague and Mathews, 1992). More distant (coastal Alaska) evidence for a glacial re-advance around 1500 cal. yr BP in the North Pacific region is provided by radiocarbon dates on *in situ* trees and stumps buried by glacio-fluvial and glacio-lacustrine sediments (Wiles et al., 1999).

Following 1500 cal. yr BP, the clastic indices from the lake basins and the varve chronology from Green Lake indicate increasing sedimentation rates to the present (figures 6.22 and 6.23). Above average sedimentation occurs following 1000 cal yr BP but century scale variability remains common in the records. In general, the magnitude and timing of these sedimentation pulses corresponds to the two-phase Little Ice Age recognized within the southern Coast Mountains (e.g. Ryder and Thomson, 1986), the mid Coast Mountains (Desloges and Ryder, 1990)and the Canadian Rockies (e.g. Osborn and Luckman, 1988; Luckman, 1993). The inception of the early phase of the LIA in the Canadian Rockies is provided by ages of 34 cross-dated trees sheared by advancing ice at Robson Glacier which were killed between 1214 and 1350AD (Luckman, 1993).

6.4.6.4 Deposit Preservation and Apparent Magnitude of Glacial Events

The timing of increased sediment delivery between 3800-1500 cal. yr BP to the lake basins is similar to reported glacial advances within the Canadian Cordillera (Figure 6.22). The variability within the records suggests that sediment delivery during the late Neoglacial period has been characterized by alternating phases of sedimentation. It suggests that the Neoglacial was likely punctuated by numerous glacial advances rather than a prolonged phase of more extensive ice cover (c.f. Ryder and Thomson, 1986).

Although there is general agreement between episodes of increased sedimentation to the lake basins of this study and terrestrial evidence of glacial ice extent within the Canadian Cordillera, several events within the sediment cores have no or minimal terrestrial counterpart. Three possibilities could explain this disparity: 1) the climatic event was not severe enough to cause an appreciable translation between increases in ice volume and downvalley position of the glacial terminus; 2) the climatic event was severe and produced a recognizable response (i.e. trees were damaged or glacial deposits constructed) but subsequent advances eroded or destroyed these deposits; or 3) that the clastic events with no apparent terrestrial counterpart are not coincident with climatological changes favorable for glacial nourishment. Because most periods of increased clastic sedimentation into the lake appear to be associated with terrestrial evidence of glacial activity within the Canadian Cordillera it is likely that the disparity between the lacustrine and terrestrial records of late Holocene glacial advances results from the combination of points 1 and 2.

Because the regional glacial chronologies have been developed from glaciers that vary in size, aspect, and location, one may expect differences in the sensitivities and response times to produce a non-synchronous response even if forced in a similar manner. Thus, only some of the largest events (e.g. the Tiedemann Phase, the Little Ice Age) are roughly coincident from site-to-site. Consequently, differences in glacial volume (and hence sensitivity) most likely explain the disparate, albeit well-dated chronologies for the Tiedemann and Bugaboo Glaciers. Consequently, decadal-to-

century scale departures in precipitation or temperature which invoke a particular glacial advance may be superimposed on millennial-scale trends which may serve to amplify or mute the absolute response of the system (e.g. the downvalley position of glacial moraines). This point is somewhat analogous to the hypothesis presented by Luckman (1993) where he suggests that monotonically-declining solar insolation (due to Milankovitch forcing) may be responsible for producing glacial advances that appear to be increasing in absolute magnitude throughout the Holocene for the Canadian Rockies. However, unlike the Canadian Rockies, the Tiedemann Phase within the Coast Mountains is recognized as a prolonged period of glacial activity that was of equal severity (based on downvalley position of terminal moraines) to the advances of Late (1000 years to present) Neoglacial time (Ryder and Thomson, 1986; Desloges and Ryder, 1990). Increased sedimentation into the lakes between 2750 and 2250 cal. yr BP, is roughly of equal magnitude and duration to clastic intervals recorded during the Late Neoglacial Period and suggest that glacial advances during the Tiedemann Phase may have been comparable in magnitude to those experienced during the late LIA. The moraine stratigraphy within the study areas partly corroborates the clastic records of sedimentation. No moraines which lie outside LIA-aged deposits are apparent within the Green Lake basin suggesting that the final glacial advances during the LIA were the most extensive. Consequently, the varve and clastic record corroborates the terrestrial stratigraphy (figures 6.23 and 6.22) and if the magnitude of the clastic flux is taken to be indicative of downvalley position, it appears that Tiedemann Advances were equal to or slightly less extensive than later advances and explain why no terrestrial evidence for these advances remains. Using a similar logic, Tiedemann glacial deposits would be expected to lie slightly downvalley from LIA moraines within the Duffey and Joffre Lake basins. Indeed, it is within these basins where deposits older than LIA advances can be found. The reason for the slightly more extensive ice cover during the Tiedemann at these localities is unknown but spatial controls on synoptic climatological conditions may be at work given the similar longitudes of these sites and their proximity to the Tiedemann Glacier.

6.4.7 Comparison of the Sediment Indices to Climate Based Proxies from the Greenland Ice Cores

The previous analysis indicated that there is much evidence to suggest changes in clastic sedimentation within the lakes of this study area caused by changes in ice cover. It is the purpose of this section to evaluate the fraction of such variability which can be shown to be linked to atmospheric variability. Thus, the final analytical section of this thesis is aimed at evaluating the trend and low frequency ($< 0.01 yr^{-1}$) components within the clastic sedimentation records. The difficulty in resolving low-frequency climate variability with the ITRDB data was discussed in section 6.2; the present analysis uses other continuous proxy records which may be better at preserving low to ultra low (e.g. 0.001 yr^{-1}) climate variance. Ice cores collected from polar environments meet these objectives and such environments are often sensitive sites for recording large-scale changes in atmospheric circulation. Climate (temperature and circulation) proxy datasets constructed from the Greenland Ice Cores (GRIP and GISP2) were available from the National Geophysical Data Center, US Department of Commerce (http://www.ngdc.noaa.gov). Details concerning the cores are summarized in a collection of papers in the Journal of Geophysical Research (Hammer et al., 1997). The dating errors of the records are low (1%) over the Holocene and age has been cross-checked using tephrochronology and by comparing the age of significant climate transitions (e.g. the Younger Dryas-Holocene transition) to their age in other, high resolution (e.g. varved sediments from Europe) climate archives (Alley et al., 1997b).

Two climate proxies were analyzed from the GRIP and GISP2 ice core records. The first time series is a proxy of air temperature produced by measuring the proportion of heavy oxygen ($\delta^{18}O$)

within the ice. Its content is linearly related to the air temperature at which the precipitation formed due to fractionation and the reliability of its use as a local paleo-thermometer has been well established in Greenland (Jouzel et al., 1997). The second climate proxy is derived from trace metals (geochemistry) within the ice cores where covariance between the species is interpreted to reflect changes in northern (global) hemispheric patterns of circulation (Mayewski et al., 1993, 1994; O'Brien et al., 1995). The time series ($EOF_{geochem}$) is the first EOF from the data reflecting the covariance between the species and only a subset of this data (11500-present) is used here. Spectral analysis (Appendix C)was completed on the Varve and $EOF_{geochem}$ time series to investigate similarity of frequency components over the last 3000 years. Complete records were analyzed and then split in half to evaluate the stability of any detected frequencies within the record. The data were tapered before analysis and the null hypothesis was based on a red noise (Gilman et al., 1963; Mann and Lees, 1996) background fitted by the methods discussed in (Mann and Lees, 1996). The $EOF_{geochem}$ time series was interpolated to yearly data from irregularly spaced data. with an average data spacing during the last 3000 years of 2.3 years. The distribution of $EOF_{geochem}$ was skewed and a log transformation was applied to the data in order to approximate a normally-distributed dataset so that errors on the spectra could be calculated in their normal fashion (c.f. equation C.13)

6.4.8 Results

6.4.8.1 Varve Records

Spectral analysis on the varve and $EOF_{geochem}$ time series indicates that both records are comprised of moderate proportions of low frequency variability (figure 6.24; table 6.9). Particularly stable and significant periodicities (within the temporal error of the time series) are found at the century-scale near 200 and 100 years. The 100 year cycle changes to an 80 yr period in the Green Lake chronology but it is unknown if this reflects a true frequency change or sampling (dating) error. Higher frequency components at the sub-decadal periods (10-5 years) appear more common in the Varve record than the $EOF_{geochem}$ time series.

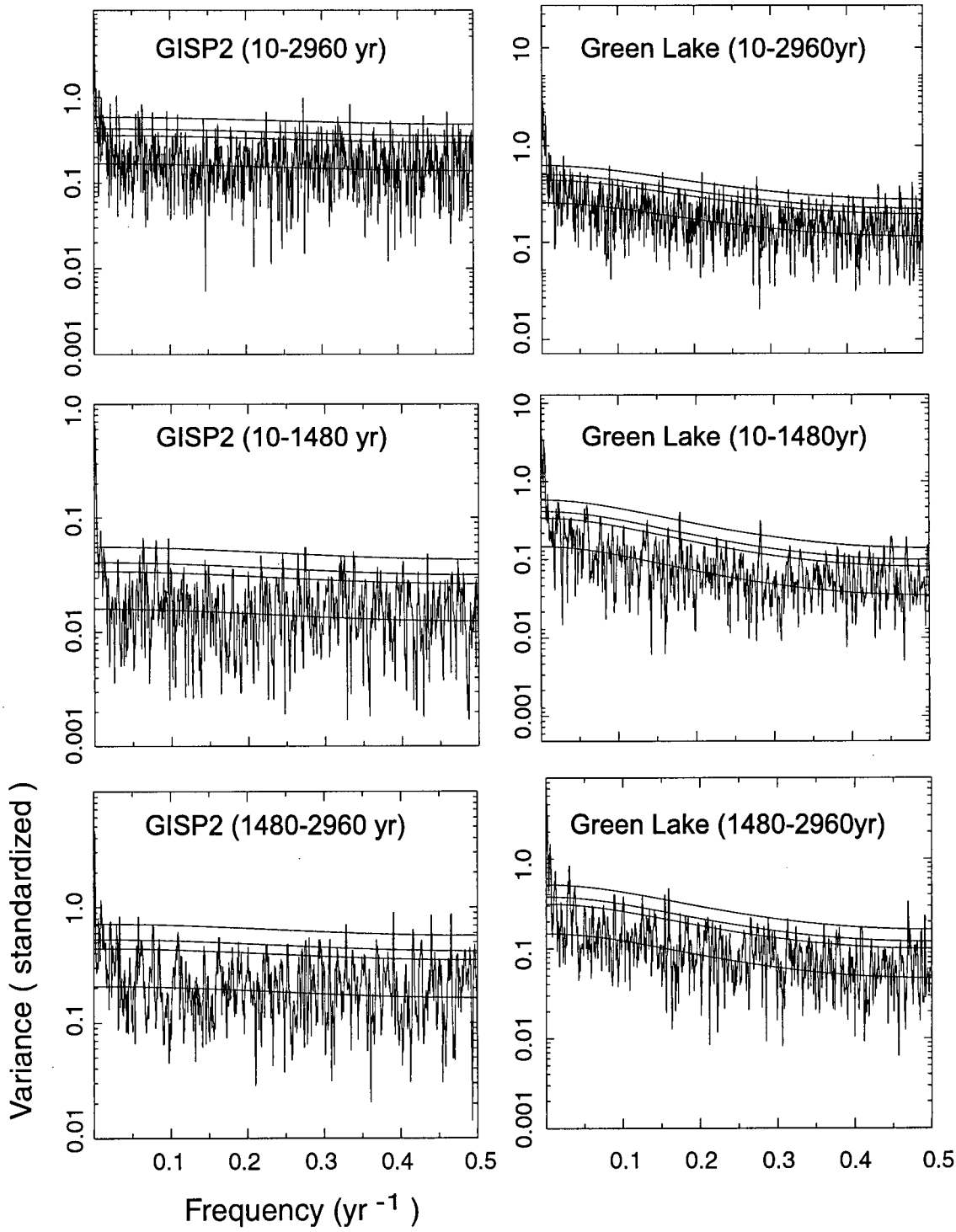

Figure 6.24: Spectra of $EOF_{geochem}$and Varve Series
Lines denote 99, 95, 90 percent, red-noise confidence limits (in order from top). Lowermost line is median fit after reshaping spectrum

Complete Record GISP2 Frequency (yr^{-1})	(10-2960 yr BP) $EOF_{geochem}$ Period (yr)	Green Lake Frequency (yr^{-1})	Varves Period (yr)
0.005	200	0.0027	370
0.007	140	0.0049	204
0.010	100	0.0090	111
0.0125	80	0.0115	86
0.0217	46	0.0286	35
0.0305	32	0.0891	11
0.0332	30		
0.0583	17		
First Half	(10-1480 yr BP)		
0.0083	120	0.0039	250
0.0630	15	0.0088	113
0.0801	12		
Second Half	(1481-2960 yr BP)		
0.0063	158	0.0054	185
0.0093	107	0.0122	81
0.0225	44	0.0293	34

Table 6.9: Spectral Power in the GISP2 and Green Lake Varve Series
Only spectral Peaks significant at 99% confidence are listed and with periods greater than 10 years.

6.4.8.2 Clastic Indices and Joffre Lake DN Record

The strongest glacial (and by inference climate) signal might be expected within the sediments of Lower Joffre Lake as it is the most heavily glacierized and the record is largely without event beds. Unfortunately the low sedimentation rates ($\approx 1mm\ yr^{-1}$) and lack of visual stratigraphy make high resolution analysis difficult. A higher resolution record of clastic delivery to the lake basin was constructed by photographing the core (wet), and constructing a continuous record of greyscale variations by digitizing the photographs into 600 dpi TIFF images (8 bit). Digital number (DN) was averaged across the central 1cm of a given photograph and the profiles were merged together to form a continuous time series to 9000 cal yr BP. Inorganic, outwash sediments have a darker color reflecting particle size (sands) rather than organic matter. The DN record was aggregated into 10-year measurements while the GRIP record was smoothed (5pt Gaussian window) to account for bioturbation within the Joffre record over approximately 5cm (100yr) of core (c.f. Willemse and Trnqvist, 1999). DN is positively correlated with organic matter and negatively to density variations and so represents a higher resolution clastic index for the lake basin.

Variations in DN appear to follow rather closely, to century-scale changes in air temperature recorded in the GRIP record (figure 6.25). Both records are only weakly correlated on the unsmoothed records over the entire period (r =0.17, n=279) but the correlation increases significantly (r=0.39) for the smoothed data over the 3500-0 cal. yr BP period with the GRIP record leading the Joffre time series (figure 6.25). The probability of chance correlation is marginally significant (p = 0.02) when corrected for autocorrelation. Spectral analysis of the time series (less trend) indicates significant power near periods 150 and 230 years.

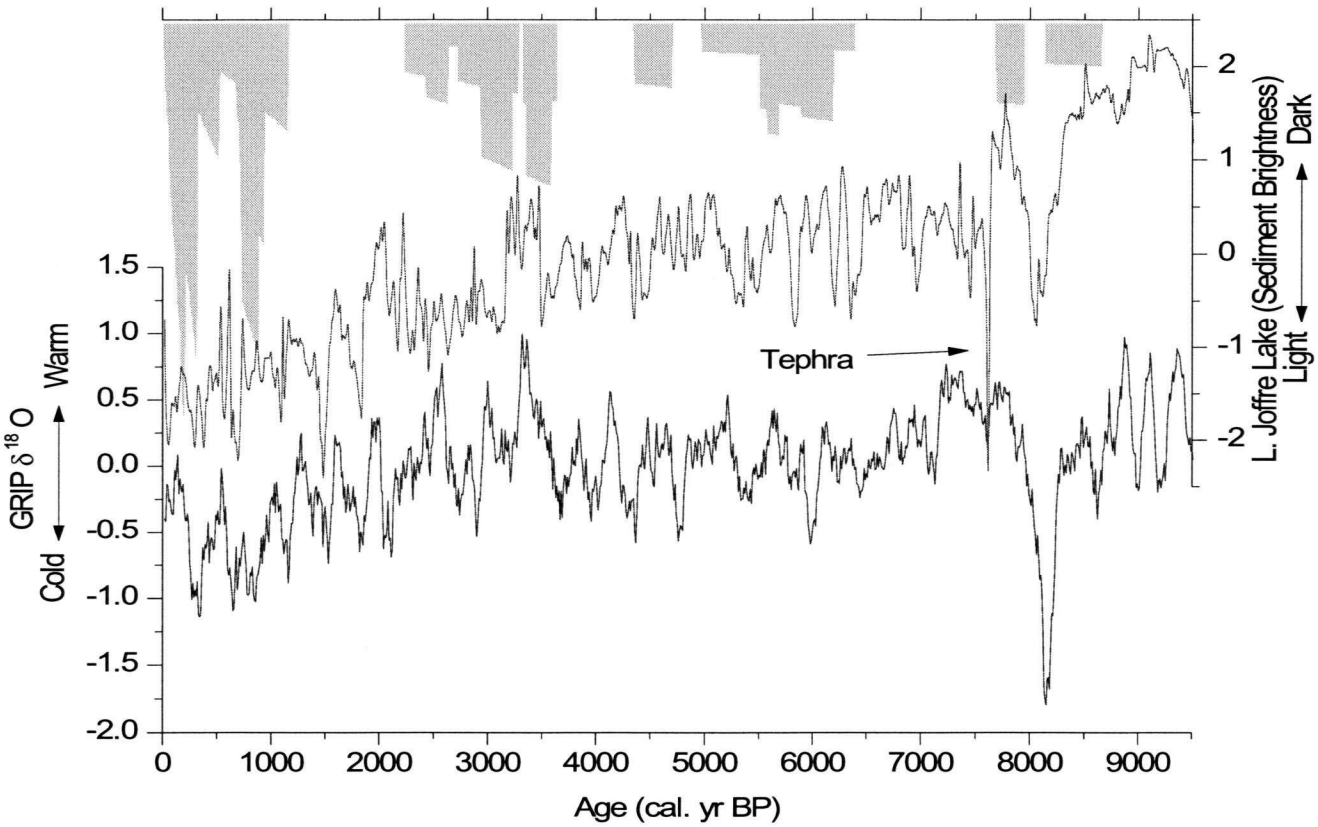

Figure 6.25: Terrestrial Glacial Record (top) , Greyscale Value (DN) of Lower Joffre Lake Sediments (middle) and Oxygen Isotope Variations (bottom) of GRIP core

Glacial record from figure 6.22. Both DN and Grip time series have been standardized (zero mean, unit variance) and smoothed with 10-year, moving average. Two event beds (17cm total) were removed from the DN chronology and sedimentation rates were recalculated. DN is correlated to GRIP δ^{18}O variations but the degree of correlation is much stronger ($r = 0.39$; $n = 334$; $p = 0.0$) for the 3500-0 cal. yr PB period. Solid (grey) lines denote terrestrial evidence for glacial advances within the Canadian Cordillera. Much less agreement (statistical and visual) exists between DN and OM with GISP2 $\delta^{18}O$ record.

Comparison of $EOF_{geochem}$ and the clastic sedimentation indices from the lake basins indicates significant differences between the series but both records are comprised of low frequency variance (figure 6.26). Similar to observations made by O'Brien et al. (1995), there is some agreement for positive $EOF_{geochem}$ loading during glacial advances though that study compared worldwide glacial records rather than evidence from the North Pacific Region. The amplitude of the middle Holocene circulation anomalies which are apparent in $EOF_{geochem}$ are much more subdued in the clastic sediment records from the lake basins and the differences may reflect local rather than global circulation anomalies as there is only fragmentary evidence for glacial advances during the middle Holocene. The amplitude of the 'Little Ice Age' differs significantly between the sites again suggesting important differences between the sites though the cause of such variability remains unknown.

6.4.8.3 Discussion

Variations in clastic delivery to the lake basins is characterized by century scale variability which is largely similar between lake basins of this study. Much of the variance within these records is primarily comprised of century-scale variations (ca. 200 and 100 yr) superimposed on a low, high amplitude cycle where local minima occur on average every 2300-2600 years. This low amplitude variability is similar in timing to changes in the common geochemistry signal recorded within ice core records from Summit, Greenland. These changes are interpreted to reflect the strength of the Polar vortex which is largely controlled by northern hemispheric changes in circulation and thus, the dominant (EOF1) from the geochemical data is interpreted to reflect large-scale, changes in northern hemispheric circulation patters (O'Brien et al., 1995). At shorter time scales there are significant differences between the records but the records appear to have similar spectral characteristics including significant components within ENSO-band frequencies (2-7yr) . The source of the temporal disparity remains unknown but because geochemistry variations with the ice cores may also reflect more localized sources such high frequency components may reflect localized rather than global changes of air trajectories to the core site. Much more agreement is recognized between air temperature proxies from GISP2 and clastic changes in the lake basins (c.f. figure 6.25) suggesting that century-scale clastic delivery to the lake basins was likely controlled by air temperature variability with preferred periods at about 100, 200 and 400 years. Leonard (1997) observed century ($\sim$ 200-250 yr) scale variations in sediment delivery to Hector Lake which was especially prevalent in the early portion of his 4500 year varve chronology. Similar preferred periods of sediment delivery were inferred by Souch (1990) for proglacial lake sedimentation in the Kwoiek River basin but she inferred that century scale-variability reflected sediment relaxation or exhaustion effects following glacial advances in the watersheds. The similarity in periodicities between the sediment yield proxies for basins of differing size, percentage of contemporary ice, and location suggests that a sizable proportion of the sediment transport variance can be explained by century-scale climate forcing. These periods appear to be particularly common in high resolution sediment records (e.g. Anderson, 1993; Dean et al., 1996) and long tree-ring records where standardization practices have been conservative and length segments contributing to the chronology are sufficiently long (e.g. Thomson, 1990). Analysis on a shorter (present to 674AD) geochemical dataset from GISP2 (Mayewski et al., 1993) indicated similar spectral power concentrated at century (400, 200, 150, 78yr) time scales.

The comparison between the DN record from L. Joffre Lake and air temperature variations at Summit, Greenland reveal some surprising and statistically significant covariation between the datasets. Most notable is the presence of the "8.2 kyr event" within both records and the timing of century-scale anomalies after ca. 3500 ^{14}C yr BP. Although other departures within the records are

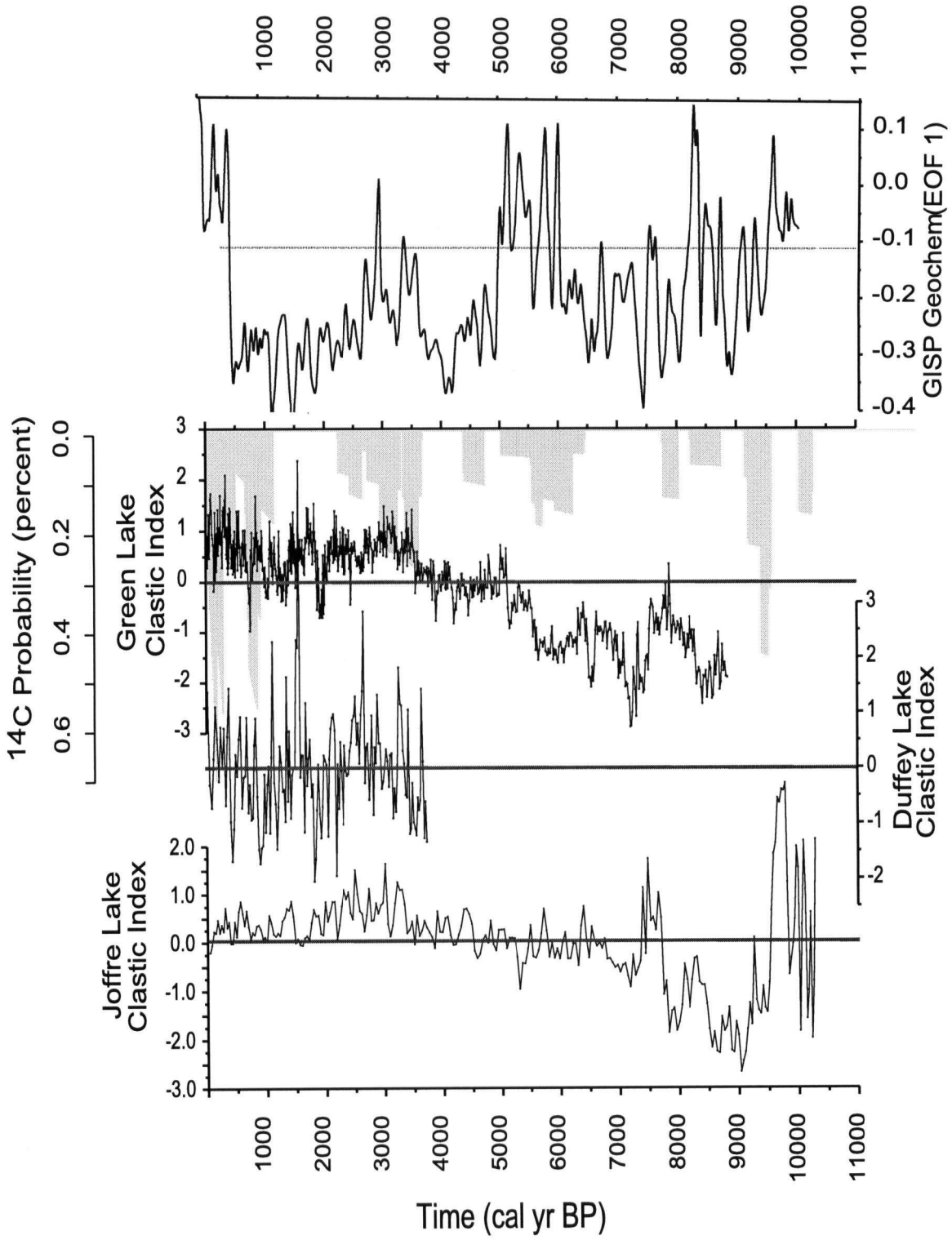

Figure 6.26: $EOF_{geochem}$ and Clastic Indices
Time series and labels similar to figure 6.22. GISP2 data smoothed with 100-year Gaussian filter.

possibly coeval, a "rubber band approach" to anchor the DN and $\delta^{18}O$ departures (e.g. Willemse and Trnqvist, 1999) is not used until the chronology is supported with addition AMS ^{14}C dating. The MC-derived error estimates for the clastic record (figure 6.21), however, suggests that many of the late Holocene correspondence between the records can not be shown to differ at 2σ. The similarities in the timing and magnitude of the century-scale variability between Lower Joffre Lake and climatic departures recorded at Summit, Greenland provides some evidence for Northern Hemispheric synchroneity of century-scale climatic events during the Holocene. It is unknown whether these similarities arise from external (e.g. solar) or internal (e.g. ocean circulation) forcing mechanisms of climate, or perhaps through atmospheric teleconnectivity between the North Pacific and North Atlantic regions. Although contemporary net mass balance of maritime glaciers within the North Pacific region is most strongly correlated to winter precipitation (e.g. Hodge et al., 1998) the data do not allow inferences to be made concerning whether precipitation or temperature anomalies were responsible for the observed century-scale variations in sediment delivery to the lake basin. Those questions must await more appropriate paleo-environmental techniques.

Over the longest time scales, clastic sediments were delivered to the lake basins with preferred structure[5] of 2300-2600 years during the Holocene and appear to corroborate those trends in proglacial lake sedimentation recognized by Souch (1994). This evidence from southern BC and those results the GISP2 and GRIP records support the theory proposed by Denton and Karlen (1973) that northern hemispheric glaciers have undergone fluctuations about every 2500 year during the Holocene. This structure appears to be particularly ubiquitous in long tree ring records from the American Southwest (e.g. Thomson, 1990), rates of ^{14}C production within the atmosphere (e.g. Damon and Cheng, 1989; Stuiver and Braziunas, 1989; Hood and Jirikowic, 1990) and within deep sea sediment cores (e.g. Bond et al., 1993, 1997). Though it is tempting to infer that the presence of the 2500 year cycle is external to climate system because it occurs in the ^{14}C record, rates of ^{14}C production can be substantially altered by sequestration changes in the deep oceans (e.g. Stuiver et al., 1991; Hughen et al., 2000b). Despite the prevalence of such a millennial period within the record from this study and many other paleoenvironmental records theories to explain such ultra-low frequency variability within the global climate system remain largely unproven.

6.5 Conclusions

This chapter has shown that a sizable fraction of variance within the sediment yield proxies from the watersheds of this study appear to be explained by variations in climate at century to millennial time periods. The effects imposed by geomorphic filtering which could introduce considerable non-linearities into the sedimentary records appears to be largely absent for the sediment records recovered from Green Lake and Joffre basins. Although low frequency changes in clastic sediment delivery to Duffey Lake agree with the trends and departures recognized in the other lake basins of this study, significant noise exists within the record at shorter time scales and the small signal to noise ratio of the record does not permit removal of climatic effects from the record. Reconstruction of temperature and precipitation patterns for the study area over the last 600 years indicates that changes in air temperature were probably the larger contributor to glacial advances during the final phases of the LIA and indicate that covariance between air temperature and varve thickness departures recognized in the early 20th century varves from Green Lake were real and remained an important control on the rates of sediment production over the last 600 years. By removing the temperature dependence from the varve record it was possible to examine how the rates of

[5]Although it may represent a frequency, the low number of cycles (4-5) within these data do not allow it to be isolated spectrally

sediment production vary primarily caused by changes in ice extent. Clastic indices from the lake basins begin to show the largest and most coherent behavior at century to millennial time scales. Based on the correspondence to the terrestrial record of glacial advances, such clastic indices record major changes in sediment production, interpreted to originate from glacial sediment sources.

Chapter 7

Conclusions

7.1 Introduction

The objective of this thesis was to evaluate the external and internal controls on sediment transfers within six glacierized watersheds of British Columbia over time scales important for sediment entrainment and production. While the dominant forcing mechanisms were assumed to be primarily of climatic origin, internal controls were suggested to introduce amplitude or phase shifts in the climate-sediment transport relation. The most important filtering mechanisms were hypothesized to include glacial response times, changes in sediment availability, and morphometric controls. Based on contemporary monitoring and a retrospective analysis of sediment transport from the watersheds, it appears that filtering is minimal in those basins where significant fluvial sediment storage of fine grained sediment (i.e. that fraction reaching monitoring sites and outlet lake basins) does not occur and where sediment production sites are directly coupled to the fluvial system. This sensitivity is in part controlled by the fine-grained nature of the transported sediments. The results of this study are easily transferable to other mountain watersheds where sediment supply is primarily governed by inter-annual to inter-decadal changes in the intensity of glacial runoff. The major findings of this study are summarized in greater detail below.

7.2 Sediment Production, Transport and its Linkage to Climate: Time and Space Scaling

The structure of the thesis was organized according to time in an attempt to isolate hydro-climatic controls of sediment entrainment and transport from those processes responsible for sediment production. With hindsight, such experimental control does not appear to be possible as sediment transfers may vary depending on such factors as the intensity of glacial runoff for a given year, sediment exhaustion effects and/or intermediate sediment storage in the fluvial network, or changes in sediment production over century-to-millennial time scales due to changes in ice cover. Nevertheless, the attention to time has helped clarify the dominant climatic and geomorphic elements which control fine-sediment transfers within glacierized watersheds of the southern Coast Mountains of British Columbia. What is most apparent in the results of this study is that sediment transport can be shown to be linked to climate variability over a range of time scales and that the proportion of variance attributable to climate forcing increases with decreasing frequency. Such frequency-variance scaling is common for geophysical time series which can be modeled as a simple Markovian process and red noise is used as the null hypothesis in the frequency (Gilman et al., 1963; Mann and Lees, 1996) or time domain (e.g. Church, 1980; Mandelbrot and Wallis, 1968; Hurst, 1951). Nevertheless, between-basin similarities in the records suggest that geomorphic filtering has been minimal and that the sediment transport records reflect trends and periodic components common to variations in air temperature and or precipitation. A stronger argument for climatic controls is provided by the similarity (time and frequency) between the sediment yield proxies and proxy-based reconstructions of climate provided by variations in tree growth and those signals captured in the GISP2 and GRIP ice cores.

An increase in variance with decreasing frequency was originally proposed by Mitchell (1976)

for the global record of climate variability during earth's history (figure 7.1). With the exception of ENSO and decadal-scale changes in ocean surface circulation (gyre), the shape and magnitude of his spectra has remained more or less unchallenged (figure 7.1) despite the multitude of proxy and coupled ocean-atmospheric GCM's data which have become available since 1976 (Stocker, 1996).

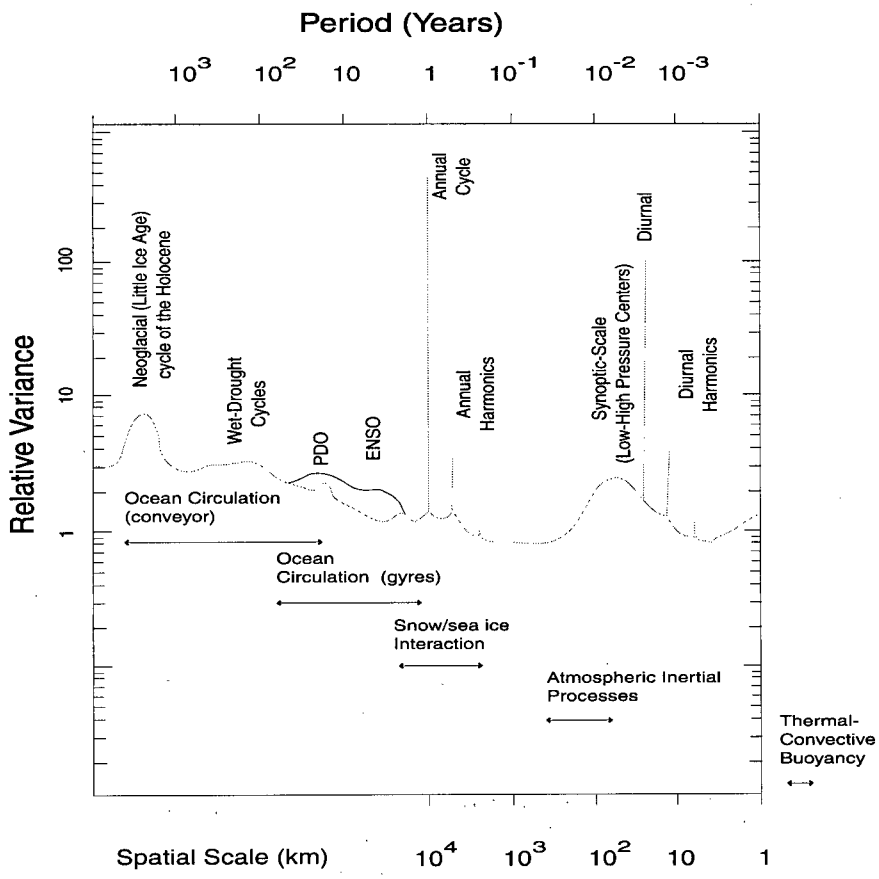

Figure 7.1: Spectrum of observed climate variability in instrumental and proxy climate-proxy records
Original figure from Mitchell 1976 and modified to show variance over the Holocene. Dotted line indices additional variance introduced to spectrum to account for ENSO and decadal-scale (e.g. PDO) climate variability which was poorly recognized or understood in 1976.

A similar time-space scaling is observed in the sediment transport data of the current study (figure 7.2) where factors controlling sediment entrainment and delivery at the event scale are primarily controlled by meteorological events which occur locally and over a period of hours to days. At this scale, effects such as topography (orography) may influence the intensity of a given hydrologic events. A good example of such effects are the observed rainshadow effects that the Coast Mountain divide has on controlling the magnitude of autumn runoff events in the study area. At the annual scale, variations in the intensity of nival and or glacial melt are influenced by wintertime precipitation and temperature changes which appear to be moderately linked to climate variability at the regional (PDO) and hemispheric (ENSO) spatial scales. Inter-annual to inter-decadal changes in the phase of the PDO or ENSO can be shown to influence minor scale changes in ice cover (sediment production) and possibly, the frequency of extreme autumn runoff events. Century to millennial changes in sediment delivery are related to large-scale changes in ice

cover. For at least the past six centuries, glacial fluctuation in the study area appear to be driven primarily by persistent anomalies in temperature. Over longer periods, variations in glacial cover within the study area were likely caused by large amplitude changes in climate driven by processes which operate at global spatial scales. Increasing ice cover through the Holocene is a likely result of changing insolation toward the present while changes in ocean circulation may be responsible for millennial-scale variations in ice cover.

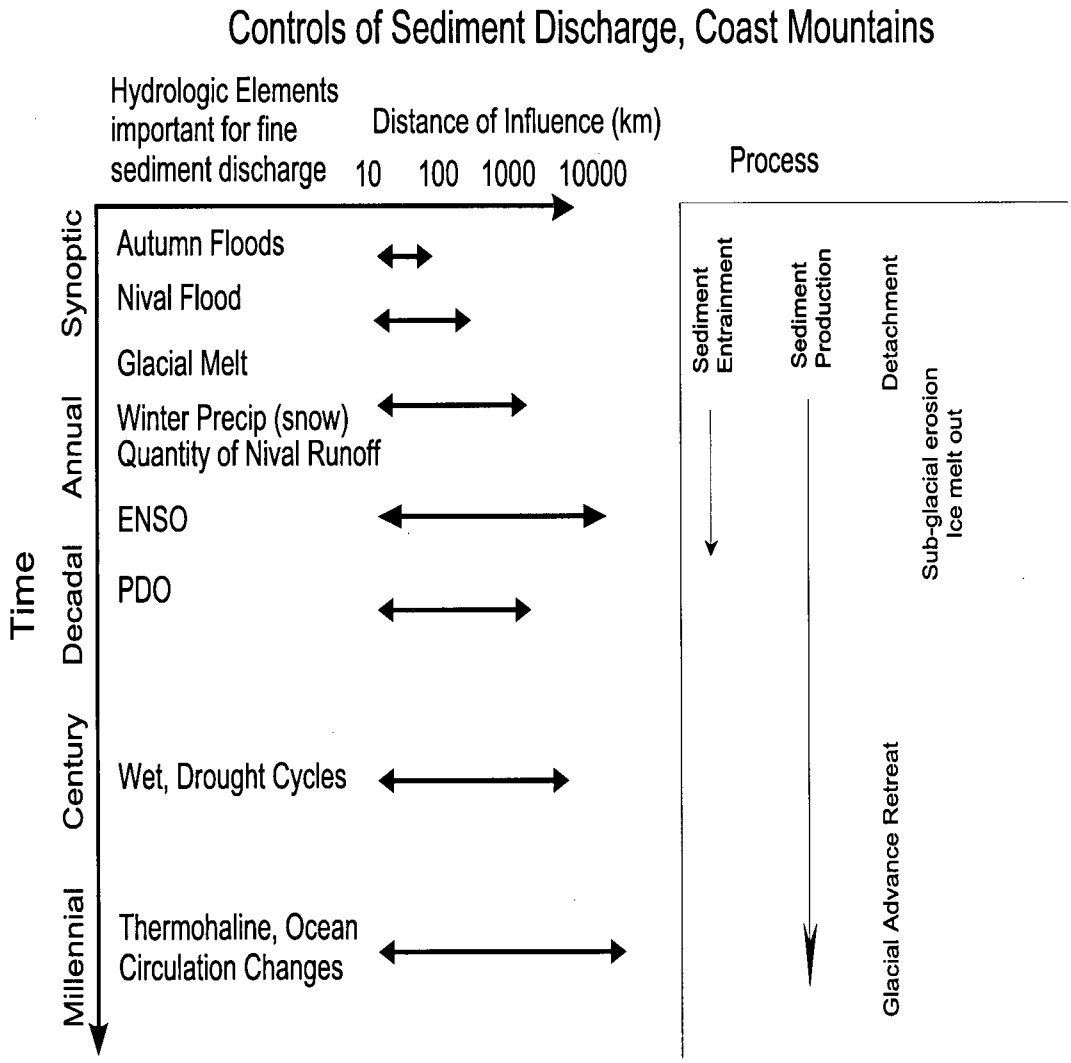

Figure 7.2: Time-Space Scaling of observed and inferred climate-sediment transport linkages, Coast Mountains BC

7.3 Other Important Findings

More specific conclusions regarding sediment transport to the lake basins can be made based largely on the varved sediment records of the study. Following 1946AD, the majority of sediment transport for a given year occurs during a 2-3 day period and originates from fluvial and hillslope sources. The importance of extreme climatological events in controlling the intensity of sediment transfers during the second half of the 20th century is exemplified by two late summer rainstorms in 1991

which caused wide-spread hillslope and fluvial instability throughout the study area. The volume of sediment mobilized during these events for one catchment (Green) is exceptional within the last 3000 years. Prior to 1946AD, sedimentation within the lake basins was also controlled by the intensity of glacial runoff for a given year which is, in turn, governed by air temperature (annual) and wintertime precipitation variability, both controlled by the PDO. The relation between air temperature variability and varve thickness variations prior to the period of instrumental records (1880AD) was assessed with proxy-based records of northern hemispheric air temperature variations. Both records are significantly correlated for the past 600 years and record abrupt early 20th century warming with little evidence for lead-lag relations. The varve chronology fails to reproduce late 20th century warming; this is interpreted to reflect diminished sediment availability following rapid glacial retreat. Little evidence for lead-lag relations between climate forcing and sediment yield response indicates that in this environment, the response time of glacial sediment systems to climate variability may be considerably less than that predicted for the glacier itself. Though debris flow and snow avalanche activity for one lake basin (Duffey) is significant in terms of mobilized sediment volume, their frequency through time appears to be random and not strongly linked to a particular climatic regime.

7.3.0.4 Importance of Glacial Cover

The contemporary monitoring and lake sediment records highlight the importance of glacial cover as a primary control on the quantity of sediment exported from the watersheds. These data provide further support for the belief that glacial cover has a significant influence on the production of fine grained sediment within mountain watersheds (e.g. Borland, 1961; Gurnell, 1995; Harbor and Warburton, 1993) though the relation between yield and glacial cover is likely spurious and scales more faithfully to basal surface area in contact with substrate (e.g. Hallet et al., 1996; Hallet, 1979). With respect to sediment yield, it has been suggested that considerable complexities are introduced to the glacial cover-sediment yield relation at decadal time scales (Leonard, 1997) and such hysteresis is likely related to a number of factors. This study has demonstrated that a sizable fraction of the decadal-scale complexity may be reduced by controlling for inter-annual variations in glacial runoff. When variations in air temperature are taken into account the relation between ice cover and sediment yield becomes more clear.

7.3.0.5 Sediment Relaxation

Sediment relaxation (paraglacial effects) was hypothesized to occur following Pleistocene ice retreat based on those descriptive models developed for British Columbia (Church and Ryder, 1972; Church and Slaymaker, 1989). Analysis and interpretation of sediment records from two of the watersheds of this study suggest that evidence of a prolonged period (e.g. ¿1000 years) of paraglacial sedimentation was not recovered in the sediment records. The evidence from lower Joffre Lake includes an abrupt (1cm) transition from a high energy, proglacial environment to one characterized by negligible inputs of clastic matter to the lake basin. Though the abrupt nature of the contact may be partly accounted for by sedimentation in the upper two lake basins, such morphometric controls are unlikely to completely alter downvalley sediment transfers especially since the availability of very fine grained sediments would be high as glacial deposits undergo stabilization. Similar rapid attenuation of downvalley sediment discharge is recorded in the inorganic, basal rhythmites in Green Lake where couplet thickness decreases more than two-fold in less than 30 years. In contrast to Joffre Lake, the lack of gravel or diamict within the basal sediments may indicate that paraglacial sediments occur deeper within the sequence and were not recovered. At least for the

early Holocene period, the sedimentary records from Green and Joffre lake basins indicate that the the fine sediment cascades were not experiencing a major phase of sediment relaxation at this time. Two probable reasons for a lack of early Holocene, paraglacial effects include rapid re-vegetation of exposed minerogenic surfaces and lower precipitation during the early Holocene. Both scenarios agree with our current knowledge of early Holocene climates for the Canadian Cordillera based on paleo-environmental reconstruction. It is also possible that watershed scale plays a part in the apparent rapid adjustment following ice retreat as the lack of significant fluvial storage sites in these watersheds would cause sediment sources to reflect detachment from upland surfaces rather than from fluvial environments (Church and Ryder, 1972; Church and Slaymaker, 1989).

For smaller amplitude sediment relaxation changes, there appears to likewise be minimal evidence for paraglacial effects following the 'Little Ice Age' within the study area. Though sediment delivery during the early 20th century was exceptional in all four varve chronologies, high rates of lake sedimentation coincided with rapid glacial retreat and ended rather abruptly in the mid 1940s when annual air temperatures returned to average or below average values. This reduction in sedimentation occurred despite the return to wetter than average conditions which would be expected to mobilize sediment from unweathered, glacial deposits if paraglacial effects were significant. Though late-lying snowcover may have reduced detachment in glacial forefield areas after 1946AD, the lack of sediment adjustments in the recent two decades (i.e. warm and dry conditions) suggests that such effects were probably minimal. Taken together, such evidence suggests that the majority of sediments reaching the lake basins originate from sub-glacial and ice melt sources rather than from mass wasting of sub-areally exposed, glacial deposits. Sub-glacial and ice melt out sources would account for the zero lag between ice retreat and sediment production while its fine caliber would allow its instantaneous transport through the fluvial system to be deposited in the downvalley lakes of this study. Finally, if paraglacial effects did occur they may be expected to be a function of sediment transport rates through the fluvial network ultimately controlled by sediment caliber, stream gradient and length, and the distribution characteristics of flood events. Such factors would suggest that sediment relaxation effects would be most apparent in the Duffey Lake basin and consequently, it is in this watershed where lags between climatological forcing and sediment transport occur.

The final example of sediment relaxation within the sediment records from this study is the trend in sediment delivery to Green Lake following the 1991 flood. After controlling for variations in flood intensity (Chapter 5), varve thickness is larger than expected and is taken to reflect increased sediment availability of channel and hillslope sediments. Increased sedimentation following the event in Cheakamus, Glacier and Lillooet Lake varve chronologies is not apparent nor is there photographic evidence for large-scale patterns of hillslope instability following the event. The regional evidence suggests that sediment transfers during the prior decade from Green Lake can not be explained by climatological events and that elevated fluxes from the watershed reflect a major disruption to the fine sediment cascade. The fluvial and hillslope sediment sources will likely continue to influence the 'normal' sediment cascade within the Fitzsimmons Creek watershed for some time to come.

7.4 Limitations of the Study and Directions for Further Research

This study has contributed to our understanding of the climatic controls associated with sediment production and transfers in glacierized basins but several important limitations require further discussion. While many of these shortcomings may be addressed with additional study or analysis, several reflect phenomena which are either stochastic, represent deficits in our understanding of sediment production in mountain environments, or can not be addressed due to limitations in

current methodological procedures.

The clarity in the climate-sediment yield relation is in part modulated by intermediate storage of sediment in the fluvial system but the relation is also complicated by important, sediment generating processes which can not be predicted in any meaningful way. Both effects appear to overwhelm any true "climate signal" preserved within the varved sediments of Duffey Lake. Hillslope-derived sediments enter the lake basin frequently and make the construction of a continuous varve chronology extremely difficult and impossible prior to ca. 1450AD. Lower sediment supply and its intermittent storage within Van Horlick introduce additional geomorphic filtering within the sediment records through bioturbation and phase shifts between sediment production and lake sedimentation. A more careful attention to evidence for hillslope instability near the lake in the planning stages of the project may have excluded the use of the basin for this study. However, many of the observed complexities such as lake morphometry and bioturbation would not have been identified without detailed analysis.

It is important to note that while much of the study has focused on reconstructing sediment yield for the watersheds, the recovered sediment records can only provide indices suggesting the most probable changes in lake-wide sedimentation patterns arising from changes in sediment delivery. Yield estimates were made for the contemporary period for Birkenhead, Duffey and Green Lakes using multiple surface cores but true estimate of sediment yield for the Holocene would require the collection of significantly more cores than were collected in this study (e.g. Evans, 1997; Lamoureux, 2000). In addition, corrections for lake outflow losses (using hydrologic models incorporating particle size, lake stratification and variable discharge) would be required and perhaps, a partitioning of yield into bedload and suspended components could be accomplished. Such methods may be possible for Green Lake where lake sediment studies continue and where bedload transport rates have been estimated for the dominant inflow to the lake basin (Pepola, 2001).

7.4.0.6 Glacial Sediment Budgets and Provenance

Sediment sources in this study were identified primarily from air photo analysis, field visitation and in several cases by determining which tributary basins contributed the largest proportion of suspended sediments to the mainstem channel systems of the study. Based on those data, glaciers and contemporary (i.e. unvegetated) glacial deposits represent the major sediment sources. Observations over the duration of the study suggest that such sediment originates primarily from sub-glacial regions and during melt of debris-laden ice. Unfortunately, field visits were made on days where precipitation was negligible and so the proportion of sediments which enter the streams from exposed glacial deposits remains unknown. Detailed sediment budgets in glacial forefield areas would help to quantify the sources and sinks of glacially-derived sediments and their overall importance in sediment discharge records from the basins.

The influence of sediment caliber appears to play an important role in controlling sediment relaxation within this study. Souch (1994; 1990) suggested that it was possible to separate glacial (silts and clays) and non-glacial sediments (sands) reaching the lake basins based primarily on sediment texture. While such effects may be true in other watersheds, much of the sediments stored within the contemporary fluvial networks of this study can be traced directly to glacial forefield areas where Holocene glacial deposits have been modified by re-advances or mass wasting. A significant fraction of this sediment is comprised of coarse to fine grained sands where its transport rate is considerably slower than finer-grained sediments. For the basins of this study, differentiation of sediment sources based on texture is not feasible and more appropriate methods are needed. Similar difficulties are encountered for identifying sediment sources based on surface weathering characteristics of transported grains using scanning electron microscopy (Souch, 1990, 1994), geo-

chemistry (e.g. Reasoner et al., 1994), or magnetic properties (Evans, 1997) of the sediments largely because lithologic differences within the basins are slight. More importantly, contemporary glacial sediments are lithologically similar to unweathered, Pleistocene glacial deposits on hillslopes and adjacent to active fluvial environments. Without the construction of a sediment budget, quantifying the importance of glacial and non-glacial sediment sources to the lake basins is difficult.

7.4.0.7 Multi-basin Varve Network

Finally, this study has demonstrated that the use of varved sediment records provides a powerful means of reconstructing proxies of sediment yield over event to century time scales. A limitation imposed by the technique lies in the inaccuracies and potential errors associated with such records. Although multiple-core chronologies can minimize error, they can not reduce it completely: the accuracy of the chronology may be compromised by bioturbation, missing varves due to low sedimentation rates, or mis-interpretation. A multiple-basin, varve network developed within a hydro-climatic region may be able to reduce the overall age errors and allow the chronologies to be used in a more precise manner. Such an approach is similar to the identification of marker rings in regional tree-ring sites. The presence of unique, flood events which are identifiable in the contemporary varve chronologies of Glacier, Cheakamus and Glacier Lake basins suggests that such an approach is possible in the study area. The analysis would allow sediment yield proxies to be developed with an accuracy approaching tree ring chronologies. More importantly, such a network could be employed to detail changes in between-basin sediment production and transport over time scales relevant for process and climate change during the Holocene.

Bibliography

P. Ackroyd. Debris transport by avalanches, Torlesse Range, New Zealand. *Zeitschrift fur Geomorphologie*, 30(1):1–14, 1986.

J.R.L. Allen. Reaction, relaxation and lag in natural sedimentary systems: general principles, examples and lessons. *Earth-Science Reviews*, 10:263–342, 1974.

R.B. Alley, P.A. Mayewski, T. Sowers, M. Stuiver, K.C. Taylor, and P.U. Clark. Holocene climate instability: A prominant, widespread event 8200 yr ago. *Geology*, 25(6):483–486, 1997a.

R.B. Alley, C.A. Shurman, D.A. Meese, A.J. Gow, K.C. Taylor, K.M. Cuffey, J.J. Fitzpatrick, P.M. Grootes, G.A. Zielinski, M. Ram, G. Spinelli, and B. Elder. Visual-stratigrapic dating of the GISP2 ice core: Basis, reproducability, application. *Journal of Geophysical Research*, 102(C12): 26367–26381, 1997b.

R.Y. Anderson. The varve chronometer in Elk Lake: Record of climatic variability and evidence for solar-geomagnetic-14C-climate connection. In *Elk Lake, Minnosota: Evidence for Rapid Climate Change in the North-Central United States*, volume Special Paper 276, pages 45–67. Geological Society of America, Boulder, Colorado, 1993.

D. Bahr, T. Pfeffer, C. Sassolas, and M. Meier. Response time of glaciers as a function of size and mass balance: 1. Theory. *Journal of Geophysical Research*, 103(B5):9777–9782, 1998.

V.R. Baker and J.C. Costa. Flood power. In L. Mayer and D. Nash, editors, *Catastrophic Flooding*, pages 1–21. Allen and Unwin, Boston, 1987.

D.C. Barber, A. Dyke, C. Hillaire-Marcel, A.E. Jennings, M.W. Kerwin, G. Bilodeau, R. McNeely, J. Southon, M.D. Morehead, and J.M. Gagnon. Forcing of the cold event of 8200 years ago by catastropic drainage of Laurentide lakes. *Nature*, 200:344–348, 1999.

T. Barnett, D.W. Pierce, M. Latif, and D. Dommenget. Interdecadal interactions between the tropics and midlatitudes in the Pacific Basin. *Geophysical Research Letters*, 26(5):615–618, 1999.

M. Bartlett. Some aspects of the time-correlation problem in regard to tests of significance. *Journal of the Royal Statistical Society*, 98:536–543, 1935.

J.E. Beget. Early Holocene glacier advance in the North Cascade Range Washington. *Geology*, 9: 409–413, 1981.

A. Berger. Support for the astronomical theory of climatic change. *Nature*, 269:44–45, 1977.

A. Berger. Long-term variations of caloric insolation resulting from the Earth's orbital elements. *Quaternary Research*, 9:139–167, 1978.

A. Berger. Milankovitch theory and climate. *Reviews of Geophysics*, 26:624–657, 1988.

F. Biondi, A. Gershunov, and D. Cayan. North Pacific decadal climate variability since 1661. *JOC*, 14(1):5–10, 2001.

C.M. Bitz and D.S. Battisti. Interannual to decadal variability in climate and the glacier mass balance in Washington, western Canada and Alaska. *Journal of Climate*, 12:3181–3196, 1999.

T. Blasing and H. Fritts. Reconstructing past climatic anomalies in the north Pacific and western North America from tree rings. *Quaternary Research*, 6:563–579, 1976.

L.H. Blikra and S.F. Selvik. Climatic signals recorded in snow avalanche-dominated colluvium in western Norway: depositional facies successions and pollen records. *The Holocene*, 8(6):631–658, 1998.

J. Bogen. Sediment transport and deposition in mountain rivers. In I.D.L. Foster, A.M. Gurnell, and B.W. Webb, editors, *Sediment and Water Quality in River Catchments*, pages 437–451. John Wiley & Sons, Chichester, 1995.

J. Bogen. Erosion rates and sediment yield of glaciers. *Annals of Glaciology*, 22:48–52, 1996.

G. Bond, W. Broecker, S. Johnsen, J. McManus, L. Labeyrie, J. Jouzel, and G. Bonanl. Correlation between climate records from North Atlantic sediments and Greenland ice. *Nature*, 365(9 September):143–146, 1993.

G. Bond, W. Showers, M. Cheseby, R. Lotti, P. Almasi, P. deMenocal, P. Priore, H. Cullen, I. Hajdas, and G. Bonani. A pervasive millennial-scale cycle in North Atlantic Holocene and glacial climates. *Science*, 278(14 November):1257–1265, 1997.

B.R. Bonsal, A. Shabbar, and K. Higuchi. Impacts of low frequency variability modes on Canadian winter. *International Journal of Climatology*, 21(1):95–108, 2001.

W.M. Borland. Sediment transport of glacier-fed streams in Alaska. *Journal of Geophysical Research*, 66(10):3347–3350, 1961.

G.S. Boulton. Processes of glacial erosion on different substrata. *Journal of Glaciology*, 23(89): 15–38, 1979.

M.J. Bovis and M. Jakob. The July 29, 1998 debris flow and landslide dam at Capricorn Creek, Mount Meager volcanic complex, southern Coast Mountains, British Columbia. *Canadian Journal of Earth Science*, 37:1321–1334, 2000.

G.E.P. Box and D.R. Cox. An analysis of transformations (with discussion). *Journal of the Royal Statistical Society*, 26:211–252, 1964.

R.S. Bradley. *Paleoclimatology: reconstructing climates of the Quaternary*, volume 68 of *International Geophysics Series*. Academic Press, San Diego, 2 edition, 1999.

K.R. Briffa, P.D. Jones, and F.H. Schweingruber. Tree-Ring Reconstructions of Summer Temperature Patterns across Western Nroth America since 1600. *Journal of Climate*, 5:735–754, 1992.

British Columbia Surveys and Resource Mapping Branch. British Columbia Specifications and Guidelines for Geomatics. Technical report, Surveys and Resource Mapping Branch, Ministry of Crown Land, Province of British Columbia, 1990.

W. S. Broecker. Massive iceberg discharges as triggers for global climate change. *Nature*, 372(1): 421–424, 1994.

W.S. Broecker. Thermohaline circulation, the Achilles heel of our climate system: will man-made CO2 upset the current balance ? *Science*, 278(28 November):1582–1588, 1997.

G.R. Brooks. The fluvial reworking of late Pleistocene drift, Squamish River drainage basin, Southwestern British Columbia. *Gographie physique et Quaternaire*, 48(1):51–68, 1994.

D. Brunsden. Tablets of stone: toward the ten commandments of geomorphology. *Zeitschrift fr Geomorphologie*, 79:1–37, 1990.

D. Brunsden. Geomorphological events and landform change. *Zeitschrift fr Geomorphologie*, 40 (3):273–288, 1996.

D. Brunsden and J.B. Thornes. Landscape sensitivity and change. *Transactions, Institute of British Geographers*, 4:463–484, 1979.

C.E. Buell. The number of significant proper functions of two-dimensional fields. *Journal of Applied Meteorology*, 17(6):717–722, 1978.

T.A. Buishand. Some methods for testing homogeneity of rainfall records. *Journal of Hydrology*, 58:11–27, 1982.

N. Caine. Geomorphic coupling of hillslope and channel systems in two small mountain basins. *Zeitschrift fr Geomorphologie*, 33(2):189–203, 1989.

N. Caine. Diurnal streamflow response by seasonal snowcover of an alpine basin. *Journal of Hydrology*, 137:245–260, 1992.

T.N. Caine. Summer rainstorms in an alpine environment and their influence on soil erosion, San Juan Mountains, Colorado. *Arctic and Alpine Research*, 8(2):183–196, 1976.

T.N. Caine. Snowpack influences on geomorphic processes in Green Lakes Valley, Colorado Front Range. *The Geographic Journal*, 161(1):55–68, 1995.

D.R. Cayan. Interannual climate variability and snowpack in the Western United States. *Journal of Climate*, 9:928–948, 1996.

D.R. Cayan, M.D. Dettinger, H.F. Diaz, and N.E. Graham. Decadal variability of precipitation over western North America. *Journal of Climate*, 11:3148–3166, 1998.

D.R. Cayan, J.V. Gardner, J.M. Landwehr, J. Namias, and D.H. Peterson. Introduction. In D.H. Peterson, editor, *Aspects of climate variability in the Pacific and Western Americas*, volume Geophysical Monograph 55, pages xiii–xvi. American Geophysical Union, Washington, D.C., 1989.

D.R. Cayan and D.H. Peterson. The influence of North Pacific atmospheric circulation on streamflow in the west. In D.H. Peterson, editor, *Aspects of climate variability in the Pacific and Western Americas*, volume Geophysical Monograph 55, pages 375–397. American Geophysical Union, Washington, D.C., 1989.

D.R. Cayan, K.T. Redmond, and L.G. Riddle. ENSO and hydrologic extremes in the western United States. *Journal of Climate*, 12:2881–2893, 1999.

X. Cheng, G. Nitsche, and J.M. Wallace. Robustness of low-frequency circulation patterns derived from EOF and rotated EOF analysis. *Journal of Climate*, 9:2003–2009, 1995.

M. Church. Records of recent geomorphological events. In R.A. Cullingford, D.A. Davidson, and J. Lewin, editors, *Timescales in Geomorphology*, pages 13–29. John Wiley & Sons, London, 1980.

M. Church. Regionalised hydrological estimates for British Columbia: first approximation of scale effects. Technical report, Resources Inventory and Data Management Branch, January 31, 1997 1997.

M. Church, R. Kellerhals, and T.J. Day. Regional clastic sediment yield in British Columbia. *Canadian Journal of Earth Sciences*, 26(31):31–45, 1989.

M. Church and M.J. Miles. Meteorological antecedents to debris flow in southwestern British Columbia; some case studies. In J.E. Costa and G.F. Wieczorek, editors, *Debris Flows/Avalanches: Process, Recognition, and Mitigation. Reviews in Engineering Geology*, volume VII, pages 63–80. Geological Society of America, Boulder, 1987.

M. Church and J.M. Ryder. Paraglacial sedimentation: a consideration for fluvial processes conditioned by glaciation. *Geological Society of America Bulletin*, 83:3059–3072, 1972.

M. Church and O. Slaymaker. Disequilibrium of holocene sediment yield in glaciated British Columbia. *Nature*, 337(2 February):452–454, 1989.

J.J. Clague, S.G. Evans, V.N. Rampton, and G.J. Woodsworth. Improved age estimates for the White River and Bridge River tephras, western Canada. *Canadian Journal of Earth Science*, 32: 1172–1179, 1995.

J.J. Clague and R.W. Mathewes. Early Holocene thermal maximum in western North America: new evidence from Castle Peak, British Columbia. *Geology*, 17:277–280, 1989.

J.J. Clague and R.W. Mathewes. Neoglaciation, glacier-dammed lakes, and vegetation change in northwestern British Columbia, Canada. *Arctic and Alpine Research*, 28(1):10–24, 1996.

J.J. Clague and W.H. Mathews. The sedimentary record of Neoglacial Tide Lake, northwestern British Columbia. *Canadian Journal of Earth Science*, 29:2383–2396, 1992.

W.S. Cleveland. Robust locally weighted regression and smoothing scatterplots. *Journal of the American Statistical Association*, 74:829–836, 1979.

A.S. Cohen. Effect of zoobenthic standing crop of laminae preservation in tropical lake sediment, Lake Turkana, east Africa. *Journal of Paleontology*, 58(2):499–510, 1984.

Contributors of the International Tree-Ring Data Bank, 2001.

E.R. Cook, K.R. Briffa, D.M. Meko, D.A. Graybill, and G. Funkhouser. The 'segment length curse' in long tree-ring chronology development for paleoclimatic studies. *The Holocene*, 5(2): 229–237, 1995.

G.D. Corner. Avalanche impact landforms in Troms, north Norway. *Geographiska Annaler*, 62A (1-2):1–10, 1980.

J.E. Costa and O'Connor. Geomorphically Effective Floods. In J.E. Costa, A.J. Miller, K.W. Potter, and P.R. Wilcock, editors, *Natural and Anthropogenic Influences in Fluvial Geomorphology*, volume Geophysical Monograph 89. American Geophysical Union, Washington D.C., 1995.

S. Dahl and A. Nesje. A new approach to calculating Holocene winter precipitation by combining glacier equilibrium line altitudes and pine-tree limits: a case study from Hardangerjokulen, central south Norway. *The Holocene*, 6:381–398, 1996.

P.E. Damon and T.W. Cheng, S.and Linick. Fine and hyperfine structure in the spectrum of secular variations of atmospheric 14C. *Radiocarbon*, 31(3):704–718, 1989.

J.C. Davis. *Statistics and Data Analysis in Geology.* John Wiley & Sons, New York, 2 edition, 1986.

P.T. Davis. Holocene glacier fluctuations in the American Cordillera. *Quaternary Science Reviews*, 7:129–157, 1988.

A.C. Davison and D.V. Hinkley. *Bootstrap Methods and their Application.* Cambridge Series in Statistical and Probabilistic Mathematics. Cambridge University Press, 1997.

W.E. Dean. Determination of carbonate and organic matter in calcareous sediments and sedimentary rocks by loss on ignition: comparision with other methods. *Journal of Sedimentary Petrology*, 44(1):242–248, 1974.

W.E. Dean. Physical properties, mineralogy, and geochemistry of Holocene varved sediments from Elk Lake, Minnesota. In J.P. Bradbury and W.E. Dean, editors, *Elk Lake, Minnesota: Evidence for Rapid Climate Change in the North-Central United States*, volume Special Paper 276, pages 135–157. Geological Society of America, Boulder, 1993.

W.E. Dean, T.S. Ahlbrandt, R.Y. Anderson, and J.P. Bradbury. Regional aridity in North America during the middle Holocene. *The Holocene*, 6(2):145–155, 1996.

G.H. Denton and W. Karlen. Holocene climatic variations-their pattern and possible causes. *Quaternary Research*, 3(155-205), 1973.

J. R. Desloges and R. Gilbert. The record of extreme hydrological and geomorphological events inferred from glaciolacustrine sediments. In *Proceedings of the Canberra Symposium*, volume 224 of *Variability and Stream Erosion and Sediment Transport*, pages 133–142, Canberra, 1994a. International Association of Hydrologic Sciences.

J.R. Desloges. *Paleohydrology of the Bella Coola River Basin: an assessment of environmental reconstruction.* Ph.d., University of British Columbia, 1987.

J.R. Desloges. Geomorphic and climatic interpretations of abrupt changes in glaciolacustrine deposition at Moose Lake, British Columbia, Canada. *JFF*, 121:202–207, 1999.

J.R. Desloges and R. Gilbert. Sediment source and hydroclimatic inferences from glacial lake sediments: the postglacial sedimentary record of Lillooet Lake, British Columbia. *Journal of Hydrology*, 159(3):375–393, 1994b.

J.R. Desloges and R. Gilbert. The sedimentary record of Moose Lake: implications for glacier activity in the Mount Robson area, British Columbia. *Canadian Journal of Earth Science*, 32: 65–78, 1995.

J.R. Desloges and R. Gilbert. Sedimentation in Chilko Lake: a record of the geomorphic environment of the eastern Coast Mountains of British Columbia, Canada. *Geomorphology*, 25:75–91, 1998.

J.R. Desloges and J.M. Ryder. Neoglacial history of the Coast Mountains near Bella Coola, British Columbia. *Canadian Journal of Earth Science*, 27:281–290, 1990.

R.W. Dirszowsky and J.R. Desloges. Glaciolacustrine sediments and neoglacial history of the Chephren Lake basin, Banff National Park, Alberta. *Geographie physique et Quaternaire*, 51(1): 1–14, 1997.

D. Drewry. *Glacial Geologic Processes.* Edward Arnold, London, 1986.

C.C. Ebbesmeyer, D.R. Cayan, F.H. McLain, D.R. Nichols, D.H. Peterson, and K.T. Redmond. 1976 step in the Pacific climate: forty environmental changes between 1968-1975 and 1977-1984. Technical Report Interagency Ecological Studies Program Technical Report 26, California Dept. of Water Resources, 1991.

I. Evans. Climatic effects of glacier distribution across the southern Coast Mountains. *Annals of Glaciology*, 14:58–64, 1990.

M. Evans. *Holocene sediment yield and geomorphic sensitivity in alpine landscapes, Cathedral Lakes, British Columbia.* Ph.d., University of British Columbia, 1997.

M.G. Evans. Neoglacial climate in the Southern Coast Mountains. Master's thesis, University of British Columbia, 1993.

C.R. Fenn. Quantifying the errors in transferring suspended sediment rating equations across ablation seasons. *Annals of Glaciology*, 13:64–68, 1989.

R.I. Ferguson. River loads underestimated by rating curves. *Water Resources Research*, 22(1): 74–76, 1986.

D.J. Finney. On the distribution of a variable whose logarithm is normally distributed. *J.R. Stat. Society. London, Ser. B,*, 7:155–161, 1941.

B.B. Fitzharris and I.F. Owens. Avalanche tarns. *Journal of Glaciology*, 30(106):308–312, 1984.

I. D.L. Foster, J.A. Dearing, R. Grew, and K. Orend. The sedimentary data base: an appraisal of lake and reservoir sediment based studies of sediment yield. In D.E. Walling, A. Yair, and S. Berkkowicz, editors, *Erosion, Transport and Depositional Processes*, volume I.A.H.S. Publ. no. 189, pages 19–43, Proc. of the Jerusalem Workshop, March-April 1987, 1990.

I.D. L. Foster, J.A. Dearing, and R. Grew. Lake-catchments: an evaluation of their contribution to studies of sediment yield and delivery processes. In M.P. Bordas and D.E. Walling, editors, *Sediment Budgets*, volume Pub 174, pages 413–424. IAHS Press, Oxfordshire, 1988.

H.C. Fritts. *Tree rings and climate.* Academic Press, San Diego, California, 1976.

H.C. Fritts. *Reconstructing Large-scale Climatic Patterns from Tree-Ring Data.* The University of Arizona Press, Tucson, Arizona, 1991.

S.R. Fuller, D.J. Easterbrook, and R.M. Burke. Holocene glacial activity in five valleys on the flanks of Mt. Baker, Washington. *Geological Society of America, Abstracts with Programs*, 15: 430–431, 1983.

Stephen J. Gale and Peter G. Hoare. *Quaternary Sediments.* Bellhaven Press, London., 1991.

J. Gardner. Geomorphic significance of avalanches in the Lake Louise area, Alberta Canada. *Arctic and Alpine Research*, 2(2):135–144, 1970.

Z. Gedalof and D.J. Smith. Interdecadal climate variability and regime-scale shifts in Pacific North America. *Geophysical Research Letters*, 28(8):1515–1519, 2001.

A Gershunov, T.P. Barnett, and D. Cayan. North Pacific Interdecadal Oscillation seen as a factor in ENSO-related North American climate anomalies. *EOS transactions*, 80(3):25–30, 1999.

A. Gershunoz and T.P. Barnett. Interdecadal modulation of ENSO teleconnections. *Bulletin of the American Meteorological Society*, 79(12):2715–2725, 1998.

B. Gilbert. *Observations of lacustrine sedimentation at Lillooet Lake, British Columbia.* PhD thesis, University of British Columbia, 1973.

G.K. Gilbert. Hydraulic-mining debris in the Sierra Nevada. Technical Report Professional Paper 105, United States Geological Survey, 1917.

R. Gilbert. Sedimentation in Lillooet Lake, British Columbia. *Canadian Journal of Earth Sciences*, 12(10):1697–1711, 1975.

R. Gilbert. Glacilacustrine environment of part of the Oak Ridges Moraine, southern Ontario. *Gographie physique et Quaternaire*, 51(1):55–66, 1997.

R. Gilbert, J.R. Desloges, and J.J. Clague. The glacilacustrine sedimentary environment of Bowser Lake in the northern Coast Mountains of British Columbia, Canada. *Journal of Paleolimnology*, 17:331–346, 1997.

D.L. Gilman, F.J. Fuglister, and J.M. Mitchell. On the power spectrum of "red noise". *Journal of the atmospheric sciences*, 20:182–184, 1963.

G. Golder Associates. Report on geotechnical investigation and stability analysis Fitzsimmons Creek Slide, Whistler, B.C. Technical report, Golder Associates, Vancouver, B.C., February 1992.

L. Granar. Dating of recent fluvial sediments from the estuary of the Angerman River. *Geol. Foren. Forhandlung*, 78:654–658, 1956.

L.J. Graumlich and L.B. Brubaker. Reconstruction of annual temperature (1590-1979) for Longmire, Washington, derived from tree rings. *Quaternary Research*, 25:223–234, 1986.

J. C. Griffiths. *Scientific method in analysis of sediments.* McGraw-Hill, New York, 1967.

K.A. Grimm, C.B. Lange, and A. Gill. Biological forcing of hemipelagic sedimentary laminae: evidence from ODP site 893, Santa Barbara Basin, California. *Journal of Sedimentary Research*, 66(3):613–624, 1996.

A.M. Gurnell. Suspended sediment. In A.M. Gurnell and M.J. Clark, editors, *Glacio-fluvial sediment transfer: an alpine perspective*, pages 305–354. John Wiley and Sons, Chicester, UK, 1987.

A.M. Gurnell. Sediment yield from alpine glacier basins. In I.D.L. Foster, A.M. Gurnell, and B.W. Webb, editors, *Sediment and Water Quality in River Catchments*, pages 407–435. John Wiley & Sons Ltd., Chichester, 1995.

A.M. Gurnell and C.R. Fenn. Box-Jenkins transfer function models applied to suspended sediment concentration-discharge relationships in a proglacial stream. *Arctic and Alpine Research*, 16(1): 93–106, 1984.

L. Haknson. Determination of characteristic values for physical and chemical lake sediment parameters. *Water Resources Research*, 17(6):1625–1640, 1981.

S. Haldorsen. Grain-size distribution of subglacial till and its relation to subglacial crushing and abrasion. *Boreas*, 10:91–105, 1981.

B. Hallet. A theoretical model of glacial abrasion. *Journal of Glaciology*, 23(89):39–50, 1979.

B. Hallet, L. Hunter, and J. Bogen. Rates of erosion and sediment evacuation by glaciers: A review of field data and their implications. *Global and Planetary Change*, 12:213–235, 1996.

D.J. Hallett, L.V. Hills, and J.J. Clague. New accelerator mass spectrometry radiocarbon ages for the Mazama tephra layer from Kootenay National Park, British Columbia, Canada. *Canadian Journal of Earth Sciences*, 34:1202–1209, 1997.

D.G. Ham and M. Church. Bed-material transport estimated from channel morphodynamics: Chilliwack River, British Columbia. *Earth Surface Processes and Landforms*, 25:1123–1142, 2000.

C. Hammer, P.A. Mayewski, D. Peel, and M. Stuiver. Preface-Greenland Summit Ice Cores. *Journal of Geophysical Research*, 102(C12):26315–26316, 1997.

J. Harbor and J. Warburton. Relative rates of glacial and nonglacial erosion in alpine environments. *Arctic and Alpine Research*, 25(1):1–7, 1993.

R.M. Hardy, N.R. Morgenstern, and F.D. Patton. Report of the Garibaldi Advisory Panel Part II. Technical report, British Columbia Department of Highways, 1978.

J.T. Harper. Glacier terminus fluctuations on Mount Baker, Washington, USA, 1940-1990, and climatic fluctuations. *Arctic and Alpine Research*, 25(4):332–340, 1993.

D.L. Hartmann. *Objective Analysis: ATM 552 Class Notes*. University of Washington, Department of Atmospheric Science, 2001.

M. Hassan, O. Slaymaker, and S. Berkowicz, editors. *The hydrology-geomorphology Interface: Rainfall, floods, sedimentation, land use*, number 261, 2000. IAHS.

C.J. Heaney. *The Northern Cordilleran*, chapter The topography of the Vancouver or Britannia Range, pages 19–32. The British Columbia Mountaineering Club, 1912.

R.J. Hebda. British Columbia vegetation and climate history with focus on 6 KA BP. *Gographie physique et Quaternaire*, 49(1):55–79, 1995.

B.J. Hegge and G. Masselink. Spectral analysis of geomorphic time series: auto-spectrum. *Earth Surface Processes and Landforms*, 21:1021–1040, 1996.

J.T. Heine. Extent, timing and climatic implications of glacier advances Mount Rainier, Washington, USA, at the Pleistocene/Holocene transition. *Quaternary Science Reviews*, 17:1139–1148, 1998.

H.G. Heinemann. A new sediment trap efficiency curve for small reservoirs. *Water Resources Bulletin*, 17(5):825–830, 1981.

E.J. Hickin. Contemporary Squamish River sediment fluxes to Howe Sound, British Columbia. *Canadian Journal of Earth Sciences*, 26:1953–1963, 1989.

D.M. Hicks, M.J. McSaveney, and T.J.H. Chinn. Sedimentation in proglacial Ivory Lake, Southern Alps, New Zealand. *Arctic and Alpine Research*, 22(1):26–42, 1990.

R.W. Higgins, J. Schemm, and A. Leetmaa. Extreme precipitation events in the western United States related to tropical forcing. *Journal of Climate*, 13:793–820, 2000.

L.. Hkanson and M Jansson. *Principles of lake sedimentology.* Springer-Verlag., New York:, 1983.

R.R. Hocking. *Method and Applications of Linear Models.* John Wiley & Sons, New York, 1996.

S.M. Hodge, D.C. Trabant, R.M. Krimmel, T.A. Heinrichs, R.S. March, and E.G. Josberger. Climate variations and changes in mass of three glaciers in western North America. *Journal of Climate*, 11:2161–2179, 1998.

R.L. Holmes. Computer-assisted quality control in tree-ring dating and measurement. *Tree-Ring Bulletin*, 44:69–75, 1983.

R.W. Holmes. Dendrochronology Program Library. Instruction and Program Manual. Technical Report 35 p., Tree-Ring Laboratory, University of Arizona, 1992.

R. Holmlund, H. Burman, and T. Rost. Sediment-mass exchange between turbid meltwater streams and proglacial deposits of Storglaciaren, northern Sweden. *AOG*, 22:63–67, 1996.

L.L. Hood and J.L. Jirikowic. Recurring variations of probable solar origin in the atmospheric delta 14C time record. *Geophysical Research Letters*, 17(1):85–88, 1990.

R. Hooke. Toward a uniform theory of clastic sediment yield in fluvial systems. *Geological Society of America Bulletin*, 112(12):1778–1786, 2000.

K.A. Hughen, J.T. Overpeck, and R.F. Anderson. Recent warming in a 500-year paleotemperature record from varved sediments, upper Soper Lake, Baffin Island, Canada. *The Holocene*, 10(1): 9–19, 2000a.

K.A. Hughen, J.R. Southon, S. Lehman, and J. Overpeck. Synchronous Radiocarbon and Climate Shift during the last deglaciation. *Science*, 290:1951–1954, 2000b.

M. Hulme. A 1951-80 global precipitation climatology for the evaluation of General Circulation Models. *Climate Dynamics*, 7:57–72, 1992.

M. Hulme, T.J. Osborn, and T.C. Johns. Precipitation sensitivity to global warming: Comparision of observations with HadCM2 simulations. *Geophysical Research Letters*, 25:3379–3382, 1998.

N.F. Humphrey and C.F. Raymond. Hydrology, erosion and sediment production in a surging glacier: Variegated Glacier. *Journal of Glaciology*, 40:539–552, 1994.

A.G. Hunt and A.A. Tsonis. On the Pacific decadal oscillation and associated long-term climate prediction. *EOS*, 81(48):581, 2000.

H.E. Hurst. Long-term storage capacity of reservoirs. *Transactions of the American Society of Civil Engineers*, 116:770, 1951.

Ross Ihaka and Robert Gentleman. R: A Language for Data Analysis and Graphics. *Journal of Computational and Graphical Statistics*, 5(3):299–314, 1996.

A. Iken and R.A. Bindshadler. Combined measurements of subglacial water pressure and surface velocity of Findelengletscher, Switzerland: conclusions about drainage system and sliding mechanisms. *Journal of Glaciology*, 32(110):101–119, 1986.

A. Iken, H. Rothlisberger, A. Flotron, and W. Haeberli. The uplift of unteraargletscher at the beginning of the melt season-a consequence of water storage at the bed? *Journal of Glaciology*, 29(101):28–47, 1983.

M. Jakob. *Morphometric and geotechnical controls of debris flow frequency and magnitude.* Ph.d., University of British Columbia, 1996.

T. Jhannesson, C. Raymond, and E. Waddington. Time scale for adjustment of glaciers to changes in mass balance. *Journal of Glaciology*, 35:355–369, 1989a.

T. Jhannesson, C.F. Raymond, and E.D. Waddington. A simple method for determining the response time of glaciers. In J. Oerlemans, editor, *Glacier Fluctuations and Climatic Change*, pages 343–352. Kluwer Academic Publishers, Dordrecht, 1989b.

P.D. Jones. Hemispheric surface air temperature variations: a reanalysis and update to 1993. *Journal of Climate*, 7:1794–1892, 1994.

P.D. Jones, M. New, D.E. Parker, S Martin, and I.G. Rigor. Surface air temperature and its changes over the past 150 years. *Review of Geophysics*, 37(2):173–199, 1999.

P. Jordan and O. Slaymaker. Holocene sediment production in Lillooet Basin, British Columbia: a sediment budget approach. *Gographie physique et Quaternaire*, 45(1):45–57, 1991.

J. Jouzel, R.B. Alley, K.M. Cuffey, W. Dansgaard, P. Grootes, S.J. Hoffmann, R.D. Koster, C.A. Shurman, M. Stievenard, M. Stuiver, and J. White. Validity of the temperature reconstruction from water isotopes in ice cores. *Journal of Geophysical Research*, 102(C12):26471–26487, 1997.

E. Kalnay and Coauthors. The NCEP/NCAR Reanlysis 40-year project. *Bulletin of the American Meteorological Society*, 77:437–471, 1996.

T. Karl, A. Koscielny, and H. Diaz. Potential errors in the application of principal component (eigenvectors) analysis to geophysical data. *Journal of applied meteorology*, 21:1183–1186, 1982.

W. Karln. Lacustrine sediments and tree-limit variations as indicators of Holocene climatic fluctuations in Lappland, Northern Sweden. *Geografiska Annaler*, 58A,:1–34, 1976.

W. Karln. Lacustrine sediment studies. *Geografiska Annaler*, 63A:273–281, 1981.

W. Karln. Scandinavian glacial and climatic fluctuations during the Holocene. *Quaternary Science Reviews*, 7:199–209, 1988.

J.T.O. Kirk. Effects of suspensoids (turbidity) on penetration of solar radiation in aquatic ecosystems. *Hydrobiologia*, 125:195–208, 1985.

A. Lambert and K.J. Hs. Non-annual cycles of varve-like sedimentation in Walesee, Switzerland. *Sedimentology*, 26:453–461, 1976.

A. Lambert, K. R. Kelts, and N.F. Marshall. Measurements of density underflows from Walensee, Switzerland. *Sedimentology*, 23:87–105, 1976.

S. Lamoureux. Five centuries of interannual sediment yield and rainfall-induced erosion in the Canadian high arctic recorded in lacustrine varves. *Water Resources Research*, 36(1):309–318, 2000.

S. F. Lamoureux. Embedding unfrozen lake sediments for thin section preparation. *Journal of Paleolimnology*, 10:141–146, 1994.

S. F. Lamoureux and R. S. Bradley. A late Holocene varved sediment record of environmental change from northern Ellesmere Island, Canada. *Journal of Paleolimnology*, 16:239–255, 1996.

S.F. Lamoureux. Catchment and lake controls over the formation of varves in monomictic Nicolay Lake, Cornwall Island, Nunavut. *Canadian Journal of Earth Sciences*, 36:1533–1546, 1999a.

S.F. Lamoureux. Spatial and interannual variations in sedimentation patterns recorded in nonglacial varved sediments from the Canadian high arctic. *Journal of Paleolimnology*, 21:73–84, 1999b.

W.B. Langbein and S.A. Schumm. Yield of sediment in relation to mean annual precipitation. *Transactions of the American Geophysical Union*, 39:1076–1084, 1958.

A. Leemann and F. Niessen. Varve formation and the climatic record in an alpine proglacial lake: calibrating annually-laminated sediments against hydrological and meteorological data. *The Holocene*, 4(1):1–8, 1994.

C.E. Leith. The standard error of time-average estimates of climatic means. *Journal of Applied Meteorology*, 12:1066–1069, 1973.

E. Leonard. An assessment of sediment loss and distortion at the top of short gravity cores. *Sedimentary Geology*, 66:57–63, 1990.

E.M. Leonard. Use of sedimentary sequences as indicators of Holocene glacial history, Banff National Park, Alberta. *Quaternary Research*, 26:218–231, 1986a.

E.M. Leonard. Varve studies at Hector Lake, Alberta, Canada, and the relationship between glacial activity and sedimentation. *Quaternary Research*, 25:199–214, 1986b.

E.M. Leonard. A varve-based calibration of the Bridge River tephra fall. *Canadian Journal of Earth Science*, 32:2098–2102, 1995.

E.M. Leonard. The relationship between glacial activity and sediment production: evidence from a 4450-year varve record of neoglacial sedimentation at Hector Lake, Alberta, Canada. *Journal of Paleolimnology*, 17:319–330, 1997.

E.M. Leonard and M.A. Reasoner. A continuous Holocene glacial record inferred from proglacial lake sediments in Banff National Park, Alberta, Canada. *Quaternary Research*, 51:1–13, 1999.

H.F. Lins. Regional streamflow regimes and hydroclimatology of the United States. *Water Resources Research*, 33(7):1655–1667, 1997.

B.K. Linsey, G.M. Wellington, and D.P. Shrag. Decadal sea surface temperature variability in the subtropical South Pacific from 1726 to 1997AD. *Science*, 290:1145–1148, 2000.

T.E. Lisle. Understanding the role of sediment waves and channel conditions over time and space. In S. Sommarstrom, editor, *Proceedings of the Sixth Biennial Watershed Management Conference*, volume 92, pages 57–67, Lake Tahoe, California, 1997. University of California Water Resources Center,.

T.E. Lisle, J.E. Pizzuto, H. Ikeda, F. Iseya, and Y. Kodama. Evolution of a sediment wave in an experimental channel. *Water Resources Research*, 33(8):1971–1981, 1997.

D.S. Lloyd, J.P. Koenings, and J.D. LaPerriere. Effects of turbidity in fresh waters of Alaska. *North American Journal of Fisheries Management*, 7:18–33, 1987.

E.N. Lorenz. An experiment in nonlinear statistical weather forcasting. *Monthly weather review*, 105:590–602, 1977.

J.A. Lowdon and W. Blake. Radiocarbon dates. *Geological Survey of Canada Paper*, 75-7:1–32, 1975.

B.H. Luckman. Dropstones resulting from snow avalanche deposition on lake ice. *Journal of Glaciology*, 14(7):186, 1975.

B.H. Luckman. The geomorphic activity of snow avalanches. *Geografiska Annaler*, 59A(1-2):31–48, 1977.

B.H. Luckman. Debris flows and snow avalanche landforms in the Lairig Ghru, Cairngorm Mountains, Scotland. *Geografiska Annaler*, 74A(2-3):109–121, 1992.

B.H. Luckman. Glacier fluctuations and tree-ring records for the last millennium in the Canadian Rockies. *Quaternary Science Reviews*, 12:441–450, 1993.

B.H. Luckman. Evidence for climatic conditions between ca. 900-1300 A.D. in the southern Canadian Rockies. *Climatic Change*, 26:171–182, 1994.

B.H. Luckman. The Little Ice Age in the Canadian Rockies. *Geomorphology*, 32(3-4):357–384, 2000.

B.H. Luckman, K.R. Briffa, P.D. Jones, and F.H. Schweingruber. Tree-ring based reconstruction of summer temperatures at the Columbia Icefield, Alberta, Canada, AD 1073-1983. *The Holocene*, 7(4):375–389, 1997.

B.H. Luckman, G. Holdsworth, and G.D. Osborn. Neoglacial glacial fluctuations in the Canadian Rockies. *Quaternary Research*, 39:144–153, 1993.

B.H. Luckman and G.D. Osborn. Holocene glacier fluctuations in the middle Canadian Rocky Mountains. *Quaternary Research*, 11:52–77, 1979.

B.H. Luckman and R. Villalba. Assessing the synchroneity of glacier fluctuations in the western cordillera of the Americas during the last millennium. In V. Markgraf, editor, *Interhemispheric climate linkages*, chapter 8, pages 121–140. Academic Press, San Diego, CA, 2002.

B. Mandelbrot and J. Wallis. Noah, Joseph, and operational hydrology. *Water Resources Research*, 4(5):909–918, 1968.

M.E. Mann, R.S. Bradley, and M. Hughes. Global-scale temperature patterns and climate forcing over the past six centuries. *Nature*, 392(23 April):779–787, 1998.

M.E. Mann, R.S. Bradley, and M.K. Hughes. Northern hemisphere temperatures during the past millennium: inferences, uncertainties, and limitations. *Geophysical Research Letters*, 26(6): 759–762, 1999.

M.E. Mann and J.M. Lees. Robust estimation of background noise and signal detection in climatic time series. *Climatic Change*, 33:409–445, 1996.

N. J. Mantua, S.R. Hare, Y. Zhang, J.M. Wallace, and R.C. Francis. A Pacific interdecadal climate oscillation with impacts on salmon production. *Bulletin of the American Meteorological Society*, 78(6):1069–1079, 1997.

N.J. Mantua and S.R. Hare. The Pacific Decadal Oscillation. *Journal of Oceanography*, 58:35–44, 2002.

R.W. Mathewes and J.A. Westgate. Bridge River Tephra: revised distribution and significance for detecting old carbon errors in radiocarbon dates of limnic sediments in southern British Columbia. *Canadian Journal of Earth Science*, 17:1454–1461, 1980.

W.H. Mathews. Historic and prehistoric fluctuations of alpine glaciers in Mt. Garibaldi map-ara, southwestern British Columbia. *Journal of Geology*, 59(4):357–381, 1951.

P.A. Mayewski, L.D. Meeker, M.C. Morrison, M.S. Twickler, S.I. Whitlow, K.K. Ferland, D.A. Meese, M.R. Legrand, and J.P. Steffensen. Greenland ice core "signal" characteristics: an expanded view of climate change. *Journal of Geophysical Research*, 98(D7):12,839–12,847, 1993.

P.A. Mayewski, L.D. Meeker, S. Whitlow, M.S. Twickler, M.C. Morrison, P. Bloomfield, G.C. Bond, R.B. Alley, A.J. Gow, P.M. Grootes, D.A. Meese, M. Ram, K.C. Taylor, and W. Wumkes. Changes in atmospheric circulation and ocean changes in ice cover of the North Atlantic during the last 41,000 years. *Science*, 263:1747–1750, 1994.

E. Mekis and W.D. Hogg. Rehabilitation and analysis of Canadian daily precipitation time series. *Atmosphere-Ocean*, 37(1):53–85, 1999.

D. Meko, E.R. Cook, D.W. Stahle, C.W. Stockton, and M.C. Hughes. Spatial Patterns of tree-growth in the United States and southeastern Canada. *Journal of Climate*, 6(9):1773–1786, 1993.

A.M. Melone. Flood producing mechanisms in coastal British Columbia. *Canadian Water Resources Journal*, 10(3):46–64, 1985.

B. Menounos. The water content of lake sediments and its relationship to other physical parameters: an alpine case study. *The Holocene*, 7(2):207–212, 1997.

B. Menounos. A Holocene debris-flow chronology for an alpine catchment, Colorado Front Range. In O. Slaymaker, editor, *Geomorphology, Human Activity, and Global Environmental Change*, pages 117–149. John Wiley & Sons, Chichester, UK, 2000.

J. Menzies and W.W. Shilts. Past Glacial Environments. chapter Subglacial environments, pages 15–136. Butterworth-Heinemann, 1996.

A. Mestas-Nunez. Orthogonality properties of rotated empirical modes. *International Journal of Climatology*, 20:1509–1516, 2000.

S. Minobe. A 50-70 year climate oscillation over the North Pacific and North America. *Geophysical Research Letters*, 24(6):683–686, 1997.

Jr. Mitchell, J.M. An overview of climatic variability and its causal mechanisms. *Quaternary Research*, 6:481–493, 1976.

J.W.S. Monger and J.M. Journeay. Guide to the geology and tectonic evolution of the Southern Coast Mountains. Open file reort 2490, Geological Survey of Canada, 1994.

R.D. Moore. Snowpack and runoff responses to climatic variability, southern Coast Mountains, British Columbia. *Northwest Science*, 70:321–333, 1996.

R.D. Moore and M.N. Demuth. Mass balance and streamflow variability at Place Glacier, Canada in relation to recent climate fluctuations. *Hydrologic Processes*, 15:3473–3486, 2001.

R.D. Moore and I.G. McKendry. Spring snowpack anomaly patterns and winter climatic variability, British Columbia, Canada. *Water Resources Research*, 32(3):623–632, 1996.

D.R. Muhs, R.M. Thornson, J.J. Clague, W.H. Mathews, P.F. McDowell, and H.M. Kelsey. Pacific Coast and mountain system. In W.L. Graf, editor, *Geomorphic systems of North America*, volume Centennial Special Volume 2, pages 517–581. Geological Society of America, Boulder, Colorado, 1986.

G.R. North, T. Bell, R. Cahalan, and F. Moeng. Sampling errors in the estimation of empirical orthogonal functions. *Monthly Weather Review*, 110:699–706, 1982.

E.B. Nuhfer, R.Y. Anderson, J.P. Bladburry, and W.E. Dean. Modern sedimentation in Elk Lake, Clearwater County, Minnesota. In J.P. Bradburry and W.E. Dean, editors, *Elk Lake Minnesota: Evidence for Rapid Climate Change in the North-Central United States: Geological Society of America Special Paper 276*, pages 75–96. Geological Society of America, Boulder, 1993.

J.F. Nye. The response of a glacier to changes in the rate of nourishment and wastage. *Proceedings of the Royal Society A*, A 275(1360):876–112, 1963.

S. O'Brien, P. Mayewski, L. Meeker, D. Meese, M. Twickler, and S. Whitlow. Complexity of Holocene climate as reconstructed from a Greenland ice core. *Science*, 270(22 December 1995): 1962–1963, 1995.

C. Ohlendorf, F. Niessen, and H. Weissert. Glacial varve thickness and 127 years of instrumental climate data: a comparison. *Climatic Change*, 36:391–411, 1997.

G. Osborn. Lateral-moraine stratigraphy and Neoglacial history of Bugaboo Glacier, British Columbia. *Quaternary Research*, 26:171–178, 1986.

G. Osborn and E.T. Karlstrom. Holocene fluctuations of the Bugaboo Glacier, British Columbia, inferred from superimposed tills and paleosols. *Geological Society of America Abstracts with Programs*, 18:712, 1986.

G.D. Osborn and B.H. Luckman. Holocene glacier fluctuations in the Canadian Cordillera. *Quaternary Science Reviews*, 7:115–128, 1988.

P.E. O'Sullivan. Annually-laminated lake sediments and the study of Quaternary environmental change–a review. *Quaternary Science Reviews*, 1:245–313, 1983.

M.J. Page, N.A. Trustrum, and R.C. DeRose. A high resolution record of storm-induced erosion from lake sediments, New Zealand. *Journal of Paleolimnology*, 11:333–348, 1994.

D. Parker, P. Jones, A. Bevan, and C. Folland. Interdecadal changes of surface temperature since the late 19th century. *Journal of Geophysical Research*, 99:14373–13399, 1994.

W.S.B. Patterson. *The physics of glaciers.* Pergamon, Oxford, 3 edition, 1994.

M.G. Pellatt and R.W. Mathewes. Holocene tree line and climate change on the Queen Charlotte Islands, Canada. *Quaternary Research*, 48:88–99, 1997.

C.P. Pepola. Bed-material transport rate derived from delta progradation in a small alpine basin, Fitzsimmons Creek, Coast Mountains, British Columbia. Master's thesis, Simon Fraser University, 2001.

J.A. Perkins and J.D. Sims. Correlation of Alaskan varve thickness with climatic parameters, and use in paleoclimatic reconstruction. *Quaternary Research*, 20:308–321, 1983.

D.H. Peterson, R.E. Smith, M.D. Dettinger, D.R. Cayan, and L. Riddle. An organized signal in snowmelt runoff over the western United States. *Journal of the American Water Resources Association*, 36(2):421–432, 2000.

T.C. Peterson and R.S. Vose. An overview of the global historical climatology network temperature data base. *Bulletin of the American meteorological society*, 78:2837–2849, 1997.

J. Pike and A.E. Kemp. Preparation and analysis techniques for studies of laminated sediments. In A.E.S. Kemp, editor, *Palaeoclimatology and Palaeoceanography from Laminated Sediments*, volume Geological Society Special Publication No. 116, pages 37–48. London Geology Society, London, 1996.

J. Pitlick. Response and recovery of a subalpine stream following a catastrophic flood. *Geological Society of America Bulletin*, 105:657–670, 1993.

S.C. Porter. Present and past glaciation threshold in the Cascade range, Washington, USA: topographic and climatic controls, and paleoclimatic implications. *Journal of Glaciology*, 18(78): 101–116, 1977.

R.W. Preisendorfer. *Principal Component analysis in meteorology and oceanography.* Elsivier, Amsterdam, 1988.

W. Press, S. Teukolsky, W. Vetterling, and B. Flannery. *Numerical Recipes in C: the art of scientific computing.* Cambridge University Press, Cambridge, 1986.

M. A. Reasoner and R.E. Healy. Identification and significance of tephras encountered in a core from Mary Lake, Yoho National Park, British Columbia. *Canadian Journal of Earth Science*, 23: 1991–1999, 1986.

M.A. Reasoner. Equipment and procedure improvements for a lightweight, inexpensive, percussion core sampling system. *Journal of Paleolimnology*, 8:273–281, 1993.

M.A. Reasoner, P.T. Davis, and G. Osborn. Evaluation of proposed early-Holocene advances of alpine glaciers in the north Cascade Range, Washington state, USA: constraints provided by paleoenvironmental reconstructions. *The Holocene*, 11(5):607–611, 2001.

M.A. Reasoner and M. Hickman. Late Quaternary environmental change in the Lake O'Hara region, Yoho National Park, British Columbia. *Palaeogeography, Palaeoclimatology, Palaeoecology*, 72:291–316, 1989.

M.A. Reasoner, G. Osborn, and N.W. Rutter. Age of the Crowfoot Advance in the Canadian Rocky Mountains: a glacial event coeval with the Younger Dryas oscillation. *Geology*, 22:439–442, 1994.

K.T. Redmond and R.W. Koch. Surface climate and streamflow variability in the western United States and their relationship to large-scale circulation indices. *Water Resources Research*, 27(9): 2381–2399, 1991.

G. Richards. Hydrologic Controls on Proglacial suspended sediment dynamics. Master's thesis, University of British Columbia, Vanvouver, British Columbia, Canada, 2001.

K. Richards. Some observations on suspended sediment dynamics in Storbregrova, Jotunheimen. *ESPL*, 9:101–112, 1984.

M.B. Richman. Rotation of Principal Components. *Journal of Climatology*, 6:293–335, 1986.

K. Ricker. Snowcap Lakes-A dramatic record of diachronous glacier movement, drainage reversals and fluctuating water levels. *Canadian Alpine Journal*, 78:59–65, 1978.

K. Ricker and B. Tupper. Wedgemount Lake and glacier studies, northern Garibaldi Park, 1978. *Canadian alpine journal*, 78:65–66, 1978.

T. Rittenour, J. Brigham-Grette, and M.E. Mann. El Nino-Like climate teleconnections in New England during the late Pleistocene. *Science*, 288:1039–1042, 2000.

H. Rothlisberger and H. Lang. Glacial hydrology. In A.M. Gurnell and M.J. Clark, editors, *Glacio-fluvial sediment transfer*, pages 207–284. John Wiley and Sons, Chicester, UK, 1987.

J. Ryder. Geomorphology of the southern part of the Coast Mountains of British Columbia. *Zeitscrift fr Geomorphologie*, 37:120–147, 1981.

J.M. Ryder and B. Thomson. Neoglaciation in the southern Coast Mountains of British Columbia: chronology prior to the late Neoglacial maximum. *Canadian Journal of Earth Science*, 23:273–287, 1986.

S.A. Schumm. Evolution of drainage systems and slopes in badlands at Perth Amboy, New Jersey. *Geological Society of America Bulletin*, 67:597–646, 1956.

S.A. Schumm. Geomorphic thresholds: the concept and its applications. *Transactions Institute British Geographers*, 4:485–515, 1979.

A. Shabbar, B. Bonsal, and M. Khandekar. Canadian precipitation patterns associated with the southern oscillation. *Journal of Climate*, 10:3016–3027, 1997.

A. Shabbar and M. Khandekar. The impact of El Nio-Southern Oscillation on the temperature field over Canada. *Atmosphere-Ocean*, 34(2):401–416, 1996.

A. Simon. Channel and drainage-basin response in the Toutle River system in the aftermath of the 1980 eruption of Mt. Saint Helens. Technical Report Open File Report 96-633, United States Geological Survey, 1999 1999.

O. Slaymaker. Mountain geomorphology: a theoretical framework for measurement programmes. *Catena*, 18:427–437, 1991.

O. Slaymaker. The sediment budget of the Lillooet River Basin, British Columbia. *Physical Geography*, 14(3):304–320, 1993.

R.J. Small. Moraine sediment budgets. In A.M. Gurnell and M.J. Clark, editors, *Glacio-fluvial sediment transfer*, pages 165–197. John Wiley & Sons, Chichester, 1987.

D. Smith, D. McCarthy, and B. Luckman. Snow-avalanche impact pools in the Canadian Rocky Mountains. *Arctic and Alpine Research*, 26(2):116–127, 1994.

D.G. Smith. Vibracoring: a new method for coring deep lakes. *Palaeogeography, Palaeoclimatology, Palaeoecology*, 140:433–440, 1998.

D.J. Smith and J.R. Desloges. Little Ice Age history of Tzeetsaytsul Glacier, Tweedsmuir Provincial Park, British Columbia. *Gographie physique et Quaternaire*, 54(2):135–141, 2000.

D.J. Smith and C.P. Laroque. Dendroglaciological dating of a Little Ice Age glacial advance at Moving Glacier, Vancouver Island, British Columbia. *Gographie Physique et Quaternaire*, 50(1): 47–55, 1996.

D.J. Smith, D.P. McCarthy, and M.E. Colenutt. Little Ice Age glacial activity in Peter Lougheed and Elk Lakes provincial parks, Canadian Rocky Mountains. *Canadian Journal of Earth Sciences*, 32:579–589, 1995.

N.D. Smith. Sedimentation processes and patterns in a glacier-fed lake with low sediment input. *Canadian Journal of Earth Science*, 15:741–756, 1978.

N.D. Smith and G.M. Ashley. Chapter 4: Proglacial Lacustrine Environments. In G.M. Ashley, J. Shaw, and N.D. Smith, editors, *Glacial Sedimentary Environments. SEPM Short Course No. 16*, pages 135–215. Society of Paleontologists and Mineralogists, Tulsa, OK, 1985.

N.D. Smith and J.P.M. Syvitski. Pelletization in a glacier-fed lake. *Journal of Sedimentary Petrology*, 52(2):503–513, 1978.

C. Souch. Holocene sedimentary environments of the goat meadows watershed, Southern Coast Mountains,British Columbia. *Gographie physique et Quaternaire*, 43(1):77–85, 1989.

C. Souch. *Lake Sediments as Recorders of Paleoenvironmental Change: Kwoiek Creek, Coast Mountains, British Columbia.* Ph.d., University of British Columbia, 1990.

C. Souch. A methodology to interpret downvalley lake sediments as records of Neoglacial activity, Coast Mountains, British Columbia, Canada. *Geografiska Annaler*, 76A:169–185, 1994.

A. Soutar and P.A. Crill. Sedimentation and climatic patterns in the Santa Barbara Basin during the 19th and 20th centuries. *Geological Society of America Bullentin*, 88:1161–1172, 1977.

R.C. Spicer. Recent variations of Blue Glacier, Olympic Mountains, Washington, USA. *Arctic and Alpine Research*, 21(1):1–21, 1989.

D.R. Sprowl. *Elk Lake, Minnisota: Evidence for Rapid Climate Change in the North-Central United States,*, chapter On the precision of the Elk Lake varve chronology, pages 69–74. Geological Society of America, special paper 276 edition, 1993.

T.F. Stocker. An overview of century time-scale variability in the climate: system: observations and models. In D.L.T. Anderson and J. Willebrand, editors, *Decadal Climate Variability*, volume I 44, pages 379–406. Spring-Verlag, Belin Heidelberg, 1996.

D.A. Stone, A.J. Weaver, and F.W. Zwiers. Trends in Canadian Precipitation Intensities. *Atmosphere-Ocean*, 38(2):321–347, 2000.

L.D. Stott, W. Berelson, R. Douglass, and D. Gorsline. Increased dissolved oxygen in Pacific intermediate waters due to lower rates of carbon oxidation in sediments. *Nature*, 407(21 September): 367370, 2000.

M. Stuiver and T.F. Braziunas. Atmospheric 14C and and century-scale solar oscillations. *Nature*, 338:405–408, 1989.

M. Stuiver, T.F. Braziunas, B. Becker, and B. Kromer. Climatic, solar, oceanic, and geomagnetic influences on late-Glacial and Holocene atmospheric 14C/12C change. *Quaternary Research*, 35: 1–24, 1991.

M. Stuiver and P. J. Reimer. Extended 14C data base and revised CALIB 3.0 14C age calibration program. *Radiocarbon*, 35:215–230, 1993.

M. Stuiver, P.J. Reimer, J.W. Beck, G.S. Burr, K.A. Hughen, B. Kromer, F.G. McCormac, J. v. d. Plicht, and M. Spurk. INTCAL98 Radiocarbon age calibration 24,000 -0 cal BP. *Radiocarbon*, 40: 1041–1083, 1998a.

M. Stuiver, P.J. Reimer, and T.F. Braziunas. High-precision radiocarbon age calibration for terrestrial and marine samples. *Radiocarbon*, 40:1127–1151, 1998b.

M. Sturm. Origin and composition of clastic varves. In Ch. Schlchter, editor, *Moraines and Varves: Origin/ Genesis/ Classification*, pages 281–285. A.A. Balkema, Rotterdam, 1979.

A. Sundborg. Lake and reservoir sedimentation: prediction and interpretation. *Geografiska Annaler*, 74A(2-3):93–100, 1992.

W. Taylor. Glacier retreat in Garibaldi Park. *Canadian Alpine Journal*, 24:103–108, 1936.

P.A. Thomas, D.J. Easterbrook, and P.U. Clark. Early Holocene glaciation on Mount Baker, Washington State, USA. *Quaternary Science Reviews*, 19:1043–1046, 2000.

M.P. Thompson. Statistical Modeling of Sediment Concentration. Master's thesis, University of British Columbia, 1987.

M.P. Thompson, H. Joe, and M. Church. Statistical Modeling of Sediment Concentration. Technical Report IWD-HQ-WRB-SS-88-1, Environment Canada, Water Resources Branch, Sediment Survey Section, 1987.

D.J. Thomson. Time series analysis of Holocene climate data. *Philosophical Transactions of the Royal Society of London Series A*, 330:601–616, 1990.

K.E. Trenberth and J.W. Hurrell. Decadal atmosphere-ocean variations in the Pacific. *Climate Dynamics*, 9:303–319, 1994.

W.N. Venables and B.D. Ripley. *Modern applied Statistics with S-Plus.* Springer-Verlag, New York, 1999.

D.J. Verardo, P.N. Froelich, and A. McIntyre. Determination of organic carbon and nitrogen in marine sediments using the Carlo Erba NA-1500 analyzer. *Deep-Sea Research*, 37(1):157–165, 1990.

I. Walker. Chironomidae (Diptera) in Paleoecology. *Quaternary Science Reviews*, 6:29–40, 1987.

J.M. Wallace and D.S. Gutzler. Teleconnections in the geopotential height field during the northern hemisphere winter. *Monthly Weather Review*, 109:784–812, 1981.

D.E. Walling and B.W. Webb. Erosion and sediment yield: a global overview. In D.E. Walling and B.W. Webb, editors, *Erosion and Sediment Yield: Global and Regional Perspectives*, pages 3–19. IAHS Press, Wallingford, Oxfordshire, 1996.

R.A. Walters and M.F. Meier. Variability of glacier mass balances in western North America. In D.H. Peterson, editor, *Aspects of climate variability in the Pacific and Western Americas*, volume Geophysical Monograph 55, pages 365–374. American Geophysical Union, Washington, D.C., 1989.

P. Ward and N.A. Skermer. The 50-year flood in Fitzsimmons Creek, Whistler, British Columbia. In *Geotecnique and Natural Hazards, a symposium*, pages 355–363, Vancouver, 1992. Vancouver Geotechnical Society.

P.J. Whiting and J.B. Bradley. A process-based classification system for headwater streams. *Earth Surface Processes and Landforms*, 18:603–612, 1993.

G.C. Wiles, A. Post, E.H. Muller, and B.F. Molnia. Dendrochronology and late Holocene history of Bering Piedmont Glacier, Alaska. *Quaternary Research*, 52:185–195, 1999.

N. Willemse and T. Trnqvist. Holocene century-scale temperature variability from West Greenland lake records. *Geology*, 27(7):580–584, 1999.

G.P. Williams. Sediment concentration versus water discharge during single hydrologic events in rivers. *Journal of Hydrology*, 111:89–106, 1989.

B. Wolfe and J.T. Teller. Sedimentological and stratigraphic investigations of a sequence of 106 varves from glacial Lake Assiniboine, Saskatchewan. *Journal of Paleolimnology*, 9:257–273, 1993.

World Meteorological Organization. Manual on stream gauging. Technical Report WMO- No. 519, World Meteorological Organization, 1980.

B. Yarnal. Relationships between synoptic-scale atmospheric circulation and glacier mass balance in south-western Canada during the International Hydrological Decades, 1965-1974. *Journal of Glaciology*, 30(105):188–198, 1984.

V. Yevjevich. *Probability and statistics in hydrology.* Water Reources Publications, Fort Collins, Colorado, 1972.

C.M. Zdanowicz, G.A. Zielinski, and M.S. Germani. Mount Mazama eruption: Calendric age verified and atmospheric impact assessed. *Geology*, 27(7):621–624, 1999.

X. Zhang, L.A. Vincent, and W.D. Hogg. Temperature and precipitation trends in Canada during the Twentieth century. *Atmosphere-Ocean*, 38:395–429, 2000.

Y. Zhang, J.M. Wallace, and D.S. Battisti. ENSO-like interdecadal variability: 1900-93. *Journal of Climate*, 10:1004–1020, 1997.

B. Zolitschka. A 14,000 year sediment yield record from western Germany based on annually laminated lake sediments. *Geomorphology*, 22:1–17, 1998.

Appendix A

Detailed Methodology

A.1 Discharge Records

Water level and temperature sites were selected on stable, straight reaches for each creek. Stream gauge sites, however, were limited to bridges (Cayoosh and Van Horlick) and stable woody debris (Phelix) given the size of the channels. Stream gauging followed standard procedure (e.g. World Meteorological Organization, 1980) for mountain streams. Stream velocity was measured with a Price current meter by wading at low-flow conditions and by attaching the current meter to a weight at higher flows. At the higher flows (Cayoosh and Van Horlick) several velocity measurements represent surface measurements. Insufficient mass of the weight (15kg) at the given flow caused the current meter to surface and velocity measurements were corrected by 0.8. Estimates of water depth at higher flows were made by detaching the current meter and using the weight as a sounding mechanism.

Water level was measured with 2m capacitance (1cm) probes which were mounted inside 4 inch, perforated ABS sewer pipe, wrapped with geocloth and attached to Unidata Starloggers. Loggers were programmed to scan sensors every 30 seconds, and writing those measurements to a buffer which was then averaged after 10 minutes and stored in memory. Capacitance sticks were favored over standard transducers both due to lower cost but also to prevent sensor damage in freezing environments. Ice build up along stilling wells prevented the collection of stage measurements during the winter (late November to early April) within the Duffey lake catchment though the nature of this project did not require estimates of low flow conditions.

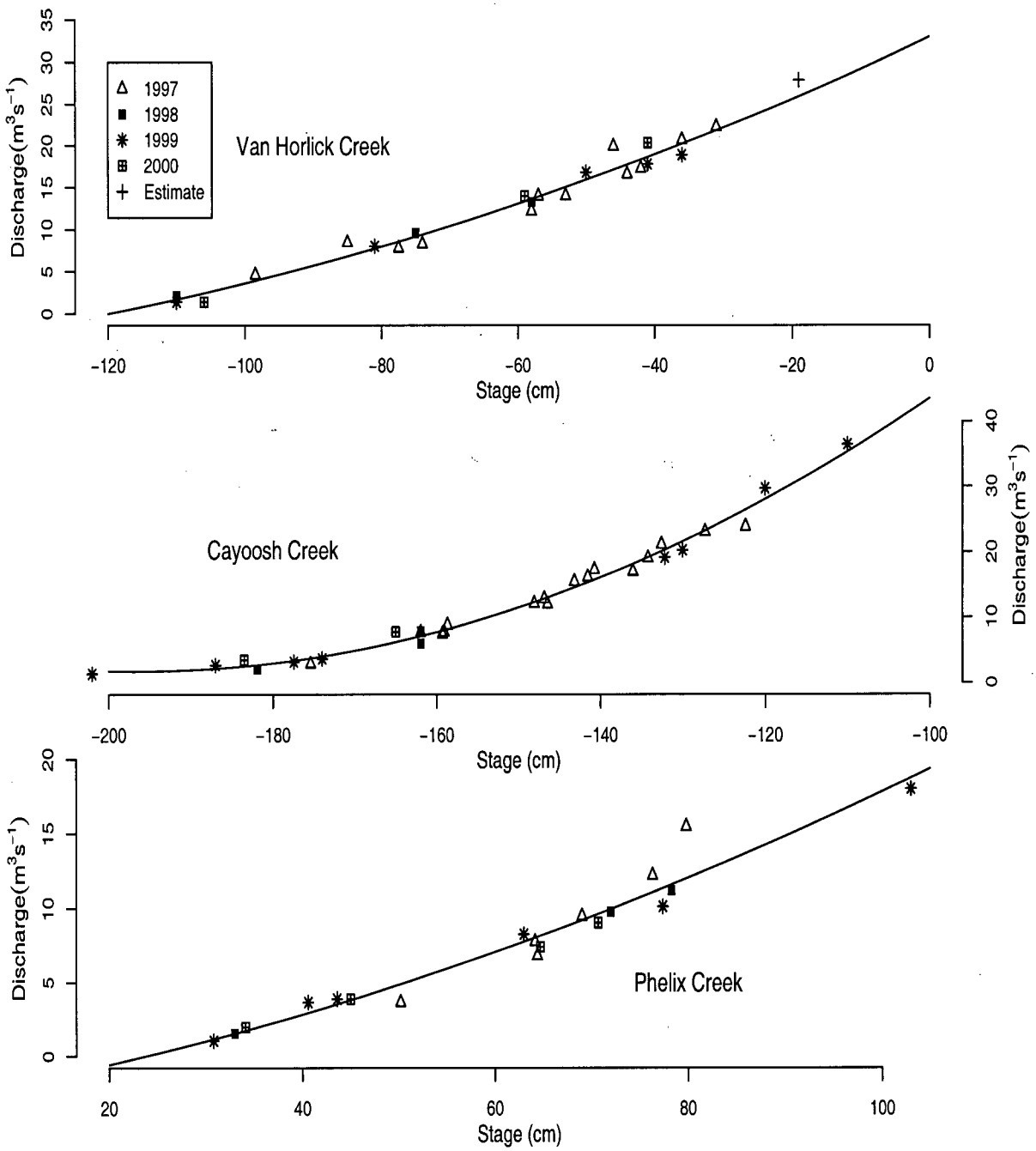

Figure A.1: Stage-Discharge Relations

Stable benchmarks were used as absolute stage indicators for SSC and stage-discharge relations in order to guarantee against data loss or systematic offsets introduced by logger malfunction, vandalism, siltation, or loss in flood. Water level recorded by the data loggers was related to the manual stage measurements through regression and all models were linear in form with very little scatter ($r^2 > 0.98$). Second order polynomials provided best fits for each stage-discharge relation with explained variance (r^2) of the models exceeding 97 % (figure A.1).

The largest degree of scatter is associated with the rating curve for Van Horlick and results from the difficulties in gauging. The only suitable location at which to gauge the flow was at the main highway bridge and flow estimates were determined by suspending the current meter and lead weight into the flow from above (10 m) and have a spotter determine the proper depth within the flow. The highest Q measurement for Van Horlick is estimated from sounding the channel and using Manning's equation to determine average velocity ($\overline{u}$) for the channel.

$$\overline{u} = \frac{AR^{0.66}S^{0.5}}{n} \tag{A.1}$$

where A is the cross sectional area of the channel, R is the hydraulic radius, S is the energy slope, and n is roughness coefficient. S was assumed to approximate the water surface slope and n was back calculated from the second largest observed discharge. The estimate of Q for was not used in the determination of the stage model but its inclusion did little to alter the parameters of the stage-discharge relation for Van Horlick Creek (figure A.1). For most of the creeks and for most years, the variability is distributed throughout the period of monitoring suggesting random errors in gauging rather than shifts in the rating relation.

A.1.1 Cayoosh Creek Discharge

Several problems were encountered with estimating water level for Cayoosh Creek which necessitated corrective measures. The first entailed removal of electrical noise from stage record. Visual inspection of the stage data collected every 10 minutes indicated spikes in water level which did not appear to be related to any physical mechanisms within the channel such as seiches originating from large organic debris jams. Spectral analysis of the time series (periods less than 24 hr) revealed no preferred frequency but the spikes were always positive (with respect to diurnal trend in data) in sign. These spikes, therefore, were assumed to be "electrical noise" of uncertain origin and subsequently removed from the record. A 5-point, boxcar running minimum filter was applied twice to the data which removed most of the spikes from the record. Given the consistent positive anomalies associated with the noise, a running minimum did not elevate the overall water height (figure A.2). Application of the filter, however, did change the sampling resolution but does not affect the results presented here.

The second difficulty encountered at Cayoosh Creek relates to a station shift following a large flood in June 1999 described in Chapter 4. The flood undermined a large organic debris jam 50 m downstream of the stilling well and the stream responded to this change by incising 50 cm in the center of the channel which abruptly altered the stage-discharge relation. In order to estimate discharge at moderate to low flow conditions, it was necessary to relocate the stilling well some 50 m upstream. Relocation could not be completed until low flow conditions and 60 days of record (15 June-15 August) was lost. Stage measurements following the flood were regressed against manual stage observations at various flows in order to develop discharge records after June 1999.

A.2 Lake Sediment Core Recovery

Long cores were cut into 3-4m sections in the field, capped and sealed in air-tight core bags. Lack of cold-storage facilities prevented the refrigeration of the longer cores between recovery and sampling but little evidence of desiccation or post-recovery diagenesis (i.e. microbial activity, molding, or color changes) were observed upon splitting. The cores were cut lengthwise with a portable power saw and split with a razor blade. On cores which were finely laminated, one half of the core was allowed to air dry to enhance subtle features related to color and texture that are commonly not visible in freshly-split cores (R. Gilbert, pers. comm.). Sampling for bulk physical properties (except particle size) was completed on split cores within 1-2 weeks as notable changes in sediment properties (oxidation and loss of water) occurred on split cores over longer time periods.

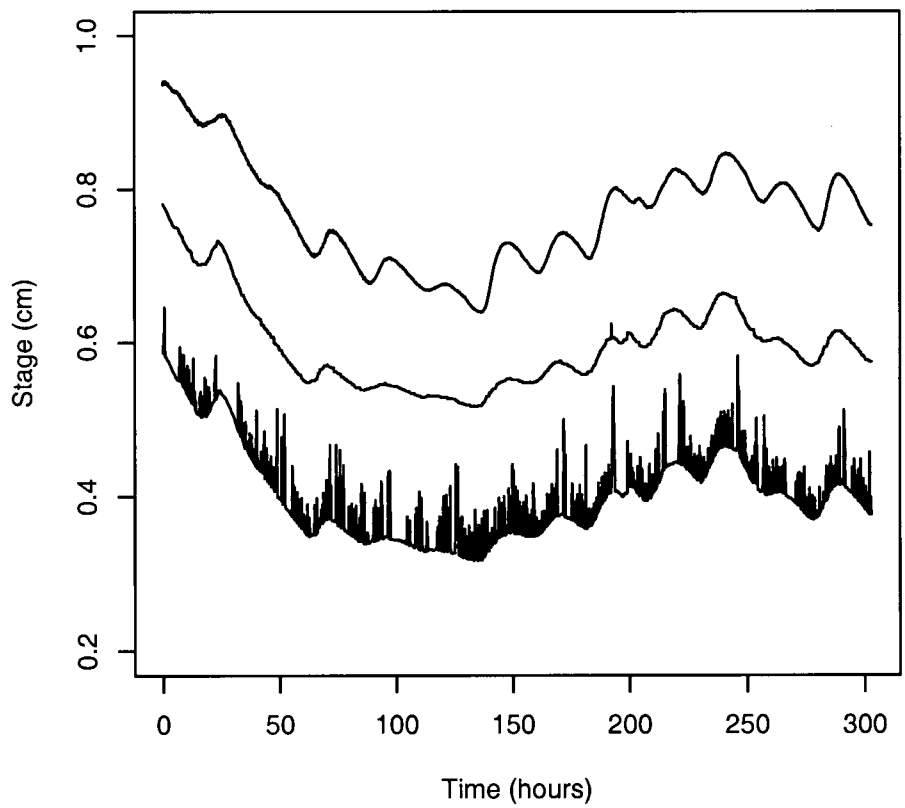

Figure A.2: Electrical Noise in Cayoosh Stage Measurement
Raw (bottom) and corrected (middle) stage level for Cayoosh Creek compared to Van Horlick (upper) for a portion of the 2000 hydrologic season. Electrical noise from Cayoosh Creek stage record was removed by applying a 5pt minimum moving boxcar average twice to the time series. 20cm was added to series in figure for visual clarity.

A.3 Laboratory Techniques

A.3.1 Organic Carbon

The loss on ignition (LOI) method (Dean, 1974) was used to estimate organic and inorganic matter content of the lake sediment samples. Sediment samples were oven dried overnight at 105 °Cand then combusted for 2 hours at 550 °C, allowed to cool in a dessicator reweighed and combusted at 950 °Cfor an hour. The mass difference between 550 °Cand 105 °Cprovided an estimate of the organic content of the sample while mass lost between 550 and 950 °Cprovides an index of the carbonate content of the sample. The loss in mass at 950 °Cis due to CO_2 evolvement during combustion (Dean, 1974).

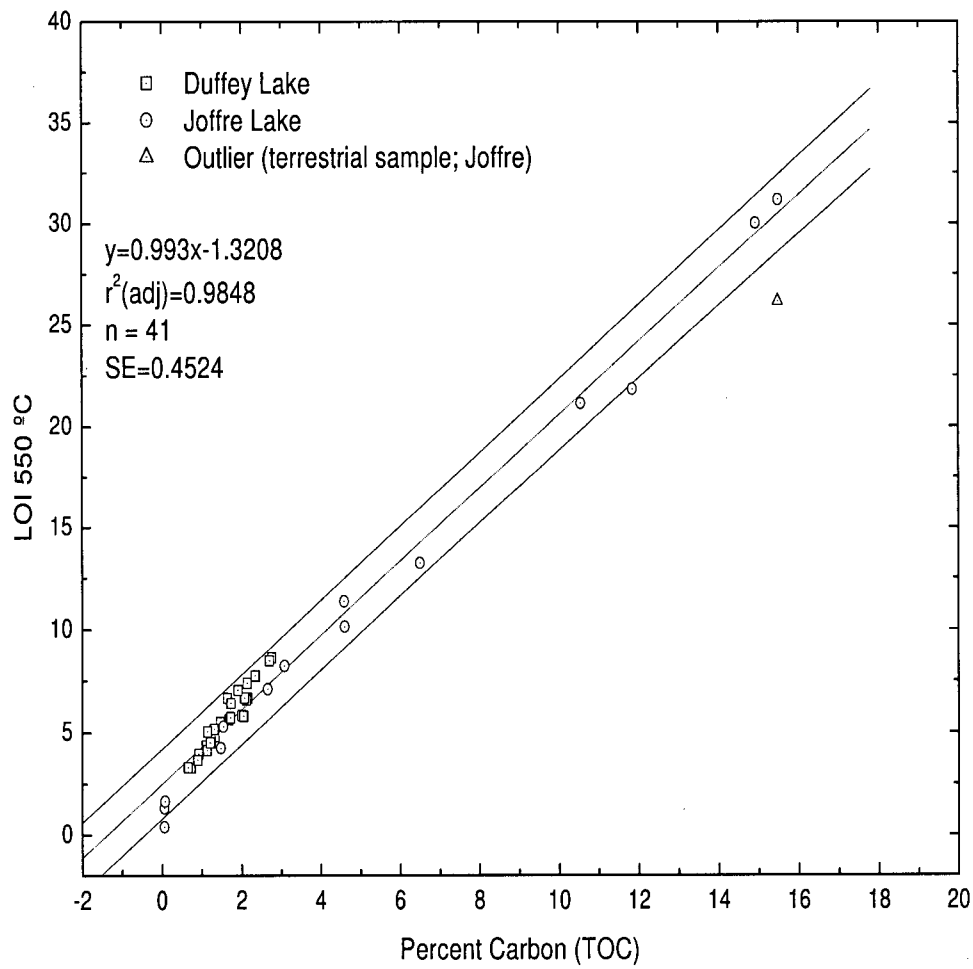

Figure A.3: LOI TOC Relation
Organic carbon and Loss on Ignition (550 °C) relation for sediment samples from Duffey and Joffre Lake basins. Outermost lines denote 95 percent prediction limits of the the regression model.

Mass lost by the LOI procedure was compared to total carbon (TC) determined with a Carlo Erba CN Analyzer (Verardo et al., 1990) with sample precision of 0.3 %. A linear model (figureA.3) explains 99 % of the variance between LOI (550 °C) and TC (n=40) while no statistically significant

correlation was found between TC and LOI (950 °C). Mass lost at 950 °C was between 1-3 percent for most samples and it is possible that this mass lost represents evolvement of lattice-bound H_2O which is common when combusting clay-rich sediment (Dean, 1974). In addition, such small changes in mass following combustion at 550 °C are at the limit of the the precision of the balance (± 1.0 mg). Therefore, even though carbonate content was estimated for the sediments it is reported as absent or below detection limits.

A.3.2 Volumetric Sampling and Particle Size Analysis

Sediment cores were sampled for bulk physical properties which varied depending on the the type of analysis which was required: a) A brass sample (3.5x1.0x7cm) sampler was used for those cores where adequate sample mass was required for other analysis (e.g. particle size) and; b) a disposable syringe which were modified and calibrated to sample 1.0 cm^3 of wet sediment. Dry density ($g\ cm^{-3}$) and water content (percent) was determined by the difference between wet and oven dry (105 °C) mass. High temperatures (> 50 °C) may alter the inherent magnetic properties of sediment and or cause sintering effects in clastic sediment with high clay content. Samples where such analysis was required were dried at 35 °C and oven dry mass (105 °C) was determined on a representative fraction and used to correct the entire sample to an oven dry basis.

Particle size analysis was completed by mechanical sieving for the sand and coarser size fraction (> 2000-63μm) and through settling in a Sedigraph particle size analyzer for the silt and clay-size sediment (63-1μm). Preparation for Sedigraph analysis entailed collection of 2.5 g of representative material which was treated with 10mL treatments of heated H_2O_2 (70 °C) to oxidize and remove fine-grained organic material which could alter "clastic" settling velocities by flocculation. Such influence of fine-grained organic complexes and an attempt to remove such material by LOI became immediately apparent which triplicate tests were completed on samples which were left untreated, teated with H_2O_2, and combusted. Depending on sample, the untreated and combusted treatments decreased the percentage of clay-sized sediment by 5-20%. Though treated sediment does not represent the true size characteristics of the sediment during settling, such treatment is the only way to standardize the results so that comparisons between studies can be made. Following peroxide treatment, the material was wet sieved (63 μm), and the coarser sized fraction was dried and dry sieved (2000-63 μm). The silts and clays were oven dried (50 °C), combined with a dispersant (Na PO_4) and sedigraphed to 1 μm. Particle size data are reported in the Wentworth grade scale and corrected for bias cause by discreet and open-ended (i.e. at the fine end) distribution characteristics (Griffiths, 1967).

A.3.3 Sediment Slabbing and Embedding Techniques

Portions of the sediment cores from Green, Cheakamus, Glacier, and Duffey lakes were embedded with low viscosity resin in order to meet two objectives: a) to increase the accuracy of varve chronologies introduced by difficulties in preparing sediment cores for visual photography; and b) to detail the micro-stratigraphy within the laminated sediments from the different lake basins. Varve counting, thickness measurements and observations of sediment fabric were originally made on color photographs of sediment cores which were left to partially dry (e.g. Gilbert, 1975; Desloges and Gilbert, 1994b). Those data were later supplemented by embedding sediment slabs which were polished and often cut into thin sections when it became apparent that discrepancies arose between varve counts on air-dry versus embedded sediment slabs. X-radiography (e.g. Grimm et al., 1996)proved unsuccessful for the sediments of this study most likely resulting from small-scale variations in sediment density which created individual X-radiographs which were both under

and over exposed.

The major source of error in using the air-dried approach in this study is believed to be caused by smearing effects. Recounts on portions of sediment cores with air-dried and embedded sediment revealed that several (2% on average) small lamina were missed on counts made on the air-dry sediment photographs. The majority of these varves were small (< 1.0mm) and underlain by thicker, clay-rich laminae interpreted to be flood deposits.

Sediment embedding techniques were modified from published sources (e.g. Lamoureux, 1994; Pike and Kemp, 1996)and more recent suggestions for improvement (Lamoureux, 2000; pers. comm). After splitting, sediment cores were sub-sampled by collecting overlapping (staggered) sediment slabs with a standard oceanographic sediment sampler (15cm x 4cm x 1cm) known as a "cookie cutter" (e.g. Grimm et al., 1996). Slabs were placed on perforated aluminum foil and arranged side by side in rectangular tupperware trays. Excess plastic around the trays was trimmed to allow 2 trays to be placed within a 22cm diameter glass, vacuum dissicator. Sediment slabs were dehydrated with acetone (e.g. Lamoureux, 1994) and by the flash-freeze/freeze-dry (ff/fd) method (e.g. Pike and Kemp, 1996). After the sediment slabs are completely dehydrated, samples were embedded under low vacuum with low viscosity resin (Spurr), left for 1-2 days and then cured in an 55 °C oven for 2 days. Once hardened, sediment slabs were either polished (to 950 grit) or made into thin sections depending on varve clarity and purpose (e.g. sediment structure description or varve measurements). *Note*: acetone replacement and embedding need to be completed under a flume hood and using protective equipment (e.g. goggles and latex gloves) as both acetone are the resin are carcinogenic.

To economize, both low and high grade acetone were used to chemically dehydrate the sediment samples. The replacement begins by submerging samples (i.e. filling tupperware containers) in low-grade acetone (acetone stored in large containers which has a higher water content), sealing and replacing acetone 3 times daily for the first 3 days. Acetone is removed and added using a large pipette. The tenth and successive exchanges use high grade acetone (H_2O <0.5 %) and exchanges continued until 18 exchanges were made. Following the last exchange, the required volume of resin (6 batches / 90cm core) is made and mixed with 1/3 acetone and placed in the dissicator over silica gel and under low vacuum.

The ff/fd method used liquid nitrogen to rapidly freeze interstitial water preventing most freezing-induced disturbances. The tupperware tray with sediment slabs is place in a Styrofoam container and liquid nitrogen is poured into the Styrofoam until the tupperware container begins to float. After the sediment slabs are completely frozen (3-5 minutes) they are placed in a freezer until they can be freeze dried which takes 2-3 days depending on the water content of the sediment.

The quality of slab and thin sections for petrographic study was highest on those sediment slabs dehydrated with acetone. Those sediments have less desiccation and freezing-crack structures and less overall disturbance of the sediment matrix. Successful embedding of sediment requires the *complete* removal of water from the sediment as the resin is hydroscopic and will not polymerize if any water is present. Sediments of Duffey Lake could be chemically dehydrated with few problems but sediments of Green (and surface sediments from Lillooet Lake) proved difficult. The difficulty of embedding within Green lake via acetone replacement became more pronounced downcore (progressively softer slab following curing). It is suspected that lattice water bound within clay (several particle size samples from Green Lake have clay percentages exceeding 80 percent) was not removed despite 18 acetone exchanges and lattice water was evolved during resin curing. Difficulties in dehydration via acetone was also experienced on sediment from Lillooet Lake (unpublished data) again most likely the result of high clay content. The ff/fd method encountered similar problems for clay-rich sediment.

Appendix B

TRIM, Geologic and Glacial Mapping

Thematic data (topographic data, land use and geologic) were obtained electronically from the Ministry of Environment, British Columbia and from the Geological Survey of Canada, co-registered and merged into overlapping coverages. Geologic mapping was conducted by the Geological Survey of Canada at a nominal scale of 1:100,000 (Monger and Journeay, 1994) and co-registered to the larger scale (1:20,000) TRIM (Terrain Resource Inventory Mapping project) data using a similar datum (NAD 1983). Positional accuracy associated with the TRIM planimetric data is 10m; discussion of this error and general specifications of the TRIM project can be found elsewhere (British Columbia Surveys and Resource Mapping Branch, 1990). Contemporary ice coverage was determined from the TRIM data (ice and snow fields coverage) and those glaciers where moraines and or former extent has been mapped were checked against recent (1990-1993) air photos. For many of the smaller glaciers there were differences in the TRIM ice coverage boundaries and those revealed in the recent air photos. The most likely source of the inconsistency lies in non-uniform classification of glacial extent (ice and or snowfield), early season photography and differences in scale between the photos sets. Such discrepancies, however, were largely limited to glacial accumulation areas (except scale effects) and not near glacial termini. Most of the ice coverage in the TRIM data consisted of single and or several polygons comprising many individual glaciers. Boundaries of individual glaciers were delimited by creating contour lines (25 m) from the DEM data and assuming that ice flow is orthogonal to slope.

Differences in the scale of mapping between the geologic (1:100,000) and TRIM (1:20,000) data created difficulties in co-registering both data types. Significant difference between ice and or water extent and surrounding geology were encountered when attempting to co-register the geological and ice/lake coverages. This is partly due to scale effects but recent glacial recession is another factor associated with this difference. In order to create "seamless" coverages, the geologic maps were edited by interpolating rock coverage from adjacent polygon edges. No attempt was made to field or photo check this interpretation given the required expertise necessary to complete such a task.

B.1 LIA Mapping

Mapping of large scale (LIA) former ice extent was accomplished by transferring interpreted boundaries under a stereoscope (when possible) from uncorrected color and black and white photographs to the TRIM dataset through screen digitization. Shaded relief maps (25m DEM data) and physiographic themes (e.g. water and digital coverages including glacial moraines) were used to register the boundaries obtained under the stereoscope to the digital coverages. Such methods are likely to be much poorer than determining boundaries with a stereoplotter. Estimation of error in the former method was assessed by replicating the digitization of a particular glacier, and comparison of glaciers where former (LIA) downvalley glacial extent was demarcated in the TRIM data. Average errors were between 10-15 percent. The magnitude of such error should not greatly affect the conclusions made in this project.

B.2 Rectification from air photos

In order to evaluate the change in sedimentation in the lake basins due to changes in glacial coverage, glacial extent for these periods was mapped from oblique, air photos and the original map base of the park and co-registered to the TRIM data. Air photos and the original base map were rectified (affine transformation) where possible and in general root mean squared errors between the control points of the TRIM data with those of the air photos were less than 15m and generally less in glacial forefield areas which were flat. Errors due to slope displacement were not corrected as many stereo pairs were not available. Control points represented prominent land marks such as moraines, stream intersections, lakes and cliff bands. It is suspected that most of the errors in the mapping arise from slope displacement and external (camera or plane tilt) factors, rather than those caused by lack of suitable ground control as the absolute displacement error of TRIM planimetric data is less than 15m. Errors caused by slope displacement were likely minimized because most of the areal changes in glacial cover occurred in ablation areas with more subdued topography. There is a general lack of complete overlap for the study area for any particular year but gross scale changes in glacial cover appear to be detectable in the analyzed air photos.

Appendix C

EOF, Spectral Analysis, and Effective Degrees of Freedom

Empirical orthogonal function (EOF) analysis is a statistical technique which seeks to reduce the spatial dimensionality of large datasets. The method has been used for some time (see introduction in Preisendorfer, 1988) and utilized in the environmental sciences to ease interpretation of dominant spatial domains of atmospheric fields, hydrologic and proxy climate data. Such patterns often provide insight into underlying geophysical processes or domains over which such processes operate. Principal component analysis (PCA) is a means of normalizing the output of EOF in the temporal domain and allows an investigator to easily interpret the proportion of variance explained by the dominant modes within the dataset in both time and space. A minor limitation associated with such a normalization is the reduction of orthogonality imposed by the transformation (e.g. Mestas-Nunez, 2000) but such non-orthogonality is usually not severe in most data sets (Preisendorfer, 1988). EOF analysis produces m (station) time series of n (sample) length which explain the time-varying nature of a given mode; such temporal analysis can also be conducted on one-dimensional time series to determine harmonic and aharmonic components in a time series; the latter of which is generally problematic using standard methods of time series analysis (i.e. Fourier decomposition).

C.1 EOF and PCA

Given S, (an n sample by m station matrix), EOF analysis begins by centering the dataset and constructing a normalized, covariance matrix:

$$\mathbf{C} = (\frac{1}{n-1})\mathbf{S}'\mathbf{S} \tag{C.1}$$

where $\mathbf{S}'$ is the transpose of $\mathbf{S}$. If necessary, the analysis can use standardized data:

$$\mathbf{R} = \frac{\mathbf{Z}'\mathbf{Z}}{n-1} \tag{C.2}$$

where $\mathbf{R}$ represents a correlation matrix and $\mathbf{Z}$ is a matrix of m centered station data divided by the standard deviation of the station. Such standardization is necessary if between-station data vary greatly in range (e.g. streamflow data), are not properly scaled (e.g. division by catchment area for the streamflow example), or have different units. Failure to normalize the data will cause non-proportional spatial weighting scaling to the observed variance of the stations. In addition, if the objective of EOF analysis is to examine the spatial components (eigenvectors), the stations must be properly weighted for the area that they represent. Preservation of spatial patterns can be preserved by resampling the data onto an equal area grid (e.g. Karl et al., 1982) or by deriving weighting coefficients based on area for the stations (e.g. Buell, 1978). Gridded data (latitude, longitude coordinate system) distributed over the earth can be weighted according to latitude (ϕ) by:

$$w \propto \sqrt{\cos|\phi|} \tag{C.3}$$

The loading matrix (basis of eigenvectors) is reverse weighted following EOF analysis to preserve variance within the dataset. Once properly weighted, N is now decomposed through standard EOF

analysis or through singular value decomposition (SVD). Both techniques compute the eigenvalues and eigenvectors from the standardized data matrix though EOF require a unique solution to the inversion of the normalized data matrix where SVD does not. For EOF analysis, eigenvectors and eigenvalues are determined by solving :

$$|\mathbf{C} - \lambda \mathbf{I}| = 0 \tag{C.4}$$

where λ represents the m eigenvalues, $\mathbf{I}$ is an m by m identity matrix and $\mathbf{C}$ is a covariance data matrix in either standardized ($\mathbf{Z}$) or unstandardized form. The solution of C.4 can be expressed by (Mann et al., 1998):

$$\mathbf{S} = \sum_{i=1}^{i=m} \lambda_m \mathbf{U}_m \mathbf{V}_m \tag{C.5}$$

where $\mathbf{U}_m$ represents the mth principal component (PC) of n length and $\mathbf{V}_m$ is the mth eigenvector (EOF) representing the loading of the this PC in the the spatial domain, λ_m is the proportion of variance explained by the mth PC. EOF and PCA will work so long as a unique solution exists for equation C.5 which generally occurs if the system is over-determined (Press et al., 1986). If this is not the case (often when m exceeds n) SVD provides an alternative method of determining required parameters of the eigensystem with the decomposition of $\mathbf{S}$ producing (Mestas-Nunez, 2000):

$$\mathbf{S} = \mathbf{B}\lambda\mathbf{A}' \tag{C.6}$$

where $\mathbf{B}$ and $\mathbf{A}'$ are the eigenvectors of $\mathbf{S}$ and λ is a diagonal matrix of normalized (powered to 0.5) eigenvalues and $\mathbf{A}$ and $\mathbf{B}$ are the eigenvector matrices from $\mathbf{S}'\mathbf{S}$ and $\mathbf{S}\mathbf{S}'$ respectively. From equation C.6, the eigenvalues (PC's) of the system are determined from:

$$\mathbf{U} = \mathbf{B}\lambda \tag{C.7}$$

Numerical algorithms used to solve eq. C.5 and C.6 have been around for some time (e.g. Press et al., 1986) and were incorporated with other computer code written in the Python computer language to complete the EOF and PCA analysis.

Because only n PC's within a given data set explain most of the variance, procedures are needed to calculate the number of PC's which will be retained so that those PC's which are not different from statistical "noise" are not interpreted as signal. Similar procedures are necessary in order to make sure that adjacent PC's represent truly differing spatial (temporal) patterns. If the data were standardized before analysis, a simple procedure is to retain those PC's which are greater than 1.0, the expected "average" eigenvalue from the standardized dataset and the value of any eigenvalue derived from a random data matrix (Preisendorfer, 1988). Often, however, the number of significant factors can be obtained by plotting the proportion of variance explained by eigenvalue n for the m eigenvalues; those dominant PC's within the dataset will plot well above the background (and physically meaningless) PC's of higher order. The number of PC's to retain can also be assessed through Monte Carlo sampling (e.g. Cheng et al., 1995) whereby comparisons are made between the eigenvectors from the original dataset with the ensemble average of temporal length (n < n original). Statistical independence of two eigenvalues can be calculated by (North et al., 1982):

$$\Delta\lambda_i = \lambda_i\sqrt{\frac{2}{N}} \tag{C.8}$$

where N is the effective sample size (after correction for autocorrelation if required) and λ_i is the ith PC. Independence can be assumed (i.e. domains in time or space are not mixed) if $\lambda_i \neq \lambda_{i+1}$.

C.1.1 Simplification of spatio-temporal patterns: Rotated Solution

The result of EOF or PCA analysis is a set of uncorrelated (in time and space) components which explain decreasing (usually logarithmically) proportions of variance within a given dataset. However, because of inherent noise within large data sets and inferential statistical treatment of the data (i.e. inferring parameter estimates of population from sample), spatial data structure obtained from standard EOF or PCA is often not robust and principal modes within the dataset may be mixed (e.g. Richman, 1986; Cheng et al., 1995). In order to clarify the spatial structure, rotation of the retained PC's was completed and is known as Rotated Principal Component Analysis (RPCA). The PC's were rotated with a varimax algorithm (Kaiser, 1958) which maximizes the variance associated with n retained PC's. The PC's are rotated in pairs until a given convergence criterion is met (Richman, 1986). A varimax algorithm written by Brian Ripley in the R language (Ihaka and Gentleman, 1996) was recoded in the Python computer language (www.python.org) and used in conjunction with Py-climate. The code was tested on smaller datasets within both packages.

C.2 Autocorrelation and the Color of Noise

Autocorrelation describes the correlation of a time or space series with itself at various lags. Most geophysical time series have some degree of autocorrelation which is often a reflection of memory within the system or a periodic structure imposed by some external forcing element. An understanding of this autocorrelation structure is important because it provides clues into signal and noise characteristics of the geophysical system in question. For example, during snowmelt runoff in mountain environments, hourly streamflow discharge has a fundamental period of 24 hours corresponding to the diurnal inputs of solar radiation. Examination of this structure at various lags indicates that the current discharge could be predicted with some degree of certainty based on the previous hour's discharge. Monthly variations is sea surface temperatures for some region through time is another example of a time series which shows strong autocorrelation. Anomaly destruction is dependent upon internal circulation characteristics of the ocean and on unpredictable atmospheric forcing.

Unlike the streamflow example, autocorrelation within the time series is principally caused by the relaxation scale of the system which can be very non-linear and non-predictable but overall response is much slower than the atmosphere. Such low frequency variations are often referred to as red noise and spectra from such processes often exhibit 1/frequency scaling, which differs from white noise which has no preferred frequency and its time domain structure is fully explained by its two first moments μ and σ. Normalized (N[0,1]) geophysical series (g) with autocorrelation can by modeled as a first-order Markovian process:

$$g_{t=}\rho_{\Delta 1}(g_{t-1}) + (1 - \rho_{\Delta 1})^{0.5}\sigma \tag{C.9}$$

where g_t, g_{t-1} is the current and previous observation respectively, $\rho_{\Delta 1}$is the estimated, lag-1 autocorrelation coefficient for the time series and σ is a normally distributed random variate which represents statistical noise with no memory. Such noise is often referred to as white. If the series is truly approximated by eq. C.9, then $\rho_{\Delta 1}$ can be approximated by the average of ρ at lag 1 and the square root of ρ at lag2 (Gilman et al., 1963).

C.2.1 Autocorrelation and Effective Degrees of Freedom

Determination of autocorrelation structure is also required in order to employ standard statistical techniques to the dataset that are not biased with respect to degrees of freedom. Autocorrelation decreases the effective number of independent samples within a dataset and will inflate the statistical significance of the correlation (r) between two time series. In the frequency domain, such effects are evident by spectra with larger proportions of power at low frequencies and a white noise background for such time series can not be made. The bias introduced by autocorrelation within the time domain has been known for some time (e.g. Bartlett, 1935) and can be corrected by determining the effective sample size (N_{eff}) of the given bivariate data (Yevjevich, 1972):

$$N_{eff} = \frac{N}{1 + 2\sum_{i=1}^{i=n} \rho_{ix}\rho_{iy}} \tag{C.10}$$

where N is the number of bivariate samples from the time series x and y , and n is the number of lags for which *both* series experience statistically significant (usually p < 0.05) autocorrelation coefficients ($\rho_{\Delta 1}$). A drawback with eq. C.10 is that it assumes that trends, periodic components and erratic behavior are removed prior to calculation. An alternative method for a single time series is provided by (Leith, 1973; Hartmann, 2001):

$$N_{eff} = \frac{N\Delta t}{2\xi} \tag{C.11}$$

where Δt is the sampling rate (time interval between successive observations) and ξ is the e-folding time, the period over which the autocorrelation of the time series drops to $1/e$. Equation C.11 makes no assumptions regarding inherent signals or irregularities within the time series. N_{eff} for the bivariate data is taken to be the smaller of the two numbers while for gridded or multiple station data (e.g. tree ring sites), $\rho_{\Delta 1}$ is averaged across the entire network.

In order to test the statistical significance of periodic components within the frequency domain, an appropriate noise background is required. Most time series examined in this thesis can be approximated by eq. C.9 and thus, frequency components can be tested against a red noise background which takes autocorrelation into account by (Gilman et al., 1963; Mann and Lees, 1996):

$$P_f = \left(\frac{\sigma^2}{1-\rho_{\Delta 1}^2}\right)\frac{1-\rho_{\Delta 1}^2}{1 - 2\rho_{\Delta 1}\cos\pi\left(\frac{f}{f_N}\right) + \rho_{\Delta 1}^2} \tag{C.12}$$

with P_f representing the spectral power at a given frequency (f) and f_N is the Nyquist frequency ($\frac{\Delta t}{2}$). Once the red-noise background is estimated for the time series in question, confidence limits for a particular frequency (f) are χ^2 distributed depending on degrees of freedom of the spectral estimate and the desired confidence limit (α) (Hegge and Masselink, 1996):

$$P_f \frac{v}{\chi^2_{(v,1-\frac{\alpha}{2})}} \geq P_f \geq_f \frac{v}{\chi^2_{(v,\frac{\alpha}{2})}} \tag{C.13}$$

Mann and Lees (1996) estimate $\rho_{\Delta 1}$ by fitting equation C.12 to the median smoothed background of the given time series in question. They suggest that such a procedure is more robust than by fitting a red-noise model by the standard approach (i.e. estimating $\rho_{\Delta 1}$ directly from the lag 1 and or lag2 autocorrelation coefficients). They find that the latter tends to misfit numerous synthetic, instrumental and proxy hydro-climatic time series at both high (lag 1 red noise model under predicts) and low (over predicts) frequencies.

Appendix D

Varve Measurements and Uncertainties

Varve chronolologies represent an important archive of lake sedimentation on an annual basis and provide a unique chronologic tool for paleoenvironmental reconstruction. Unfortunately, varve identification is subjective and subject to multiple sources of error which may be caused by incorrect varve identification or loss of varves by erosion and destruction through hydrologic or biologic reworking. Less common is the possibility of missing varves caused by lack of sedimentation at the core site for the year in question. Most secure chronologies are developed in lake settings where varves represent the end product of biologic processes within lake setting which follow the annual, predictable rhythms of the earth such as the seaonal cycle of air temperatures at temperate latitudes (e.g. Nuhfer et al., 1993; Zolitschka, 1998; O'Sullivan, 1983). Reported errors are considerably larger in varve chronologies which reflect allochthonous accumulations because sedimentation is partially controlled by inflow events which may occur irregularly. For example, low inflow may occur during times of severe drought, failing to produce a varve for the year in question or a second inflow may occur late in the hydrologic season after thermal structure within a lake has broken down. Such an inflow event may produce a couplet which is then counted as a small (false) varve for the year in question.

Over time scales exceeding the contemporary period, uncertainty in the varve chronologies for Green and Duffey lake basins was assessed in three ways. The first procedure entailed replicating varve counts back to a particular depth in a single core and provided a gross-scale estimate of errors in varve identification (e.g. Sprowl, 1993). Such methods are common for ice core records where important replication provided by multiple cores is often severely limited or absent (e.g. Alley et al., 1997b). The repeat counts were separated by 2 months and there was no attempt to identify marker horizons but only to record the number of varves within a given depth of core. The second approach utilized multiple cores and cross correlated varves based on conspicuous marker horizons such as turbidites or uniquely laminated varves (e.g. Lamoureux and Bradley, 1996). This approach provides a means of assessing the type of error causing the discrepancy (i.e. missing or false varve) and is the standard approach of developing and assessing the reliability of a given varve chronology. The third method of evaluating counting errors is to estimate sediment age at a given depth independently such as well-dated pollen horizons or tephras (e.g. Leonard, 1995) or with radiocarbon dating (e.g. Desloges and Gilbert, 1995).

Errors observed in the Green Lake chronology are lowest and most consistent between cores and between methods (table D.1) for the two lake basins. Higher errors are observed for counts based on sections of cores which were partially dried where small couplets were obscured by smearing of clay-rich sediment from underlying flood deposits. The error in the chronology is similar in magnitude to those reported for other varve chronologies developed from clastic lake sediments (e.g. Leonard, 1995; Lamoureux and Bradley, 1996). Much larger varve-identification errors were observed for the Duffey Lake varve chronology where varves are often eroded under, coarse grained events beds or obscured by bioturbation (table D.1). Up to 22 couplets were eroded under the largest and thickest event bed, based on cross-core correlation. Repeat varve counts for Duffey Lake gave the largest errors of the lake basins (table D.1). The large uncertainty in repeat counting for the Duffey Lake chronology is based on initial varve counts on photos of partially-dried sediment. Recounts using thin sections and slabs indicate that significantly more laminae were considered to be true varves

on photographs of partially dried cores. Much of the difficulty appeared to arise in sections which were moderately bioturbated and where couplet boundaries were poorly defined.

Method	*Green Lake*	*Duffey Lake*
Cross-correlation	1.7-2.8	4.7-8.7
Repeat Counting	1.5 (600 yr)	11.3 (550 yr)
$AMS\ ^{14}C$ Dating	7.8 (1300yr)	3.97-5.28 (550yr)
Mean Error	3.82	7.54

Table D.1: Uncertainty (percent) in Varve Chronologies, Duffey and Green Lake Basins

The large uncertainty of the Green Lake varve chronology based on independent dating is believed to originate from the result of the lack of identifiable varves in the 5cm bioturbated section of core around 150cm depth. Without adding missing varves to the chronology, the best estimate for the varve age at 242cm is 920AD±20 yr while the 2σ $AMS\ ^{14}C$ calibrated age range for terrestrial macrofossils from this interval (648-865AD) and to not overlap at 2σ. The uncertainty (1σ) from the varve-based estimate is the average uncertainty from errors based on cross-correlation and repeat counting. Assuming this interval represents 40 yr of sedimentation ($\approx 1.25\ mmyr^{-1}$) the varve and calibrated radiometric age can not be shown to be statistically different at 2σ. The sedimentation estimate is based on average varve thickness in other portions of the sediment cores where laminae are moderately bioturbated but boundaries are still recognizable. Further verification of the varve counts is provided by a second $AMS\ ^{14}C$ age obtained from terrestrial macrofossils at 342cm depth (table 6.7). Even without the addition of 40 missing varves into the chronology, the varve based (365AD±20) and the calibrated $AMS\ ^{14}C$ age (5-324AD) overlap at 2σ.

In summary, multiple derived estimates of uncertainty indicate that for at least the last 1700 years, the Green Lake varve chronology has consistent and acceptable levels of error. Though it is much larger than uncertainty associated with tree-ring chronologies, it is consistent with error estimates derived for other clastic varve chronologies (e.g. Lamoureux and Bradley, 1996; Leonard, 1995; Sprowl, 1993) . Unfortunately, the Duffey Lake chronology has a much larger (> 5 percent) average uncertainty which makes it less useful for investigating climate-sediment transport linkages and general paleoenvironmental reconstruction. The origins of the errors relate mainly to difficulties in varve identification, erosion of varves by coarse-grained debris flows and strong turbidity currents, and through bioturbation. Thus, although seaonal core recovery and radiometric dating indicate that a true clastic varve interpretation for the non-event laminae is reasonable, their use as a precise chronologic tool is not possible.